

# **Geometric Complexity of Urban Road Networks**

BY

FARIDEDDIN PEIRAVIAN  
B.S., Shiraz University, 1985  
M.S., McMaster University, 1994

THESIS

Submitted as partial fulfillment of the requirements  
for the degree of Doctor of Philosophy in Civil Engineering  
in the Graduate College of the  
University of Illinois at Chicago, 2014

Chicago, Illinois

Defense Committee:

Dr. Sybil Derrible, Chair and Advisor  
Dr. Abolfazl Mohammadian  
Dr. Bo Zou  
Dr. Mohsen Issa  
Dr. Thomas Theis  
Dr. Nebiyu Tilahun, Urban Planning and Policy

بِسْمِ اللَّهِ الرَّحْمَنِ الرَّحِيمِ

To my beloved father and mother

## ACKNOWLEDGMENTS

“In the Name of God, the Merciful, the Compassionate”

“Life is a journey, from *being* to *becoming*”

- SVCF

First and foremost, thanks to Allah (SWT), Master of the universe, for giving me life; the pleasure of loving and being loved; the joy of being a child and having a child; the gift of senses to feel, explore, experience and learn about His creation; and the opportunity and excitement to indulge in knowledge. I ask Him to help me be humble like a blade of grass and generous in spreading my knowledge like a tree laden with fruit.

When I look back, I cannot imagine being here without the company, help, support, and encouragement of many others. I hope this work will be seen as a "Thank you" to the many people who have helped me through my journey.

My special thanks goes to Dr. Sybil Derrible, my advisor and my friend, who walked with me through the course of my research, and skillfully guided me, encouraged me, pushed me and inspired me. He showed a high level of professionalism, maturity, and integrity. He taught me how to be, as a person and a professional.

I am grateful to my advisory committee members for their invaluable comments, suggestions, and ideas; specifically my former advisor, Dr. Abolfazl Mohammadian, for continually offering me guidance and encouragement.

Many thanks to my little angel and wonderful daughter, Elham, for helping me with data collection and preparation for my research. I am also grateful to my lovely wife, Dawn; my little big man, my son Ali; my loving brothers and sisters; and my uncle (peace be upon his soul) and aunt, each of whom played an important role in my success.

And last, but not least, I am greatly indebted to my beloved father (peace be upon his soul) and mother, who patiently and quietly stood by me from near and far, never gave up on me, always gave me hope and blessing, and sacrificed everything they had for me. I wrote each page of this work while having them in my mind and heart. Their presence can be found here weaving in and out of every page. I proudly dedicate this work to them as a token of my appreciation. God bless them.

## TABLE OF CONTENTS

1. INTRODUCTION .....	1
1.1. The need to understand cities .....	1
1.2. Defining Complexity .....	4
1.2.1. Simple Systems.....	4
1.2.2. Complicated Systems.....	5
1.2.3. Complex systems .....	5
1.2.4. Definition of Complex Systems.....	6
1.3. Complex Urban Systems .....	8
2. LITERATURE REVIEW .....	15
2.1. The origin .....	15
2.2. Definition of a network .....	17
2.3. Network indicators .....	17
2.4. Network Science .....	18
2.4.1. Definition of Network Science .....	18
2.4.2. Small-World Networks.....	19
2.4.3. Scale-Free Networks.....	20
2.4.4. Applications of network science.....	21
2.5. Science of complexity .....	22
2.5.1. Definition of science of complexity .....	22
2.5.2. Branches of science of complexity .....	23
2.6. Recent Applications in Transportation Systems .....	24
2.7. Research ideas .....	33
3. THE BOX-COUNTING METHOD .....	35
3.1. Introduction .....	35



3.2.	The Box-Counting Method.....	36
3.3.	Investigating the validity of box-counting method.....	38
3.3.1.	Creation of the base network .....	39
3.3.2.	Creating fishnets .....	40
3.3.3.	Application of the box-counting method .....	42
3.4.	Analytical investigation.....	45
3.5.	Further rigorous mathematical induction .....	46
3.6.	Conclusions .....	48
4.	AREA, LINE, AND POINT THRESHOLDS .....	50
4.1.	Introduction .....	50
4.1.1.	Transportation Networks as Complex Systems .....	50
4.1.2.	Geometry of Transportation Networks .....	51
4.2	Methodology .....	53
4.2.1.	Geometric Information .....	53
4.2.2.	Grid Creation .....	56
4.2.3.	Geometric Equivalency .....	57
4.3.	Results and Discussion .....	60
4.4.	Conclusions .....	70
5.	THE RING-BUFFER METHOD .....	72
5.1.	Introduction .....	72
5.1.1.	Cities and Complexity .....	72
5.1.2.	Transportation Systems .....	73
5.2	Methodology .....	75
5.2.1.	Description of the ring-buffer approach .....	75
5.2.2.	Verification of Ring-Buffer Method for Fractal Analysis .....	78

5.2.3. Application of Ring-Buffer Method to Urban Road Networks .....	82
5.2.4. Coupled Complexity .....	85
5.2.5. Grid Equivalency .....	86
5.2.6. Verification of the Equivalent Grid .....	88
5.2.7. Revealing the Functional Form for the Ring Road Density .....	90
5.2.8. Deriving the Functional Form for the Total Toad Length $N$ .....	93
5.2.9. Calibration of the Formulation for the Total Toad Length $N$ .....	94
5.3. Results and Discussion .....	97
5.4. Conclusions .....	100
6. APPLICATIONS AND EXTENDED RESEARCH .....	104
6.1. People versus buildings: Characterization and Correlation .....	104
6.1.1. Introduction .....	104
6.1.2. Methodology .....	107
6.1.2.1. The Ring-Buffer Method .....	107
6.1.3. Application .....	107
6.1.3.1. Case Study: Chicago .....	107
6.1.4. Data .....	110
6.1.5. Results .....	111
6.1.6. Analysis .....	113
6.1.7. Discussion .....	115
6.1.8. Conclusion .....	116
6.2. Development and Application of the Pedestrian Environment Index (PEI) .....	118
6.2.1. Abstract .....	118
6.2.2. Introduction .....	119
6.2.3. Background .....	121
6.2.4. Methodology .....	128

6.2.4.1. Land-use Diversity Index (LDI) .....	128
6.2.4.2. Population Density Index (PDI).....	130
6.2.4.3. Commercial Density Index (CDI).....	131
6.2.4.4. Intersection Density Index (IDI) .....	132
6.2.4.5. Pedestrian Environment Index (PEI) .....	134
6.2.5. Notes on Area and Data Requirements.....	135
6.2.6. Case Study .....	136
6.2.6.1. Data Sources .....	137
6.2.6.2. Application.....	137
6.2.7. Results and Discussion .....	142
6.2.8. Conclusion .....	146
7. CONCLUSIONS.....	149
7.1. Introduction .....	149
7.2. Summary of the Achievements .....	152
7.3. Suggestions for Future Work .....	157
REFERENCES .....	159
APPENDICES .....	177
APPENDIX A: List of 50 U.S. Urban Systems Studied.....	178
APPENDIX B: Road Networks for 50 U.S. Urban Systems .....	183
APPENDIX C: Details of Grid Creation for Chicago MSA.....	197
APPENDIX D: Area, Point, and Line Thresholds for 50 U.S. Urban Road Networks .....	201
APPENDIX E: Density and Decay Indices for 50 U.S. Urban Road Networks .....	204
APPENDIX F: Characteristic Maps for 50 U.S. Urban Systems .....	207
APPENDIX G: Copyright Authorizations.....	258
VITA.....	261

## LIST OF TABLES

Table 1 Data sources .....	110
Table 2 Scaling properties of component densities .....	113
Table 3 Data Sources .....	137
Table 4 List of 50 U.S. urban systems studied .....	179
Table 5 Area, point, and line thresholds for 50 U.S. urban road systems.....	202
Table 6 Density and Decay Indices for 50 U.S. Urban Road Networks.....	205

## LIST OF FIGURES

Figure 1 Comparison of the growth of world's urban and rural population. ....	2
Figure 2 Research trend on “urban complexity”.....	3
Figure 3 Example of a simple system: a pendulum. ....	4
Figure 4 Example of a complicated system: an airplane. ....	5
Figure 5 Example of a complex system: a flock of birds .....	6
Figure 6 Characteristics of Complex Systems .....	7
Figure 7 U.S. Interstate highway system. ....	9
Figure 8 The Seven Bridges of Königsberg.....	15
Figure 9 Graph representation of the Königsberg Bridges problem.....	16
Figure 10 Comparison of different network types .....	20
Figure 11 Comparison of different transportation network structures with direct links versus the more-efficient fractal pattern .....	24
Figure 12 Street network in London, U.K. ....	25
Figure 13 The paradox of measuring the length of Britain's coastline.....	27
Figure 14 Application of box-counting method to Britain's coastline. ....	27
Figure 15 a) U.S. Population Dot Map and Light pollution at night in the U.S.. ....	28
Figure 16 Box-counting method .....	36
Figure 17 Patterns expected from box-counting results. ....	38
Figure 18 Steps taken for the creation of the base network. ....	39
Figure 19 The base network.....	40
Figure 20 Comparison of the effect of fishnet offset on the box counts.....	41
Figure 21 Box-counting results.....	42
Figure 22 Various Networks and their box-counting results. ....	44
Figure 23 Chicago MSA road network. ....	54
Figure 24 Comparison of the service area of the road system created by closed road polygons and the MSA area for the city of Las Vegas.....	55
Figure 25 Road polygons and 10x10 km grid network.....	56
Figure 26 Chicago road network and its equivalent grids with respect to area, road length, and number of intersections.....	58

Figure 27 Determining the three thresholds for Chicago MSA road network:.....	60
Figure 28 Area, Line, and Point thresholds within U.S. urban areas.....	62
Figure 29 Comparison of Phoenix and Chicago road polygons variations .....	63
Figure 30 Comparison of Salt Lake City and Chicago road length variations .....	64
Figure 31 Spatial Distributions of Area, line, and point thresholds for 50 U.S. urban areas. ....	65
Figure 32 Relationship between the area threshold and the age of the urban system. ....	66
Figure 33 Relationship between Population density and Line and Point thresholds.....	67
Figure 34 Relationship between the Average travel time for all modes and Total transit travel time and the Line threshold.....	68
Figure 35 Relationship between Walk time per capita and Point threshold. ....	69
Figure 36 Ring creation in the ring-buffer method. ....	76
Figure 37 Normal plot of the power law relationship.....	77
Figure 38 Log-log plot of the power law relationship. ....	77
Figure 39 Greek Cross grid with 1000 m cells created within Chicago MSA. ....	79
Figure 40 Examples of full and partial rings. ....	80
Figure 41 Log-log plots of buffer road length versus radius for different grid cell sizes.....	81
Figure 42 Road Density map for Chicago MSA road network, and the selected “center”.....	83
Figure 43 Log-log plot of buffer road length versus radius and power law fit for Chicago road network. ....	84
Figure 44 Buffer with radius $r$ around the center of the road network. ....	85
Figure 45 A portion of a uniform grid network with block size of $l$ . ....	87
Figure 46 Radially-varying equivalent grid network for Chicago MSA road network.....	89
Figure 47 Ring-buffer results for Chicago MSA road network and its equivalent grid. ....	89
Figure 48 Log-log plot of the inverse of the equivalent grid block size for Chicago, IL road network versus radius and the power law fit. ....	91
Figure 49 Log-log plot of the inverse of the equivalent grid block size for Chicago, IL road network versus radius and the exponential fit.....	91
Figure 50 Variation of the inverse of grid block size versus radius for Austin, TX with a power law fit. ....	92
Figure 51 Variation of the inverse of grid block size versus radius .....	93
Figure 52 Semi-log plot of buffer road density for Chicago, IL with an exponential fit.....	95

Figure 53 Semi-log plot of buffer road density for Austin, TX with a power law fit.....	96
Figure 54 Semi-log plot of Buffer Road Density for Los Angeles, CA with a logarithmic fit. ...	96
Figure 55 Spatial Distributions of the Density and Decay Indices.....	101
Figure 56 Location Map for Chicago, Illinois .....	108
Figure 57 The “Loop”, CBD of Chicago .....	109
Figure 58 Rings, splitting Chicago into rings from the center.....	109
Figure 59 Chosen urban components within equi-distance rings around the Center. ....	110
Figure 60 Plots of component densities vs. radius.....	111
Figure 61 Log-log plots of components densities vs. radius. ....	112
Figure 62 Correlation between Population+Employment and Gross Floor Area Densities .....	114
Figure 63 Examples of intersection equivalency factor values. ....	133
Figure 64 Comparison of zonal geometries. ....	138
Figure 65 Chicago sub-TAZ system. ....	139
Figure 66 Excluded and remaining areas.....	140
Figure 67 Extracted individual land uses.....	141
Figure 68 Street Network and Intersections.....	142
Figure 69 Spatial distributions of Land-use Diversity Index (LDI), Population Density Index (PDI), Commercial Density Index (CDI), and Intersection Density Index (IDI). ....	143
Figure 70 Spatial distribution of the Pedestrian Environment Index (PEI) .....	144

## SUMMARY

An urban system has a starting point when it has been founded, and from where it has spread into its current form. Previous research has suggested that no matter how an urban system has evolved, from a larger perspective it has inherent order and organization. As a result, cities are considered as complex systems consisting of many inter-related components and features. And similar to complex living organisms, they exhibit orderly characteristics that are lying beneath their physical forms.

In order to better understand the complex nature of an urban system, studies have been focused on the characterization of its components. A transportation network provides a window into the complex world of its encompassing urban system, because they have followed the same path during their evolution.

This work focuses on a better understanding of the complex geometric characteristics of urban road networks. It tries to develop novel methodologies to study and characterize them, which can in turn lead to a better understanding of their corresponding urban systems.

Along that line, this study develops new methodologies to characterize the complex geometry of urban road networks and develops new indicators representing their unique multi-dimensional characteristics. The study also succeeds in uncovering the coupled geometric complexity of road networks and offers a novel approach towards their characterization.



## **1. INTRODUCTION**

“The whole is greater than the sum of its parts.”

- Aristotle (384–322 BC)

### **1.1. The need to understand cities**

In her famous book, “The Death and Life of Great American Cities”, Jacobs (1961) raises the need for a better understanding of cities, best described as “evolving networks of relationships” (Batty, 2013a) that connect people together. She argues that it is not sufficient anymore to only study where things are located within a city. Instead, we need to focus on understanding how the inter-related and connected network of things within a city work together to evolve into something far more complex, hidden under the face of the urban environment that we see.

In the past, cities were conceptualized as systems that were in equilibrium, managed in a top-down fashion, and mostly unaffected by their wider surrounding environment. They could not experience any significant changes unless external stimuli disturbed this equilibrium. In

short, this view considered cities as “machines” that were manufactured and controlled by central brains, while their individual parts and members had no or little decision-making role in how they functioned. But empirical evidence suggests that the opposite is true. Cities are not only dynamic and thus in ever-changing and evolving state, the inter-city as well as intra-city interactions are becoming more and more profound, which in turn add to the bottom-up direction of their functionality.

Although cities can decline and even disappear, the current trend forecasts massive urbanization in the coming century with not only an increase in the number of cities but also in the size of cities, reaching new heights in population levels. The 20th century has seen the rise of mega metropolitan areas around the world. This phenomenon becomes more important as cities will continue to grow even faster in the future, both horizontally and vertically. As a result, now for the first time in the history of mankind more than half of the world’s population live in urban areas (United Nations, 2014). Figure 1 exhibits the growth rate of urban population, compared with rural population.

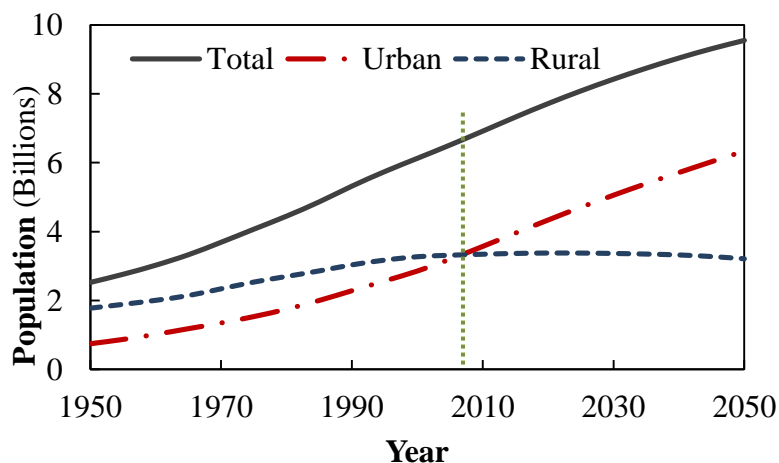


Figure 1 Comparison of the growth of world’s urban and rural population.  
adapted from (United Nations, 2014).

The growing trend in the expansion of urban areas and their populations has resulted in a rapid increase in research interest focused on understanding cities, how they function, and how seemingly-invisible driving forces shape their evolution. Thanks to this research, we now understand that the evolution of cities is the result of the collection of the interactions between their constituents, their responses to the changes in their environments, and the decisions made by their inhabitants. The fact that cities function as collectives that determine the evolutionary paths they follow has strengthened the idea of considering cities as “living” organisms and “complex” entities.

This, of course, does not mean that the process is unidirectional. Naturally the feedback effect and the action-reaction cycle persist. Nonetheless, it is important to know what the main players that affect their course of evolution are. For that reason, the angle from which cities are looked at and the approaches used to study and understand them has been improve to include the science of complexity. Figure 2 exhibits the research trend on the topic of “urban complexity”, showing that it has been gaining significant momentum since 1990s, and has been exponentially increasing ever since.

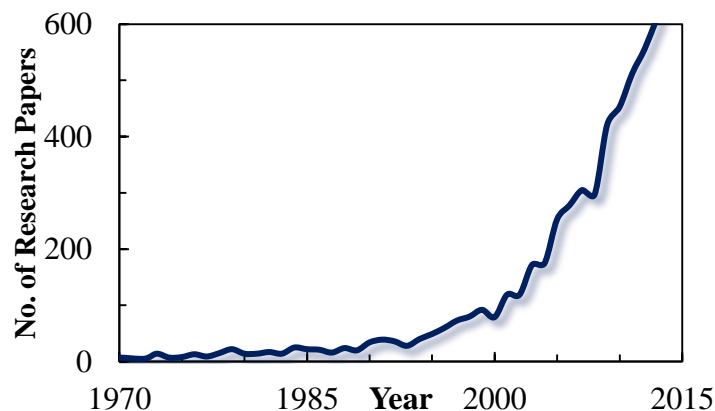


Figure 2 Research trend on “urban complexity” (Scopus, 2014).

## 1.2. Defining Complexity

Before going any further, it is desirable to define what “complexity” means. Different systems exhibit various properties at different levels with varying degrees of strength. From the complexity point of view, regardless, they can be categorized into the following three classes (Nicolis, 2012; Ollhoff, 2002; Wolfram, 2002):

### 1.2.1. Simple Systems

A simple system consists of a small number of components that work together according to well-understood principles. A good example is perhaps a pendulum (Figure 3), which is made of only a few parts. The behavior of such a system and its response to external forces can easily be described in terms of well-known Physics laws.

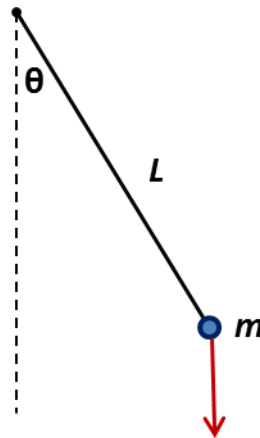


Figure 3 Example of a simple system: a pendulum.

### 1.2.2. Complicated Systems

In contrast, a complicated system is made of a large number of components, but still with well-defined roles and governed by well-understood rules. An example is an airplane that could have in the order of millions parts, which have to work together in order for it to fly and maneuver. This means that if a critical part is out of order, it can prevent the entire system from providing the expected service. For that reason, redundancy is normally built into the design of complicated systems to avoid system failure. Despite their complicated structure, however, they still follow the expected and known rules.



Figure 4 Example of a complicated system: an airplane.

### 1.2.3. Complex systems

Complex systems typically, though not necessarily, have a large number of components as well. The difference, however, is that they are “adaptive” and “self-organizing”. This means that their internal structures, as well as external appearances, are in constant change and transformation due to the fact that they are reactive to external stimuli and also the internal interactions between their components.

A good example of a complex system is a flock of birds (Figure 5) that is indeed a complex system, even though it consists of fewer and very similar components in contrast to an airplane. Not only the flock responds to changes in its environment, i.e., adaptive property (e.g., by changing direction), it self-organizes without the need for a leader to tell the rest of the flock what to do. This is revealed by observing the dynamic and ever-changing patterns generated by the birds as they adjust their flying formations during their flight. And it is this and other similar features of a complex system that also gives it robustness and resilience, since no single component is critical enough to cause a total system breakdown should it fail. In a flock of birds, it is the adaptability to the changing environment that matters and not its number of participating birds.



Figure 5 Example of a complex system: a flock of birds (robwolstenholme.co.uk, 2014)

#### 1.2.4. Definition of Complex Systems

There is no single definition of “complex systems” that is commonly agreed upon. The following definition, however, might serve the purpose:

“A complex system is a system with a large number of elements, building blocks or agents, capable of interacting with each other and with their environment. The interaction between elements may occur only with immediate neighbors or with distant ones; the agents can be all identical or different; they may move in space or occupy fixed positions, and can be in one of two states or of multiple states. The common characteristic of all complex systems is that they display organization without any external organizing principle being applied. The whole is much more than the sum of its parts.” (Dougherty, 2013)

The evolution of a system toward complexity consists of two basic phenomena: “juxtaposition and integration” (Chapouthier, 2009). Moreover, the pattern of interactions between components of a complex system creates a new level of order, which results in systematic feedbacks between cause and effect, in space or time.

The following diagram visualizes the characteristics of a typical complex system:

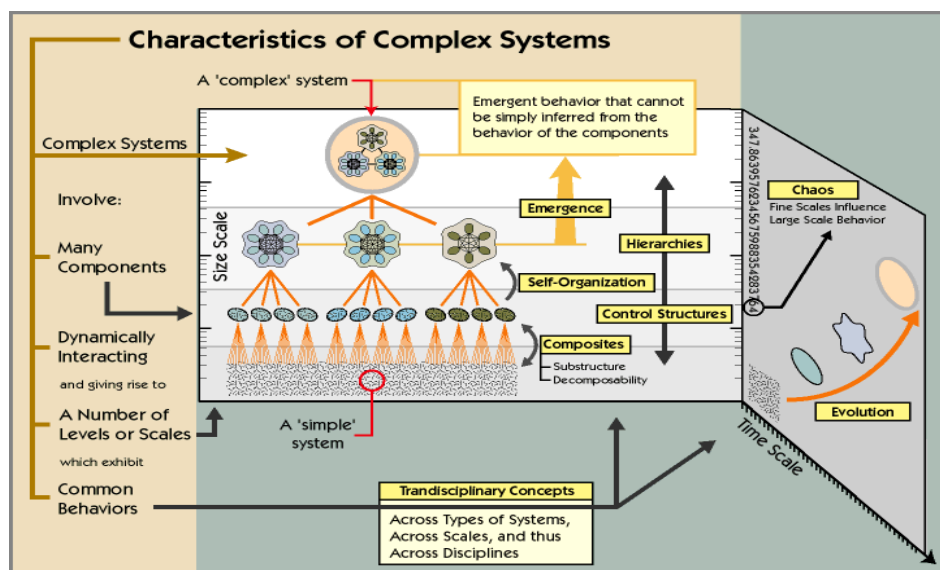


Figure 6 Characteristics of Complex Systems (www.necsi.edu)

### **1.3. Complex Urban Systems**

Urban systems can be defined as human settlement agglomerations with high population densities, which are characterized by the existence of a variety of components and infrastructure, such as: transportation networks, housing, utilities, ecological conditions, economic relations, social connections, cultural environments, and so on, all of which work together for the whole system to exist and evolve (Batty, 2005). Urban areas are the largest creation of mankind, helped with the opportunities and resources provided by nature.

Most urban areas have not had a coherent and well-designed plan from the beginning. Together with the impacts of nature and man, they have resulted in cities to be seen as a “loosely-organized” amalgamation of many components. However, urban systems are believed to possess an underlying order that links those components. To verify that hypothesis, the characteristics of such an order need to be captured and expressed in a more quantifiable form. Unfortunately, however, “there is no single paradigm that has come to dominate our understanding of cities” (Batty, 2013a). But that is the nature of complexity not to be confined by one perspective or to one definition or description.

Based on the definition and description provided, an urban system is a very good example of a complex system; it is made of a large number of components (including people), it is adaptable, i.e. reacts to and evolves in response to changing environment, it does not have a fixed and central decision maker that controls all its components, i.e. the course of its evolution is determined by the collective result of all the decisions made by its constituting elements. That



is why “to understand cities, we must simplify, we must abstract. We must dig below the surface of what we see and reveal the foundations of how cities function” (Batty, 2013a).

One approach taken towards such understanding of urban environments has been to find parallels between their characteristics and other natural-occurring phenomena. For example, cities and their geomorphologies have been compared to human systems and physical systems, respectively (Haggett and Chorley, 1969). Figure 7 shows the continental United States and its interstate highway system. Compare the country to a body, and the first thing that comes to one’s mind as an analogy for its highway system is the body’s circulatory system.

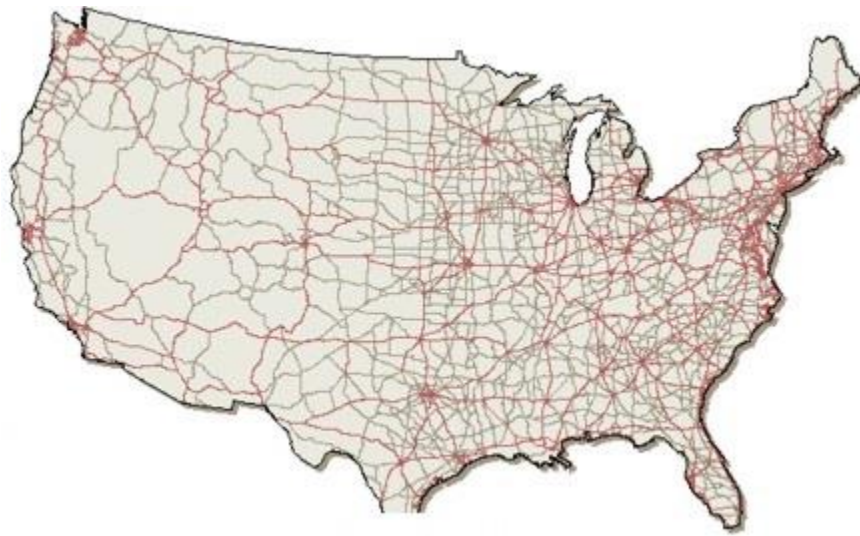


Figure 7 U.S. Interstate highway system.

Moreover, in another recent study on slime mold, Tero et al. (2010) demonstrated that by creating conditions similar to the ones on the ground in and around Tokyo, the slime mold grows and forms a network with similar patterns to that of the real Tokyo rail system.

There are many other examples where one can find similarities between a physical system and a biological one. These analogies enable us to utilize the methods used for, and the knowledge about, the biological systems towards a better understanding of cities (Samaniego and Moses, 2008a). The better we know how the urban system components work, the better we can use this knowledge to make cities more efficient, sustainable, and livable. Recent advances in “Complex Systems” concepts and methods have opened the door to the challenging and intriguing field of understanding cities as a joint complex creation of man and nature.

Having said that, one should note that a complete understanding of the complex nature of urban systems requires many fields of science, including, but not limited to: civil engineering, transportation theory, network science, system engineering, urban geography, regional science, social physics, urban economics, etc. (Batty, 2013a).

While a number of researchers have studied cities as non-spatial networks and processes, the science of evolution of cities is mostly focused on physical form of the urban systems. To better understand how cities function, we need to think of them as the space within which people connect and interact. Such interactions happen through physical as well as virtual networks, by which exchange of goods, money, service, and information occur between people. Based on this picture, characterizing those networks will be the first step towards understanding the complex nature of cities and urban systems.

At the core of this dissertation, the rationale for attempting to characterize transportation networks as the window to the complex nature of urban systems is simply that in order to “understand place, we must understand flows, and to understand flows we must understand

networks” (Batty, 2013a). Having said that, it is fair to say that the transportation system within an urban environment is considered as the main network that facilitates the interactions that occur continuously, something which is the driving forces behind the gradual evolution of its encompassing urban system.

The importance of the transportation network in a city comes from the fact that it facilitates not only the movements of people and goods, but also the social and economic livelihood and functionality of that urban system. Transportation networks are practically spatial networks that are usually, but not always, planar, within which the road network is understandably the largest and perhaps the most important element. When looking at the map of an urban road network, the first thing that catches one’s eyes is its geometry that is shaped by the locations of its intersections and the road segments that connect them.

A comparison of road systems in different cities with one another points to the fact that they have similar characteristics, many of which have been explored through prior studies. Among them, researchers have always been looking for properties that are universal and that can summarize and represent networks of different shapes with simple and general indicators, such as the “scaling” property that is said to be the signature of natural evolution. This is in fact a very important and fundamental property, because it supports the idea that cities are indeed like organisms, and thus their evolution follows a trend that we also observe in nature.

“Scaling” property represents the self-similarity and replication of similar forms at different scales within an entity such as a transportation network. Indeed, the resemblance of road networks in an urban system to circulatory system in the human body is an indicator of the

existence of this property, which can be studied in order to extract the universal characteristics of these systems. For that reason, geometric analysis of road networks is the main focus of this study, in which not only are the current available methods studied in depth, but new approaches are also developed and applied.

This work focuses on a small corner of this area of science and that is the geometry of urban road systems. What makes this goal realistic is the intrinsic similar properties we see in the road networks all around the world, and the fact that even though they do not look exactly the same, they still show similar patterns and order in terms of shape and size, and potentially other hidden characteristics that we are yet to discover. Along this line of thought, the main aspiration behind this study is **“to develop novel methodologies to study and characterize the complex geometry of urban road networks, which can in turn lead to a better understanding of their encompassing urban systems.”**

More specifically, this study attempts to achieve the following detailed objectives:

- **Review the history of the methods used for geometric analysis of urban road systems from a complexity point of view,**
- **Investigate the validity of the box-counting method, as the traditionally dominant method of choice, for capturing the complex nature of road networks,**
- **Explore the information that can be extracted from the outputs of the application of box-counting method, and define new metrics,**
- **Propose different methods to analyze the geometrical properties of urban road networks,**

- **Develop new methodologies to characterize the complex geometry of road systems,**
- **Explore other relevant areas of study toward a better understanding and classification of urban environments.**

Achieving the above objectives requires collection and processing of large amounts of spatial data for a large number of urban road networks with various geographical, topological, morphological, ecological, and demographic conditions. This makes performing repetitive steps a necessity in order for detailed analysis of those urban systems, and hence requires the use of proper and powerful tools. Geographic Information Systems (GIS) provide the tools that can be used with efficiency, accuracy, and speed for the analysis, comparison, replication, verification, and visualization of spatial data. Moreover, they facilitate the automation of the whole process, thus avoiding manual repetition of identical steps for different urban systems. This provides the opportunity for more detailed and in-depth analyses of the collected spatial data toward testing the relevant hypotheses, both old and new, about the complex nature of urban road networks. This study will utilize the powerful technology of GIS throughout the analyses performed in order to ensure the reliability and accuracy of the results.

This dissertation is organized in the following order. Chapter 2 presents an extensive review of the existing literature that attempts to characterize urban road networks, and specifically their complex nature. In chapter 3, a critical review of the box-counting method, which has traditionally been the method of choice for the analyses of road network patterns, is presented, concluding with the invalidation of that method for physical networks. Chapter 4

includes a novel methodology for using the outputs of the application of the box-counting method to urban road networks. That leads to the definition of three area, line, and point thresholds as representative characteristics of the complexity of urban road networks. Chapter 5 focuses on the development and application of a proposed ring-buffer method, through which the intrinsic mixed complexity of urban road networks is unraveled. The discussion then leads to a new set of characteristic models for urban road networks, along with the definition of two more parameters; density and rate of decay indices. Chapter 6 presents an expansion of the idea developed in Chapter 5 to other components of urban systems, followed by another related work within the realm of transportation planning that defines a new pedestrian environment index by using characteristics of various urban system components. A brief conclusion follows in Chapter 7, which summarizes the contributions of this research, as well as ideas and a layout for relevant future work. Following the References, Appendix A presents a collection of related information about the 50 U.S. cities that were studied during the course of this research, while Appendix D provides a tabular summary of the results and indices for the same cities.

## 2. LITERATURE REVIEW

### 2.1. The origin

There is no clear date as to when methodological analysis of road networks started. One of the earliest works that used a scientific approach to approach a route-based problem is that of the Swiss mathematician Leonhard Euler (Euler, 1741). The challenge brought to him was related to the city of Königsberg in then Prussia, now city of Kaliningrad in Russia. The city was split by the Pregel River into four areas with seven bridges connecting them, as shown in Figure 8 (Preussen Chronik, 2013).

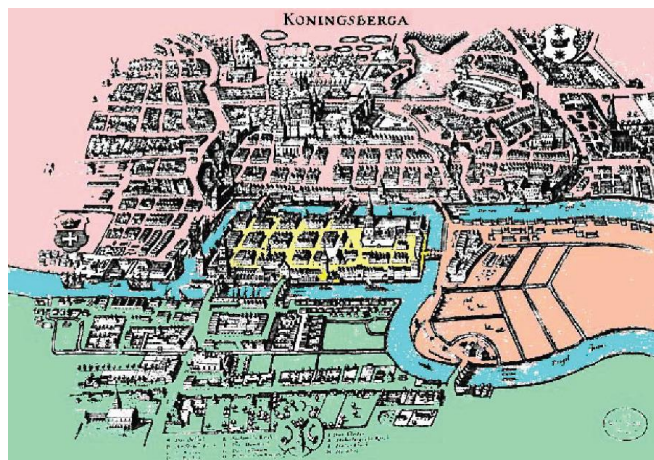


Figure 8 The Seven Bridges of Königsberg.

The question put forward to him was if it were possible to visit every part of the city but in a way that each bridge was crossed once and only once. Euler showed that the problem had no solution. In doing so, however, he faced the difficult task of devising a sound technique to approach the problem in a scientific way, and that is when he came up with a graph representation of the problem and used it to answer the question. Figure 9 presents an idealized representation of the routes network in that problem (Königsberg, 2013).

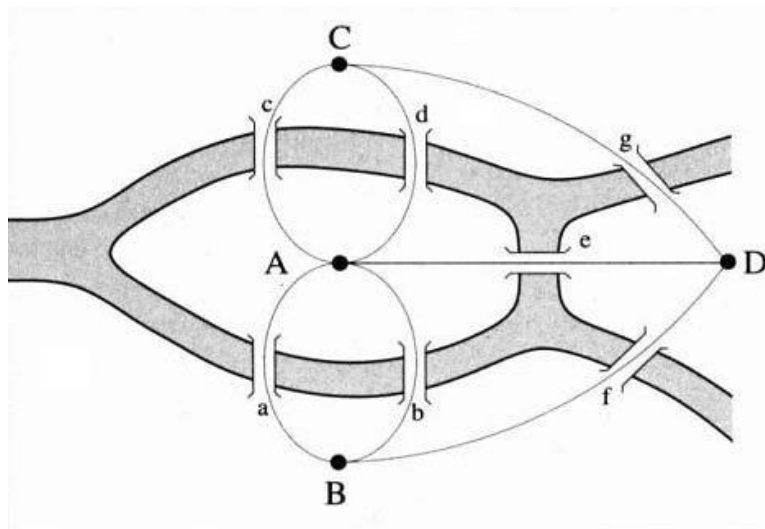


Figure 9 Graph representation of the Königsberg Bridges problem.

The approach used by Euler started Graph Theory as a new branch of science, and that opened the way for a tremendous amount of research in the centuries that followed. The methodologies used, understandably, improved over time to include modern graph theory, which evolved into network science that is a main method used in the science of complexity.



## **2.2. Definition of a network**

There are a variety of definitions for networks that vary based on the field they are used in. For the purpose of this research, the following concise definition is preferred:

“A network is a collection of nodes (or vertices) joined by links (or edges).” (Derrible, 2010)

## **2.3. Network indicators**

After its emergence, graph theory gradually found applications in the analysis of transportation systems. One of the early pioneers in this area was Garrison (1960), who introduced some descriptive approaches based on graph theory, while pointing to the fact that the application of graph theory provides the opportunity to study the whole system as one entity, or alternatively focus on individual parts while being still considered as the members of the system. Berge (1962) defined the first index for expressing the number of loops in a network, which in a way represents “robustness” of a network, because loops practically provide alternative routes. As a result, this index has been widely used ever since in conjunction with other indices developed later. Avondo Bodino (1962) used some indicators that were developed based on graph theory and applied them to road networks. It was, however, Garrison and Marble (1962) who revolutionized this field by defining three new network indicators and using them to describe the structural characteristics of transportation systems. The indices they defined represented the cyclicity, redundancy, and connectivity of the network.

Around the same time, Kansky (1963) did a study on transportation systems, in which he attempted to correlate the structural properties of road networks within an urban area to the regional characteristics of that area, especially its economic characteristics. In doing so, he defined four indices, each capturing a relevant aspect of transportation networks. They represented the average edge length, spread, average flow per node, and distribution of the network.

## **2.4. Network Science**

The review of the literature will now focus on the evolved form of graph theory, i.e. network science, for which the following definition is selected.

### **2.4.1. Definition of Network Science**

There are various definitions for Network Science, among which the following official definition presents a proper description:

"The study of network representations of physical, biological, and social phenomena leading to predictive models of these phenomena." (NCHRP, National Research Council, 2010)

Roads and highways, power transmission lines, water and wastewater networks, and other similar physical infrastructure possess network appearance. It is easily understood, therefore, that network science is a proper method to study their network aspects. One should

know, however, that network science can also be utilized to analyze many other non-classic networks that exist hidden within complex systems, and/or with no physical form, such as financial networks, epidemics, the World Wide Web, or social networks to name a few. The usefulness of network science is that it makes it easier to “identify general patterns present in a system without getting into the details of the system specificities” (Derrible, 2010).

Network science first emerged by an original works on random graphs by Erdős and Rényi (1959, 1961). But it did not as much attention until the publication of the work by Watts and Strogatz (1998), in which they introduced the idea of small-world networks. The year after saw another major article, by Barabasi and Albert (1999), presenting new ideas about scale-free networks. Those two papers revolutionized network science and gave it a momentum that has lasted to date. To better understand their works, the following definitions are presented.

#### 2.4.2. Small-World Networks

A small-world network is one in which most nodes are connected to both their immediate as well as distant neighbors, in a way that most nodes can be reached from every other by a small number of steps. Social networks are good examples of small-world networks, because two seemingly complete strangers can get acquainted through a small number of intermediary friends. Figure 10 shows network variations (Watts, 2003, Watts and Strogatz, 1998).

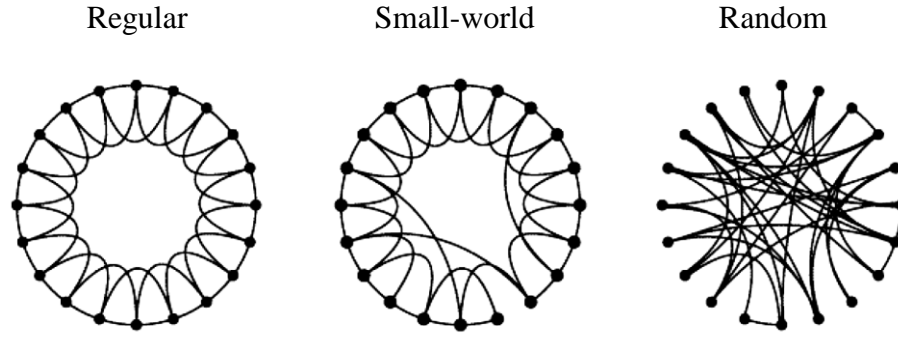


Figure 10 Comparison of different network types

In a small-world network, the number of steps between two randomly-chosen nodes, also called their distance, is proportional to the logarithm of the number of nodes in the network (Watts and Strogatz, 1998), i.e.:

$$L \sim \log(N) \quad \text{Eq. 2.1}$$

in which:

$L$  = the distance between the two nodes

$N$  = the number of nodes in the network

#### 2.4.3. Scale-Free Networks

Scale-free networks are the ones whose number of nodal connections follows a power law (Barabasi and Albert, 1999). In other words, the probability that a node in the network has a given number of connections to the other nodes is:

$$p(k) \sim k^{-\gamma} \quad \text{Eq. 2.2}$$

in which:

$p(k)$  = probability of the node having  $k$  connections, which is in the form of a power law,

$\gamma$  = scaling factor

As a result, in a scale-free network, there are few nodes that have many links, while at the same time there are many nodes that only have a few links (Barabasi and Albert 1999), which is a signature property of power law. A good example of a scale-free network is the World Wide Web.

#### 2.4.4. Applications of network science

The groundbreaking ideas discussed in the previous parts resulted in an explosion of the applications of network science in many different areas; from physics to virtual networks to sociology to financial markets to social networks to epidemiology to ecology, and more, the majority of which are out of the scope of this research, especially for the fact that the work presented here does not explicitly use a network science approach.

An example of the application of network science to transportation systems is the work done by Derrible and Kennedy (2011), in which he employed the fundamentals of networks science towards characterization of urban subway systems. During the process, he not only used the indicators developed before, but also defined new relevant indicators of his own for subway systems. Combined together, he was able to extract information from his findings that could be used for proper classification and thus better design of metro systems.

## **2.5. Science of complexity**

Science of complexity is much broader, and in some aspects older (Alexander, 1964; Simon, 1965), than network science that now is considered as a subset of it. Complexity science offers a variety of methods for analyzing and characterizing complex systems, some of which cannot be studied by network science.

### **2.5.1. Definition of science of complexity**

Despite its recent popularity, there is still no single definition that everybody agrees upon. Among the descriptions offered, the following offers an adequate definition:

“Complexity is a system in which large networks of components with no central control and simple rules of operation give rise to complex collective behavior, sophisticated information processing, and adaptation via learning or evolution” (Mitchell, 2009).

At the same time, one should also note that complexity science is not “general systems theory, or a postmodern science, or a set of metaphors or analogies based on resemblance thinking” (Phelan, 2001).

Therefore, the main characteristics of a complex system that differentiate it from other systems are: being “adaptive” and exhibiting nontrivial “emergent” and “self-organizing” behavior. In a complex system, not only the components perform their individual tasks, but also

together they work as a collective that functions as a whole. That is when the famous phrase of Aristotle, “The whole is greater than the sum of its parts”, finds its place.

A proper example of a complex system is an urban system, which is composed of many components, working together to change and evolve their encompassing system endlessly. Interestingly enough, many of those components are complex systems in their own realm and deserve their own proper analysis. Transportation network within an urban system is a good example, as it possesses its own complex nature that needs to be investigated and understood, something which is the main focus of this research.

#### 2.5.2. Branches of science of complexity

In addition to network science, there are many other areas of knowledge that fall under complexity science’s umbrella. Examples are chaos theory, fractals, self-organization, cellular automata, nonlinear dynamics, percolation models, feedback control, machine learning, information theory, statistical mechanics, game theory, evolutionary design, population genetics, artificial life, simulation modelling, autonomous computing, and so on so forth.

The research presented in this work was originally inspired by the signs of the presence of fractal properties in transportation systems. The objective was to incorporate that idea into a better understanding of urban road networks, which lead to studying their complex geometrical characteristics. For that reason, the rest of this literature review will mostly cover the studies on fractal and geometric properties of transportation networks, although it will occasionally include relevant works that have used other approaches.

## 2.6. Recent Applications in Transportation Systems

Michael Batty, one of the pioneers of promoting complexity as the new science of cities, proposes an example that explains how the transportation network in a city could grow to be similar to fractals. Assume that there are 16 locations within a city, positioned around a circle, as shown in Figure 11a (Batty, 2008a). The goal is to transport goods from a central location (the center of the circle) to the other 16 locations in the most efficient way, i.e. while minimizing the transport costs.

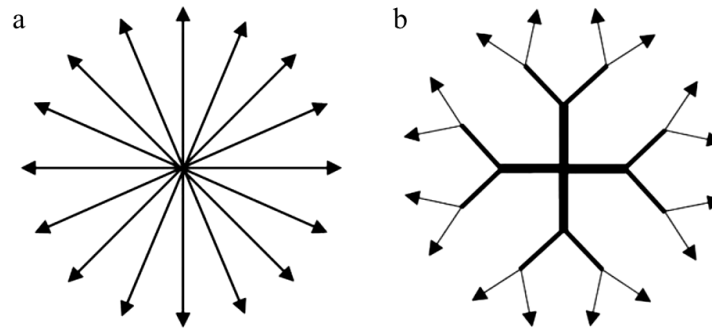


Figure 11 Comparison of different transportation network structures  
a) direct links, versus b) the more-efficient fractal pattern.

Even though the network shown in Figure 11a is a simple and feasible solution, it is not an efficient one. In comparison, it can be shown that the network presented in Figure 11b (Batty, 2008a), which shows fractal properties, demonstrated by its recursive branching pattern, requires between  $\frac{1}{4}$  to  $\frac{1}{2}$  less road length, depending on the way it is created. The difference is due to the characteristic of fractal entities, which by nature try to create efficient forms that produce the



most by using the least while adapting to the constraints imposed on them yet still achieving their objectives.

It is understood that during the evolution of an urban system, the interference by man and nature at different points in time results in an irregularly and randomly structured transportation network, but the argument still stands. Moreover, one should note that transportation networks exhibit a more complex recursive pattern than what is shown in Figure 11, because they include loops or branch-joining due to the fact that it makes them robust and more resilient towards disruptions.

Having said that, Figure 12 demonstrates a representation of the street network in London, U.K. (Batty, 2013a), in which the coloring is based on the link traffic volumes, with red being the most congested.

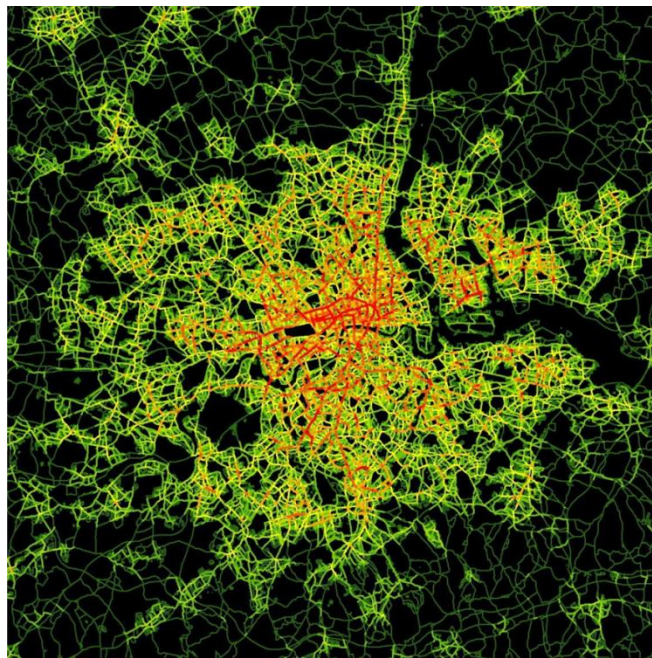


Figure 12 Street network in London, U.K.

With the above analogy in mind, we now present a summary of the literature on fractal and complex properties of urban systems and their transportation networks.

It was Benoit B. Mandelbrot who first brought up the complexity of physical forms. He used coastal lines as examples in which fractal nature translates into complex properties. He put forward a challenge that has amazed many ever since: “How long is the coast of Britain?” Mandelbrot (1967). In his words the answer was:

“Geographical curves are so involved in their detail that their lengths are often infinite or, rather, undefinable. However, many are statistically "self-similar," meaning that each portion can be considered a reduced-scale image of the whole. In that case, the degree of complication can be described by a quantity  $D$  that has many properties of a "dimension," though it is fractional; that is, it exceeds the value unity associated with the ordinary, rectifiable, curves” Mandelbrot (1967).

In short, it is impossible to measure the length of a coastline with 100% accuracy, because no matter how much the measurement precision is increased, there are still smaller details that are missed during the measurement. Figure 13 shows a demonstration of the above statement, in which the shorter the ruler used to measure the coastline, the longer the total length will be. And since the ruler size can hypothetically get infinitely small, the length of the coastline can get infinitely large accordingly. As a result, the total length remains undefined.

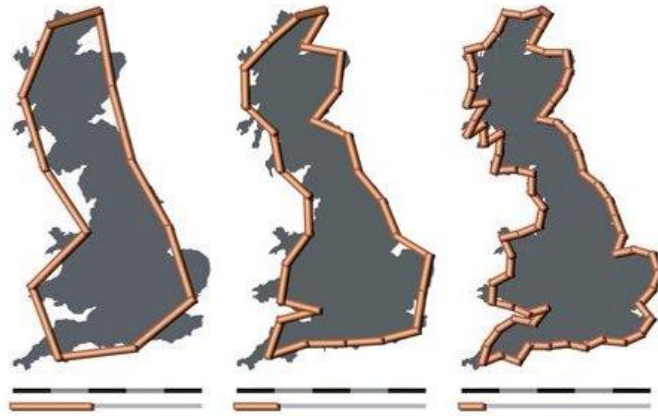


Figure 13 The paradox of measuring the length of Britain's coastline (Wikipedia, 2014a).

Instead of using a ruler, some have used box-counting method to highlight the challenge in measuring the length of a coastline. Due to the relevance of box-counting method to our future discussion, Figure 14 is presented here to demonstrate the application of box counting to the same problem.

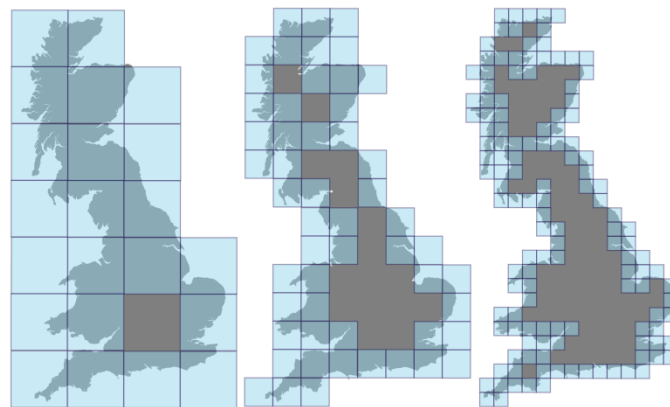


Figure 14 Application of box-counting method to Britain's coastline (Wikimedia, 2014).

Mandelbrot's introduction of fractals through his publications, e.g. (Mandelbrot, 2004, 1977; Mandelbrot et al., 1998; Mandelbrot and Blumen, 1989), has fascinated the scientific world to date. His theory of fractals opened the door to numerous studies in the area of physical sciences.

The 1980's started to see applications of fractal geometry to physical features, e.g. geographical features (Goodchild, 1980), landscapes (Burrough, 1981), coastal lines (Burrough, 1984), and geographic surfaces (Goodchild and Mark, 1987), etc.. But it was Batty (1985) who first highlighted the fractal properties of urban forms. That idea was followed by a flood of articles, each trying to focus on a component of urban systems and show that fractal properties exist in every corner of a city (Barthélemy and Flammini, 2009; Batty, 2013a, 2008a, 2008b, 2005; Batty et al., 2008, 1989; Batty and Longley, 1987a, 1987b, 1986; Bettencourt et al., 2010; Chen, 2011; Chen and Zhou, 2004; Frankhauser, 1998a, 1998b; Milne, 1988; Shen, 2002; Tannier et al., 2012). Figure 15 presents fractal similarities between two urban features.

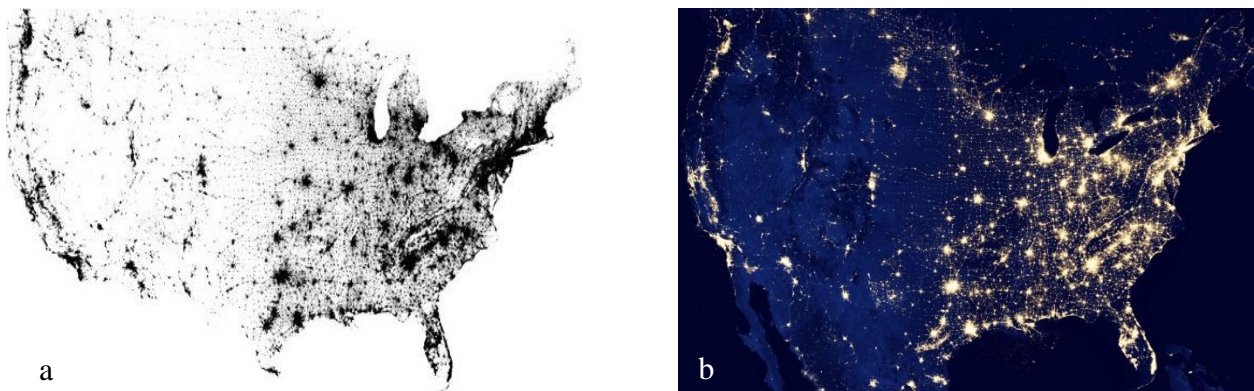


Figure 15 a) U.S. Population Dot Map (theatlanticcities.com),  
b) Light pollution at night in the U.S. (nasa.gov).

In parallel with studies on general characteristics of urban systems, some researches started to focus on the fractal applications in transportation networks. Benguigui and Daoud (1991), Benguigui (1992), and Benguigui (1995) did a series of studies on the subway systems in a few European cities including Paris using fractal methods. The public transportation system in Paris is composed of two networks. One is the metropolitan system that serves the city of Paris itself. The other one, being the suburban system, provides service to the suburbs of Paris. By counting the number of stations, they showed that a naïve analysis using power law property resulted in the conclusion that both networks were fractal. Through further analysis, however, they showed that despite initial observation, the metropolitan network is really not a fractal, and it is only the suburban network that does have fractal properties. They also devised a method for generating networks which were analogous to the real ones, further analysis of which confirmed their findings. The importance of that work was mainly because of the fact it demonstrated that following some rules blindly can result in erroneous conclusions, especially when it comes to complex geometries of transportation systems. Hence, one should always exercise engineering judgment in applying the method and also evaluating the results.

Using a qualitative approach based on length-area relationship, (Rodin and Rodina, 2000) investigated the existence of fractal properties in different parts of Tokyo's street network, which is famous for its old maze-fashion geometrical base structure. While their conclusion was that their study revealed signs of fractal properties, they admitted that the margin of errors in the results were high. Nonetheless, they made an interesting observation, unnoticed by many researchers, that the studies performed on road networks routinely ignores the presence of

topography that can potentially have profound impact on road length calculations, especially in mountainous urban areas. While agreeing with this observation in principle, we have to admit that topographic information are usually either not easily available, or are not accurate enough to be combined with horizontal distance measurements for road length recalculations.

Shen (2002) used box-counting method to find the fractal dimension for 20 large American urban areas. Since the objects under study were areas and not boundaries or road networks, he used pixel-based (raster) maps of the selected cities. He then plotted the results versus the total area as well as total population of the corresponding urban systems. The results showed that while the fractal dimension of a city is correlated with its area, it cannot explain the population variations throughout the urban system. Moreover, the results of the analyses were very dependent on the resolution of the maps used.

Kim et al. (2003) studied the properties of Seoul's surface rail and subway lines, for which they used the data collected for several time periods. They employed a combination of box-counting method along with radial measurement. By comparing the calculations for the line lengths for the two systems, they concluded that both exhibit fractal properties that are very close, meaning that they both have similar structures. Moreover, their time analyses showed that the fractal dimensions of the public transportation system had increased every time new lines were added. In addition to that, they used the radially-counted number of stations to show that they also possess fractal nature. By comparing the two sets of results, they showed that the public transport system of Seoul has a smaller fractal dimension than its stations. While their comparative conclusions could be usable, the individual results are not reliable because the

output plots did not exhibit acceptable linear patterns, and thus they could not support the conclusion that the two components of the urban system were indeed fractals.

Tang (2003) used a fractal growth approach to study the relationship between the population and road network in Bexar County urban area, TX. The study showed that there was an acceptable linear relationship, based on the statistics provided, between the above two parameters, and thus they concluded that the fractal approach used was valid. The methodology employed, however, was flawed (as will be shown in the next chapters), because even though the study claimed that the two parameters followed power law (the signature of fractal properties), the diagrams provided visibly contradict that claim, thus refuting the methodology.

Legrand et al. (2004) studied several road profiles in France using wavelet fractal approach. Their finding was that road profiles do show fractal properties. They also investigated the correlation between the fractal characteristics of the road profiles and their corresponding friction coefficients. While no significant correlation was found between the two using the same method, they found that there is a significant correlation between the friction factors and “Pointwise Holder Exponent” of the local fractal characteristics of the road profiles that were studies. The latter finding, however, is questionable because fractal properties of road profiles depend on their geometries while friction coefficients are properties of the materials used in the road surface construction, and the two are not related.

Based on the data collected for the road networks in and around Dallas-Fort Worth, TX, metropolitan area, Lu and Tang (2004) used a revised box-counting method to study the relationship between fractal dimension and population size as an indicator of the urban growth.

Their results showed that there was an exponential relationship between the two variables. As they noticed, however, the results from the application of the box-counting method showed some problems that they attributed to the fact that the method uses discrete observations to derive a continuous property.

Doménech (2009) employed a power law approach related to both fractals as well as small worlds to study the data collected over a long period of time for London, Paris, and Madrid metros, as well as Madrid and Valencia tramways. He concluded that the metro and tramway systems studied were basically identical with respect to topology, in a way that their total length and also total number of stations variations with respect to the total population show a small-world characteristic that further transform into fractal behavior. Once again, however, the diagrams he produced using the data do not really exhibit power law trends that can be considered significant. Moreover, he used the total populations for his analysis, and not the populations that are served by the metro or tramway, a weakness that he himself admits but justifies based on the lack of data.

Using the road network data for the city of Dalian, China; Sun et al. (2012) investigated the fractal pattern of urban road networks by employing an improved version of box-counting method. They showed that their proposed method was able to capture the heterogeneity of the road network at various locations. Due to the fact that their log-log plots of the results did not confirm a significantly linear relationship, as well as based on our findings to be presented in the next chapter, their overall methodology is under question.



There have been numerous other studies that have looked at urban road networks from various angles and through focusing on their non-geometric characteristics (Buckwalter, 2001; Gülgen and Gökgöz, 2011; Jiang, 2007; Jiang and Claramunt, 2004; Kalapala et al., 2006; Lämmer et al., 2006; Levinson, 2012, 2007; Levinson et al., 2012; Levinson and Yerra, 2006; Louf et al., 2014, 2013; Samaniego and Moses, 2008a; Strano et al., 2012; Sundquist et al., 2011; Xie and Levinson, 2009a, 2009b, 2007, 2011; Yamins et al., 2003; Yerra and Levinson, 2005; Zhang and Li, 2011; Zhang and Levinson, 2004). Even though those studies are not directly related to the subject matter of this research, the reader is encouraged to browse through them for general information.

## **2.7. Research ideas**

As mentioned before, the work presented here was inspired by observing signs of fractal properties in urban road networks, which was influenced by some of the works mentioned in the review of the literature.

At first, the research idea was to employ the box-counting method by applying it to selected urban road networks and then try to see what new information could be extracted from the results. As we will see in the next chapter, however, the study ended up with rejecting the box-counting method as being able to capture the fractal properties, if any, of transportation networks, or in general physical networks. This changed the course of the research toward a new direction, including devising a new method to do the job, the outcomes of which will be presented in the next chapters.

As the research progressed, moreover, it gradually became clear that the complexity observed in transportation systems is not a simple complexity (power law, which means fractal nature), but a coupled complexity. The new finding presented a challenge as how to decouple this mixed complexity and uncover the true nature of urban road networks.

### **3. THE BOX-COUNTING METHOD**

#### **3.1. Introduction**

With the emergence of complexity theory, numerous studies have focused on studying the characteristics of physical systems that show “scaling” properties, which essentially means they are fractal in nature (Hastings, 1993; Batty and Longley, 1994; Czegledy and Katz, 1995; West, 1999; Batty, 2005). A fractal can be described as an entity that possesses self-similarity on all scales. It is important to note that a fractal only needs to exhibit a similar type of, but not necessarily exactly the same, structure at all scales. Moreover, according to Mandelbrot (2004): "A fractal set is one for which the fractal dimension strictly exceeds the topological dimension." In practice, this means that while a line feature has a dimension of one in classical geometry, it must have a fractal dimension larger than 1 (but no more than 2) if it is to have fractal properties.

Among the methods used, box-counting method has traditionally been the method of choice, especially for physical urban infrastructures, and more specifically the road networks. As a result, a large number of those studies have used box-counting method for analyzing the features under study in order to show that they have complex nature, and if so, extract the

relevant metrics (Ahammer and Mayrhofer-Reinhartshuber, 2012; Han and Lu, 2008; Karperien et al., 2008; Li et al., 2009; Song et al., 2007; Zheng, 2010).

This chapter will investigate the validity of the box-counting method for studying and confirming the nature of physical fractal features, i.e. if it is capable of revealing a power law trend based on its outputs. Along this way, we first apply the box-counting method to several well-known fractal features and make in-depth observation of the results. Then we follow an analytical approach to verify our conclusions made in the previous part, followed by a more rigorous mathematical analysis of the subject matter to support our conclusion further.

### 3.2. The Box-Counting Method

The box-counting method has been proposed and applied based on the idea that in a self-similar system one should be able to find parts at different scales that demonstrate similar patterns. To capture this characteristic, box-counting method is applied via the following steps (Burduk et al., 2011; Song et al., 2007), which are also demonstrated in Figure 16 (Biehl, 2008).

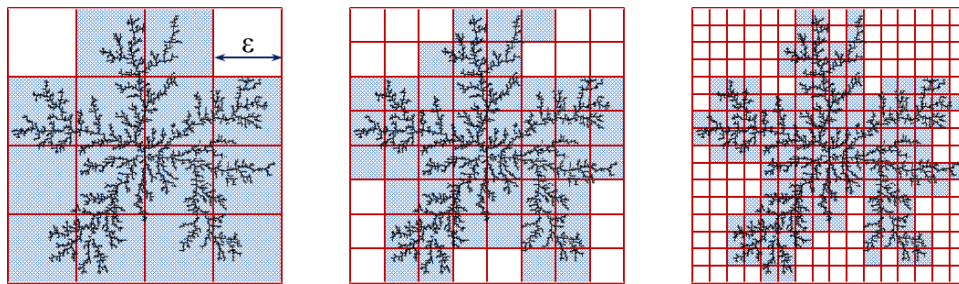


Figure 16 Box-counting method.

- i. A fishnet/mesh consisting of squares with size  $\varepsilon$ , large enough to cover the whole feature, is created,
- ii. The number of non-empty boxes overlaying the feature ( $N$ ) is counted,
- iii. Size of the squares ( $\varepsilon$ ) in the original fishnet are halved, i.e. each square is split into four smaller squares,
- iv. The number of new non-empty boxes overlaying the feature is again counted,
- v. The process is repeated until the size of the squares become too small for practical purposes.

For a fractal entity, the relationship between the number of non-empty squares or boxes ( $N$ ) and the inverse of the size of squares ( $1/\varepsilon$ ) is supposed to fit a power law (Schroeder, 1991; Voss, 1987; Iannaccone and Khokha, 1996), as shown in Eq. 1 and illustrated in Figure 17a. This property comes from the definition of fractals. As a result, if the diagram is plotted in a log-log format instead, a linear graph is expected to appear, as shown in Eq. 3.2 and also in Figure 17b.

$$N \sim (1/\varepsilon)^D \quad \text{Eq. 3.1}$$

$$\log(N) \sim D \log(1/\varepsilon) \quad \text{Eq. 3.2}$$

There are different methods proposed for verifying the linearity of the fit in the log-log plot, for which the reader is referred to Clauset et al. (2009). Once the log-log plot shows a linear trend, it is regarded as a proof of the fractal properties.

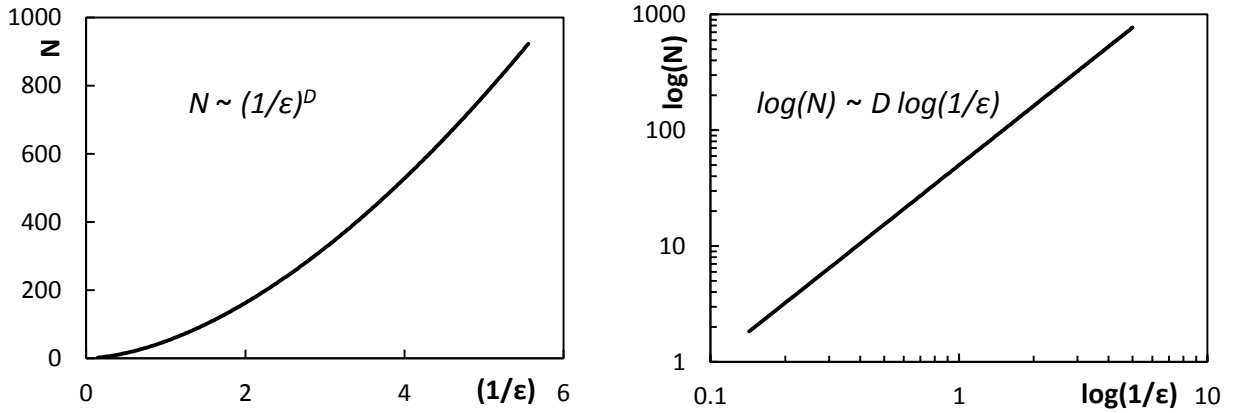


Figure 17 Patterns expected from box-counting results.

a) Normal plot with power law pattern

b) Log-log plot with linear pattern

For practical purposes, the slope of the fit line is then extracted and used as the fractal dimension of the feature, i.e.:

$$\text{Fractal Dimension} = D = -(\text{Slope of the linear fit}) \quad \text{Eq. 3.3}$$

Mathematically, however, the fractal dimension is defined as:

$$\text{Fractal Dimension} = D = \lim_{\epsilon \rightarrow 0} \left( \frac{\log(N)}{\log(1/\epsilon)} \right) \quad \text{Eq. 3.4}$$

Eq. 3.4 means that in fact it is the asymptotical slope, and not the average slope, of the log-log plot that is equal to the fractal dimension.

### 3.3. Investigating the validity of box-counting method

As mentioned before, after applying the box-counting method, traditionally a line is fitted to the log-log plot of the box counts, assuming that the line represents a power-law behavior, and then the slope of the lines is extracted as the fractal dimension of the feature being studied. The

objective of this work is to investigate the ability of the box-counting method to capture the characteristics of fractal networks. This investigation is especially pertinent considering the resurgence of studies on fractal systems, supported by the availability of new and large amounts of data along with increasing computational power.

### 3.3.1. Creation of the base network

To start with, a fractal network (hereafter referred to as the base network) of 5120 m x 5120 m consisting of 160 m x 160 m blocks was created, as shown in Figure 18. To create fractal properties, the network was generated by starting with the outside square (i.e. the largest block). Next, each side was split in two halves, and then two lines equal to one half was drawn perpendicular to that side at its middle point. Practically this means that the middle points of the opposite sides were connected, resulting in four smaller squares, each a quarter size of the original square. In Figure 18, we demonstrate the first few steps of creating the base network.

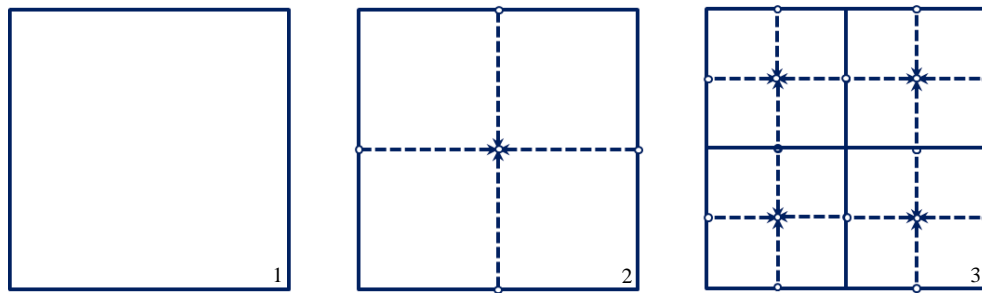


Figure 18 Steps taken for the creation of the base network.

The final base network consisted of  $2^5 \times 2^5$  (i.e. a total of 1024) squares of 160 m x 160 m as shown in Figure 19. This geometry is in fact a variant of the well-known Greek Cross.

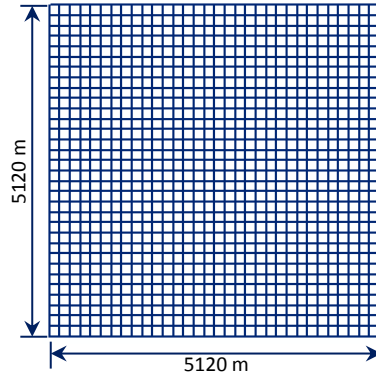


Figure 19 The base network.

### 3.3.2. Creating fishnets

The application of box-counting method involves using fishnets with varying box sizes ( $\epsilon$ ), while keeping everything else unchanged. At the time of creating a fishnet, however, it is important to pay attention to the choice of the location for the origin of the fishnet as compared to the origin of the network, as it can affect the count of the matching boxes. In other words, if one considers the bottom left corner of the network as its origin and create two different fishnets, one with the same origin (Figure 20a) and one with offsets in both horizontal and vertical directions (Figure 20b), the number of boxes needed to cover the network in the two cases will be different since in Figure 20a any link to the right of and above the origin will be counted twice, because it is common between adjacent fishnet boxes, as shown below:



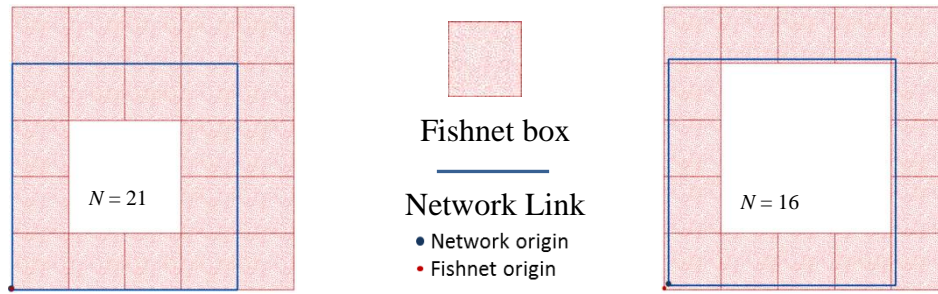


Figure 20 Comparison of the effect of fishnet offset on the box counts  
a) Fishnet origin without offset, b) Fishnet origin with offsets

In order to avoid double-counting, small offsets were introduced to the location of the origin of the fishnet in both horizontal and vertical directions. This choice can be further supported by the fact that most, if not all, real physical networks do not have a regular shape and as a result their links do not align with the edges of the fishnet boxes.

Creation of the base network, as well as the fishnets, was performed using the commercial platform ArcGIS. The rationale for using GIS (Geographic Information Systems) software was the fact that it can create a network in vector format (as opposed to pixel format) that does not lose its resolution when zooming in it. As a result, the process of box counting is performed accurately, especially when the box sizes become very small. Moreover, the data for many physical networks (e.g. transportation, power grid, etc.) are increasingly available in shapefile format, for which GIS is the right analysis platform.

### 3.3.3. Application of the box-counting method

GIS software was used to perform the box counting, using fishnets with box size dimensions of 5160 m, 1280 m, 640 m, 320 m, 160 m, 80 m, 40 m, 20 m, 10 m, and 5 m. Figure 21 shows the results obtained from the application of the box-counting method to the base network, plotted in a log-log diagram.

The plot of the results clearly show non-linear trend over the full span of the data. This means that the box-counting results do not follow a power law. In fact, they follow two distinct regimes, one quadratic and one linear, shown in Figure 21. This observation directly refutes the existence of a power law, and as a result rejects the applicability of the box-counting method.

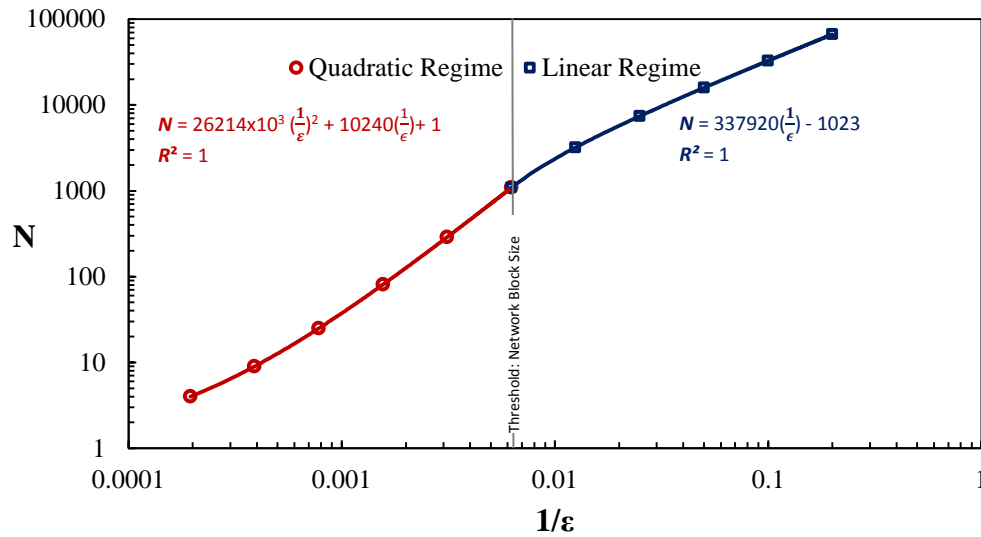


Figure 21 Box-counting results.

To further validate this finding, we applied the box-counting method to a variety of other networks, including Greek Cross as well as Sierpinski Triangular networks, which are both well-known fractals. Except for the Sierpinski Triangle, all the selected networks had an outer square boundary of 5120 m x 5120 m.

Plot of the results for every network, shown in Figure 22, systematically exhibits two distinct parts, one quadratic and one linear, akin to the above analysis. The transition between the quadratic and linear regions for each network was determined based on careful examination of the goodness of fit for both trends as well as the behavior of the coefficients in their equations. In all cases, the goodness-of-fit  $R^2$  values calculated for the corresponding linear or quadratic fit were 1. In contrast,  $R^2$  values for power law fits were all less than 1. Residuals also showed consistent bias in power law fits in contrast with linear and quadratic fits.

In Figure 22, network A was created by adding successively smaller squares at increments of 160 m using arithmetic reduction. Network B was created similarly, but with the difference that at each step the size of the new square was chosen to be half of the size of the previous square, i.e. geometric reduction. Networks C and D were both created by splitting the first square to 4 equal parts, then choosing the two diagonally opposing squares and applying the same process to them. Network E was also created using a repeating reduction pattern. The Greek Cross and Sierpinski Triangular were also created and tested thanks to their well-known fractal nature.

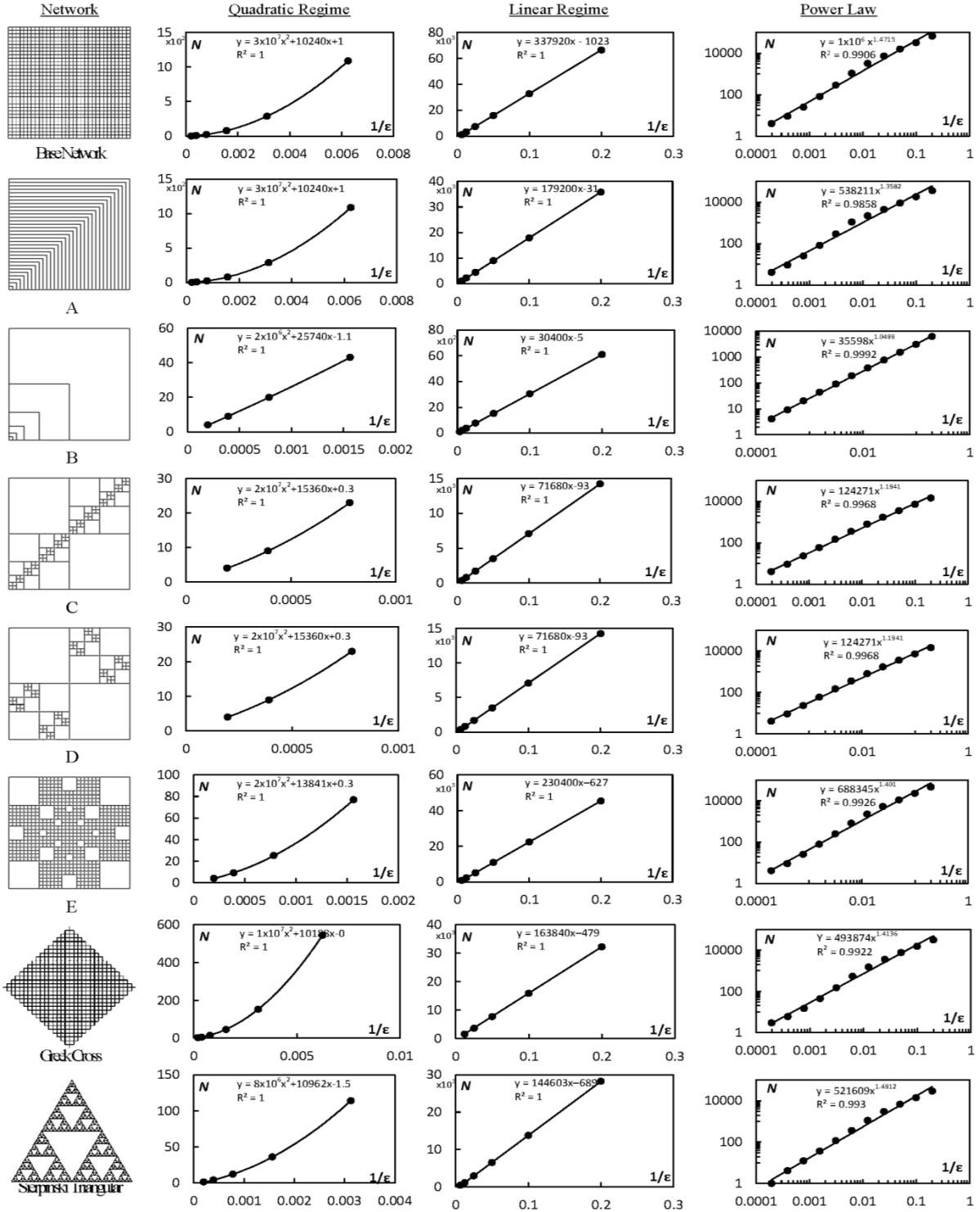


Figure 22 Various Networks and their box-counting results.

### 3.4. Analytical investigation

The unexpected conclusion in the previous part deserves proper mathematical investigation. To do so, it should be noted that the main variables of importance in box-counting method are  $\varepsilon$ , or better to say  $1/\varepsilon$ , and  $N$  = number of fishnet boxes needed to cover the network. For this reason, we aim to express  $N$  in terms of powers of  $1/\varepsilon$ .

If for the chosen network and also any given fishnet:

$\Delta$  = network block size (here 160 m),

$\varepsilon$  = fishnet box size, and

then while referring to Figure 20, we find mathematically:

$$\text{for } \varepsilon \geq \Delta \quad N = \Delta^2 M^2 \left(1/\varepsilon\right)^2 + 2\Delta M \left(1/\varepsilon\right) + 1 \quad \text{Eq. 3.5}$$

$$\text{for } \varepsilon \leq \Delta \quad N = 2\Delta M(M + 1)\left(1/\varepsilon\right) - M^2 + 1 \quad \text{Eq. 3.6}$$

in which:

$N$  = number of fishnet boxes needed to cover the network,

$M$  = number of network blocks in horizontal or vertical direction.

The above relationships can be further confirmed by the fact that both are equal when  $\varepsilon = \Delta$ , i.e. where the fishnet box size and the network block size become equal.

Noting the fact that  $M = L/\Delta$ , where  $L$  is the network size (here 5120 m):

$$\text{for } \varepsilon \geq \Delta \quad N = L^2 \left(1/\varepsilon\right)^2 + 2L \left(1/\varepsilon\right) + 1 \quad \text{Eq. 3.7}$$

$$\text{for } \varepsilon \leq \Delta \quad N = 2L \left(L/\Delta + 1\right) \left(1/\varepsilon\right) - \left(L/\Delta\right)^2 + 1 \quad \text{Eq. 3.8}$$

The first observation from the above expressions is that they demonstrate two different regimes, meeting where the fishnet box size equals the network block size. One regime, for fishnets with box sizes larger than the network block size ( $\varepsilon \geq \Delta$ ), exhibits a quadratic trend. The other regime follows a linear trend, which is for fishnets with box sides smaller than the network block size ( $\varepsilon \leq \Delta$ ). The above statements mean that a log-log plot of the results cannot be linear, which is exactly what we observed previously. This conclusion again rejects the ability of box-counting method in capturing the power law in features that are undoubtedly fractal.

### 3.5. Further rigorous mathematical induction

At this point, we take a deeper look at the theoretical definition of box-counting dimension of a fractal entity. Theoretically, the box-counting dimension of a fractal entity should be calculated at the limit when  $\varepsilon$  approaches zero, i.e. it is essentially equal to the asymptotic slope of the plot at infinity (as  $1/\varepsilon \rightarrow \infty$ ), i.e.:

$$\text{Fractal Dimension} = D = \lim_{\varepsilon \rightarrow 0} \left( \frac{\log(N)}{\log(1/\varepsilon)} \right) \quad \text{Eq. 3.9}$$

For the base network used in this study, the above equation corresponds to Eq. 3.8 (i.e. for small values of  $\varepsilon$ ), as shown again below:

$$\text{for } \varepsilon \leq \Delta \quad N = 2L \left( \frac{L}{\Delta} + 1 \right) \left( \frac{1}{\varepsilon} \right) - \left( \frac{L}{\Delta} \right)^2 + 1 \quad \text{Eq. 3.10}$$

Substituting  $N$  from Eq. 3.10 into Eq. 3.9 results in:

$$D = \lim_{\varepsilon \rightarrow 0} \left( \frac{\log[2L \left( \frac{L}{\Delta} + 1 \right) \left( \frac{1}{\varepsilon} \right) - \left( \frac{L}{\Delta} \right)^2 + 1]}{\log(1/\varepsilon)} \right) \quad \text{Eq. 3.11}$$

If  $z = 1/\varepsilon$ , then Eq. 3.11 is re-written as:

$$D = \lim_{z \rightarrow \infty} \left( \frac{\log[2L(L/\Delta+1)(z) - (L/\Delta)^2 + 1]}{\log(z)} \right) \quad \text{Eq. 3.12}$$

Since the above limit is indeterminate, using L'Hôpital's Rule, Eq. 3.12 is converted to:

$$D = \lim_{z \rightarrow \infty} \left( \frac{d(\log[2L(L/\Delta+1)(z) - (L/\Delta)^2 + 1])/dz}{d(\log(z))/dz} \right) \quad \text{Eq. 3.13}$$

Performing the above operations results in:

$$D = \lim_{z \rightarrow \infty} \frac{2L(L/\Delta+1)/[2L(L/\Delta+1)(z) - (L/\Delta)^2 + 1]}{1/z} \quad \text{Eq. 3.14}$$

or if simplified:

$$D = \lim_{z \rightarrow \infty} \frac{2L(L/\Delta+1)}{[2L(L/\Delta+1) - ((L/\Delta)^2 - 1)/z]} \quad \text{Eq. 3.15}$$

Finally, by applying the limit:

$$D = \frac{2L(L/\Delta+1)}{2L(L/\Delta+1)} = 1 \quad \text{Eq. 3.16}$$

This means that the fractal dimension for the base network used in this study using box-counting method is equal to one, which is equal to its topological dimension, i.e. according to the box-counting method it is not a fractal. Even if we account for the finite property of the figure, above the block size the relationship is quadratic and is therefore not power law. The comparison of the linear plots of the box-counting results for other networks with that of the base network also points to the fact that for all of them the box-counting method results in a fractal dimension of one, i.e. the box counting method cannot capture any of the fractal properties of the analyzed networks. This observation leads to the conclusion that for those networks, and in fact for any real network in which the self-similarity stops at some finite scale, the box-counting method is incapable of producing a fractal dimension. The diagrams for Greek Cross (with a known fractal

dimension of 2) in Figure 22, in which a quadratic pattern is followed by a linear trend exist, support the above statement further.

### **3.6. Conclusions**

Box-counting method has been used in numerous studies for analyzing features that have shown fractal properties. It accomplishes that by showing that a power law relationship exists among the results of its application to the feature under study.

This chapter presented computational, analytical, and rigorous mathematical approaches in investigating the validity of box-counting method toward capturing the nature of fractal networks. The observation made was that box-counting method is incapable of producing a power law relationship between the outputs obtained from its application. As a result, this finding invalidates box-counting method as an appropriate technique for capturing the characteristics of physical networks that possess fractal properties.

The methodology followed through this study is general and can be verified by using any other network. This means that even if the repeating patterns used in creating the above networks are continued to smaller scales, it will only shift the transition point between the quadratic and linear regimes, after which the linear trend will eventually appear, leading to a fractal dimension of one, i.e. no fractality, even if the feature is indeed fractal.

Through robust analytical as well as computational investigation of the box-counting method, this work has successfully demonstrated that for physical networks, even those with known fractal characteristics, the application of box-counting method results in data exhibiting



two distinct patterns in a normal plot, one quadratic and another one linear. These findings invalidate the box-counting method as being able to capture the existence of a power law, and thus the fractality of a feature.

## **4. AREA, LINE, AND POINT THRESHOLDS**

### **4.1. Introduction**

Cities are complex systems, consisting of a variety of interacting elements. From the time of its inception, an urban settlement goes through an evolutionary process that affects all of its constituents, among them its transportation system. Since a road network grows, expands, and evolves along with and similar to its encompassing urban system, it offers a proper means to study the complexity of its corresponding urban system and to express it using meaningful indicators (Batty, 2013a). As Samaniego and Moses have described it: “understanding the topology of urban networks that connect people and places leads to insights into how cities are organized” (Samaniego and Moses, 2008b).

#### **4.1.1. Transportation Networks as Complex Systems**

Moreover, similar to other emerging (Yerra and Levinson, 2005) and self-organizing systems (Xie and Levinson, 2009a), the evolution of road networks is not a simple “product of conscious design” (Levinson and Yerra, 2006), but rather a complex and dynamic process (Xie

and Levinson, 2009b) that is the result of the interaction of many different factors. Such influencing parameters include not only the system users and its infrastructure (Xie and Levinson, 2009a), but also topological, morphological, technical, economic, social, and political factors (Xie and Levinson, 2009b), all of which are also determinants of the changes in the road network's encompassing urban system. In fact, even for cities that 'look' different, their transportation systems can demonstrate a variety of similarities (Barthélemy, 2011; Batty, 2005; Cardillo et al., 2006; Jiang and Claramunt, 2004; Lämmer et al., 2006).

Many researchers have focused on presenting a broad picture of transportation networks by showing that they possess general properties such as self-organization (Yerra, 2003; Yerra and Levinson, 2005; Levinson and Yerra, 2006; Samaniego and Moses, 2008a; Barthélemy and Flammini, 2009), fractal (Batty and Longley, 1994; Li, 2002; Batty, 2008b), scale-free or power-law distribution (Lämmer et al., 2006; Porta et al., 2006; Kalapala et al., 2006; Jiang, 2007; Jiang and Liu, 2012), Zipf's rank law (Gabaix, 1999; Chen and Zhou, 2004; Gonzalez-Val, 2011; Chen and Wang, 2014), or other properties (Scellato et al., 2006; Crucitti et al., 2006; Kuran and Thiran, 2006; Barthélemy and Flammini, 2008; Levinson, 2012; Louf et al., 2013) to name a few.

#### 4.1.2. Geometry of Transportation Networks

Among other characteristics, transportation systems have geometric properties. While their topologic characteristics can be examined as graphs (Garrison and Marble, 1962; Karsky, 1963; Haggett and Chorley, 1969; Taaffe, 1973), complex analysis approaches and more

specifically network topological methods (Watts and Strogatz, 1998; Barabasi and Albert, 1999; Newman, 2003; Derrible and Kennedy, 2009; Antunes et al., 2009; Barthélemy, 2011) have recently been extensively used for this purpose (Buhl et al., 2006; Courtat et al., 2011). There are a number of studies of urban systems that have used simulated grid networks for different purposes (Levinson and Yerra, 2006; Masucci et al., 2009; Xie and Levinson, 2007; Yerra, 2003; Yerra and Levinson, 2005).

At the first glance, and from a network perspective, a road system is simply seen as a collection of connected segments or links. Understandably, this perspective shifts the main attention towards studying its links as a way of understanding the whole network. This ‘link’ aspect of urban transportation systems is paramount in terms of geometry and perhaps more closely related to the concept of ‘lines’ (although not related to Space Syntax (Hillier, 1999)). We will therefore look for a *line* indicator that can represent the links in a road system.

An urban road network, however, is more than the sum of its links or lines. Similar to the circulatory system that serves the whole body, a road system serves its encompassing urban area by dividing it into smaller blocks that make it easier to reach every corner of the system. The coverage area of the road network is therefore another important factor to be studied. Thus, we will also represent the coverage area of a given road system by an *area* indicator.

Moreover, the locations where the road segments cross, i.e. their intersections, also play an important role in the daily operation of a road network. For that, their representation should also be a part of any complete study of the complexity of their corresponding transportation

system. And that provides another objective for this study, which is to find a *point* indicator for a given road network.

Based on the above argument, this work will focus on measuring inherent geometric characteristics of urban road networks through studying their grid equivalents. It will be further extended by investigating the relationships between the results and their corresponding urban systems' demographic and socio-economic characteristics as well as travel patterns. We first develop the methodology to perform those measurements and then apply it to 50 urban areas in the United States to extract and analyze the characteristics of their road systems.

This study contributes to a better understanding of the complex nature of urban road networks by offering a robust and efficient approach that serves as a complement to other existing methods.

## **4.2 Methodology**

In order to explain the methodology towards the development of the three geometric indicators of a given road network, Chicago's urban system is used as an example, for which the process can be summarized in the following three steps.

### **4.2.1. Geometric Information**

As the first task, the extent of the urban system for the given city is determined. In the U.S., the commonly-used representation of such an influence area is the city's Metropolitan

Statistical Area (MSA). MSA is defined as the “geographical region with a relatively high population density at its core and close economic ties throughout the area” (Nussle, 2008). Essentially, an MSA is a Core Based Statistical Areas that comprises the central county plus adjacent outlying counties (Census Bureau, 2013), e.g. Chicago.

More precisely, “Metropolitan Statistical Areas have at least one urbanized area of 50,000 or more population, plus adjacent territory that has a high degree of social and economic integration with the core as measured by commuting ties” (U.S. Office of Management and Budget, 2008). The choice of MSA not only provides a consistent means for the selection of the extents of an urban area, but it also makes data collection easier as the MSA boundaries are readily available in shapefile format. Figure 23 exhibits Chicago MSA and its road network.

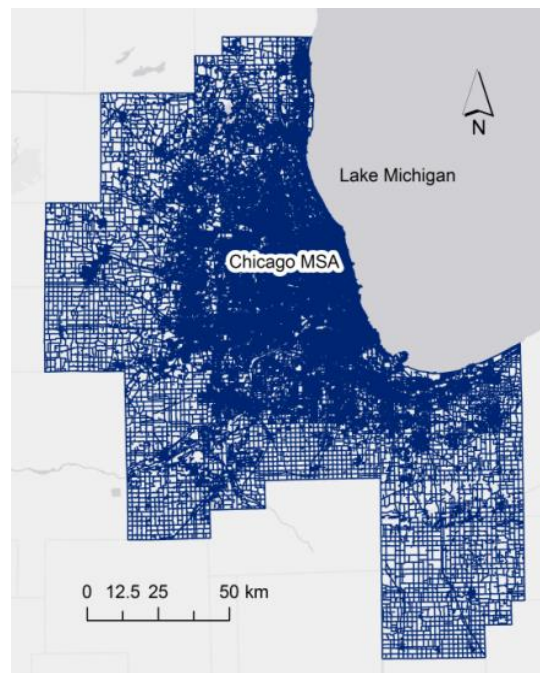


Figure 23 Chicago MSA road network.

Next, using the corresponding road network, polygons are created within the MSA area wherever the road network within that area creates a closed loop. The rationale for that is to exclude large peripheral areas without roads as well as outer road segments that extend beyond the built environment of a MSA that follows county boundaries. This is desirable since far areas of the full MSA easily artificially inflate the area of an urban system instead of focusing on the main area serviced by the road network.

This proved to be an important choice, especially for cities like Las Vegas, NV. Figure 24 demonstrates the difference between the road polygons area created using the above approach versus the MSA area for the Las Vegas MSA, which makes a substantial difference in the service area to be analyzed.

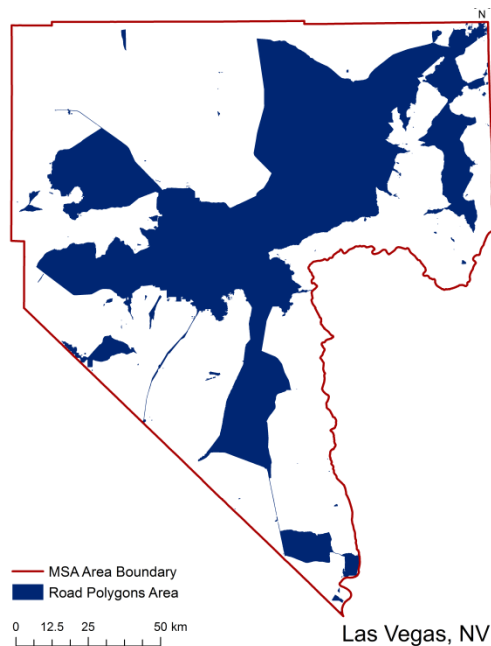


Figure 24 Comparison of the service area of the road system created by closed road polygons and the MSA area for the city of Las Vegas.

Having completed the previous part, the total area of the combination of the polygons is calculated and reported as the total area (A) of the road network that is serviced by the road segments within them.

Moreover, for the same road network, the lengths of its roads segments are calculated and added to find the total length (L), while also the network's intersections are counted, and their number is recorder as the total number of points (P).

#### 4.2.2. Grid Creation

This step involves successive creation of grids with varying cell sizes and overlaying them on the road network in a way that the grid cells cover all the road segments. Figure 25 demonstrates the creation of such a grid with 10 km x 10 km cells that covers Chicago MSA road network. Note that this process resembles the box-counting methodology in fractal analysis, but here different information is collected from the results.

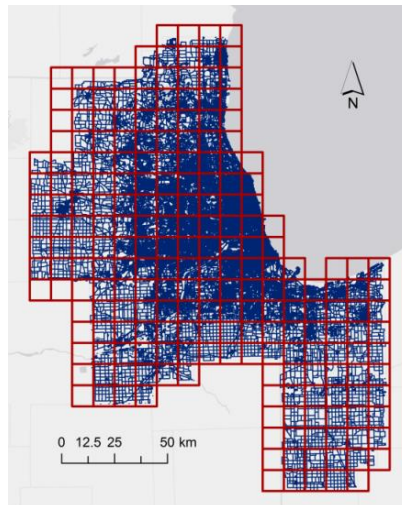


Figure 25 Road polygons and 10x10 km grid network.



During the grid network creation step, if there are any grid cells that do not contain any portion of the road network is removed. Having completed that task, and for each grid network, the total coverage area (a), total length of links (l), and total number of nodes (p) are calculated. Details of grid creation for Chicago MSA are presented in APPENDIX B.

#### 4.2.3. Geometric Equivalency

The final task involves a comparison of the values obtained from the previous two steps. The goal is to find the grids that are equivalent to the given road network with respect to total coverage area, total road length, and total number of intersections. As mentioned before, those criteria represent the given road network's area, line, and point characteristics, successively. The idea is that while a given urban road system might have an irregular configuration, something which is a part of its complex identity; there are equivalent grid networks that possess the same area, line, or point geometric properties.

Naturally, there are more than one equivalent grid network that satisfy the condition for any of the above geometric indicators. An additional condition must therefore be set to result in a unique equivalent grid network. For that, we required the coverage area of the grid network to cover all the road segments of the urban road network under study, which was set and achieved in the previous step.

For each of the calculated geometric properties of the given road network, there will be one equivalent grid. The block size of that equivalent grid network will then be considered as an indicator, or as called hereafter: the "*threshold*" for its corresponding geometric property. This

means that at the end any given road network will have a set of unique indicators: area, line, and point thresholds.

The procedure explained above is applied to the Chicago MSA road network. Due to its dense configuration, however, only a south-western section of the road network along with its equivalent grid networks are magnified and demonstrated in Figure 26.

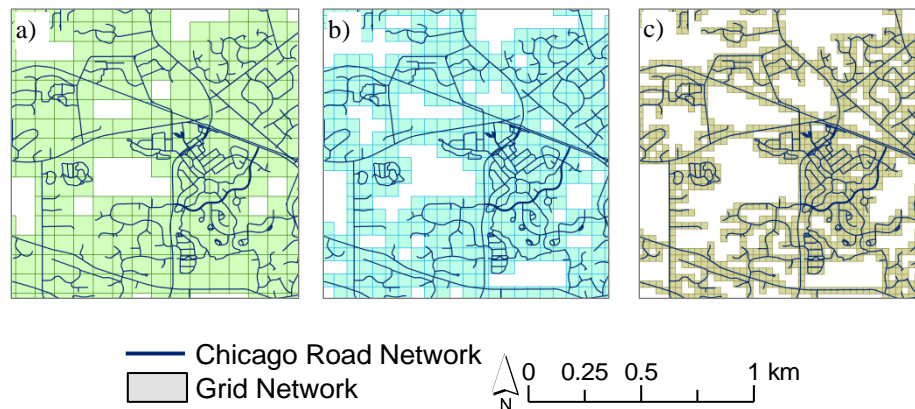


Figure 26 Chicago road network and its equivalent grids with respect to a) area, b) road length, and c) number of intersections.

To explain their differences, the process involves overlaying grids with gradually decreasing block sizes over the original road system. At the beginning, the area covered by the grid is larger than the corresponding area of the road network under study. As the cell size of the grid is gradually reduced, at some point the two areas become equal (Figure 26a). At that very moment, the grid network crosses a threshold. Since it marks the point where the two networks are equivalent in an “area” dimensional perspective, the grid network’s block size is then designated as the *area threshold*.

After that point, the focus shifts to the comparison of the total road lengths of the two networks. As the grid network's block size becomes smaller and smaller, its total road length gradually increases, up to a point at which it becomes equal to the total road length of the original network (Figure 26b). That moment marks another threshold, at which the block size of the grid network is designated as the *line threshold*, i.e. when the two networks are equivalent in a “line” dimensional sense.

The same process continues further, until a point when the total numbers of intersections (points) in both networks become equal (Figure 26c). That marks the third threshold, at which the block size of the grid network is designated as the *point threshold*. At that very moment, the two networks are equivalent in a “point” dimensional sense.

As discussed before, a given urban road network can be examined from different perspectives. One is the area it encompasses or serves. Another one is the links (lines) that facilitate the services it provides. And the third one is the intersections (points) that in turn facilitate the transfer of services between links (lines). Measuring these three components, and their corresponding thresholds (as explained above), can help better characterize the road network itself.

In order to find the three area, line, and point thresholds accurately, the following approach is taken.

For a given urban road network, its coverage area ( $A$ ), total road length ( $L$ ), and total number of intersections ( $P$ ) can be calculated and extracted from its shapefile, easily obtainable from Census TIGER/Lines dataset (U.S. Census Bureau, “TIGER/Lines Shapefiles”).

In comparison, for any chosen grid network with a block size of  $\varepsilon$ , the area it serves ( $a$ ), the total road length it consists of ( $l$ ), and the total number of intersections that it has ( $p$ ), can also be extracted from its shapefile.

Instead of comparing the two sets of numbers, the grid network values are standardized by dividing them by the road network's corresponding values and then comparing the result with unity (one), i.e. plots of  $a/A$ ,  $l/L$ , and  $p/P$ , are drawn and intersected with a horizontal line with the value of 1. At the point of intersection, the block size ( $\varepsilon$ ) of the grid network is extracted and reported as the corresponding threshold. Examples of the diagrams for the area, line, and point thresholds for the Chicago MSA road network are presented in Figure 27.

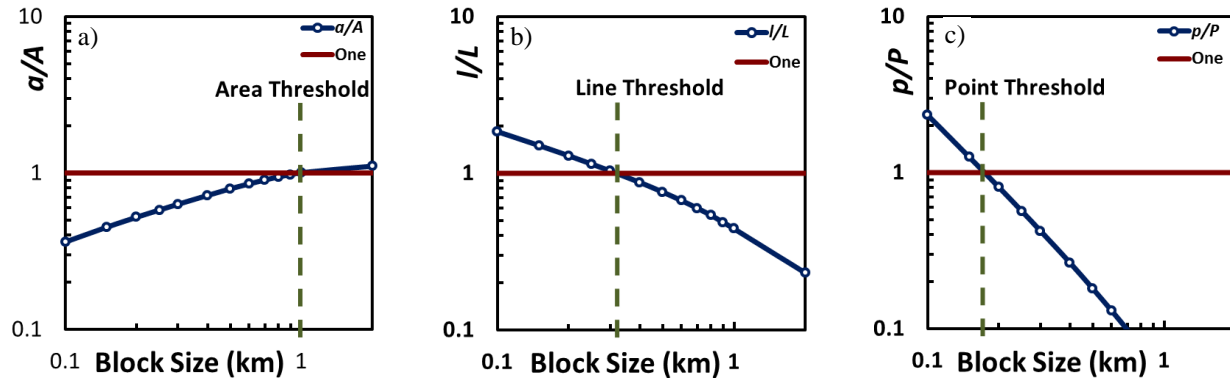


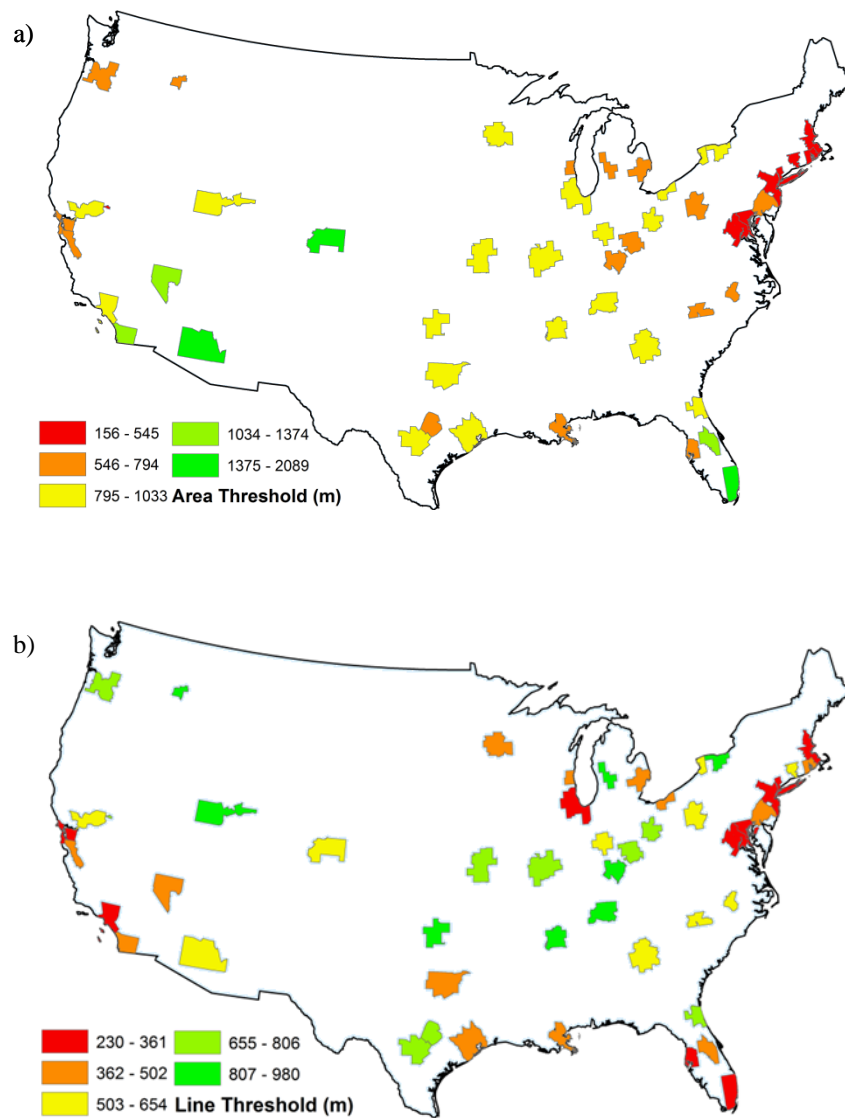
Figure 27 Determining the three thresholds for Chicago MSA road network:  
a) Area, b) Line, and c) Point Thresholds

### 4.3. Results and Discussion

Similar steps were repeated for a total of 50 urban areas across the U.S. (see Appendix A for a complete list of cities, and Appendix C for the thresholds for individual cities). These cities

cover a wide and diverse range of parameters such as road network structure, topology, morphology, history, size, population, area, and socio-economic conditions.

The results of the analyses performed are presented in Figure 28 in the form of three maps, showing the geospatial variations of the three thresholds (area, line, and point) calculated for those urban areas.



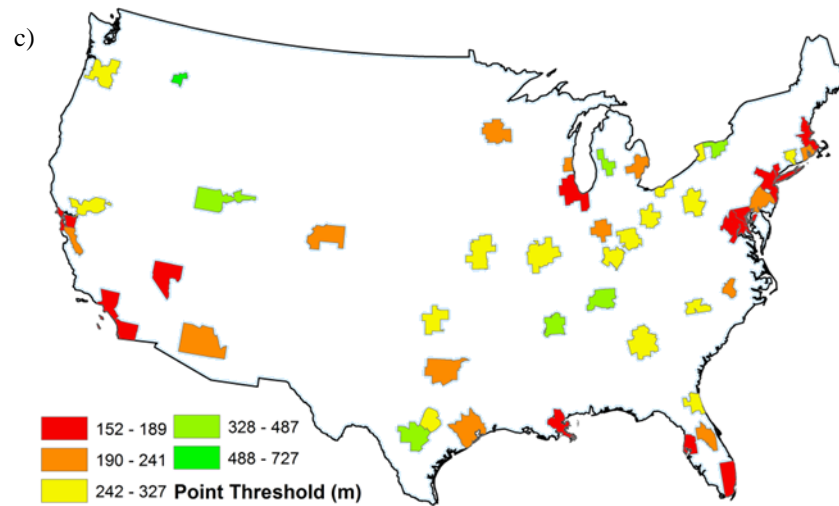


Figure 28 a) Area, b) Line, and c) Point thresholds within U.S. urban areas.

Figure 28a for area threshold shows lower values for older cities (mostly in the north-eastern states) as compared to those for younger cities. This difference is related to the advent of the motorized transportation in the 20<sup>th</sup> century. ‘Older’ cities tend to be more walkable and have smaller blocks, while ‘younger’ cities tend to have larger block sizes. A same-scale comparison between the road polygons in Phoenix, AZ with Chicago, IL that have the largest and medium area thresholds, respectively, sheds light on this fact, as shown in Figure 29. We can see that in general Chicago offers a more inviting environment towards walking than Phoenix.

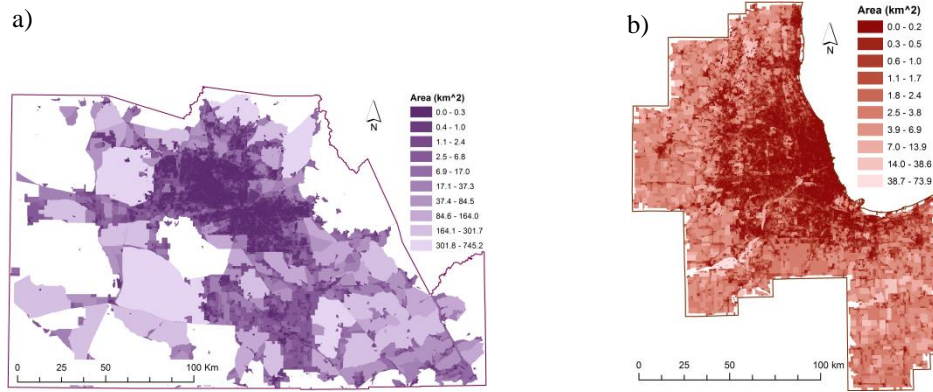


Figure 29 Comparison of a) Phoenix, and b) Chicago road polygons variations

As for the line thresholds, and different from the previous figure, we see that the line thresholds for the cities along the costal lines are smaller than for the cities inside the country. The reason is partly due to the fact that coastal cities often perform as logistics hubs (e.g., ports) and thus are centers of import and export activities. As a result, their road networks are more compact and have more uniform road segments as compared to inland cities that have larger variations in their road segment lengths. A comparison of the length variations within the road networks of Salt Lake City, UT with Chicago, IL that have the largest and medium line thresholds, respectively, presents a visual explanation of this characteristic, as shown in Figure 30. This is an example of the inland Salt Lake City versus a logistic hub coastal city like Chicago that is a center of freight activity. We see that as a result, Chicago's road network is more compact and has a more uniform distribution of road segments as compared to the non-coastal Salt Lake City that has larger variation in its road segment lengths.

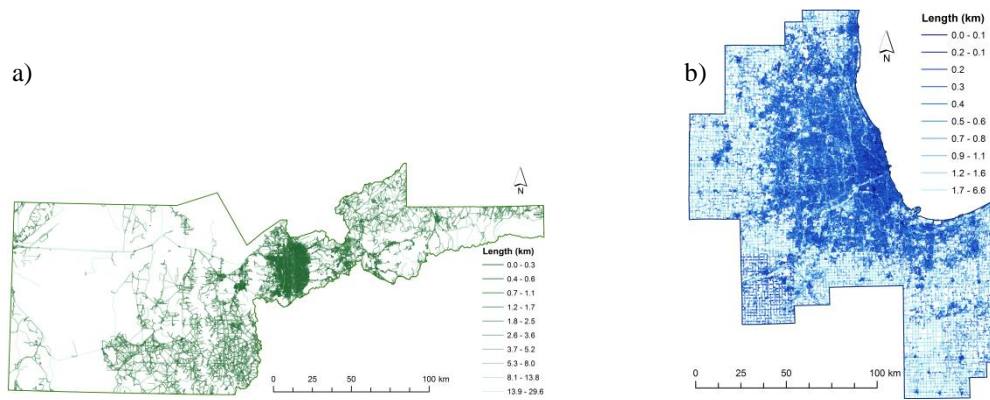


Figure 30 Comparison of a) Salt Lake City, and b) Chicago road length variations

For the point threshold, while we might expect to see the same trend for it as the line threshold, since intersections are merely where the roads intersect, this is not always the case. A good example is Denver, CO that has a mid-range line threshold, but a small point threshold. One of the factors affecting the point threshold is the way the intersections are created, i.e. 6- or 4- way intersections as compared to T- intersections or cul-de-sacs, each affecting the point-threshold differently. This means that cities with similar line thresholds could have different point threshold, and vice versa.

The above figures demonstrate interesting and insightful aspects of the diversity of the inner complexity of the urban systems studied here. Of relevance, overall no single indicator can completely capture and describe all the complexities at play. This emphasizes the fact that any given urban system has its own unique multi-dimensional complex characteristics, all of which need proper representation in order to gain a complete picture of its corresponding urban system's characteristics.



In order to better present and visually compare the thresholds calculated for the cities studied in this work, all the values obtained are plotted in one diagram. Figure 31 clearly shows that each threshold has its own variation and no two thresholds are behaving similarly, again a manifestation of the complex nature of urban systems and their road networks.

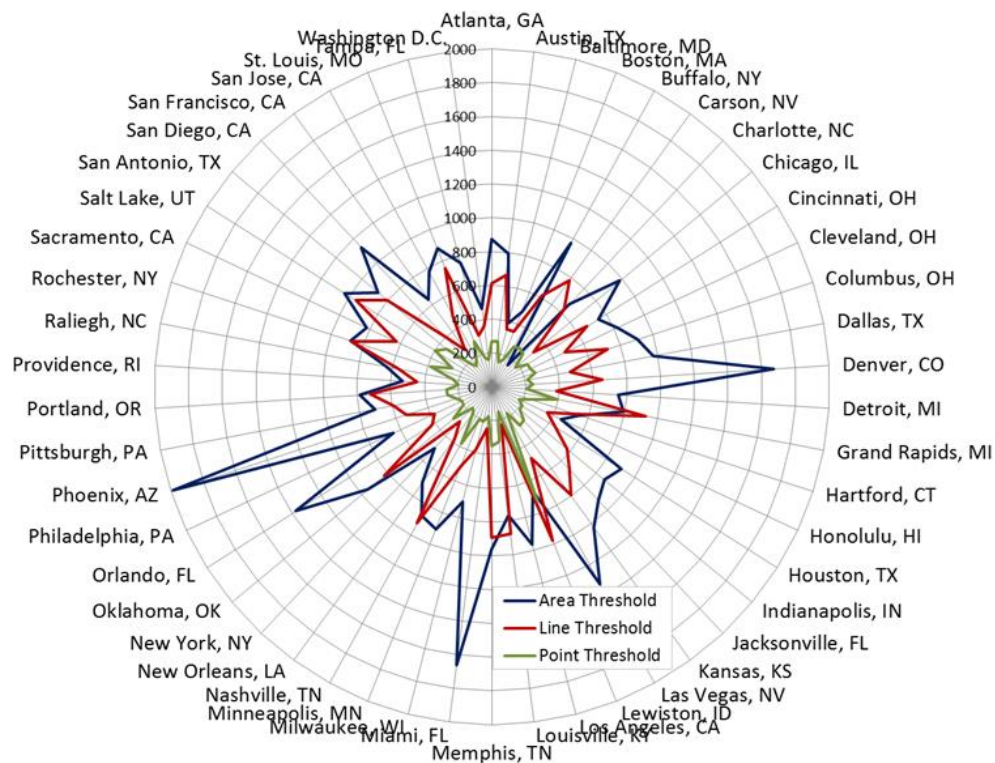


Figure 31 Spatial Distributions of Area, line, and point thresholds for 50 U.S. urban areas.

The significance of the three thresholds found in this work was further investigated through analyzing their relationships with several socio-economic parameters as well as travel patterns related to their corresponding urban areas.

A plot of the area threshold versus the age (Wikipedia, 2014b) of the urban systems studied here is presented in Figure 32.

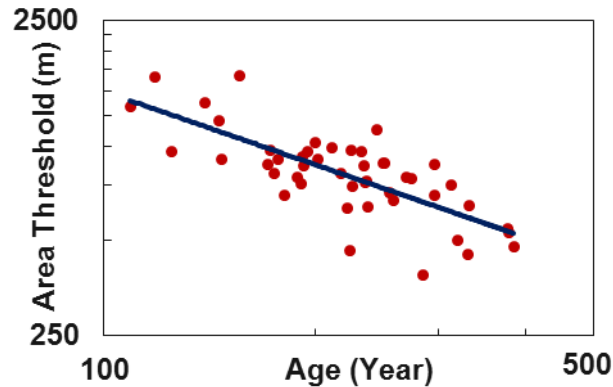


Figure 32 Relationship between the area threshold and the age of the urban system.

Figure 32 shows a power law trend ( $Area\ Threshold = 52057\ Age^{-0.772}$  with  $R^2 = 0.51$  and  $|t\text{-score}| = 6.8$ ), which means that the older a city is, the shorter its area threshold will be. This supports the fact that in older cities the polygons created by road networks are smaller due to their more developed state, while in younger cities one would see larger polygon sizes. This figure is able to capture nearly two hundred years of urban and regional planning theory and the advent of motorized transportation as discussed earlier.

From another perspective we witness a relationship between population density and line and point thresholds, as shown in Figure 33. This phenomenon is common and expected (Jacobs, 1961; Hanson and Giuliano, 2004; Peiravian et al., 2014), since, if other conditions remain the same, neighborhoods with smaller blocks (i.e. higher road and intersection density, as compared

to larger blocks) tend to create safer environments and thus attract more people, hence higher population density.

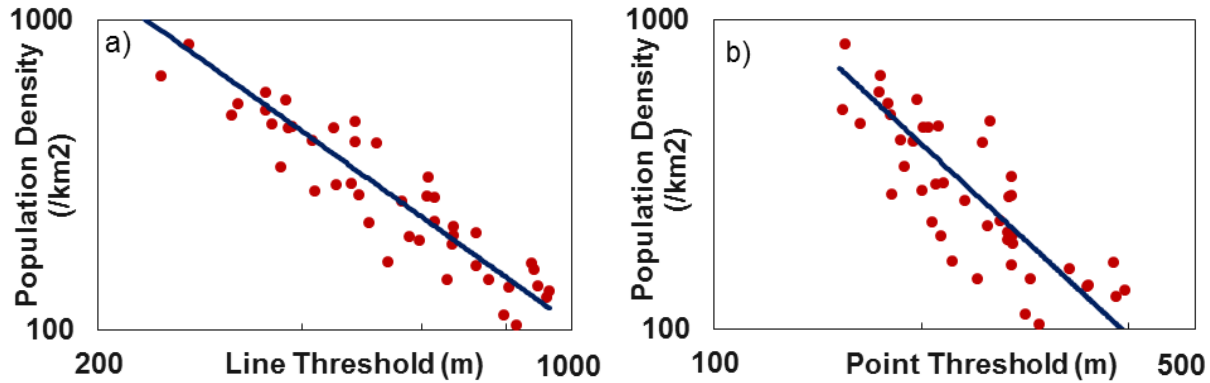


Figure 33 Relationship between Population density and a) Line and b) Point thresholds.

Figures 33a shows that an increase in line threshold, which means larger block size, has a negative power law impact on the population density, i.e.  $Population\ density = 5 \times 10^6 \cdot Line\ threshold^{1.566}$  (with  $R^2 = 0.56$  and  $|t\text{-score}| = 7.6$ ). The reason is that longer road segments, i.e., larger block sizes, essentially translate into larger residential units. Similarly, population density is affected by point threshold ( $Population\ Density = 2 \times 10^7 \cdot Point\ threshold^{2.061}$  with  $R^2 = 0.43$  and  $|t\text{-score}| = 5.8$ ), as shown in Figure 33b. This shows the fact that closer and denser intersections translate into city blocks that are smaller and thus more suitable for housing with higher concentration of people per area.

Using the 2010 American Community Survey (ACS) data (U.S. Census Bureau, “American Community Survey (ACS)”), we find that many travel patterns within the U.S. have power law relationships with the line threshold. Figure 34 exhibits the variations of the average

travel time for all modes and also total transit travel time with respect to the line threshold. Other travel patterns found to possess similar trends, including all-modes total travel time, total number of trips, and total number of transit trips.

The power law trend seen in Figure 34a (*All-modes avg. travel time* =  $60.725 \text{ Line threshold}^{0.134}$  with  $R^2 = 0.38$  and  $|t\text{-score}| = 5.2$ ) shows that as the line threshold increases, the average travel time for all modes decreases. The reason is that an increase in the length of the road segments, which partially represents the existence of freeways and thus lower road density, results in a higher car use as the dominant choice of transportation mode in the U.S. A similar trend exists for the reduction in the use of public transit, shown in Figure 34b (*Total transit travel time* =  $7 \times 10^{12} \text{ Line threshold}^{-2.475}$  with  $R^2 = 0.30$  and  $|t\text{-score}| = 4.4$ ). In this case, we use total as opposed to average travel time since cities with denser road networks tend to generate more as well as longer transit trips. As a result the total number of transit trips and thus the total transit travel time drop as line threshold increases.

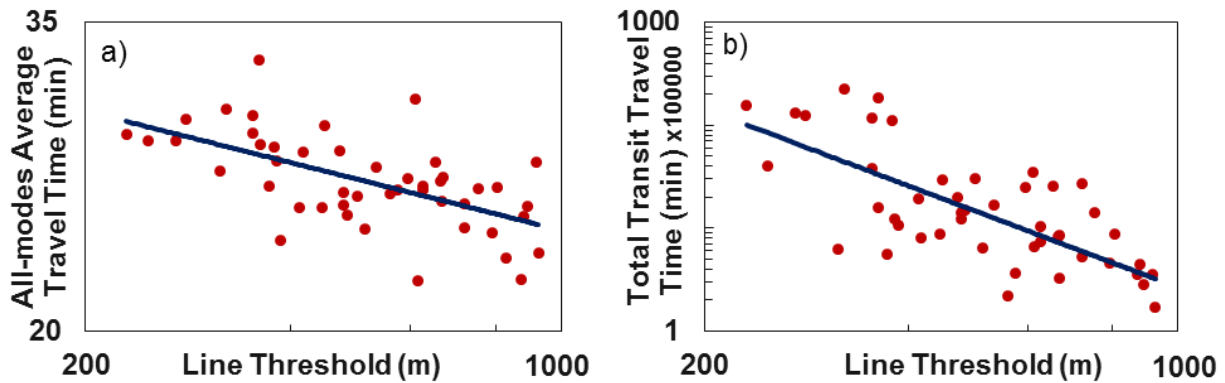


Figure 34 Relationship between the a) Average travel time for all modes, and b) Total transit travel time, and the Line threshold.

As for the point threshold, studies (Brown et al., 2013; Peiravian et al., 2014) have shown that denser road networks, which translate into closer and more compact intersections, support active modes of transportation, including walking. Walking data from 2010 American Community Survey (ACS) supports this idea, as shown in Figure 35.

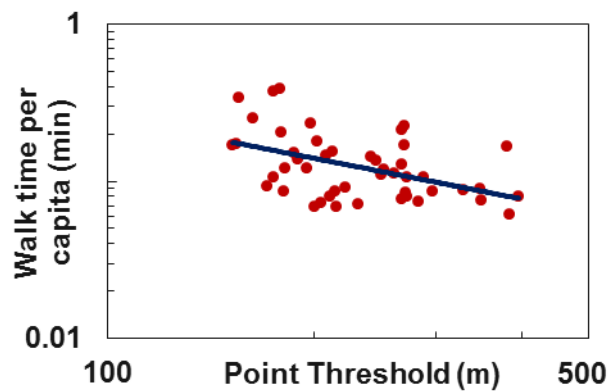


Figure 35 Relationship between Walk time per capita and Point threshold.

Based on this figure, urban areas with shorter point thresholds, i.e. with more and closer intersections, have higher walk time per capita, i.e.  $Walk\ time\ per\ capita = 13.405\ Point\ threshold^{0.861}$  with  $R^2 = 0.38$  and  $|t\text{-score}| = 3.1$ . Although not as statistically significant, this result simply reflects the fact that among other parameters the closer the intersections, the more encouraging and supportive the environment is for pedestrians. In other words, pedestrians are willing to walk longer distances if the environment is encouraging.

#### 4.4. Conclusions

Transportation networks serve as windows into the complex world of urban systems. By properly characterizing a road network, we can therefore better understand its encompassing urban system. This chapter offers a geometrical approach towards capturing inherent properties of urban road networks.

Based on the arguments presented, an analysis of a road network, as a representative of the complexity of its encompassing urban system, requires three different yet related geometric indicators: *area*, *line*, and *point*. From a mathematical perspective, these three indicators also represent the three main geometric dimensions of an urban system,  $D^2$ ,  $D^1$ , and  $D^0$ , respectively.

This study resulted in the development of a unified and systematic approach for the characterization of urban road networks through their *area*, *line*, and *point* indicators, later referred to as *thresholds*. It offers a robust and efficient methodology towards defining and extracting the three relevant indicators of road networks through measures of their grid equivalents.

By creating grid networks of varying block sizes and overlaying them on the road networks under study, three indicators were extracted, each representing an individual geometric property of the network. Together, the area, line, and point thresholds obtained through the method developed in this study succeed in capturing important and complex characteristics of an urban system.

By applying the methodology to 50 U.S. urban systems, we successfully observe differences between eastern versus western, coastal versus inland, and old versus young, cities. Moreover, we show that many socio-economic characteristics as well as travel patterns within urban systems are directly correlated with their corresponding area, line, and point thresholds. While two cities may share similarities for one of the thresholds, they may not be similar with respect to the other two, thus allowing us to capture their unique properties from different perspectives.

## **5. THE RING-BUFFER METHOD**

### **5.1. Introduction**

#### **5.1.1. Cities and Complexity**

Cities are complex systems consisting of many inter-related components and features. They possess both visible as well as hidden characteristics. Similar to complex living organisms, they exhibit orderly characteristics that are lying beneath their physical forms. The evolution and spread of an urban system and its components happen over many years. It is the aggregated outcome of numerous individual and collective choices, each influenced by the prevailing conditions in its time. Each new change is overlaid on previous changes. In other words, any urban system and its components have a starting point when and where they are founded; tens or in some cases hundreds of years ago.

While we may assume that the older a city is, the less coherent its founding blocks have been, many researchers suggest (Batty, 2008b; Batty et al., 2008; Batty and Longley, 1994), and even demonstrate (Wong and Fotheringham, 1990; Friedrich et al., 1994; Rodin and Rodina,



2000; Doménech, 2009; Chen, 2010a), that no matter how an urban system has evolved or what foundations it has been built on, from a larger perspective it has inherent order and organization.

As complex systems, cities have been studied heavily in the scientific literature, leading for a push towards a new “Science of Cities” (Batty, 2013b). In order to better understand the complex nature of an urban system, studies have been focused on the characterization of its components (Hillier and Hanson, 1984). As a result, the hidden, and presumably orderly, characteristics of different components of a given urban system have been a matter of interest in recent time (Shen, 2002; Levinson, 2007; Terzi and Kaya, 2011). These studies have looked at a large number of characteristics, from the travel behavior of their residents (Gonzalez et al., 2008; Wang et al., 2012), to the amount of energy that is being consumed (Bristow and Kennedy, 2013; Kennedy et al., 2014), to how they scale with size (Bettencourt et al., 2007; Batty, 2008; Samaniego and Moses, 2008; Bettencourt, 2013) to name a few.

#### 5.1.2. Transportation Systems

Studying urban systems require proper analysis methods capable of capturing their complex nature. The complex behavior of cities has been studied through their transportation systems (Batty and Longley, 1994; Samaniego and Moses, 2008c), because “understanding the topology of urban networks that connect people and places leads to insights into how cities are organized” (Samaniego and Moses, 2008c). Urban transportation systems are particularly interesting to study since they have evolved at the same pace as their encompassing cities, and thus they offer virtual snapshots of the past through the changes in their characteristics from

downtowns to the suburbs. Measuring the complex properties of transportation systems can therefore pave the way to a better understanding of city formation and growth.

In the case of the road network of a city, one can visually observe that such an order manifests itself in a self-similar pattern (L. M. A. Benguigui, 1995; Kim et al., 2003). In other words, the evolution of a transportation network is very similar to a tree trunk that grows, then splits into branches, and those branches also grow and then split again into smaller branches, and so on so forth. One main difference, however, is that transportation networks create loops through branch-joining. Additionally, order can manifest itself by showing similar shapes and patterns even if scales differ. This is particularly true in road networks that tend to be denser in a downtown while keeping the same overall pattern throughout the city.

With the advent of new technologies, and in particular powerful Geographic Information System (GIS) tools, as well as the availability of more disaggregate datasets including extensive geospatial data, we are now enabled to perform a more detailed analysis of transportation networks towards a better understanding of their encompassing urban systems as complex adaptive entities.

Based on the above discussion, the main objective of this work is to employ a proposed ring-buffer approach to capture the complex characteristics of urban transportation systems. The steps to take are first applied to Chicago metropolitan area as a case study. After making proper observations and analyzing the results, the method is then applied to 50 U.S. urban systems. Overall, this work fits within the global endeavor to analyze cities and their infrastructure as complex systems (Doménech, 2009; Batty, 2005; Luis M. A. Bettencourt et al., 2007; Derrible

and Kennedy, 2009; Bettencourt et al., 2010; Derrible and Kennedy, 2010; Kennedy, 2011; Derrible, 2012; Levinson, 2012). Taking a complex analysis approach to analyze an urban system and its components offers many benefits, including the provision of measurable metrics, as is the case here.

## **5.2 Methodology**

### **5.2.1. Description of the ring-buffer approach**

The ring-buffer method used in this study is based on the assumption that urban systems and their components, specifically their road networks, evolve similar to living organisms. A living being comes to life as a single cell. Then it grows and spreads around that center, subject to its prevailing conditions and constraints. Similar to that, a city spreads around a point of origin, or “center” (Frankhauser, 1998b; Levinson and Xie, 2011), and then gradually expands outwards, while avoiding the physical constraints around it such as water bodies, etc. The widely accepted assumption is that the spread of any component of the urban system, e.g. its road network, at a given point is proportional to its distance from that center. Mathematically, for this assumption to hold true, it needs to manifest itself in the form of a power law. In other words, if measurements follow a power law, then the urban system, or its component, will be considered to be a *fractal*.

A fractal can be described as an entity that possesses self-similarity on all scales. It is important to note that a fractal needs to only exhibit similar (but not exactly the same) type of

structure at all scales. Moreover, according to Mandelbrot (2004): “A fractal set is one for which the fractal dimension strictly exceeds its topological dimension.” In practice, this means that while a line feature (e.g. a road) has a dimension of 1 in classical geometry, it must have a dimension larger than 1 (to a maximum of 2), if it is to have fractal properties.

The existence of a power law appears in the form of Eq. 5.1:

$$N(r) = a \cdot r^D \quad \text{Eq. 5.1}$$

in which  $r$  is the radius (with respect to a point of origin or center),  $N$  is the number quantifying the object under consideration within a circle of radius  $r$ ,  $a$  is a constant, and  $D$  is the exponent, also called the *fractal dimension*. Figure 36 illustrates the idea, in which circles with increasing radii are created around the center. The quantities of the feature are calculated for each ring, and then successively added to obtain the quantities within consecutive circles (or buffers) with corresponding radii. The variation of the total length of the feature with respect to the buffer radius can then be examined for the presence of the power law, according to Eq. 5.1, as shown in Figure 37.

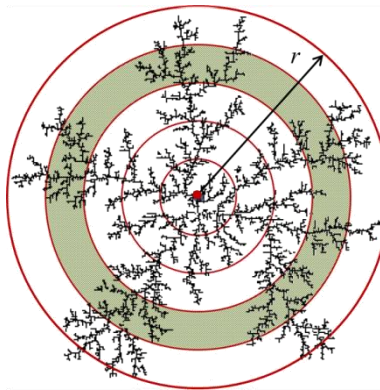


Figure 36 Ring creation in the ring-buffer method.

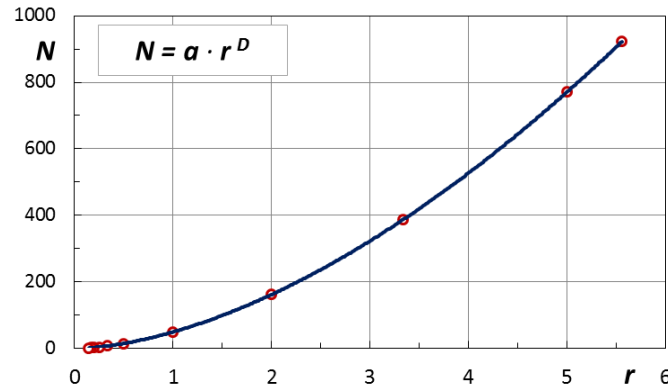


Figure 37 Normal plot of the power law relationship.

In order to facilitate the examination of the data, the measurements are re-plotted in log-log scale. Taking the log of both sides in Eq. 5.1 results in Eq. 5.2, as shown below:

$$\text{Log}[N(r)] = \log(a) + D \cdot \log(r) \quad \text{Eq. 5.2}$$

This means that the log-log plot of the data should be linear, as shown in Figure 38.

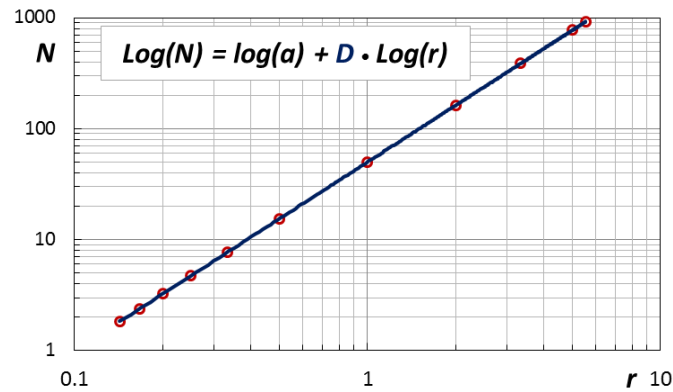


Figure 38 Log-log plot of the power law relationship.

Exhibition of the linear trend by the logs of the data not only proves the existence of the power law, but also enables us to extract the fractal dimension of the feature from the slope of the log-log plot, as per Eq. 5.3:

$$D = Slope \quad \text{Eq. 5.3}$$

Because the data points are ordered and successively plotted based on  $r$  values, a regression analysis will be sufficient to linearly fit the outputs of this method to Eq. 5.2. The reader, however, is referred to Clauset et al. (2009) for a further discussion regarding statistical methods that can be used to fit power laws to overlapping data.

### 5.2.2. Verification of Ring-Buffer Method for Fractal Analysis

As the first step, the validity of the ring-buffer approach as a proper method for capturing the fractal nature of features is investigated. In order to do so, the Greek Cross grid, which is a well-known fractal with dimension of 2, is chosen. The rationale behind this choice is the resemblance of Greek Cross pattern to urban road systems, especially grid road networks. Also, to investigate if the grid cell size has any impact on the results, a total of 20 Greek Cross grids are created with varying cell sizes from 100 m to 10000 m. Moreover, and in order to capture the impact of boundary shapes on the results, the Greek Cross grids are all clipped by the Chicago MSA area. Figure 39 demonstrates one of the grids created via the above steps.

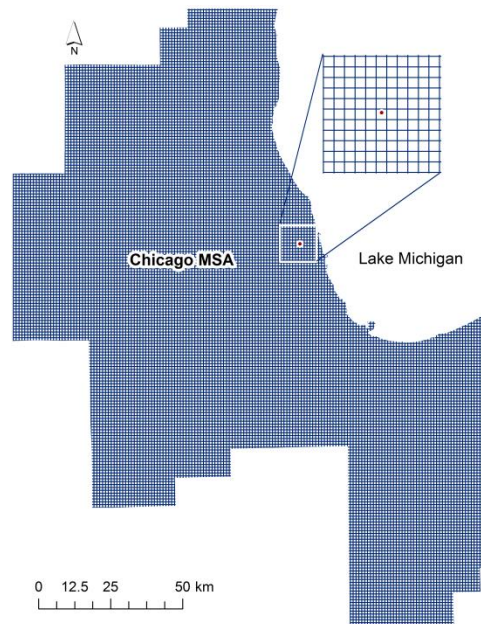


Figure 39 Greek Cross grid with 1000 m cells created within Chicago MSA.

As it can be seen, however, there is no apparent center to the above grid network, mainly due to its uniform structure. As for the point around which the circles are to be created, therefore, the center chosen for the actual Chicago road network (as explained later) is used. The ring-buffer method is then applied to every grid created through the above steps, during which circles with the radii from 1 km to 100 km are created around the chosen center at the increments of 1 km. This results in the creation of a total of 100 rings of 1 km width. The rings are then intersected with the grid networks, and the total road length within each ring is calculated for every grid.

An important note to mention here is that at some radius, as shown in Figure 40, the boundary of the MSA representing an urban system starts to cut through some of the rings, thus

reducing the road lengths within the affected rings, as compared to the smaller rings that are uncut and complete.



Figure 40 Examples of full and partial rings.

To rectify this problem, the density of the roads within the partial rings are calculated and then extended to their corresponding full rings, as if no parts of them are cut. This allowed us to successively add the ring road lengths to obtain the total road lengths within buffers (circles) around the center at the selected radii. The values obtained, which represented  $N$  in Eq. 5.1, are then plotted versus the radii in a log-log diagram, as shown in Figure 41.



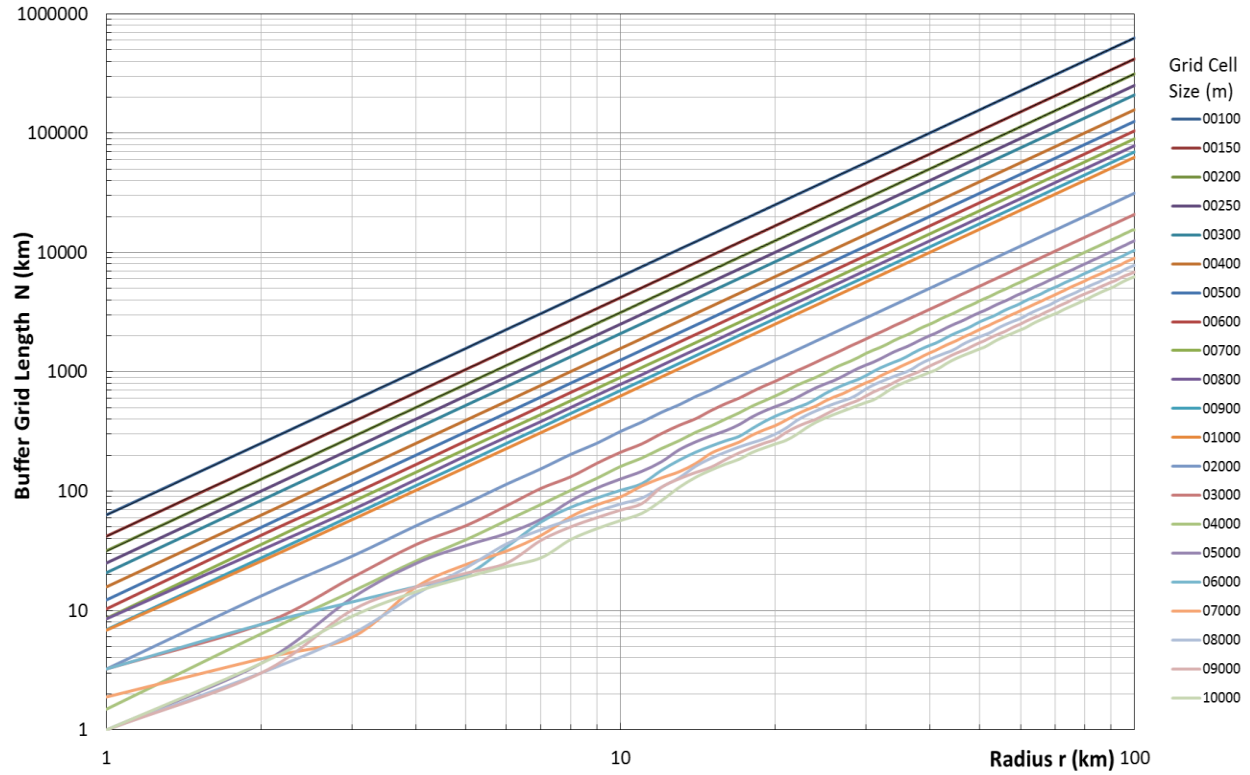


Figure 41 Log-log plots of buffer road length versus radius for different grid cell sizes.

The above Figure 41 shows that the fits to all the above plots follow linear patterns, i.e., they display power law relationships, supporting the existence of fractal properties. Moreover, the slopes of the fits to all the plots are equal to 2, meaning that the fractal dimensions of all the grids are 2, as expected. Moreover, for grids with large cell sizes ( $> 1000$  m or 1 km), the plots show oscillations at the beginning, but still around a line. The reason is that the chosen ring width (1 km) becomes too small for grids with cell sizes of larger than 1 km. Nonetheless, all of the plots eventually become lines with slope of 2. This investigation therefore validates the ability of the ring-buffer method to capture the characteristics of a fractal feature. In other words,

if this method does not show a linear pattern in a log-log plot for a given feature, it will mean that the feature is not a fractal.

Another observation that is made from the above experiment is that the outcomes of the application of the ring-buffer method are insensitive to the shape of the boundary of the chosen urban system, i.e. the shape and size of the MSA of a given urban system will not have an impact on the results.

Moreover, the size of the grid cells used also does not affect the outcome of the ring-buffer method. Of course, the smaller the grid cell size, the clearer the linear relationship, but even for larger grid sizes, the oscillations remains around a line with the slope of 2.

### 5.2.3. Application of Ring-Buffer Method to Urban Road Networks

In order to investigate the complex properties of urban road networks, we apply this ring-buffer approach to the same 50 U.S. urban systems chosen in Chapter 4.

The first step, however, is to select a consistent method for determining the “center” for any given road network. Based on the earlier discussion, we first use the distribution of the road density of the whole network over its MSA area to identify and select the densest area. Then, we choose the point with the highest road density within the selected area as the “center” for the whole network. An example of the application of this method to the Chicago MSA road network, and the selected center, is presented in Figure 42. Similar maps are generated for all 50 U.S. urban systems and are included in Appendix F.

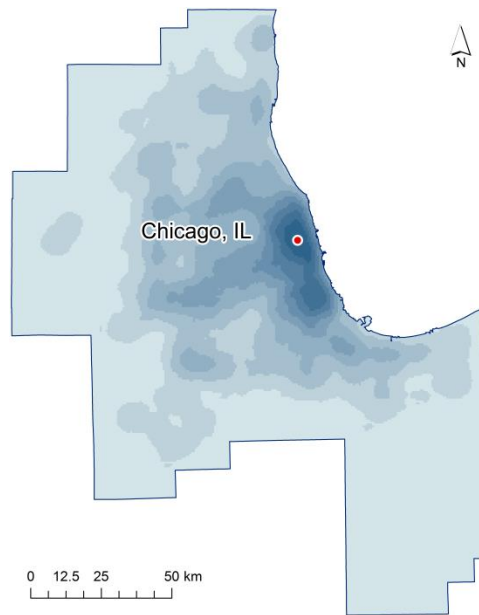


Figure 42 Road Density map for Chicago MSA road network, and the selected “center”.

Naturally, this method is most applicable to mono-centric cities that show a clear center. Although some cities have evolved to become poly-centric, our analysis shows that their road networks have often remained mono-centric, simply related to the fact that denser streets tend to locate in older areas of the cities. Even in a relatively young country as the U.S., only two cities out of the 50 cities studied did not have a clear center. In that case, a point between them is chosen as the center, for which the results are found to be still acceptable (as shown in Appendix F).

Having determined the “center”, the ring-buffer method is applied to the 50 urban road networks. The results of the process for Chicago MSA road network are displayed in Figure 43. Looking purely at the data points (i.e., the blue dots), the trend looks close to linear, but the power law fit (i.e., red line) clearly shows a systematic bias. Based on Figure 43, some may

claim that the plot is piece-wise linear, i.e. each part represents a power law and thus a fractal, albeit with different slopes or fractal dimensions. Further examination of the results, however, shows that the slope of the plot in Figure 43 is nowhere constant, i.e., even after selecting any number of points, adding another or more points (or removing them) changes the slope. In other words, the Chicago road network is neither a fractal nor a multi-fractal.

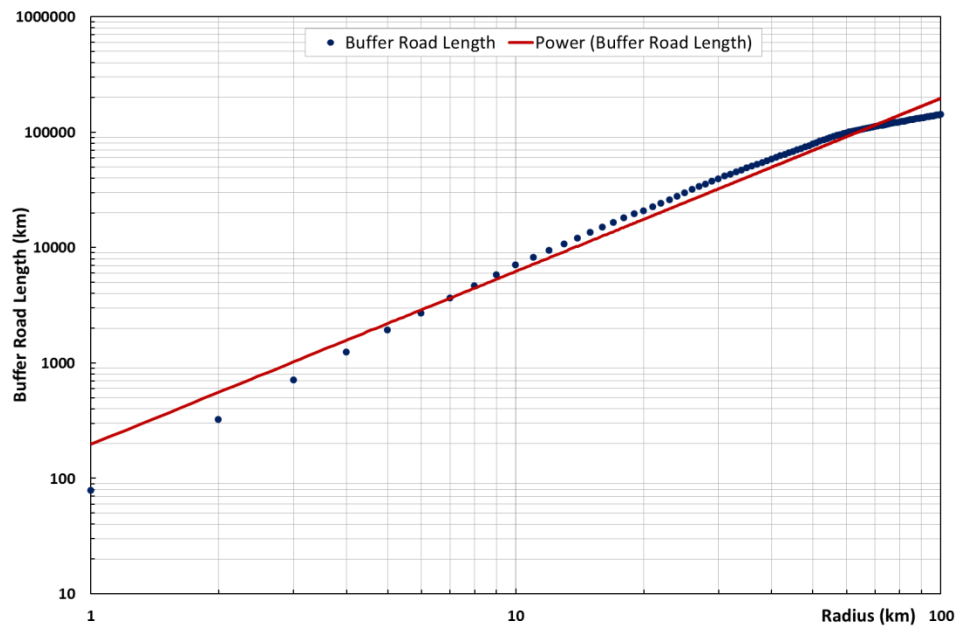


Figure 43 Log-log plot of buffer road length versus radius and power law fit for Chicago road network.

Similar steps are taken for all 50 U.S. urban areas chosen for the study. The majority of the diagrams show similar issue too. This fact supports the conclusion that the general assumption of the existence of a power law for any urban road networks is flawed. Therefore, the

universality of power law as the manifestation of the evolution of urban road networks, and as a result the sole existence of fractal properties, is rejected.

#### 5.2.4. Coupled Complexity

The question that naturally follows is: “Are we able to find a general rule that captures and explains the complex nature of urban road networks?” In order to answer this question, let us assume that the average density of a road network within a buffer of radius  $r$  around its center, as shown in Figure 44, is equal to  $\rho(r)$ .

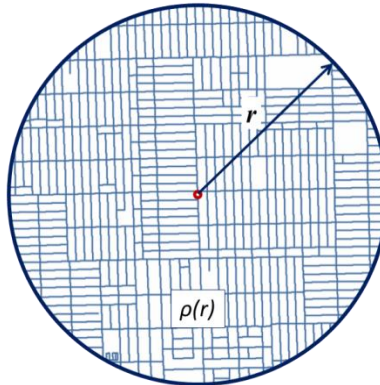


Figure 44 Buffer with radius  $r$  around the center of the road network.

The buffer area is given by:

$$A = \pi r^2 \quad \text{Eq. 5.4}$$

As a result, the total road length within the buffer with radius  $r$  can be written as:

$$N(r) = A \cdot \rho(r) = \pi r^2 \cdot \rho(r) \quad \text{Eq. 5.5}$$

The above relationship, despite its simple appearance, has a profound meaning. The first part of the right side,  $\pi r^2$ , is in fact a power law representing a fractal with the dimension of 2, similar to the Greek Cross or a uniform grid. This means that a given road network does in fact have an intrinsic component similar to fractal features, which represents some kind of scaling in our system and akin to many other studies (Batty, 2013b; Clark, 1967). It is, however, coupled with another component represented by  $\rho(r)$ .

What makes the above finding interesting is how these two components are coupled, which represents complexity at a higher level than what the power law alone offers. This presents the challenge of separating these two components ( $\pi r^2$  and  $\rho(r)$ ), thus isolating  $\rho(r)$ , in order to examine its properties.

#### 5.2.5. Grid Equivalency

To tackle this challenge, we recall that a grid network is represented by a power law of exponent 2, as we observed in Figure 44. This means that the appearance of  $\pi r^2$  in the Eq. 5.5 is equivalent to the existence of a uniform grid network. But, we also need a component that changes along  $r$  to represent  $\rho(r)$ . As a result, the combination can be represented by a non-uniform grid network, i.e., one in which the block size evolves with  $r$ , yet overall it stays equivalent to the real road network. By choosing an equivalent non-uniform grid network, the  $\pi r^2$  component will be represented by its grid nature, while the block size that is varying along  $r$  will represent the  $\rho(r)$  component.

In order to find out how to create such a grid network with varying block size, let us first consider a uniform grid network with block size of  $l$ . By isolating an intersection from this grid network, and drawing a hypothetical square of side  $l$  around that intersection, we obtain Figure 45.

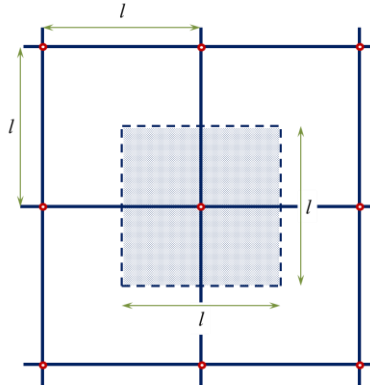


Figure 45 A portion of a uniform grid network with block size of  $l$ .

Using the above figure, we can calculate the total road length inside the shaded square, as shown in Eq. 5.6.

$$\text{Total length} = 4(l/2) = 2l \quad \text{Eq. 5.6}$$

Moreover, the area of the shaded square is equal to:

$$\text{Area} = l^2 \quad \text{Eq. 5.7}$$

As a result, the road density within the shaded square, which is also the road density for the whole uniform grid, is calculated to be:

$$\rho = 2l / l^2 = 2 / l \quad \text{Eq. 5.8}$$

This means that having the density  $\rho$  of a grid network, we can find its block size,  $l$ :

$$l = 2 / \rho \quad \text{Eq. 5.9}$$

This also means that if the average density of a given road network is known within an area, using Eq. 5.9 an equivalent grid network can be found for that area that has the same road density as the given network. Moreover, Eq. 5.9 highlights that the grid block size and the density are actually inversely proportional.

Having Eq. 5.9 in mind, we now recall that during the application of the ring-buffer method, we measured the average road densities within the consecutive rings with varying radii (i.e. as a function of radius  $r$ ). With those measurements, we can therefore calculate an equivalent grid block size for every single ring by using Eq. 5.9. We can then substitute the actual roads within each ring with their equivalent grids. This way, any given road network can be represented by an equivalent non-uniform grid network with radially-varying block sizes. This means that the block sizes of the equivalent grid network will change as a function of the distance,  $r$ , from its center, thus representing  $1/\rho(r)$  according to Eq. 5.9.

This process is applied to Chicago MSA road network, and its equivalent grid network with radially-varying block sizes is created, as shown in Figure 46.

#### 5.2.6. Verification of the Equivalent Grid

The ring-buffer method is then applied to the radially-varying equivalent grid created for Chicago MSA road network. Figure 47 shows the results for the equivalent non-uniform grid (red line) versus the real Chicago MSA road network (blue markers).



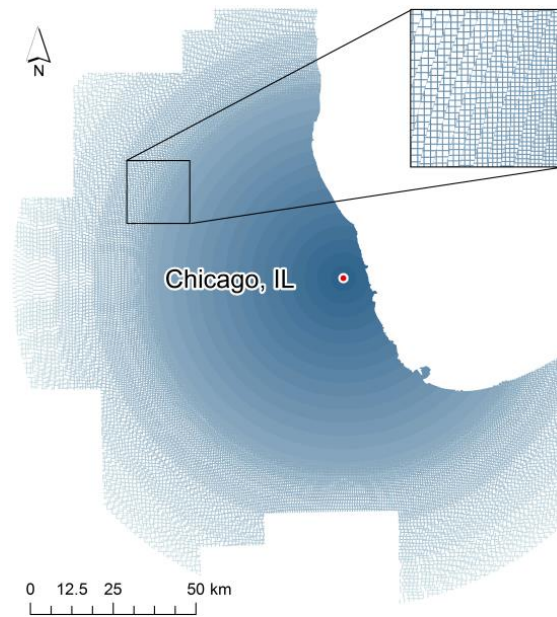


Figure 46 Radially-varying equivalent grid network for Chicago MSA road network.

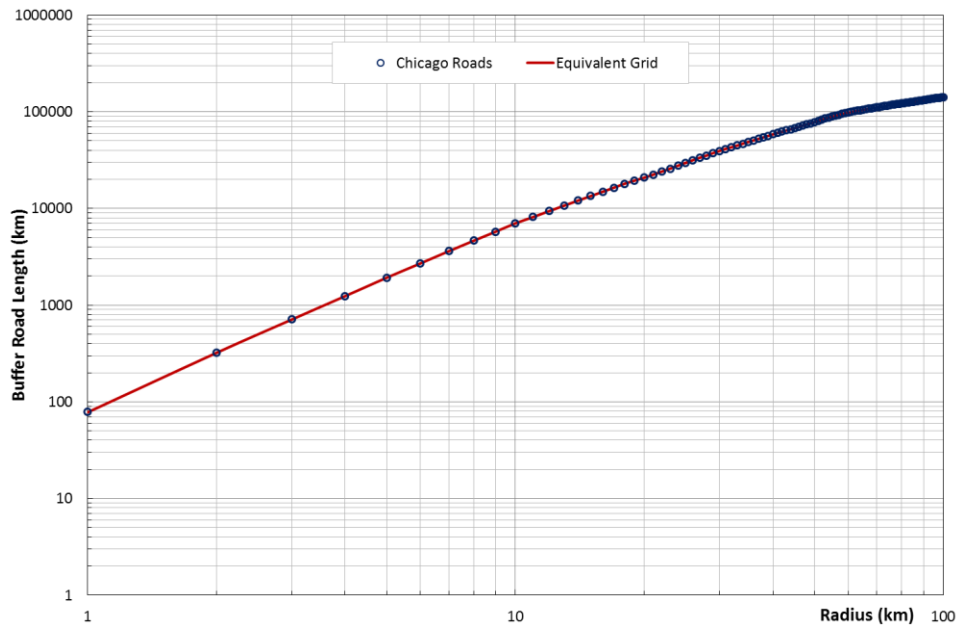


Figure 47 Ring-buffer results for Chicago MSA road network and its equivalent grid.

The above figure shows that the results are extremely close. This confirms that the approach developed is valid, i.e. a grid network whose properties vary radially (as a function of  $r$ ) has been found that is equivalent to the real network with respect to the ring-buffer method.

#### 5.2.7. Revealing the Functional Form for the Ring Road Density

As mentioned before, the equivalent grid network already represents the  $\pi r^2$  component in Eq. 5.5 through its grid nature. As for the representation of the  $\rho(r)$  component, we note that it is the block size, or better to say the inverse of the block size, of the equivalent grid network that varies as a function of  $r$ . This means that if we plot the variation of the inverse of the grid block size versus  $r$ , it will reveal the form of the  $\rho(r)$  component.

To do so, at first a log-log plot of the inverse of grid block size versus radius is created for Chicago's equivalent grid network, and a power law fit to the data is performed, shown in Figure 48.

Figure 48 clearly shows that the data does not follow a power law, which is another proof that a simple power law does not exist.

Several other types of fits are also performed on the data, among which the exponential fit is found to be the best. As shown in Figure 49, semi-log plot is used to plot the data and its corresponding exponential fit, which clearly fits well.

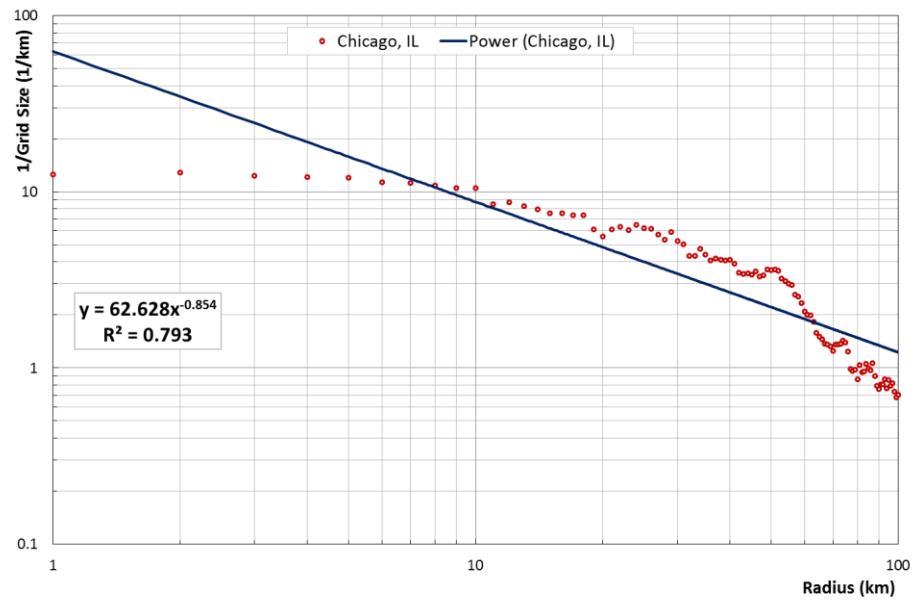


Figure 48 Log-log plot of the inverse of the equivalent grid block size for Chicago, IL road network versus radius and the power law fit.

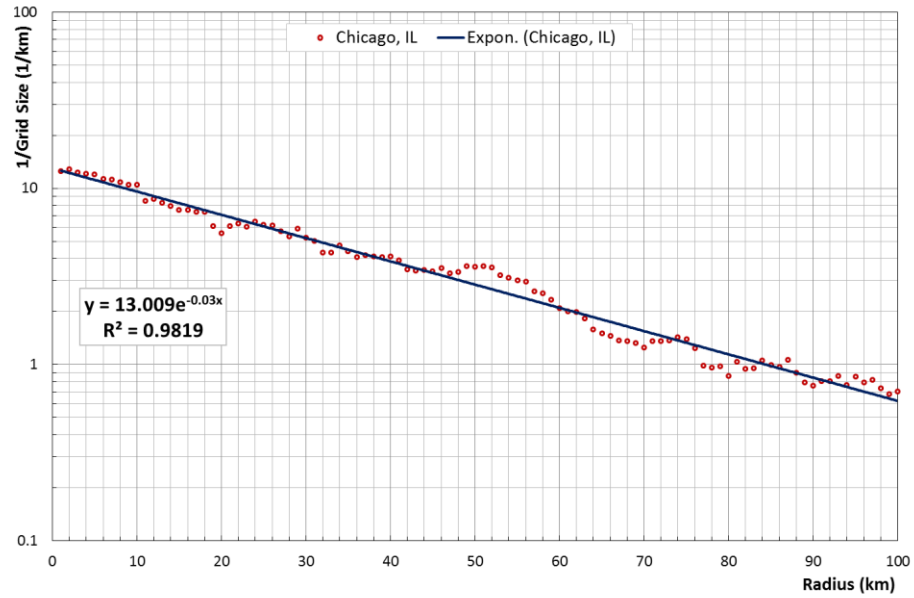


Figure 49 Log-log plot of the inverse of the equivalent grid block size for Chicago, IL road network versus radius and the exponential fit.

The whole process presented in this part has two main outcomes. One is that we were able to decouple the mixed complexity of the urban road networks and reveal that in fact it consists of a combination of two different components; one with a power law or fractal nature, coupled with another component of unknown form. Moreover, we were able to devise a novel method to reveal the nature of the second component, which in the case of Chicago MSA road network turned out to possess an exponential form.

The above steps are applied to the selected 50 U.S. urban road networks. It is found that the second component for some networks follows an exponential form, similar to Chicago, IL, shown in Figure 49, while for some others it indeed exhibits power law properties, e.g. Austin as shown in Fig 50, and some others show logarithmic trend, e.g. Los Angeles as shown in Figure 51.

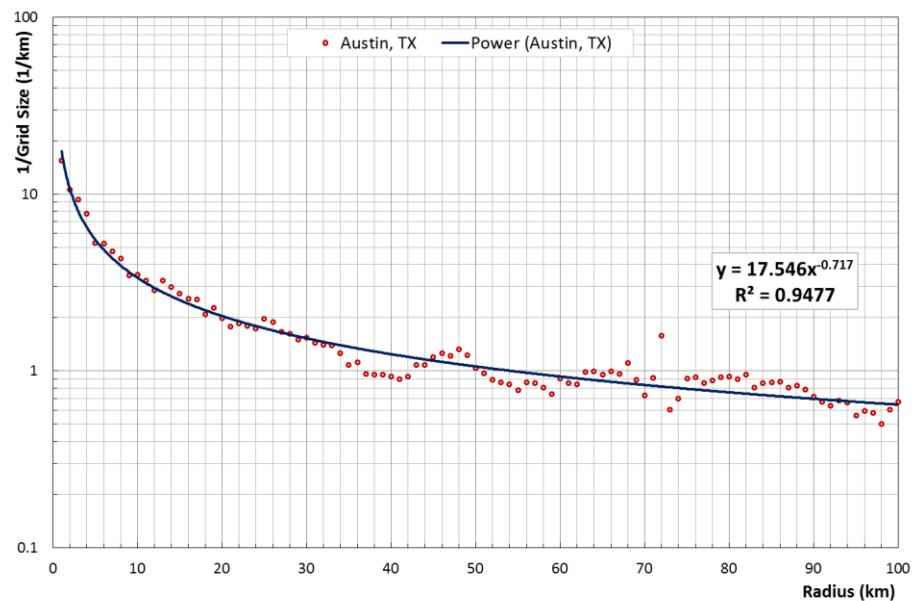


Figure 50 Variation of the inverse of grid block size versus radius for Austin, TX with a power law fit.

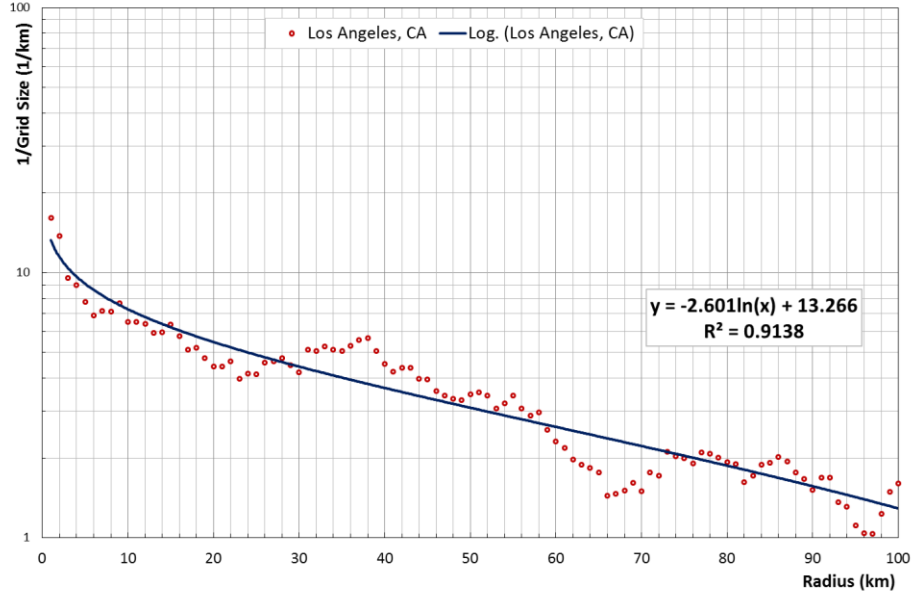


Figure 51 Variation of the inverse of grid block size versus radius for Los Angeles, CA with a logarithmic fit.

#### 5.2.8. Deriving the Functional Form for the Total Toad Length $N$

The ultimate objective of the application of the ring-buffer method to an urban road network is to come up with an expression for  $N(r)$ , which is the total road length within a buffer of radius  $r$  around the center. As explained before, Eq. 5.1 (i.e.,  $N(r) = a \cdot r^D$ ) suggests power law property for features that are fractal in nature. Based on the results from this work, we are now in a position to reject it as a universal rule representing urban road systems. Instead, our observation has been that each urban road networks has its own inner mixed complexity, which may or may not be the same as another one. Because of that, investigation of the nature of the complexity of a given urban road network needs to be performed on its own.

As an example, we take another look at the outputs of the application of ring-buffer method to Chicago MSA road network. In accordance with Eq. 5.1, we present the expression developed in Eq. 5.5 here again:

$$N(r) = \pi r^2 \cdot \rho(r) \quad \text{Eq. 5.5}$$

Moreover, we now know that in addition to  $\pi r^2$  that follows a power law, for the case of Chicago MSA road network  $\rho(r)$  follows an exponential trend of the form shown in Eq. 5.10.

$$\rho(r) = a \cdot e^{-br} \quad \text{Eq. 5.10}$$

which means:

$$N(r) = \pi r^2 \cdot a \cdot e^{-br} \quad \text{Eq. 5.11}$$

The final goal is to find a fit to  $N(r)$ , through which the values of the parameters  $a$  and  $b$  can be found. Performing a fit to Eq. 5.11, however, is difficult due to the fact that it consists of a combination of two different trends. But since the first component of Eq. 5.11, i.e.  $\pi r^2$ , does not include any parameters, the whole equation can be divided by the  $\pi r^2$  component to obtain a relationship with only the second component remaining on the right hand side:

$$N(r)/\pi r^2 = a \cdot e^{-br} \quad \text{Eq. 5.12}$$

#### 5.2.9. Calibration of the Formulation for the Total Toad Length $N$

Now a fit can be performed to Eq. 5.12 to find the values for parameters  $a$  and  $b$ . Due to the exponential nature of the right hand side, we use a semi-log paper to plot the left hand side (which is essentially the buffer road density) versus radius, with the expectation to observe an exponential pattern. The resulting diagram for Chicago MSA road network is shown in Figure

52. We see that the data points clearly follow an exponential trend, as expected, from which parameters  $a$  and  $b$  are found.

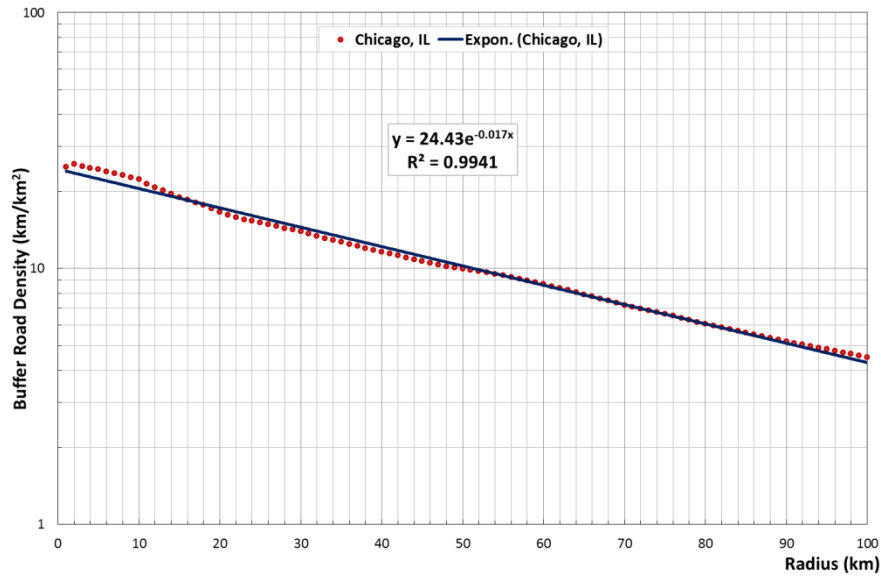


Figure 52 Semi-log plot of buffer road density for Chicago, IL with an exponential fit.

Similar procedure is repeated for all the selected 50 U.S. urban road networks with satisfactory results. The outputs are included in Appendix F. The results for some urban road networks indeed followed power law, e.g. Austin, TX as shown in Figure 53, while for some others showed logarithmic trend best, e.g. Los Angeles, CA as shown in Figure 54.

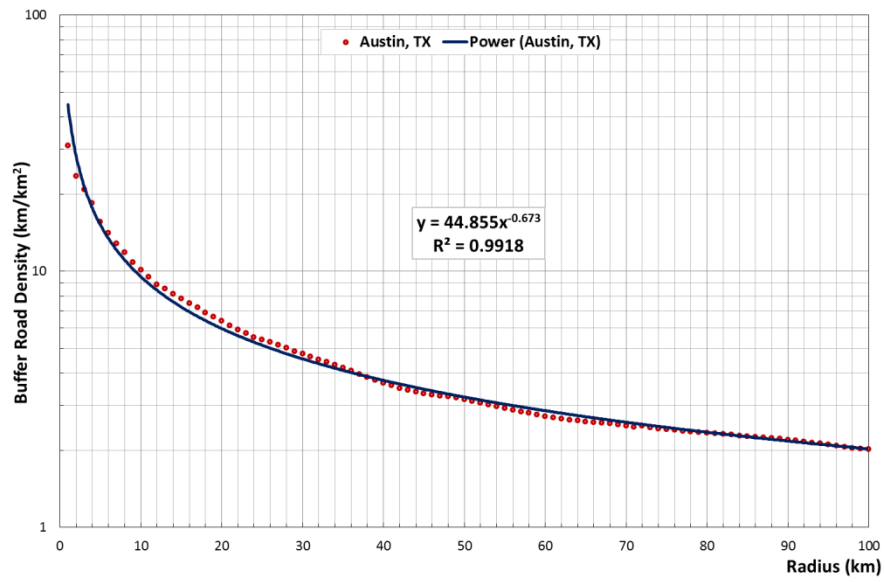


Figure 53 Semi-log plot of buffer road density for Austin, TX with a power law fit.

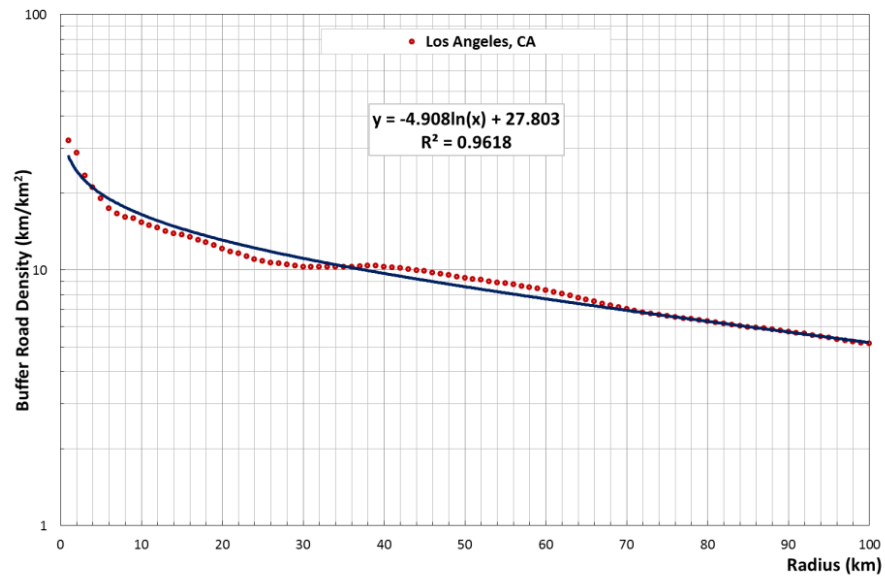


Figure 54 Semi-log plot of Buffer Road Density for Los Angeles, CA with a logarithmic fit.



### 5.3. Results and Discussion

Based on the methodology developed in this study, we now understand that the inner complexity of urban road networks consists of two components that are intertwined: one is the power law component, which is a manifestation of the fractal nature common in all road networks. The other one, however, is a property that is specific to the urban system under study, and thus differentiates between various road networks, and therefore needs to be characterized separately for any given urban system. The methodology developed in this study is able to decouple this mixed complexity of urban road networks.

The proposed ring-buffer method is applied to 50 U.S. urban road networks. Complete results are provided in Appendix F. The results clearly show that there are three possible trends for the second component representing the complexity of urban road networks; exponential, power law, and logarithmic. Overall, the results confirm that the methodology developed in this study is sound, efficient, and robust.

As for the exponential trend, e.g. Figure 52 for the case of Chicago MSA road network, the total road length  $N$  within a buffer of radius  $r$  can be written in the following general form:

$$N(r) = \pi r^2 \cdot a \cdot e^{-br} \quad \text{Eq. 5.11}$$

As mentioned before, the  $\pi r^2$  part represents the hidden fractal nature of road network under study, in this case Chicago MSA's. This is expected to some degree, because in general most urban road networks have grid elements imbedded in them, a property that is fractal in

nature, as confirmed by Figure 41. In other words,  $\pi r^2$  represents the scaling property of the road network.

More interestingly, however, is the second part, i.e.  $a \cdot e^{-br}$ , that represents the road density of the network. It is easily understood that  $a$  is the maximum road density of the network (at  $r = 0$ ). This also means that the larger  $a$  is, the larger  $N$  value will be, i.e. they have a direct and positive linear relationship. In other words, given  $r$  and  $b$  values,  $a$  represents how compact or sparse the road network is. Because of that,  $a$  can be considered as an overall *compactness* or *density index* for urban road networks. In comparison,  $b$  has a different impact on  $N$ . We note that  $b$  appears with a negative sign in the exponent of the exponential function. This means that for a given set of  $a$  and  $r$  values, the larger  $b$  is, the smaller  $N$  will be. On the other hand, and unlike  $a$ ,  $b$  has a non-linear impact on  $N$ . As a result,  $b$  can be interpreted as a *decay index*, i.e. how fast the rate of change of  $N$  value (i.e. the road density value) drops, or how fast the equivalent grid size increases.

As for the power law trend, e.g. Figure 53 for the case of Austin MSA road network, the total road length  $N$  within a buffer of radius  $r$  can be written in the following general form:

$$N(r) = \pi r^2 \cdot a \cdot r^{-b} \quad \text{Eq. 5.13}$$

Again, and as mentioned before, the  $\pi r^2$  part represents the hidden fractal nature of road network under study, in this case Austin MSA's. Therefore,  $\pi r^2$  represents the scaling property of that road network.

Moreover, similar to the previous part, the second part, i.e.  $a \cdot r^{-b}$ , that represents the road density of the network, is also a form of power law. Once again, it is easily understood that  $a$  is a

representative of the maximum road density of the network (at  $r = 1$ ). This also means that the larger  $a$  is, the larger  $N$  value will be, i.e. they have a direct and positive linear relationship. In other words, and similar to the case of the exponential component, and given  $r$  and  $b$  values,  $a$  represents how compact or sparse the road network is. Because of that,  $a$  can again be considered as an overall *compactness* or *density index* for that urban road network. In comparison, moreover,  $b$  has a different impact on  $N$ . We note that  $b$  appears with a negative sign in the exponent of  $r$  in the right hand side of Eq. 5.12. This means that for a given set of  $a$  and  $r$  values, the larger  $b$  is, the smaller  $N$  will be. On the other hand, and unlike  $a$ , again  $b$  has a non-linear impact on  $N$ . As a result,  $b$  can be interpreted as a *decay index*, i.e. how fast the rate of change of  $N$  value (i.e. the road density value) drops, or how fast the equivalent grid size increases.

Moreover, for the logarithmic trend, e.g. Figure 54 for the case of Los Angeles MSA road network, the general form for the total road length  $N$  within a buffer of radius  $r$  can be written as:

$$N(r) = \pi r^2 \cdot [-b \cdot \ln(r) + a] \quad \text{Eq. 5.14}$$

Again, similar to the previous cases, the  $\pi r^2$  part represents the hidden fractal nature of Los Angeles MSA's road network, and therefore represents its scaling property.

The second part, i.e.  $[-b \cdot \ln(r) + a]$ , on the other hand, represents the road density of the network, which follows a logarithmic trend. Even though Eq. 5.13 looks partially different from Eq.s 5.11 and 5.13, it essentially conveys the same meaning, i.e. that  $a$  is the density of the network (at  $r = 1$ ). This also means that  $a$  and  $N$  have a direct and positive linear relationship, in the sense that the larger  $a$  is, the larger  $N$  value will be. Similar to the case of the exponential and power law versions, and given  $r$  and  $b$  values, again  $a$  represents how compact or sparse the road

network is. This means that  $a$  can again be considered as an overall *compactness* or *density index* for this group of urban road networks. Similar to the previous cases, the impact of  $b$  is still the same but with a different look. In the sense that due to its negative sign, and for a given set of  $a$  and  $r$  values, the larger  $b$  is, the smaller  $N$  will be. Moreover, due to the fact that  $b$  is the coefficient of  $\ln(r)$ , it again has a non-linear impact on  $N$ . Therefore, and once again,  $b$  can be interpreted as a *decay index*, i.e. how fast the equivalent grid size increases, or how fast the  $N$  value (or the road density value) drops.

The overall observation is that even though three different patterns are observed for the way  $N$  values change for different U.S. urban road networks, the parameters  $a$  and  $b$  obtained from the calibration of the fits continue to have similar meanings.

Comparing the above three patterns, we see that they represent different rates of decay in the urban transportation networks, where the exponential fit is the fastest, followed by the power law and finishing with the logarithmic fit. Another difference is that the logarithmic trend, which is slow by nature, also exhibits an “additive” property, as opposed to the “multiplicative” nature of the two other fits.

Figure 55a illustrates the distributions of the density index within the three categories of cities. It can be seen that cities such as Minneapolis, Boston, and Chicago have denser centers as compared to cities such as Nashville, Charlotte, and Miami, respectively.

Moreover, Figure 55b demonstrates how the decay index varies among the same cities, based on which we see that in cities like Las Vegas, Portland, and Denver, the road networks’ densities fall faster than in cities such as Sacramento, Buffalo, and San Francisco, respectively.

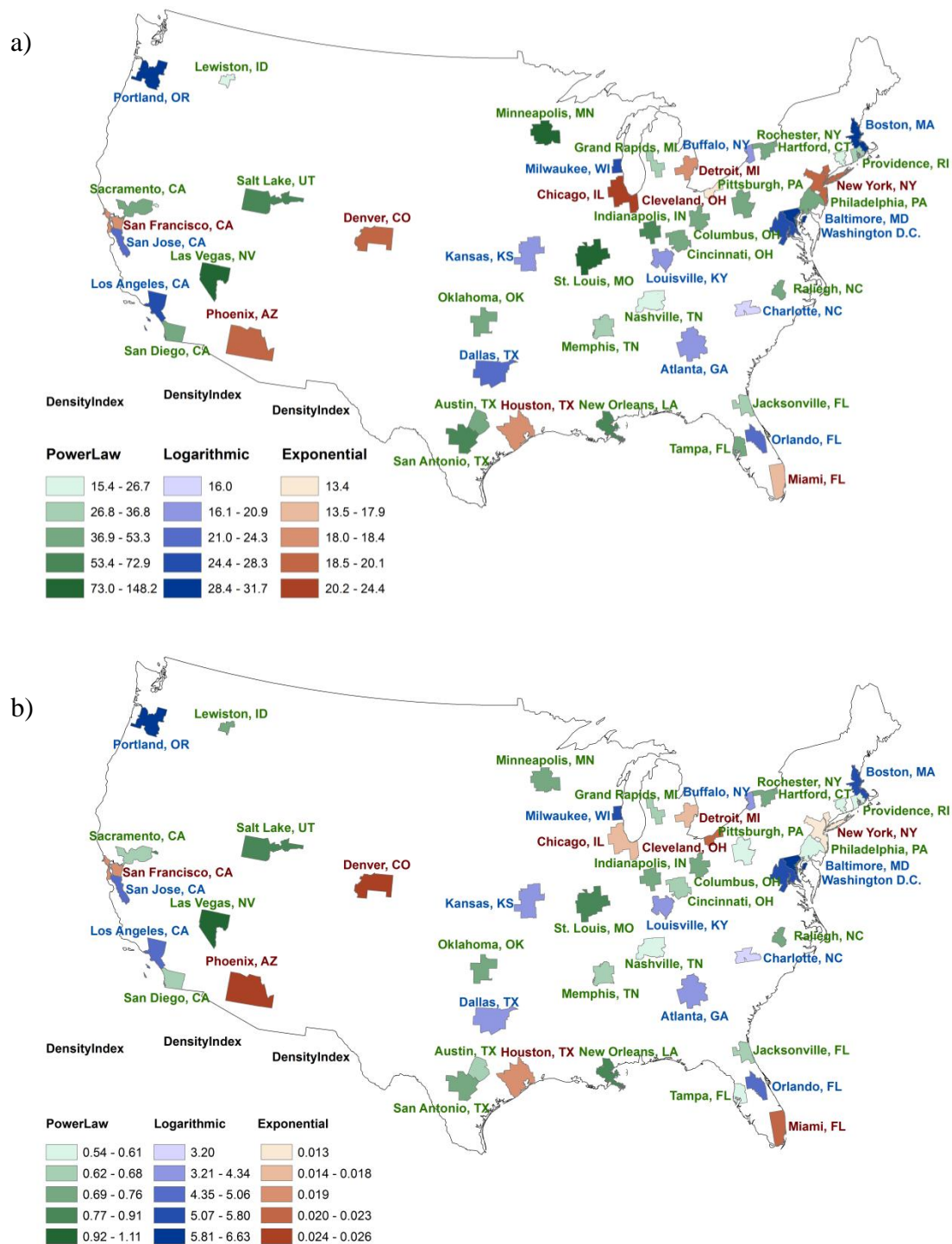


Figure 55 Spatial Distributions of the a) Density Index, and b) Decay Index.

## 5.4. Conclusions

In the past, many studies have been done with the final conclusions that the transportation networks (as well as many other components) of urban systems follow power law, and thus are fractals (Shen, 2002; L. M. A. Benguigui, 1995; Kim et al., 2003; Lu and Tang, 2004).

In this study, we developed a methodology for the application of a ring-buffer method as a tool for analyzing complex urban road networks. Even though the mathematical foundations of this method has been originally developed based on the assumption of the existence of a power law for the features being studies, thus proving that they are fractal, we used it to reject that assumption as a universal rule for urban road networks. Moreover, we used a novel approach to decouple the mixed complex nature of urban transportation systems, through which we concluded that such features possess characteristics that are influenced by two components that are mixed. One is a power law with exponent 2 that captures the fractal aspect, or scaling property, of the road networks. The other component can come in three different forms, either exponential, or another power law, or logarithmic, thus separating the urban road networks to three classes based on their complex nature.

Nevertheless, for any of the cases, two parameters are identified. One that has a direct and positive linear relationship with the total length of the road network, and because of that can be considered as a *compactness* or *density index*. And the other one that has a negative nonlinear inverse impact on the total length of the road network, and thus can be considered as a *decay index*. Using those two indices, various urban road networks can then be properly classified.

In short, through rigorous computational as well as analytical work, we show that regardless of the choice of the city, urban road networks possess similar attributes while also exhibit unique properties at the same time. More specifically, our study rejects the universality of power law as a means of describing the evolution of urban road networks, something that has been suggested by many researches in the past. Instead, we show that urban road networks possess a combination of two characteristics; a scaling component related to the square of the radius, as well as a second component that can follow a number of trends (exponential, or logarithmic, or power law).

## **6. APPLICATIONS AND EXTENDED RESEARCH**

### **6.1. People versus buildings: Characterization and Correlation**

#### **6.1.1. Introduction**

In the previous chapters we discussed the fact that the evolution and spread of an urban system and its components; whether it is its transportation network, or buildings, or even distribution of people themselves, evolve during its life that could be for decades or perhaps centuries. Moreover, present morphology and demographic characteristics of an urban system is the aggregated outcome of all actions and interactions that have occurred between its own components with one another or with external factors during that period. An urban system starts with a small settlement or development that expands over time in accordance to various factors affecting its direction and speed of growth and subject to the constraints imposed on it. This means that any urban system has a starting point around which it has evolved.

Even though that central point might gradually move as the system readjusts the way it functions, its location at any point in time can easily be known by looking at the distribution of the buildings within its greater urban system. Usually that falls where the city's central business



district (CBD) is, especially in North-American cities. On the other hand, the distribution of the population within an urban system does not necessarily match the spread of its buildings. One reason could be that people tend to live more in areas where the rents or house prices are comparatively lower. This means that there are more people living in the suburbs than in downtowns where housing is more expensive.

Yet, buildings and population are naturally linked, since buildings are physical places of origins or destinations for people, and both should be related at some level. Indeed, referring back to the idea that cities possess inherent organization (Batty, 2008b), we can reasonably expect that the two integral components of any urban system, i.e. its people and buildings, can be shown to be correlated.

As for the complexity of the building component of a city, it can be justified that the construction of buildings and their spread resembles the expansion of living organisms. They start from a central area, and then spread and expand in different directions while avoiding natural, as well as man-made, barriers. Moreover, since a building not only spreads horizontally, but also vertically, and because its footprint alone does not capture that characteristic, total building gross floor area (equal to the footprint multiplied by the corresponding number of floors) is the proper attribute for it in any study.

Moreover, instead of population alone, population+employment data should be selected to represent the people. This essentially means that population and employment numbers are summed together. The rationale is that downtown areas tend to host few households but many jobs, while the opposite is true as we move towards suburbs. In comparison, downtowns are

usually centers of financial and commercial activities, which attract many people for work or business, while the number of employment opportunities falls as we go away from the downtown.

By choosing the above attributes, therefore, we are suggesting that the buildings (i.e. a *supply*) are constructed to meet a *demand*, which is mostly (though not completely) generated by the needs to live and/or work.

The characteristics of different components of a given urban system have been a matter of interest in recent time (Shen, 2002; Terzi and Kaya, 2011), more specifically about the population (Appleby, 1996; Chen, 2010b; Lu and Tang, 2004) and buildings (Frankhauser, 1998a; Batty et al., 2008). Such studies have showed that scaling patterns exist within the spatial distributions of these components, which manifest itself in the form of a power law. That, as we learned in previous chapters, shows that those components do have complex nature. While the characteristics of population and also buildings have been studied to some degree before, new technologies as well as more disaggregate datasets, and in particular extensive Geographic Information Systems (GIS) tools and spatial data, now allow us to perform a more detailed analysis of their complex relationship.

Based on the above discussion, the objective of this part is to employ the ring-buffer technique, that was developed in Chapter 5, toward studying the characteristics of, and relationship between, population+employment and building gross floor area, as proxies for people and buildings, respectively. As a case study, Chicago, one of the oldest and most populous cities in North America, was chosen.

Similar to the studies presented in previous chapters, this work fits within the overall effort to look at, and analyze, cities and their constituting components as complex systems (Batty, 2005; Bettencourt et al., 2010; Luis M. A. Bettencourt et al., 2007; Kennedy, 2011). Taking a complex analysis approach provides the opportunity through which we can analyze and compare different urban systems components such as people and buildings.

### 6.1.2. Methodology

#### *6.1.2.1. The Ring-Buffer Method*

The procedure for applying the ring-buffer method is the same as explained in Section 5.2.3. The only difference is how to select the center. In this study, buildings are chosen as the main feature, and therefore the place where they have the highest concentration is chosen as the “center”. Moreover, unlike a road network that is mostly planar, buildings are in three dimensions. In fact, their third dimension, i.e. height, is usually longer than the other two dimensions, especially in high-rise buildings. That is why the method used to determine the center for road networks is not applicable here.

### 6.1.3. Application

#### *6.1.3.1. Case Study: Chicago*

In this part, we study the spread of people and buildings in one of the oldest cities in North America, i.e. Chicago. The hypothesis is that not only they have inherent order, but also that they are highly correlated.

What made Chicago a unique choice was not only its long history during which it had experienced different periods of urban evolution, but also its unique morphology. Chicago is restricted on the east side by Lake Michigan (Figure 55), which means it has only been able to expand towards the west. Moreover, two branches of Chicago River run through it from north and south which join together to the west of the center of the city and then run eastward towards Lake Michigan. Such natural constraints on the evolution of its urban system, in addition to the man-made barriers such as its two international airports, offer intriguing challenges against the task at hand.

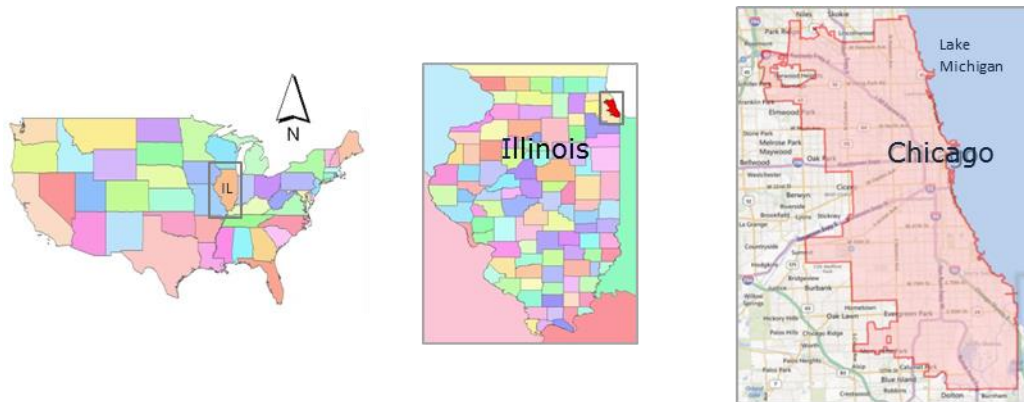


Figure 56 Location Map for Chicago, Illinois. (Background: Bing Maps Hybrid)

Moreover, Chicago has a well-defined center, called the “Loop”. The “Loop” is Chicago’s Central Business District (CBD), hosting the Chicago Mercantile Exchange, as well as being the city’s administrative center. It is a well-defined 1.0 km x 1.2 km rectangle surrounded

by freeways and partially the Chicago River (Figure 56). For that reason, the “Loop” seemed to be a natural choice for the “center” (or the “heart”) of the city.



Figure 57 The “Loop”, CBD of Chicago (Background: Bing Maps Hybrid).

Having done so, rings were then created around it with radii from 1 km to 21 km, in increments of 1 km (Figure 57). As shown, the physical or natural barriers to the city’s expansion, such as the lake, rivers, valleys, airports, etc., have been cut out of the rings.

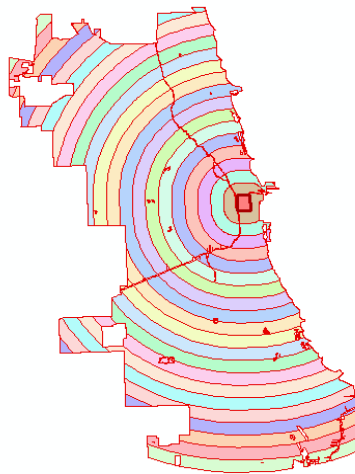


Figure 58 Rings, splitting Chicago into rings from the center.

#### 6.1.4. Data

The data for this study was obtained from different sources, as shown in Table 1.

Table 1 Data sources

Data	Source
Census Tracts and Population Data	U.S. Census Bureau, American FactFinder
Building footprints, Land-Use, and Employment Data	Chicago Metropolitan Agency for Planning

Having obtained the data for both urban system components, their quantities in each ring and the areas of the rings are calculated. That information is then used to calculate the densities of those components for buffers around the center at the selected radii (Figure 58).

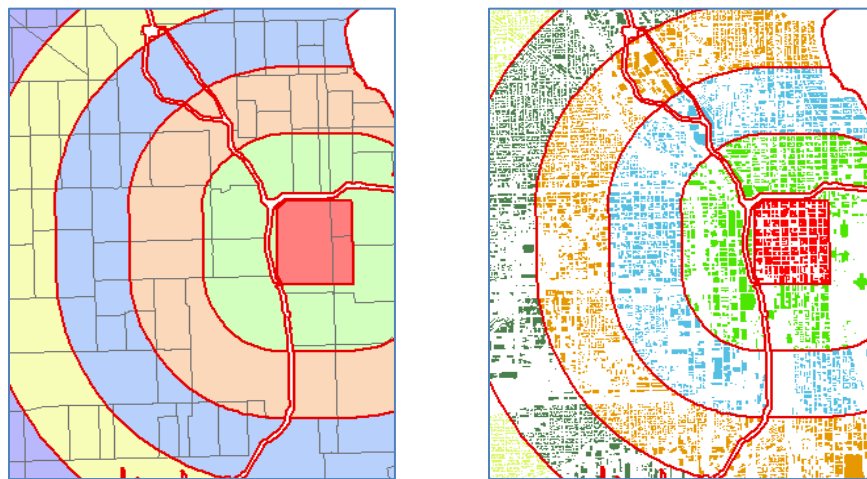


Figure 59 Chosen urban components within equi-distance rings around the Center.  
a: Population+Employment      b: Gross Floor Area

### 6.1.5. Results

In order to compare the two components, their densities are calculated for buffers at the radii from 1 km to 21 km at increments of 1 km. The results are plotted in Figure 59. The diagrams provide an opportunity to observe the variations in the overall cumulative (average) value of the given components as a function of the distance from the center.

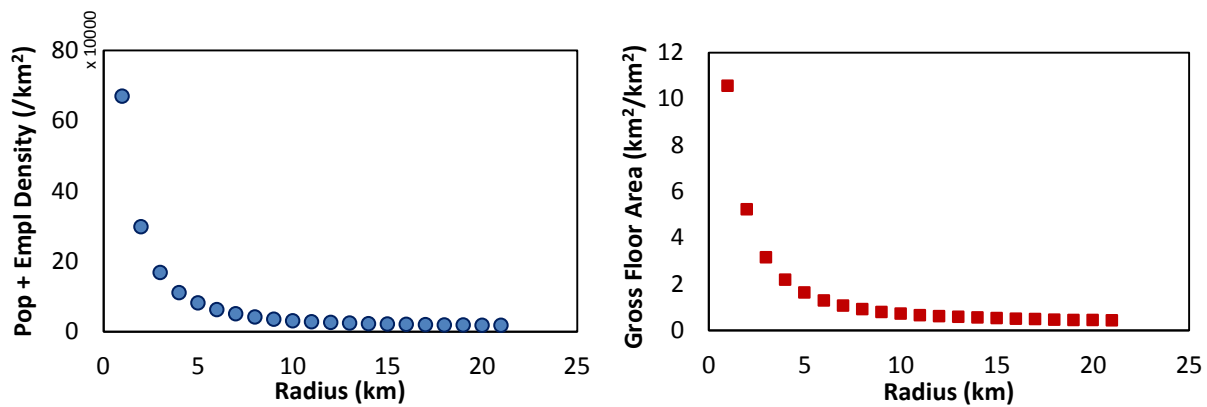


Figure 60 Plots of component densities vs. radius.  
a. Population+Employment      b. Gross Floor Area

The initial observation is that both the above plots seem to exhibit similar properties, though not exactly the same. Nevertheless, the population+employment density as well as the gross floor area density figures show power law patterns. As mentioned before, the presence of a power law is a manifestation of scaling property, which is a signature of complex systems. In accordance to power law properties, both Figures 59a and 59b show that the density values for them are expectedly high at the center, and then drops sharply as one moves away from the center. Moreover, the rates of change of the slopes for both plots gradually start decreasing,

demonstrating the reduced sensitivity of the population+employment as well the gross floor area densities with respect to the distance from the center. This is also expected; because the further away from the center, the less percentage change in the radius.

To further investigate the existence of the power law, the same data are redrawn on log-log diagrams, which transform power laws into straight lines (Figure 60).

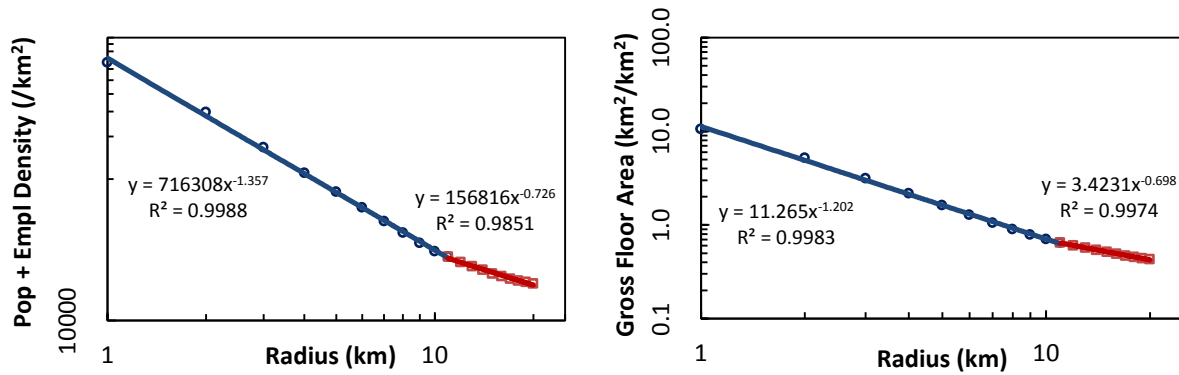


Figure 61 Log-log plots of components densities vs. radius.  
a. Population+Employment      b. Gross Floor Area

As a mega city, Chicago has absorbed many smaller urban areas within itself during its evolution history, and therefore changes were expected in the patterns observed over the selected range of the radii. The log-log plots indeed confirmed this expectation, as there are break points in the linear trends in the plots, both at the same distance from the center, which one can observe in Figure 60. Nevertheless, using the piece-wise linear patterns observed in the log-log plots, the fractal dimension values for the chosen components of the city were extracted. Also, statistical analyses were performed on the data and the results are presented in Table 2. The  $R^2$  and t-stat values show that all the results are statistically significant.



Table 2 Scaling properties of component densities

Component	Radius (km)	Fractal Dimension	St. Dev.	R <sup>2</sup>	t-stat	Significant?
<b>Population+Employment</b>	1 to 10	1.36	0.02	0.99	77	Yes
	11 to 21	1.73	0.03	0.98	22	Yes
<b>Gross Floor Area</b>	1 to 10	1.20	0.02	0.99	66	Yes
	11 to 21	1.70	0.02	0.99	45	Yes

#### 6.1.6. Analysis

Both the log-log plots of population+employment and gross floor area densities show very well-defined piece-wise linear relationships, which are signs of the existence of scaling property, which in turn is a signature of complex properties.

Moreover, the linear trends start from the center and move outwards up to the radius of 10 km, at which the slopes of both population+employment and gross floor area curves change simultaneously. Interestingly, the location of the change, which appears in both log-log diagrams, corresponds to the boundary of old Chicago City with old Cicero Township, which are now completely merged. This fact explains the sudden, yet similar, changes in the trends of both log-log plots in Figure 60, as well as the ability of the method to capture the hidden characteristics of Chicago urban system.

Moreover, the diagrams show that the rates of change of both densities have slowed down beyond the 10-km radius, which reflect the fact that after that point the sensitivities of the population+employment and gross floor area densities with respect to the distance to the center

of the city have fallen, i.e. people and businesses are less reactive to a slight change in the distance to the downtown area after that point. Nevertheless, the linear trends of both diagrams continue after the 10 km radius, though with different slopes.

In order to further investigate the similarity between the population+employment and gross floor area densities, the corresponding values are plotted against each other (Figure 61), which clearly shows linear relationship between them with a significant  $R^2$  value of 0.997.

This confirms our hypothesis that the two different-in-nature components of the urban system are indeed strongly correlated. Moreover, one would appreciate that the fractal dimensions of the population+employment and the gross floor area densities are also very close. This observation also points to the high degree of similarity between the two.

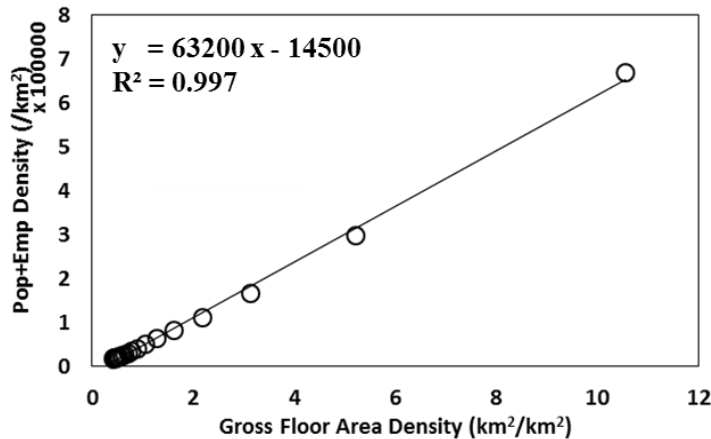


Figure 62 Correlation between Population+Employment and Gross Floor Area Densities

#### 6.1.7. Discussion

The two important components of the urban system, population+employment and building gross floor area, show strong similarities with one another. Moreover, their fractal dimensions are close. Although a further investigation is necessary, this result seems to attest the presence of an equilibrium between the *supply* (i.e. buildings) and the *demand* (i.e. people) within that range.

The patterns of both diagrams therefore correspond to the fact that the further one moves away from the center of an urban system, the less dense it gets in terms of population+employment and building gross floor area, something which is expected. Moreover, their rates of change, expectedly, are higher at the beginning but slow down quickly as the distance increases. This, again, is the exhibition of the power law, which is a representative of fractal behavior.

Overall, the results strongly support the hypothesis that the two components that are studied, i.e. population+employment and gross floor area, exhibit scaling properties, and thus are complex in nature, as demonstrated by the presence of power law relationships.

Nevertheless, not all fractals are exactly the same, and as such each possess its own characteristics, including its own fractal dimension. Sudden changes in the behavior of these fractal entities can enable one to identify where the inherent characteristics of a system have changed. This could be a clue to the causes behind such changes, which can then be used to identify the shortcomings or deficiencies of the system.

Despite the old history of city of Chicago, both chosen components show fairly similar patterns. For example, they both showed a change in their trends where the old boundary of the

city used to be. This could be used as a tool to identify hidden underlying attributes of an urban system.

The presence of a power law here, unlike in road systems, is interesting and likely related to the fact that buildings are not constrained in two-dimensional space. Indeed, buildings have a third dimension, and an increase in demand can therefore be accommodated by building upwards.

#### 6.1.8. Conclusion

The work presented in this article employed the simple yet efficient ring-buffer fractal approach towards the identification, analysis, and comparison of the characteristics of the components of an urban system. The results showed that the ring-buffer method is capable of exposing the hidden features of a city, even an old and diverse city such as Chicago with its unique physical and topological barriers.

The study was also able to achieve its objectives, namely: to analyze the characteristics of the two urban system components, i.e. population+employment and gross floor area, of Chicago; to show the similarities between the fractal representations of those components; and to demonstrate that the two components, despite their different natures, are strongly correlated.

The presence of a power law is also interesting and it is likely related to the fact that building systems have a third dimension that can accommodate growing demand, unlike transport systems as we saw in previous chapters.

A further expansion of this work could be the application of the method used in this study to other cities, so that the results can be compared and analyzed and the findings can be used to improve the quality of the observations and conclusions from this fractal approach. This is a project that is currently under way in which world cities with different regulations are being studied. An example is Paris, where regulations are in place that prohibits buildings from being built too high, something that is expected to show in the results.

Moreover, the approach can be used to explore the evolution of urban complex systems through time, i.e. temporal analysis, which could help in following their evolutionary paths and analyze the impacts of natural or man-made events on how they are shaped today.

The accuracy of complex analysis of urban systems not only depends on the appropriateness of the methods employed, but also on the quality of the data used. The reliability of analyses that involve non-stationary subjects, such as people (population, as well as employment) can greatly be improved if the advances in mobile technology are integrated with the data collection process (Tilahun and Levinson, 2011).

Overall, this approach could potentially be used towards a better understanding of how a city, as a complex system, works and how its intertwined components can be studied and improved.

## **6.2. Development and Application of the Pedestrian Environment Index (PEI)<sup>1</sup>**

### **6.2.1. Abstract**

The objective of this work is to develop a new and easily computable measure of pedestrian-friendliness for urban neighborhoods that makes the best use of the available data and also addresses the issues concerning other models in use. The Pedestrian Environment Index (PEI) is defined as the product of four components representing the Land-use Diversity (based on the concept of entropy), Population Density, Commercial Density, and Intersection Density. The final PEI is bound between 0 and 1 and it uses data that is typically readily available to planners and MPOs (metropolitan planning organizations). The results of this method is region-specific, i.e. they are comparable only between the zones within the given study area. As a case study, the city of Chicago is analyzed at the sub-TAZ (Traffic Analysis Zone) level. The results agree closely with the expectation of pedestrian friendliness across different parts of the city. Possible extensions are also listed, including a further study to determine statistical relationships between the PEI and common socio-economic characteristics. The method can also be further improved should more types of data become available.

---

<sup>1</sup> This section is an authorized reproduction of the recently published paper by Peiravian et al. (2014): Peiravian, F., Derrible, S., Ijaz, F., 2014. "Development and application of the Pedestrian Environment Index (PEI). *Journal of Transport Geography* 39, 73–84."

### 6.2.2. Introduction

The two active transportation modes, walking (Gotschi and Mills, 2008) and cycling (Tilahun et al., 2007), have received much attention in recent transportation literature. Not only do they possess significant health benefits as well as being natural and integral means in reducing our dependence on fossil fuels for transportation (Woodcock et al., 2007; Derrible et al., 2010), they offer a myriad of benefits including the provision of Jane Jacobs' "eyes on the street" (Jacobs, 1961, pp. 54). In her own words: "... there must be eyes upon the street, eyes belonging to those we might call the natural proprietors of the street." (Jacobs, 1961, pp. 35). A study by Gauvin et al. (2005 pp. 126) has confirmed that "safety of the environment was positively associated with neighborhood affluence." Relevant to that view, a study has shown that the social cohesion, e.g. "people in my neighborhood can be trusted", can result in a significant increase in the time they spend walking (Clark and Scott, 2013, pp. 284).

While the modernist movement in the 20th century, and the infamous Buchanan report (Great Britain and Ministry of Transport, 1963), focused mostly on accommodating the private transportation mode, ideas of smart growth and new urbanism have embraced new planning and design techniques that favor walking and cycling (Tilahun et al., 2007). Indeed, concepts of new urbanism attempt to address a variety of human needs through promoting communities in which "people can live, work, and socialize without being totally dependent on cars" (Saligaros, 2010, pp. 11). The goal of this movement is to create pedestrian-friendly neighborhoods where most of the residents' needs (e.g. living, working, shopping, entertainment, etc.) are met within walkable distances (Saligaros, 2010).

The new urbanism philosophy has received much acceptance and has gained momentum among the academic community as well as practitioners. Consequently, there has been much interest lately in developing and promoting pedestrian-friendly neighborhoods in urban areas (Azmi and Karim, 2012). The goal is to create walkable communities with mixed land-use, facilitating periodic activities of less than 15 minutes that would make the use of cars unattractive, and instead make walking or biking viable alternatives.

In recent times, there have been numerous studies aimed at defining a proper index that can capture the urban design elements which affect the friendliness of a neighborhood towards pedestrians. The models developed so far, however, more or less have shortcomings that are discussed later. To address that, Parks and Schofer (2006, pp. 251) have emphasized the “need for a method to characterize neighborhood pedestrian environments that can be applied objectively using commonly available data.” They have also recommended measures for the development of such a method that will still agree well with the commonly-used subjective measures.

The main impetus for this work is to offer a simple yet useful index that assists urban planners in using the publicly available data towards comparatively evaluating current, proposed, and future community designs in different stages of their plans. The rest of the article goes as follows. First, a brief review of the current literature is presented, which notably shows current gaps that need to be address. Then, the pedestrian environment index (PEI) is introduced and all of its constituting sub-indices and its final formulation are detailed. Then, the approach is laid



out by going through the case study of Chicago. The results are then presented and discussed for Chicago.

### 6.2.3. Background

A study by Millward et al. (2013, pp. 101) has shown that “most walks are shorter than 600 m, and very few exceed 1200 m”. Nonetheless, designing more walkable neighborhoods is not necessarily straightforward. Many factors can impact the propensity to walk or bike for any given trip, including the three Ds: Density, Diversity, and Design (Cervero and Kockelman, 1997; Lee and Moudon, 2006). Overall, pedestrian-friendly urban design offers at least four benefits (Burian, 2012):

- Practical impact: making it easy to walk or bike to the destination by making the distances shorter (Millward et al., 2013),
- Social impact: increasing social interaction by facilitating meeting between people (Clark and Scott, 2013),
- Health impact: highlighting the fact that the level of physical activity of people is greatly affected by their neighborhood environment, thus improving their health (Smith et al., 2008; Gebel et al., 2010; Hoehner et al., 2011; Smith et al., 2011; Brown et al., 2013),
- Economic impact: creating public and consumer cost savings, more efficient land-use, community livability, and economic development (Litman, 2003; Cavill et al., 2008, 2012).

Using a “path choice to investigate the causal effect of the pedestrian environment on the utility of walking”, Guo (2009, pp. 343) has concluded that “the pedestrian environment can significantly affect a person’s walking experience and the utility of walking along a path”. Moreover, Lund (2003) has found that the perception of walking environment in the neighborhood has direct positive relationship with participation in social activities there. Another study within the framework of transit-oriented development (TOD) (National Research Council (U.S.) et al., 2004) has focused on the pedestrian access between their neighborhoods and the transit stops in their vicinities using some walkability indicators. During the process, the streets were classified into two groups: friendly to pedestrians and hostile to pedestrians (National Research Council (U.S.) et al., 2004). The analysis highlighted the fact that "the presence and location of pedestrian-hostile streets have a significant, negative influence on the pedestrian environment surrounding transit stops, often cutting off more-pedestrian-friendly environments from the transit stops" (Schlossberg and Brown, 2004, pp. 34). The built environment naturally has an impact on people’s mode choice and travel patterns as well (Ewing and Cervero, 2010).

Measuring how friendly an environment is to the pedestrians represents a major challenge, for which a few methods and indices have been developed. For instance, Schlossberg (2006) used Topologically Integrated Geographic Encoding and Referencing (TIGER) street data from U.S. Census Bureau for areas surrounding transit stops and schools. The goal was to visually and quantitatively analyze the path network around key urban destinations in order to provide tools for evaluation and planning applications in pedestrian-oriented projects. During the process, three GIS (Geographic Information Systems) techniques, namely; “intersection density”,

“street network classification”, and “pedestrian catchment areas” were used. He introduced “impedance” as a measure that could help identify pedestrian-oriented neighborhoods from automobile-oriented areas (Schlossberg, 2006). From another perspective, Weyman et al. (2008) used GIS to analyze nine previously-identified urban environmental variables to measure and compare walkability between neighborhoods with pre- versus post- mid-20th century buildings in Toronto. They concluded that “urban development in Toronto dating from the mid-20th Century and earlier generated higher walkability, while development since the mid-20th century has been inconsistent in generating built environments amenable to pedestrians” (pp. 320). Mayne et al. (2012) used a set of four indices to study the walkability of different neighborhoods in Sydney, Australia. They had to use an abridged approach, however, due to the lack of data for one of the indices.

The reader is also referred to Kelly et al. (2011) for some survey-based studies and to Clifton et al. (2007) and Hoedl et al. (2010) for environmental audit approaches. From another perspective, Lwin and Murayama (2011) have modeled “green space walkability” for urban areas by utilizing web-based GIS along with Advanced Land Observing Satellite (ALOS) to use the green space areas in neighborhoods to calculate their ecofriendly walk scores.

Arguably, one of the most famous of indices that has been created to date is perhaps the Walk Score measures resource proximity and density. It uses the address entered by the user and finds amenities within a one mile radius that address (Brewster et al., 2009). Weinberger and Sweet (2012) have used data from walkscore.com to assess walking behavior in four U.S. cities. They developed three models in order to understand the correlation between walk scores and

walking, in which they looked at walk scores and walk mode shares for different trip types. Their results suggested that "walk scores may be used as a reasonable heuristic to assist with assessing trip impacts for individual projects" (pp. 20). More recently, Lee et al. (2013) have done a literature of the topic based on which they developed another walk score that notably uses elements of space syntax (Hillier, 1999).

Health impacts of walkable neighborhoods have also been the subject of numerous studies, some of which have used Walk Score as a tool. Carr et al. (2010) did a study that showed significant positive correlations between the Walk Score and several physical activity environment measures, both objective as well as subjective. A research by Duncan et al. (2011) used the data obtained from "YMCA-Harvard After School Food and Fitness Project" and concluded that "Walk Score is a valid measure of estimating certain aspects of neighborhood walkability, particularly at the 1600-meter buffer" (pp. 4175). Also, another study (Duncan, 2013) has recommended that neighborhood walkability tools (e.g. Walk Score) to be used as a part of health-related intervention tools. As mentioned before, however, a disadvantage of Walk Score is that it measures the walkability of a given address (Brewster et al., 2009) and not a neighborhood. Perhaps due to that reason, many studies have developed or used other approaches in order to capture the health impacts of walkable neighborhoods. Bahrainy and Khosravi (2013) did a cross-sectional study to collect data on health and walkability. They found that "continuity has the largest effect on walkability." They also concluded that the walking environment "has a stronger influence on female residents than on male residents," as "safety was the most important factor for women, whereas distance to destinations was the most

important factor for men” (pp. 17). Another study by Brown et al. (2009) concluded that “the presence of walkable land uses, rather than their equal mixture, relates to healthy weight (pp. 1130). A study by Owen et al. (2007) used regression analysis to demonstrate the correlation between the frequency of walking and measures representing network design (census-block density, block length and intersection type), pedestrian facilities (sidewalks), as well as the built environment along the roads (parkings and setbacks). Several parts of data collection, however, had to be done manually due to the lack of available data. The reader is also referred to works by Hou et al. (2010); Van Dyck et al. (2010); Gray et al. (2012).

Among the research on the definition of pedestrian-friendliness of neighborhoods, works by Frank et al. are probably the most significant ones to-date, which deserves proper review. Frank and Pivo (1994); Frank (2000); Frank and Engelke (2001) laid the foundations for developing a walkability index to capture the impact of micro-scale urban form on walking, and biking, as forms of physical activity. Frank et al. (2004a, 2004b) defined built environment measures affecting walkability as being: connectivity (number of 3+-leg intersections per square kilometer), net residential density (defined as the number of persons per residential acre), and land use mix (represented by an entropy-type function). Based on that, Frank et al. (2005) used those concepts to define a walkability index as the summation of the weighted z-scores of the above measures.

Later, Frank et al. (2006, 2007) added a fourth variable (the ratio of retail floor to the retail ground area) to the previous three, using which the walkability index definition was revised to simple (un-weighted) summation of the z-cores of the measures used. The most recent version

of their model was presented by Frank et al. (2010), in which they used the same variables to define a walkability index as:  $\text{Walkability} = 2 (\text{z-intersection density}) + (\text{z-net residential density}) + (\text{z-retail floor area ratio}) + (\text{z-land use mix})$ .

Frank et al.'s works, while impressive, possess shortcomings such as inconsistency in the geographic extents used for the variables, dependency on the number and spatial distribution of participants, combining the impact of different variables by addition and hence the inability to capture the interaction and feedback loop between the variables, and the use of z-score to normalize the variables Frank et al. (2007, pp. 1903) without proper statistical justification, to mention a few.

In an effort to “develop objective measures of the pedestrian environment that still correlate well with accepted subjective measures”, Parks and Schofer (2006, pp. 251) concluded that “there is a need for a method to characterize neighborhood pedestrian environments that can be applied objectively using commonly available data.” They suggest that:

“Any new measure of the pedestrian environment should meet these criteria:

- Measures should not require field visits to decrease the time and cost associated with application.
- The rating method should be objective to avoid problems of inter-rater reliability.
- There must be a balance between the level of detail and data collection costs. The method should capture the key walking related aspects of the neighborhood but should be simple enough to apply easily to many neighborhoods.
- It must be possible to develop ratings for proposed designs.

- Measures should be based on reliable data sources that are systemically updated, so that measures stay current.”

Having the above recommendations in mind, the main goal of this article is to develop a new index, called the Pedestrian Environment Index (PEI), which uses GIS data most commonly available to urban planners and metropolitan planning organizations (MPOs) without having similar shortcomings as other models that were discussed before. In order to support the use of spatial (GIS-based) methodology for this paper, the reader is referred to a recent study by Hajna et al. (2013), which has concluded that “The GIS-derived measure of walkability correlated well with the in-field audit, suggesting that it is reasonable to use GIS-derived measures in place of more labor-intensive audits” (Hajna et al., 2013, pp. 55).

The PEI takes into account characteristics of land use diversity (using concepts of entropy), population and commercial densities, as well as intersection density, based on which it assigns a value at the zonal level. This new index has the benefits of being region specific, which is helpful to compare different areas within a city with one another, a problem that seems pertinent to walkscore.com for instance (Kelbaugh, 2013). Moreover, the PEI is most useful to urban planners and metropolitan planning organizations (as opposed to the general public), who most often have access to the data required while having the leverage to modify the variables used in the PEI at a policy level.

#### 6.2.4. Methodology

The Pedestrian Environment Index (PEI) consists of four sub-indices: Land-use Diversity (LDI), Population Density (PDI), Commercial Density (CDI), and Intersection Density (IDI). These four sub-indices are specifically selected because they capture relevant aspects of a neighborhood design for walking, while addressing the concerns by Parks and Schofer listed in the previous section. They have also been repeatedly used in the literature and shown to have positive influences on walking. As an example, Rutt and Coleman (2005) used statistical analysis of their data to show that the land-use diversity and BMI in a low-income Hispanic neighborhood had positive relationship. Moreover, using improved sampling and analysis methods for the data collected from 715 participants, Forsyth et al. (2007) concluded that the purpose of walking is affected by the density of the residential environment. At the same time, Boer et al. (2007) used the data collected for ten American cities to show that the walking mode is directly and positive related to the level of business (commercial) diversity and percentages of four-way intersections within a neighborhood.

Having emphasized the relevance of the chosen indices, in the following, the four individual sub-indices are defined, followed by the complete PEI model.

##### *6.2.4.1. Land-use Diversity Index (LDI)*

The LDI is a measure of land-use homogeneity or heterogeneity (i.e. mix of residential, commercial, and other uses). It shows how diverse the land-use in a given zone is. It is calculated



using concepts of entropy, originally defined in statistical mechanics and applied famously in information theory by Shannon (1948). More closely related to measuring inequalities, an entropy index was defined to study biodiversity, and it was applied in many other fields, including economics (Sen, 1973) and transportation (Xie and Levinson, 2007). A version of this index was first used in a classic mode choice study (Frank and Pivo, 1994) in which it was found that walking, biking, and transit trips possessed a positive relationship with land-use diversity (Manaugh and Kreider, 2013) Mathematically, the entropy is defined as:

$$E_i = - \frac{\sum_{j=1}^k (p_j * \ln(p_j))}{\ln(k_i)}, \text{ for } k_i > 1 \quad \text{Eq. 6.2.1}$$

$$= 0 \quad , \text{ for } k_i = 1$$

where:

$p_j$  = the ratio of the surface area of land-use type  $j$  over the total area of the study zone  $i$ ,

$k_i$  = the total number of different land-use types within the study zone  $i$ .

Here, the LDI of a zone is calculated as the entropy of that zone,  $E$ , divided by the maximum entropy found in all the zones in the studied area. As a result:

$$LDI_i = \frac{E_i}{\max[E_i]} \quad , \quad 0 \leq LDI_i \leq 1 \quad \text{Eq. 6.2.2}$$

The numerator in Eq. 6.2.2 is maximized when all land-use types in the study zone have equal proportions. For instance, an area with 50% residential and 50% commercial leads to:

$$E = - [0.5 \times \ln(0.5) + 0.5 \times \ln(0.5)] / \ln(2) = 1.$$

The rational for the denominator in Eq. 6.2.2, which is the maximum value of the numerator across all zones studied in a city, is to normalize the index in order to keep its value

between 0 and 1. This process allows for the sub-index to be region-specific, therefore making it more convenient for citywide comparative analyses.

Consequently, a higher LDI translates into a more diverse land-use. This diversity in land-use is likely to facilitate performing one's daily activities by walking between different destinations (Loo and Chow, 2006). As a result, the relationship between LDI and PEI is direct and positive.

#### 6.2.4.2. Population Density Index (PDI)

The PDI represents population density in a given zone. It is a measure of the community environment, which encourages people to get to their destinations by walking. Mathematically, the PDI is defined as:

$$PDI_i = \frac{\left(\frac{Pop_i}{A_i}\right)}{\max\left(\frac{Pop_i}{A_i}\right)}, 0 \leq PDI_i \leq 1 \quad \text{Eq. 6.2.3}$$

where:

$Pop_i$  = Total population in the study zone  $i$ ,

$A_i$  = Area of the study zone  $i$ .

The PDI index has also been normalized (i.e. keeping its value between 0 and 1) using the same method that was used for the LDI.

A higher PDI means more people reside in the neighborhood. The rationale for a denser neighborhood links back to Jane Jacobs' conditions for diversity (Jacobs, 1961), since more "eyes on the street" will provide a safer and more secure environment to walk in. Moreover,

dense population makes social services easily accessible within walking distance for low-mobility groups (Loo and Chow, 2006). High PDI values are mostly observed in city centers where walking distances are expectedly shorter (Burian, 2012). Here again, the relationship between PDI and PEI is direct and positive.

#### 6.2.4.3. Commercial Density Index (CDI)

Commercial establishments act as destinations for work-, shopping-, entertainment-, and service-related trips. The higher the commercial density, the more people's needs can be satisfied within a small area, encouraging them to walk rather than drive to farther places. The CDI represents the existence of different commercial, financial, and other services that are typically needed during one's daily activities in an area. Koh and Wong (2013) found that the percentage of commercial land-use, among other factors, influences the propensity of walking. Mathematically, the CDI is defined as:

$$CDI_i = \frac{\left(\frac{GFA_i}{A_i}\right)}{\max\left(\frac{GFA_i}{A_i}\right)}, 0 \leq CDI_i \leq 1 \quad \text{Eq. 6.2.4}$$

where:

$GFA_i$  = Total Gross Floor Area of commercial establishments in the study zone  $i$ ,

$A_i$  = Area of the study zone  $i$ .

The GFA represents the total area available for commercial activity in a given zone (i.e. it is the sum of the products of building footprints multiplied by their corresponding number of

floors). As compared to a simple building footprint, GFA was preferred because commercial buildings typically have more floors than residential buildings, especially in downtown areas.

Once again, the denominator in the CDI is used as a normalizing measure (i.e. keeping its value between 0 and 1), similar to the LDI and PDI.

In general, a higher CDI suggests closer and more diverse commercial services in an area. Consequently, people may be more encouraged to walk. Here as well, the relationship between CDI and PEI is direct and positive.

#### 6.2.4.4. Intersection Density Index (IDI)

The IDI measures the density of intersections (i.e. street crossings) in an area. It can also be seen as a proxy to block size, which is also one of the four conditions for diversity by Jacobs (1961). It is defined as:

$$IDI_i = \frac{\left(\frac{\sum_j n_{ij}}{A_i}\right)}{\max\left(\frac{\sum_j n_{ij}}{A_i}\right)}, 0 \leq IDI_i \leq 1 \quad \text{Eq. 6.2.5}$$

where:

$n_{ij}$  = Intersection equivalency factor for intersection  $j$  in zone  $i$ ; i.e. number of links meeting at node  $j$  (see Figure 62),

$\sum_j n_{ij}$  = Sum of intersection equivalency factors in zone  $i$ ,

$A_i$  = Area of zone  $i$ .

As shown in Figure 62, the intersection equivalency factor value for a given intersection is equal to the number of links originating from, ending at, or continuing through that

intersection. This means that a regular 4-way intersection will have an intersection equivalency factor value of 4, while that of a cul-de-sac will be 1.

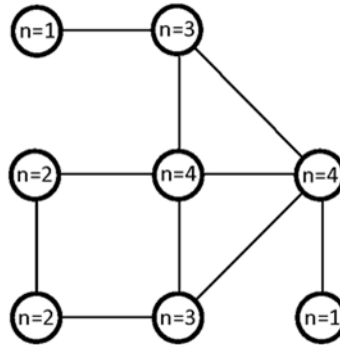


Figure 63 Examples of intersection equivalency factor values.

In practice, a higher IDI essentially suggests smaller block sizes, which is a desirable feature and part of Jacobs' conditions for diversity (Jacobs, 1961). Indeed, smaller block sizes tend to provide a more pleasant environment to pedestrians, while offering more route choices and the option to change course more easily. Even though a smaller block size results in a higher number of crossings and hence increased safety concerns, the fact that in this context the streets will be narrower, and thus the crossing times will be shorter, compensate for those concerns to some degree. In addition, smaller block sizes also tend to discourage car use due to increased delay at intersections. Akin to the three other sub-indices, the relationship between IDI and PEI is direct and positive.

Finally, we wish to highlight that since highways artificially inflate the number of intersections (because of their multiple lanes as well as their access and egress ramps that intersect with each other and with the overpasses/underpasses in planar maps), they were

excluded from the network. The fact that they are not suitable for walking in the first place also supports such a decision. In addition to the highways, areas of water bodies and rivers were also subtracted from the zonal areas (Burian, 2012).

#### 6.2.4.5. Pedestrian Environment Index (PEI)

As discussed previously, the PEI combines the four sub-indices of LDI, PDI, CDI and IDI, each capturing an important characteristic of a neighborhood. The final PEI is defined as:

$$PEI_i = \frac{1}{16} [(1 + LDI_i) \times (1 + PDI_i) \times (1 + CDI_i) \times (1 + IDI_i)],$$

$$0 < PEI_i \leq 1 \quad \text{Eq. 6.2.6}$$

where:

$LDI_i$  = Land-use Diversity Index for zone  $i$ ,

$PDI_i$  = Population Density Index for zone  $i$ ,

$CDI_i$  = Commercial Density Index for zone  $i$ ,

$IDI_i$  = Intersection Density Index for zone  $i$ .

The PEI combines the impact of each component by multiplication and not by summation. The rationale behind this form is that factors affecting the pedestrian environment within a neighborhood have cause-and-effect or non-linear feedback impacts on each other, i.e. a change in one can result in changes in the other factors. For example, by increasing the number or variety of commercial activities in a neighborhood, more people will be encouraged to move to that area and live there, resulting in an increase in the household density. That, in turn, will

attract more cause-and-effect or non-linear feedback impact on each other, i.e. an improvement in one magnifies the impacts of the other factors. For example, by increasing the number or variety business to the neighborhood, positively affecting the commercial density.

Having the rationale for multiplication in mind, and in order to avoid a null value for PEI should any of the sub-indices turn out to be zero (e.g., if there is only one zone type, i.e.  $k = 1$ , then LDI will be zero), a value of “1” was added to every sub-index value. Since the final values of PEI are used only for comparing different zones, and thus relative values (as opposed to absolute values) are important, the final outcome of the comparative analysis remains unchanged with such a precautionary measure.

At last, since the maximum possible value of the product of the components shown in the PEI formulation is 16, the introduction of a  $1/16$  coefficient will help to normalize the calculated values and keep the PEI values within a  $(0,1]$  range.

Based on the above definition, a value of PEI close to 1 will mean that the neighborhood environment better supports pedestrian activities, while a value of PEI close to 0 will mean that people in that neighborhood will be encouraged to depend on using cars in their everyday activities due to unwelcoming walking environment.

#### 6.2.5. Notes on Area and Data Requirements

The definition of “zone” in the PEI can be applied to any zonal system, ranging from neighborhoods, blocks, block groups, traffic analysis zones (TAZ) or sub-TAZ, census tracts, or even to an entire city (i.e. to compare small suburban cities). Custom sizes can also be

envisioned; e.g., 1 km by 1 km squares. The limit is not imposed by the definition of the PEI but by the data availability and the scope of the study. That being said, and unlike WalkScore, the PEI needs to be calculated for an area as opposed to a point.

As mentioned before, one of the objectives of the formulation of PEI was to provide a simple, yet efficient, index for comparative analysis. This included the simplicity in obtaining the data required for the analysis. The formulation requires data that is mostly available publicly, including the population, land-use, buildings, zonal and geographic, and street network data, all of which should be easy to find. A more complex formulation could include other parameters such as sidewalk widths, etc., which is very difficult to obtain. This is why only the data that is expected to be available in many cities across North America and around the world is used in the proposed model.

#### 6.2.6. Case Study

To fully explain the approach, use, and application of the PEI, the city of Chicago is chosen as a case study. Chicago is a particularly good candidate for any pedestrian index since it has a variety of diverse neighborhoods with vastly changing pedestrian environments, from extremely friendly to the north (e.g., Lincoln Park) to extremely hostile to the south (e.g., close to Midway Airport).



#### 6.2.6.1. Data Sources

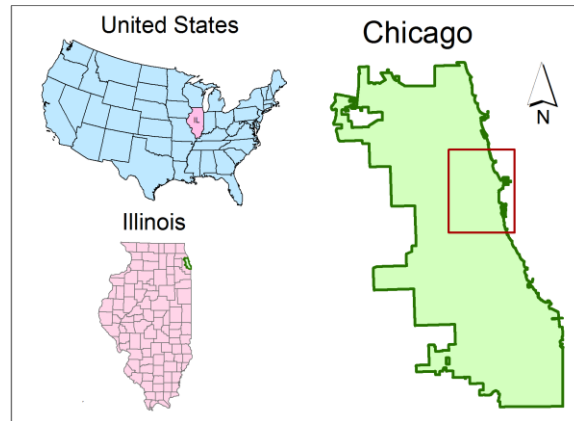
Several sets of data were needed to compute the PEI. Table 3 presents the type of data required and their sources for our case study.

Table 3 Data Sources

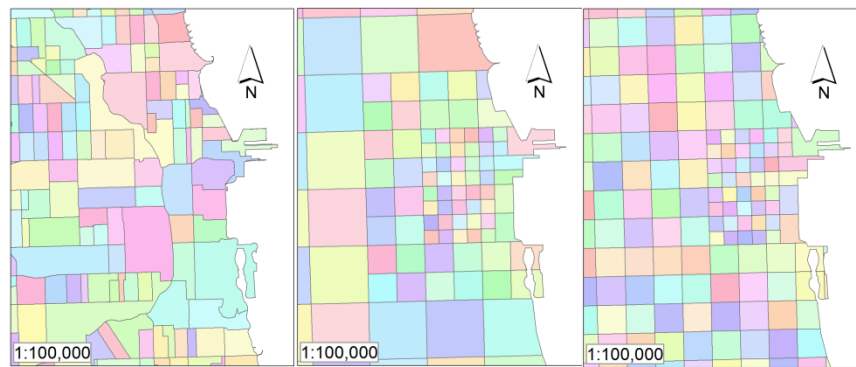
<b>Data</b>	<b>Source</b>
Census Tracts 2010	(U.S. Census Bureau a), TIGER/Line Data
TAZ (Traffic Area Zone) 2009	(Chicago Metropolitan Agency for Planning)
City of Chicago boundary 2010	(City of Chicago), Data Portal
Household data 2010	(U.S. Census Bureau b), American FactFinder
Land-use data 2005	(Chicago Metropolitan Agency for Planning)
Building data 2000	(Chicago Metropolitan Agency for Planning)
Street networks 2010	(U.S. Census Bureau a), TIGER/Line Data

#### 6.2.6.2. Application

When applying the PEI, the first task is to determine the desired zonal geometry, i.e. Block, Block group, Census Tract, TAZ (Traffic Analysis Zone) or sub-TAZ (see Figure 63), and even neighborhoods that can have different sizes and shapes.



a) Location Map



b) Sub-TAZ

c) TAZ

d) Census Tract

Figure 64 Comparison of zonal geometries.

For this case study, the sub-TAZ level was chosen since it offers fairly high spatial resolution and for that reason is traditionally used by the Chicago Metropolitan Agency for Planning (CMAP). In total, there are 985 sub-TAZs within the city of Chicago. The sub-TAZ geography was then used to extract the city of Chicago zones from Cook County, as shown in Figure 64.

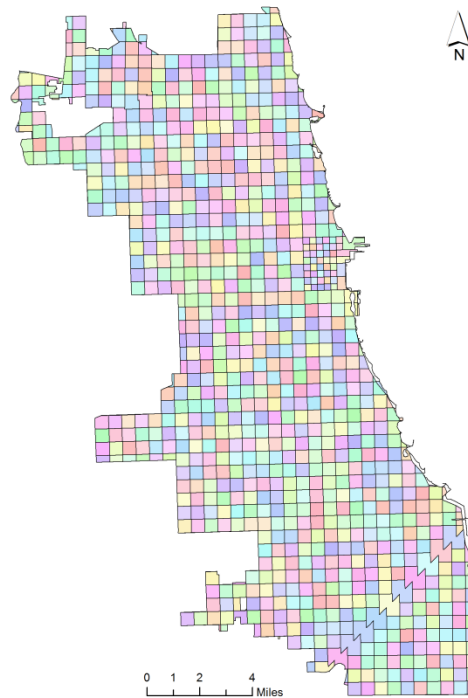


Figure 65 Chicago sub-TAZ system.

The second task was to remove land areas that do not directly affect pedestrians and are therefore not relevant for this study (e.g., highways, waterways, airports). To do so, land-use designations in the GIS shapefiles that were provided by CMAP were used to identify the lands that had to be excluded from the analysis. They were clipped from all analysis zones (Figure 65).

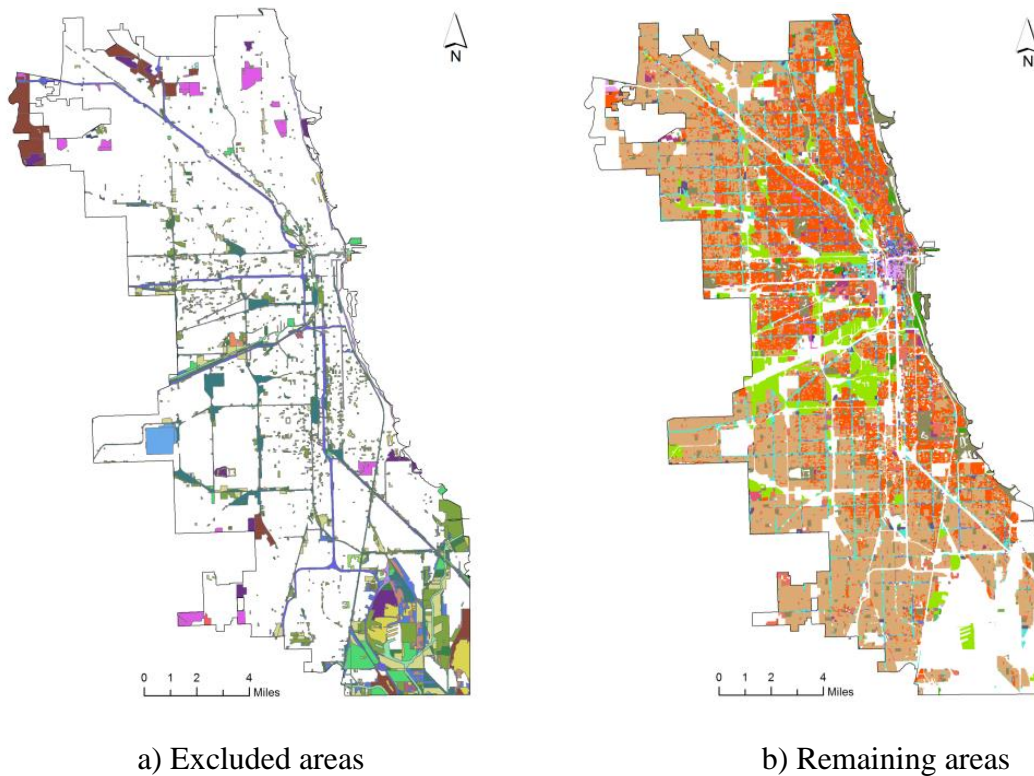


Figure 66 Excluded and remaining areas.

Individual land-uses were then extracted from the study zones, examples of which are shown in Figure 66. Although the residential land-use apparently dominates other land use types in this figure, one should not forget the third dimension (i.e. the building height or number of floors), which is not captured by the figure. Indeed and as mentioned, most of commercial and other non-residential land-uses include tall buildings, resulting in large gross floor areas. The outputs were then spatially joined with sub-TAZ areas in order to obtain the numbers and areas corresponding to individual land-use classes

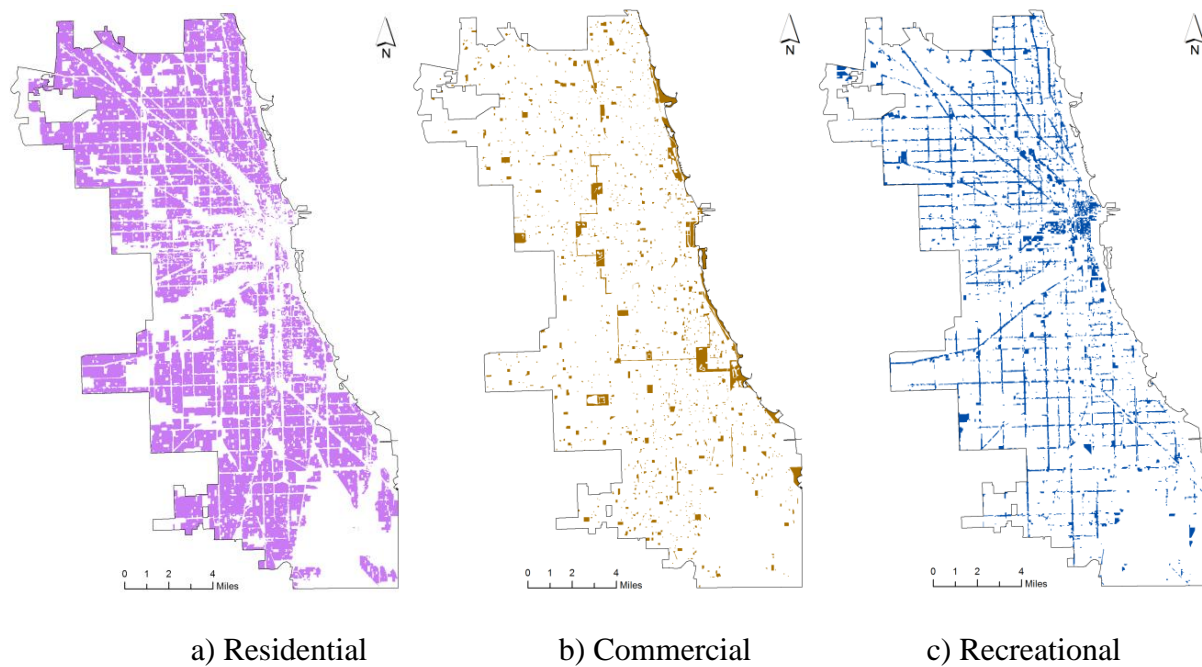


Figure 67 Extracted individual land uses.

To determine gross floor areas (GFA), the building footprints were multiplied by their corresponding number of floors (as explained previously). This information along with the land-use data was then used to extract the gross floor areas but only for the commercial buildings from the data obtained previously (to be used in CDI calculations).

The fourth task dealt with the IDI specifically. The street network was used to create a network dataset for the city, in which the intersections (junctions) were identified, for which the intersection equivalency factors (as explained in Figure 62) were calculated as shown in Figure 67.

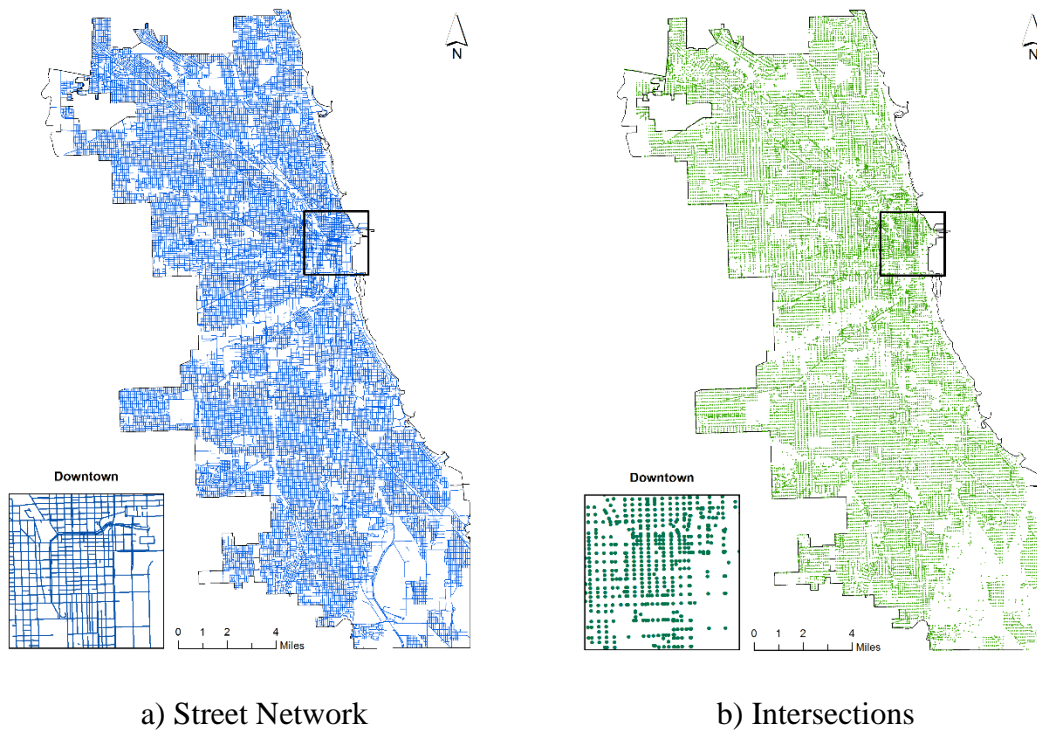


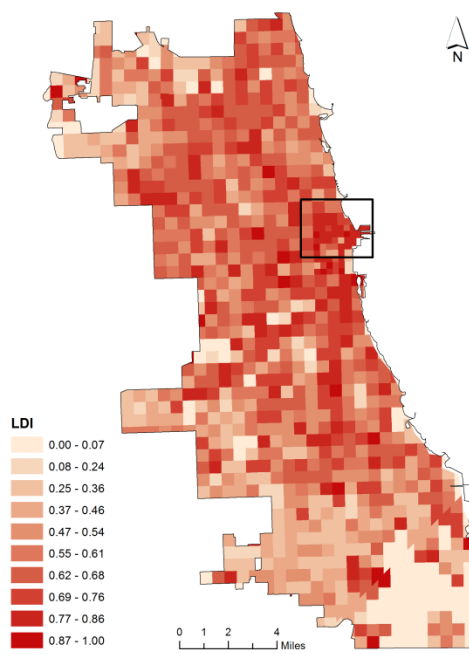
Figure 68 Street Network and Intersections.

As the fifth task, the results of the previous steps were used to calculate the four individual sub-indices. For each sub-TAZ in Chicago, the Land-use Diversity Index (LDI), the Population Density Index (PDI), the Commercial Density Index (CDI), and the Intersection Density Index (IDI) were calculated and displayed in Figure 68, which is discussed in the next section.

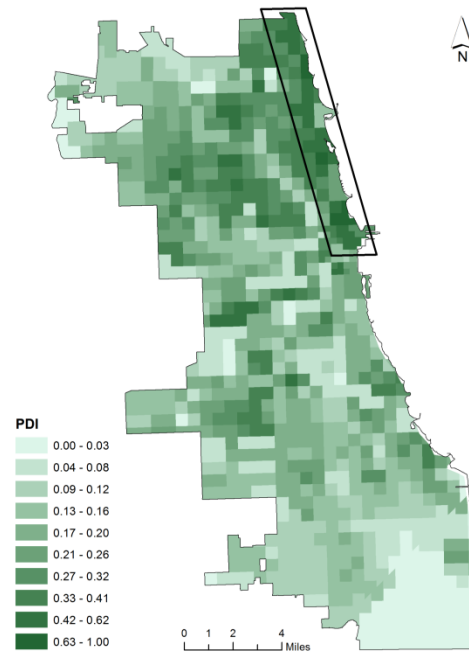
The sixth and final task was to calculate the Pedestrian Environment Index (PEI) values for each zone using equation 6. The results are shown and discussed in the next section

#### 6.2.7. Results and Discussion

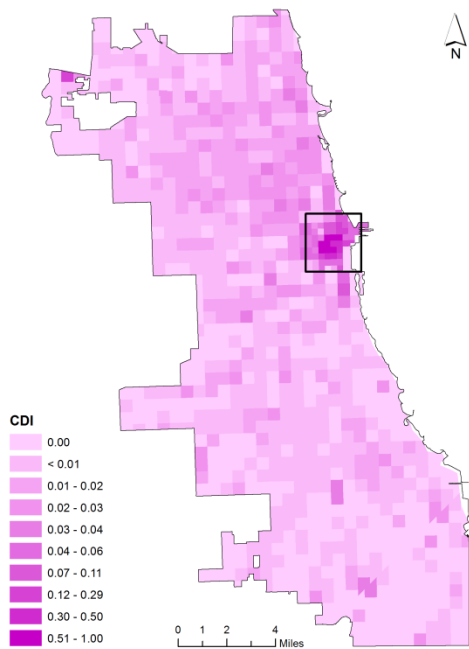
The spatial distributions of individual sub-indices are shown in Figure 68.



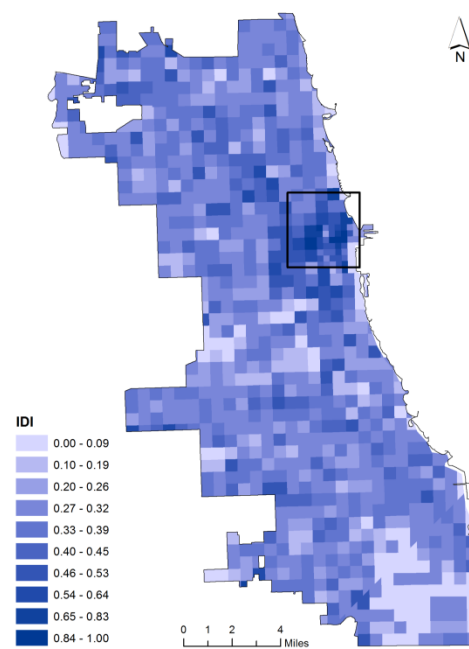
a) Land-use Diversity Index (LDI)



b) Population Density Index (PDI)



c) Commercial Density Index (CDI)



d) Intersection Density Index (IDI)

Figure 69 Spatial distributions of Land-use Diversity Index (LDI), Population Density Index (PDI), Commercial Density Index (CDI), and Intersection Density Index (IDI).

As expected, the LDI map (Figure 68a) shows higher values in the downtown area, i.e., the “Loop” (shown by a rectangle). The LDI is also fairly high directly west of the downtown as well as along the lakefront. Considering the PDI map (Figure 68b), higher values tend to be present towards the northeastern part of the city. This phenomenon is notably due to the existence of higher number of tall residential buildings in those areas, especially by the lakefront, which results in higher population densities. As expected, Figure 68c also shows higher values of CDI in the downtown area, as well as towards the northeastern areas of the city. That again, is due to the existence of more commercial sectors as well as tall buildings in those areas, resulting in higher commercial densities. Looking at the IDI map, Figure 68d shows higher values in the downtown area. As expected, IDI values tend to decrease with distance from that area.

Finally, the overall PEI results were calculated for the city of Chicago (Figure 69).

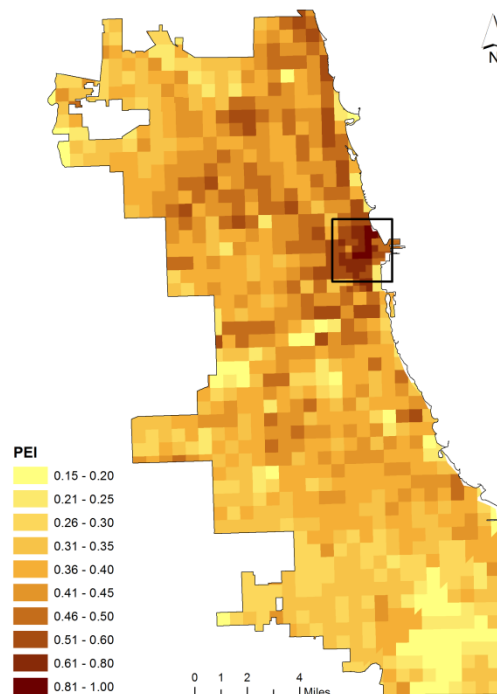


Figure 70 Spatial distribution of the Pedestrian Environment Index (PEI)



Unsurprisingly, PEI values are highest in the downtown areas, as well as around the University of Illinois at Chicago's east campus (shown in the map), which are compatible with the expected performance of those areas with respect to their pedestrian-friendliness environments. PEI values are also high northeast of the downtown, especially in areas close to the lakefront, which are also compatible with the facts on the ground, partially validating the PEI.

The Figure 69 also succeeds in highlighting the serious differences in pedestrian-friendliness throughout the city. A reverse process can then be adopted to identify the roots of the cause for a low PEI value, i.e., whether a low PEI is linked with a poor LDI, or PDI, or CDI, or IDI, or a combination of those four sub-indices, which can then be helpful to devise and recommend relevant policies. As an example, the PEI values below the center of the map in Figure 69 are comparatively low. A look at the sub-indices values show that while the commercial and intersection density sub-indices values for that area are in medium to high ranges, it is its land-use diversity and population density sub-indices that are very low. A more detailed look at the area reveals that it mostly consists of industrial lots without much land-use diversity and with very low population, confirming the outputs of the analysis.

Two natural further extensions can be thought of. First, the PEI could be further validated by comparing its zonal values with walk mode data from the American Community Survey. This process may also help determine other important characteristics that have been omitted in the current version of the PEI. Second, a subsequent study could investigate the spatial statistical relationships between the PEI and other socio-economic characteristics such as poverty, crime

rate, income, etc. In fact, this work could be repeated in various cities across the United-States, which could then offer insights about the relevance of each of the four sub-indices.

Another possible extension would be to include specific amenities in the index, for instance in the form of entropy (i.e. looking at the number of grocery stores, schools, banks, dry cleaners, etc. akin to [walkscore.com](http://walkscore.com)), although caution should be taken since this data is rarely available to planners.

Furthermore, in addition to land-use mix, population and commercial densities, and street connectivity (via intersection density), the inclusion of the impact of the urban design could be studied, because what makes a place walkable is to some degree the way it is designed.

Moreover, further research will be needed as to how the PEI can be used to devise policies, improve the pedestrian environment, or evaluate community designs.

#### 6.2.8. Conclusion

All across the urban planning community, much effort is currently being put into providing safe and friendly environments that encourage walking in cities. The main goal of this study was to develop a simple yet efficient measure that captures properties of pedestrian friendliness, which is region-specific and, that can be particularly useful to urban planners and metropolitan planning organizations.

The Pedestrian Environment Index (PEI) that is developed is based on four sub-indices: Land Diversity Index (LDI), Population Density Index (PDI), Commercial Density Index (CDI), and Intersection Density Index (IDI). These four sub-indices each capture a specific

characteristic of an area relevant to active transportation. The index is also compiled in such a way that the final PEI value cannot be 0 because of one single index.

As a case study, the PEI of each sub-TAZ in Chicago was calculated and mapped. The final output of the project was in agreement with the overall expectation based on the prior knowledge about the current urban configuration of the city of Chicago. That serves as the validation of the model.

The method developed in this study can be used to compare neighborhoods, which are within the same study area, in terms of their pedestrian-friendliness. Using this method, planners and policy makers can compare and rank already-built areas and identify the ones where investment can improve the pedestrian environment. This will be an important tool for optimizing funding allocation for projects geared towards the renovation and revitalization of neighborhoods that are suffering from low economic activities and high levels of crime, poverty, and obesity, which are all correlated. As an example, considering the high crime rate in Chicago, the results of the case study presented in this paper can be used to list the neighborhood for which improvements in the built environment can support and encourage safe walkability and improve the living condition due to increased economic activity.

The Pedestrian Environment Index can also be used as a tool to compare designs for future developments and select ones that can offer better environment for pedestrian activities that in turn are major players in future prosperity and sustainability of those communities.

Moreover, a reverse analysis of the outputs from the application of this method to different zones or neighborhoods within a given city or urban area can reveal the deficiencies in

their urban design and other relevant factors for areas with low PEI values. This in turn can help policy makers devise customized plans specific to such areas in order to make them more walkable and thus encourage people to engage more in community and group activities as well as reduce their dependence of motor vehicles.

While active transportation seems to have a bright future, measuring the friendliness of neighborhood to accommodate for walking and cycling and as a policy tool remains non-trivial, and much work remains to be done. This work provides a starting point for such a task.

## **7. CONCLUSIONS**

### **7.1. Introduction**

With the growth in world population and the increasing trend of urbanization, the need to understand how cities function is becoming more important than ever. The reason is simple, forming settlements and agglomerating offers a multitude of positive economies of scale, and cities are growing around the globe, both in number and in size. Understanding these economies of scale is therefore essential if we aspire to design more livable cities.

As a city grows and its population increases, and especially as technology advances, the interactions between the city's components become more frequent, more diverse, and with higher level of sophistication. The combination of these factors gives that city a unique identity in its own realm. Similar to living organism, the building blocks of cities have their own individual functions and roles, yet together they create a much bigger entity and in a much larger scale.

The sheer number of components that form a city and the fact that these components are more or less autonomous, and the diversity of interactions that occur between them as well as many other apparent and hidden factors make the understanding how cities form and grow a gargantuan task. Similar to any living being, however, and despite the presence of seemingly

aleatory changes in the appearance of cities, an underlying order exists, and capturing and understanding this order is highly desirable to better design the city of the 21<sup>st</sup> century.

Luckily, the overarching task to understand cities is greatly facilitated by the growth in human knowledge and further advancements in technology. Indeed, we are now equipped with tools and techniques that were not available a short while ago. This provides us with the opportunity to perform a more detailed analysis of our surroundings and obtain a deeper understanding of cities.

From this need to better understand cities, a new branch of knowledge has emerged. Since the early 20<sup>th</sup> century with the works of Geddes et al. (1915) and now often grounded within the realm of Complexity Theory, a new Science of Cities has steadily been growing, providing us with the necessary tools towards a better understanding of the complex nature of the urban systems. Even though understanding the holistic nature of cities is not yet possible, we nonetheless possess sufficient knowledge to investigate one or more of components of cities individually. This approach opens a path through which we can enter the inner world of urban systems, and lay some of the ground work to understand the whole by understanding some of the parts.

Among the components of an urban system, its transportation network is one that carries traces of its evolution. From an original small settlement to a metropolis, the residents of a city need physical infrastructure to travel to be able to connect with one another, and this is not possible without building roads, even from the very early years of a city. For that, the evolution of an urban system and its transportation network are inseparable. In theory, this suggests that

understanding the evolution of the transportation system of a city, we may be able to understand the evolution of the entire city.

The research exposed in this dissertation started with the aim **“to develop novel methodologies to study and characterize the complex geometry of urban road networks, which can in turn lead to a better understanding of their encompassing urban systems”**.

The above goal required a set of objectives to be met, which were to:

- **Review the history of the methods used for geometric analysis of urban road systems from a complexity point of view,**
- **Investigate the validity of the box-counting method, as the traditionally dominant method of choice, for capturing the complex nature of road networks,**
- **Explore the information that can be extracted from the outputs of the application of box-counting method, and define new metrics,**
- **Propose different methods to analyze the geometrical properties of urban road networks,**
- **Develop new methodologies to characterize the complex geometry of road systems,**
- **Explore other relevant areas of study toward a better understanding and classification of urban environments.**

Most notably, this thesis was the summary of the accomplishments that have been made, through the course of which old knowledge was rejected as new knowledge was born.

The achievements made during this research were included in the previous chapters, a summary of which is summarized is presented here.

## **7.2. Summary of the Achievements**

Chapter 1 of this thesis presented the reason why we need to understand urban systems, It also described the complex nature of cities, and the fact that they are similar to living organisms. This meant that despite their rather chaotic appearances, there is an intrinsic order hidden beneath urban system. We learned that studying components of an urban system opens windows into its inner world. The idea was that by understanding different elements, and the interactions among them, we can better understand the whole. Among the components of urban systems, we chose to study transportation networks, more specifically road networks. The rationale was that transportation networks evolve along with and at the same pace as their encompassing urban systems. In fact they carry the signature of their evolutions, because any new change is overlaid on the previous ones, thus preserving the history for us to study.

In Chapter 2 we talked about the history; how the origins of the knowledge and tools we have at hand started. It was first the idea of graphs, which then became graph theory. Combining a more cohesive foundation with new knowledge, it evolved to network science, one of the main themes used for studying complex phenomenon. In parallel, the idea of complexity and the need to have a branch of knowledge to understand and characterize the nature of complexity took form. This new breed evolved to something very big that connects and includes a spectrum of many other sciences. Among those, we chose the knowledge that was developed based on fractal properties of living organisms. The rationale was that road networks resemble, and evolve like, fractals. We reviewed previous literature on the application of fractal approaches used for characterization of transportation networks, and noted their shortcomings. At the end, we made a



case for the need to new ideas and tools towards a better understanding of road networks as representatives of their encompassing urban systems.

Chapter 3 focused on box-counting as the traditionally method of choice for fractal characterization of transportation networks. A characteristic of naturally-evolved organisms is the existence of inherent “scaling”, which means that the object consists of parts that are similar at different scales. This essentially means that similar patterns of different characteristics, e.g. shape, are repeated everywhere within that entity. The scaling property traditionally exhibits itself in the form of a power law. Therefore, one could say that power law is the manifestation of fractal properties. As a result, prior researches have tried to show the existence of power law behavior in different features, including road networks. And for that, the box-counting method has been extensively used. By trying to critically assess the results collected when employing the box-counting method, we realized that the power law could not be applied. This led us to investigate the validity of the box-counting methodology to capture fractal properties. Through rigorous mathematical induction, along with computational effort, we concluded that in fact the box-counting method is incapable of properly capturing the fractal nature, if any, of physical networks such as transportation systems. This was an important finding, considering the fact that the box-counting method has been used in numerous studies in the past decades.

Although it cannot capture fractal properties, the box-counting method can be useful towards some understanding of the complexity of urban transportation networks. The idea discussed in Chapter 4 was that as the grid network created during the employment of box-counting method evolve, at some point and based on a single criteria it becomes equivalent to the

real road network under study. We presented the results of our efforts to extract meaningful information from the results we had obtained through the application of the box-counting method to 50 urban road networks around the country. Our research concluded with the definition of three new indicators for urban road networks, namely: area, line, and point thresholds. They represent the block size at which the created grid network becomes equivalent to the real road network in terms of the coverage area, total length, and total number of intersections, respectively. We also studied the relationships between the three newly-defined indicators and a variety of travel and demographic statistics, and showed that each threshold exhibits correlations with one or more of the statistics used. We provided maps, demonstrating the distribution of each threshold within the U.S. and discussed the findings.

Chapter 5 presented a ring-buffer method as an alternative approach towards studying complex features, including urban road networks. Again, and understandably, the application of the method was based on the existence of power law, though a variant form of it. We first investigated the validity of the method by applying it to a series of grid networks created from Greek Cross, a well-known fractal, and concluded that the method is indeed capable of capturing the existence of fractal nature in those networks. Next, we applied the ring-buffer method to the same 50 U.S. urban system road networks that were studied in Chapter 4. The results, however, did not support the presence of fractal properties in the majority of the networks studied. This took us on a journey to understand the complex nature of urban road network. Through a novel approach with both analytical as well as computational steps, we managed to reveal the mixed complexity that road networks possess. We showed that their complexity consists of two parts;

one part that follows power law and thus exhibits scaling or fractal property. The other part, which is specific to any urban road network, that could take different forms (exponential, or power law, or logarithmic). This second part includes two new parameters, named as density and decay indices, respectively, that are unique to any given urban road system. We provided a method as how to measure those two indices. We demonstrated the distribution of each index within the U.S. and discussed it.

In Chapter 6 we presented to related extensions of this research, in both of which components of urban systems were used towards achieving the objectives defined. In 6.1, we applied the ring-buffer method to the distribution of two different-in-nature components, i.e. people and buildings, within Chicago, IL. The hypothesis was that the spread of population+employment as well as building gross floor area; as proxies for people and buildings, respectively, not only possess complex nature, but are also correlated. Our study confirmed both hypotheses. Moreover, we showed that the method used is capable of capturing and unraveling the hidden characteristics of an urban system, e.g. the city of Chicago's old boundary, something that might not be discovered by simply looking at the corresponding road network. In 6.2, we combined the information we tried to use the characteristic of different urban system components to define an index that can describe the friendliness of a neighborhood towards pedestrians. We developed a sound methodology, in which we incorporated a variety of relevant urban system components; road network (number of intersections), population and commercial, and land use data. This resulted into a new index, named "Pedestrian Environment Index (PEI)" that measures

how inviting and supporting an urban area is towards walking. We then applied the model to the city of Chicago, and discussed the results with relevant conclusions.

To summarize, this research was successful to meet the objectives set, during which we managed to develop a sound, efficient, and robust methodology towards a better understanding of the complexity of urban road networks. Moreover, we also defined five new indices to characterize them, as well as a new index to measure the friendliness of an urban environment towards walking. At last, the contributions of this work can be listed as follows:

- **Invalidation of box-counting method for fractal analysis of physical networks,**
- **Devising the methodology for an alternative application of box-counting method,**
- **Developing three new indices; area, line, and point thresholds, that can be used for classification purposes,**
- **Developing a methodology using which the ring-buffer method can be used for complexity analysis of urban road networks,**
- **Unraveling and decoupling the mixed complexity of the nature of urban road networks,**
- **Developing the two new density and decay indices that can be used for classification of road networks,**
- **Demonstrating the complex nature of the spread of people and buildings, and their strong correlation,**

- **Developing a new descriptor, Pedestrian Environment Index (PEI) that measures the friendliness of an urban area towards pedestrians, that can be used for comparison and planning purposes.**

### **7.3. Suggestions for Future Work**

The research presented in this thesis laid the foundations for an area of knowledge that can be further explored and expanded in a variety of ways and directions.

Our study showed that the complexity of a road network consists of two parts; one being a universal fractal component, and the one a components whose form is determined by the specific road network under study. A potential extension to this work is finding the underlying factors that determine the overall characteristics of an urban road network. This can help explain why different networks exhibit different forms for the second component.

The question also arises whether or not similar forms exist in cities in the rest of the world. For instance, many cities in Europe are much older, and their road densities might not present similar patterns. Most European cities also have regulations that prohibit the construction of buildings above a certain height, therefore limiting this vertical expansion to meet the demand. Cities in newly develop counties like Seoul in South Korea, Tokyo in Japan, Hong-Kong or Singapore may also show different patterns symptomatic of their local conditions.

As importantly, effort should be put into understanding the growth of cities in fast emerging countries like India and China, so that design recommendations can be given to limit an ever-increasing carbon footprint.

Another important task is to link the indices developed in this study to travel patterns and other relevant parameters such as demographic and socio-economic characteristics of the corresponding urban system. This can be further developed into design and or policy-making tools.

Applying the ring-buffer to other systems is also highly desirable. This includes other types of transportation networks, especially public transportation, which is essential if we aspire to lower our greenhouse-gas emissions.

Another potential extended topic for further research is to study the impact of topography and climate on the complex evolution of urban systems and travel behavior. This will help to link sustainability and complexity and employ the strength of both towards the betterment of our cities. A paper based the same idea has been prepared, which is currently under review for publication.

## REFERENCES

- Ahammer, H., Mayrhofer-Reinhartshuber, M., 2012. Image pyramids for calculation of the box counting dimension. *Fractals* 20(03n04), 281–293.
- Alexander, C., 1964. A city is not a tree. 1965.
- Antunes, A.L., Bavaud, F., Mager, C., 2009. Handbook of theoretical and quantitative geography. Université de Lausanne, Faculté de géosciences et de l'environnement.
- Appleby, S., 1996. Multifractal characterization of the distribution pattern of the human population. *Geographical Analysis*, 28(2), 147–160.
- Avondo Bodino, G., 1962. Economic Applications of the Theory of Graphs. Gordon and Breach Science Publishers, New York.
- Azmi, D.I., Karim, H.A., 2012. Implications of Walkability Towards Promoting Sustainable Urban Neighbourhood. *Procedia - Social and Behavioral Sciences* 50, 204–213.
- Bahrainy, H., Khosravi, H., 2013. The impact of urban design features and qualities on walkability and health in under-construction environments: The case of Hashtgerd New Town in Iran. *Cities* 31, 17–28.
- Barabasi, A.-L., Albert, R., 1999. Emergence of Scaling in Random Networks. *Science* 286(5439), 509–512.
- Barthélemy, M., 2011. Spatial networks. *Physics Reports* 499(1-3), 1–101.
- Barthélemy, M., Flammini, A., 2008. Modeling Urban Street Patterns. *Physical Review Letters* 100(13).
- Barthélemy, M., Flammini, A., 2009. Co-evolution of Density and Topology in a Simple Model of City Formation. *Networks and Spatial Economics* 9(3), 401–425.
- Batty, M., 1985. Fractals: Geometry between Dimensions. *New Scientist* 105, 31–35.
- Batty, M., 2005. Cities and complexity: understanding cities with cellular automata, agent-based models, and fractals. MIT Press, Cambridge, Mass.
- Batty, M., 2008a. Generating Cities from the Bottom-Up: Using Complexity Theory for Effective Design. *Cluster Magazine*.
- Batty, M., 2008b. The Size, Scale, and Shape of Cities. *Science* 319(5864), 769–771.

- Batty, M., 2013a. *The new science of cities*. MIT Press, Cambridge, Massachusetts.
- Batty, M., 2013b. *The New Science of Cities*. MIT Press, Cambridge, MA.
- Batty, M., Carvalho, R., Hudson-Smith, A., Milton, R., Smith, D., Steadman, P., 2008. Scaling and allometry in the building geometries of Greater London. *The European Physical Journal B* 63(3), 303–314.
- Batty, M., Longley, P.A., 1986. The fractal simulation of urban structure. *Environment and Planning A* 18(9), 1143–1179.
- Batty, M., Longley, P.A., 1987a. Fractal-based description of urban form. *Environment and Planning B: Planning and Design* 14(2), 123–134.
- Batty, M., Longley, P.A., 1987b. Urban Shapes as Fractals. *Area* 19(3), pp. 215–221.
- Batty, M., Longley, P.A., 1994. *Fractal Cities, A Geometry of Form and Function*. Academic Press Inc.
- Batty, M., Longley, P.A., Fotheringham, S., 1989. Urban growth and form: scaling, fractal geometry, and diffusion-limited aggregation. *Environment and Planning A* 21(11), 1447–1472.
- Benguigui, L., 1992. The fractal dimension of some railway networks. *Journal de Physique I* 2(4), 385–388.
- Benguigui, L., 1995. A fractal analysis of the public transportation system of Paris. *Environment and Planning A* 27(7), 1147–1161.
- Benguigui, L., Daoud, M., 1991. Is the Suburban Railway System a Fractal? *Geographical Analysis* 23(4), 362–368.
- Benguigui, L.M.A., 1995. A fractal analysis of the public transportation system of Paris. *Environment and Planning A* 27, 1147–1161.
- Berge, C., 1962. *The theory of graphs and its applications*. Methuen, London.
- Bettencourt, L.M.A., 2013. The Origins of Scaling in Cities. *Science* 340(6139), 1438–1441.
- Bettencourt, L.M.A., Lobo, J., Helbing, D., Kühnert, C., West, G.B., 2007. Growth, innovation, scaling, and the pace of life in cities. *Proceedings of the National Academy of Sciences* 104(17), 7301–7306.



- Bettencourt, L.M.A., Lobo, J., Helbing, D., Kuhnert, C., West, G.B., 2007. Growth, innovation, scaling, and the pace of life in cities. *Proceedings of the National Academy of Sciences* 104(17), 7301–7306.
- Bettencourt, L.M.A., Lobo, J., Strumsky, D., West, G.B., 2010. Urban Scaling and Its Deviations: Revealing the Structure of Wealth, Innovation and Crime across Cities. *PLoS ONE* 5(11), e13541.
- Biehl, M., 2008. A brief introduction to self-similar fractals.
- Boer, R., Zheng, Y., Overton, A., Ridgeway, G.K., Cohen, D.A., 2007. Neighborhood Design and Walking Trips in Ten U.S. Metropolitan Areas. *American Journal of Preventive Medicine* 32(4), 298–304.
- Brewster, M., Hurtado, D., Olson, S., Yen, J., 2009. Walkscore. com: A new methodology to explore associations between neighborhood resources, race, and health.
- Bristow, D.N., Kennedy, C.A., 2013. Urban Metabolism and the Energy Stored in Cities. *Journal of Industrial Ecology* 17(5), 656–667.
- Brown, B.B., Smith, K.R., Hanson, H., Fan, J.X., Kowaleski-Jones, L., Zick, C.D., 2013. Neighborhood Design for Walking and Biking. *American Journal of Preventive Medicine* 44(3), 231–238.
- Brown, B.B., Yamada, I., Smith, K.R., Zick, C.D., Kowaleski-Jones, L., Fan, J.X., 2009. Mixed land use and walkability: Variations in land use measures and relationships with BMI, overweight, and obesity. *Health & Place* 15(4), 1130–1141.
- Buckwalter, D.W., 2001. Complex topology in the highway network of Hungary, 1990 and 1998. *Journal of Transport Geography* 9(2), 125–135.
- Buhl, J., Gautrais, J., Reeves, N., Solé, R.V., Valverde, S., Kuntz, P., Theraulaz, G., 2006. Topological patterns in street networks of self-organized urban settlements. *The European Physical Journal B* 49(4), 513–522.
- Burduk, R., Kurzynski, M., Wozniak, M., Zołnierak, A. (Eds.), 2011. Fractal Dimension in the Landscape Change Estimation by Piotr Łabędź and Agnieszka Ozimek. In: *Computer*

- Recognition Systems 4: Fractal Dimension in the Landscape Change Estimation by Piotr Labedz and Agnieszka Ozimek. Springer, Berlin, pp. 507–515.
- Burian, J. (Ed.), 2012. Walkability Index in the Urban Planning: A Case Study in Olomouc City. In: *Advances in Spatial Planning*, Ch. 10. InTech, pp. 179–196.
- Burrough, P.A., 1981. Fractal dimensions of landscapes and other environmental data. *Nature* 294(5838), 240–242.
- Burrough, P.A., 1984. The application of fractal ideas to geophysical phenomena. *Bull. Inst. Math. and Applications*.
- Cardillo, A., Scellato, S., Latora, V., Porta, S., 2006. Structural properties of planar graphs of urban street patterns. *Physical Review E* 73(6).
- Carr, L.J., Dunsiger, S.I., Marcus, B.H., 2010. Walk Score™ As a Global Estimate of Neighborhood Walkability. *American Journal of Preventive Medicine* 39(5), 460–463.
- Cavill, N., Kahlmeier, S., Dinsdale, H., Gtschi, T., Oja, P., Racioppi, F., Rutter, H., 2012. The Health Economic Assessment Tool (HEAT) for walking and cycling: From evidence to advocacy on active transport. *Journal of Science and Medicine in Sport* 15, S69.
- Cavill, N., Kahlmeier, S., Rutter, H., Racioppi, F., Oja, P., 2008. Economic analyses of transport infrastructure and policies including health effects related to cycling and walking: A systematic review. *Transport Policy* 15(5), 291–304.
- Census Bureau, 2013. Metropolitan Statistical Area [WWW Document]. URL [census.gov/glossary/#term\\_MetropolitanStatisticalArea](http://census.gov/glossary/#term_MetropolitanStatisticalArea) (accessed 9.14.13).
- Cervero, R., Kockelman, K., 1997. Travel demand and the 3Ds: Density, diversity, and design. *Transportation Research Part D: Transport and Environment* 2(3), 199–219.
- Chapouthier, G., 2009. Mosaic structures – a working hypothesis for the complexity of living organisms. *E-LOGOS ELECTRONIC JOURNAL FOR PHILOSOPHY*.
- Chen, Y., 2010a. Characterizing Growth and Form of Fractal Cities with Allometric Scaling Exponents. *Discrete Dynamics in Nature and Society* 2010, 1–22.
- Chen, Y., 2010b. A new model of urban population density indicating latent fractal structure. *International Journal of Urban Sustainable Development* 1(1-2), 89–110.

- Chen, Y., 2011. Modeling Fractal Structure of City-Size Distributions Using Correlation Functions. *PLoS ONE* 6(9), e24791.
- Chen, Y., Wang, J., 2014. Recursive subdivision of urban space and Zipf's law. *Physica A: Statistical Mechanics and its Applications* 395, 392–404.
- Chen, Y., Zhou, Y., 2004. Multi-fractal measures of city-size distributions based on the three-parameter Zipf model. *Chaos, Solitons & Fractals* 22(4), 793–805.
- Clark, A.F., Scott, D.M., 2013. Does the social environment influence active travel? An investigation of walking in Hamilton, Canada. *Journal of Transport Geography* 31, 278–285.
- Clark, C., 1967. Von Thunen's Isolated State. *Oxford Economic Papers* 19(3), 370–377.
- Clauset, A., Shalizi, C.R., Newman, M.E.J., 2009. Power-Law Distributions in Empirical Data. *SIAM Review* 51(4), 661–703.
- Clifton, K.J., Livi Smith, A.D., Rodriguez, D., 2007. The development and testing of an audit for the pedestrian environment. *Landscape and Urban Planning* 80(1-2), 95–110.
- Courtat, T., Gloaguen, C., Douady, S., 2011. Mathematics and morphogenesis of cities: A geometrical approach. *Physical Review E* 83(3).
- Crucitti, P., Latora, V., Porta, S., 2006. Centrality in networks of urban streets. *Chaos: An Interdisciplinary Journal of Nonlinear Science* 16(1), 015113.
- Czegledy, F., Katz, J., 1995. Analysis and modeling of biological systems using fractal geometry. *Open Systems & Information Dynamics* 3(2), 189–199.
- Derrible, S., 2010. The Properties And Effects Of Metro Network Designs. University of Toronto, Toronto, Ontario, Canada.
- Derrible, S., 2012. Network Centrality of Metro Systems. *PLoS ONE* 7(7), e40575.
- Derrible, S., Kennedy, C., 2009. Network Analysis of World Subway Systems Using Updated Graph Theory. *Transportation Research Record: Journal of the Transportation Research Board* 2112(-1), 17–25.

- Derrible, S., Kennedy, C., 2010. Evaluating, Comparing, and Improving Metro Networks. *Transportation Research Record: Journal of the Transportation Research Board* 2146(-1), 43–51.
- Derrible, S., Kennedy, C., 2011. Applications of Graph Theory and Network Science to Transit Network Design. *Transport Reviews* 31(4), 495–519.
- Derrible, S., Saneinejad, S., Sugar, L., Kennedy, C., 2010. Macroscopic Model of Greenhouse Gas Emissions for Municipalities. *Transportation Research Record: Journal of the Transportation Research Board* 2191(-1), 174–181.
- Doménech, A., 2009. A topological phase transition between small-worlds and fractal scaling in urban railway transportation networks? *Physica A: Statistical Mechanics and its Applications* 388(21), 4658–4668.
- Dougherty, G., 2013. *Pattern Recognition and Classification: An Introduction* [Kindle Edition]. Springer.
- Duncan, D.T., 2013. What's Your Walk Score®? *American Journal of Preventive Medicine* 45(2), 244–245.
- Duncan, D.T., Aldstadt, J., Whalen, J., Melly, S.J., Gortmaker, S.L., 2011. Validation of Walk Score® for Estimating Neighborhood Walkability: An Analysis of Four US Metropolitan Areas. *International Journal of Environmental Research and Public Health* 8(12), 4160–4179.
- Erdős, P., Rényi, A., 1959. On Random Graphs I. *Publicationes Mathematicae* 6, 290–297.
- Erdős, P., Rényi, A., 1961. On the evolution of random graphs. *Bull. Inst. Internat. Statist* 38(4), 343–347.
- Euler, L., 1741. *Solutio problematis ad geometriam situs pertinentis*. *Commentarii academiae scientiarum Petropolitanae* 8, 128–140.
- Ewing, R., Cervero, R., 2010. Travel and the Built Environment. *Journal of the American Planning Association* 76(3), 265–294.
- Forsyth, A., Oakes, J.M., Schmitz, K.H., Hearst, M., 2007. Does Residential Density Increase Walking and Other Physical Activity? *Urban Studies* 44(4), 679–697.

- Frankhauser, P., 1998a. The Fractal Approach, A New Tool for The Spatial Analysis of Urban Agglomerations. *Population: An English Selection* 10(1), 205–240.
- Frankhauser, P., 1998b. Fractal Geometry of Urban Patterns and their Morphogenesis. *Discrete Dynamics in Nature and Society* 2, 127–145.
- Frank, L.D., 2000. Land Use and Transportation Interaction: Implications on Public Health and Quality of Life. *Journal of Planning Education and Research* 20(1), 6–22.
- Frank, L.D., Andresen, M.A., Schmid, T.L., 2004a. Obesity relationships with community design, physical activity, and time spent in cars. *American Journal of Preventive Medicine* 27(2), 87–96.
- Frank, L.D., Engelke, P.O., 2001. The Built Environment and Human Activity Patterns: Exploring the Impacts of Urban Form on Public Health. *Journal of Planning Literature* 16(2), 202–218.
- Frank, L.D., Engelke, P., Schmid, T., 2004b. Public health and the built environment: emerging evidence and complexity. *Canadian Journal of Dietetic Practice and Research* 65(2).
- Frank, L.D., Pivo, G., 1994. Impacts of mixed use and density utilization of three modes of travel: single-occupant vehicle, transit, and walking. *Transportation Research Record* 1466, 44 – 52.
- Frank, L.D., Saelens, B.E., Powell, K.E., Chapman, J.E., 2007. Stepping towards causation: Do built environments or neighborhood and travel preferences explain physical activity, driving, and obesity? *Social Science & Medicine* 65(9), 1898–1914.
- Frank, L.D., Sallis, J.F., Conway, T.L., Chapman, J.E., Saelens, B.E., Bachman, W., 2006. Many Pathways from Land Use to Health: Associations between Neighborhood Walkability and Active Transportation, Body Mass Index, and Air Quality. *Journal of the American Planning Association* 72(1), 75–87.
- Frank, L.D., Sallis, J.F., Saelens, B.E., Leary, L., Cain, K., Conway, T.L., Hess, P.M., 2010. The development of a walkability index: application to the Neighborhood Quality of Life Study. *British Journal of Sports Medicine* 44(13), 924–933.

- Frank, L.D., Schmid, T.L., Sallis, J.F., Chapman, J., Saelens, B.E., 2005. Linking objectively measured physical activity with objectively measured urban form. *American Journal of Preventive Medicine* 28(2), 117–125.
- Friedrich, A., Kaufman, S., Kaufman, M., 1994. Urban Property Values, Percolation Theory and Fractal Geometry. *Fractals* 02(03), 469–471.
- Gabaix, X., 1999. Zipf's Law for Cities: An Explanation. *The Quarterly Journal of Economics* 114(3), 739–767.
- Garrison, W.L., 1960. Connectivity of the InterState Highway System. *Papers in Regional Science* 6(1), 121–137.
- Garrison, W.L., Marble, D.F., 1962. The structure of transportation networks. Ft. Belvoir Defense Technical Information Center, Evanston, IL.
- Gauvin, L., Richard, L., Craig, C.L., Spivock, M., Riva, M., Forster, M., Laforest, S., Laberge, S., Fournel, M.-C., Gagnon, H., Gagné, S., Potvin, L., 2005. From walkability to active living potential. *American Journal of Preventive Medicine* 28(2), 126–133.
- Gebel, K., Bauman, A., Owen, N., Sugiyama, T., 2010. Misperceptions of neighborhood walkability attributes: Prospective relationships with changes in walking and BMI. *Journal of Science and Medicine in Sport* 12, e57–e58.
- Geddes, S.P., Geddes, P., Biologist, S., Geddes, P., Biologiste, S., Urbaniste, G.B., 1915. Cities in evolution: an introduction to the town planning movement and to the study of civics. Williams & Norgate London.
- Gonzalez, M.C., Hidalgo, C.A., Barabasi, A.-L., 2008. Understanding individual human mobility patterns. *Nature* 453(7196), 779–782.
- Gonzalez-Val, R., 2011. Deviations from Zipf's Law for American Cities: An Empirical Examination. *Urban Studies* 48(5), 1017–1035.
- Goodchild, M.F., 1980. Fractals and the accuracy of geographical measures. *Journal of the International Association for Mathematical Geology* 12(2), 85–98.
- Goodchild, M.F., Mark, D.M., 1987. The Fractal Nature of Geographic Phenomena. *Annals of the Association of American Geographers* 77(2), 265–278.

- Gotschi, T., Mills, K., 2008. Active Transportation for America: The Case for Increased Federal Investment in Bicycling and Walking. Rails-to-Trails Conservancy, Washington, DC.
- Gray, J.A., Zimmerman, J.L., Rimmer, J.H., 2012. Built environment instruments for walkability, bikeability, and recreation: Disability and universal design relevant? *Disability and Health Journal* 5(2), 87–101.
- Great Britain, Ministry of Transport, 1963. Traffic in towns: a study of the long term problems of traffic in urban areas. H.M. Stationery Off., London.
- Gülen, F., Gökgöz, T., 2011. A block-based selection method for road network generalization. *International Journal of Digital Earth* 4(2), 133–153.
- Guo, Z., 2009. Does the pedestrian environment affect the utility of walking? A case of path choice in downtown Boston. *Transportation Research Part D: Transport and Environment* 14(5), 343–352.
- Haggett, P., Chorley, R.J., 1969. Network Analysis in Geography. Edward Arnold, London.
- Hajna, S., Dasgupta, K., Halparin, M., Ross, N.A., 2013. Neighborhood Walkability. *American Journal of Preventive Medicine* 44(6), e55–e59.
- Han, J., Lu, G., 2008. Research on the Vector Box-counting Algorithm in Fractal Dimension Measurement. *Journal of Image and Graphics* 13(3), 525–530.
- Hanson, S., Giuliano, G. (Eds.), 2004. The geography of urban transportation, 3rd ed. ed. The Guilford Press, New York.
- Hastings, H.M., 1993. Fractals: a user's guide for the natural sciences. Oxford University Press, Oxford ; New York.
- Hillier, B., 1999. Space is the Machine. Cambridge University Press, Cambridge, UK.
- Hillier, B., Hanson, J., 1984. The social logic of space. Cambridge university press, Cambridge [Cambridgeshire] ; New York.
- Hoedl, S., Titze, S., Oja, P., 2010. The Bikeability and Walkability Evaluation Table. *American Journal of Preventive Medicine* 39(5), 457–459.

- Hoehner, C.M., Handy, S.L., Yan, Y., Blair, S.N., Berrigan, D., 2011. Association between neighborhood walkability, cardiorespiratory fitness and body-mass index. *Social Science & Medicine* 73(12), 1707–1716.
- Hou, N., Popkin, B.M., Jacobs Jr., D.R., Song, Y., Guilkey, D., Lewis, C.E., Gordon-Larsen, P., 2010. Longitudinal associations between neighborhood-level street network with walking, bicycling, and jogging: The CARDIA study. *Health & Place* 16(6), 1206–1215.
- Iannaccone, P.M., Khokha, M.K. (Eds.), 1996. *Fractal geometry in biological systems: an analytical approach*. CRC Press, Boca Raton, FL.
- Jacobs, J., 1961. *The Death and Life of Great American Cities*. Vintage Books, New York.
- Jiang, B., 2007. A topological pattern of urban street networks: Universality and peculiarity. *Physica A: Statistical Mechanics and its Applications* 384(2), 647–655.
- Jiang, B., Claramunt, C., 2004. Topological analysis of urban street networks. *Environment and Planning B: Planning and Design* 31(1), 151–162.
- Jiang, B., Liu, X., 2012. Scaling of geographic space from the perspective of city and field blocks and using volunteered geographic information. *International Journal of Geographical Information Science* 26(2), 215–229.
- Kalapala, V., Sanwalani, V., Clauset, A., Moore, C., 2006. Scale invariance in road networks. *Physical Review E* 73(2).
- Kansky, K.J., 1963. *Structure of transportation networks: relationships between network geometry and regional characteristics*. The University of Chicago, Chicago, IL.
- Karperien, A.L., Jelinek, H.F., Buchan, A.M., 2008. Box-counting analysis of microglia form in Schizophrenia, Alzheimer's disease and affective disorder. *Fractals* 16(2), 103–107.
- Kelbaugh, D., 2013. *Two Brothers, Two Radically Different Walk Scores*. Congress for the New Urbanism.
- Kelly, C.E., Tight, M.R., Hodgson, F.C., Page, M.W., 2011. A comparison of three methods for assessing the walkability of the pedestrian environment. *Journal of Transport Geography* 19(6), 1500–1508.



- Kennedy, C., 2011. *The Evolution of Great World Cities: Urban Wealth and Economic Growth*. University of Toronto Press, Toronto, Canada.
- Kennedy, C.A., Ibrahim, N., Hoornweg, D., 2014. Low-carbon infrastructure strategies for cities. *Nature Clim. Change* 4(5), 343–346.
- Kim, K.S., Benguigui, L., Marinov, M., 2003. The fractal structure of Seoul’s public transportation system. *Cities* 20(1), 31–39.
- Koh, P.P., Wong, Y.D., 2013. Comparing pedestrians’ needs and behaviours in different land use environments. *Journal of Transport Geography* 26, 43–50.
- Königsberg, 2013. Königsberg Bridges Problem [WWW Document]. URL <http://physics.weber.edu/>
- Kurant, M., Thiran, P., 2006. Extraction and analysis of traffic and topologies of transportation networks. *Physical Review E* 74(3).
- Lämmer, S., Gehlsen, B., Helbing, D., 2006. Scaling laws in the spatial structure of urban road networks. *Physica A: Statistical Mechanics and its Applications* 363(1), 89–95.
- Lee, C., Moudon, A.V., 2006. The 3Ds+R: Quantifying land use and urban form correlates of walking. *Transportation Research Part D: Transport and Environment* 11(3), 204–215.
- Lee, S., Hickman, M., Tong, D., 2013. Development of a temporal and spatial linkage between transit demand and land-use patterns. *Journal of Transport and Land Use* 6(2), 33.
- Legrand, P., Véhel, J.L., Tan, D.M., others, 2004. Fractal properties and characterization of road profiles. In: *FRACTAL04, Complexity and Fractals in Nature*, 8th International Multidisciplinary Conference. pp. 189–198.
- Levinson, D., 2007. Density and dispersion: the co-development of land use and rail in London. *Journal of Economic Geography* 8(1), 55–77.
- Levinson, D., 2012. Network Structure and City Size. *PLoS ONE* 7(1), e29721.
- Levinson, D., Xie, F., 2011. Does First Last? The Existence and Extent of First Mover Advantages on Spatial Networks. *Journal of Transport and Land Use* 4(2).
- Levinson, D., Xie, F., Oca, N.M., 2012. Forecasting and Evaluating Network Growth. *Networks and Spatial Economics* 12(2), 239–262.

- Levinson, D., Yerra, B., 2006. Self-Organization of Surface Transportation Networks. *Transportation Science* 40(2), 179–188.
- Li, J., 2002. Research on Fractal Characteristics of Urban Traffic Network Structure Based on GIS. *Chinese Geographical Science* 12(4), 346–349.
- Li, J., Du, Q., Sun, C., 2009. An improved box-counting method for image fractal dimension estimation. *Pattern Recognition* 42(11), 2460–2469.
- Litman, T., 2003. Economic Value of Walkability. *Transportation Research Record* 1828(1), 3–11.
- Loo, B.P., Chow, S.Y., 2006. Sustainable Urban Transportation: Concepts, Policies, and Methodologies. *Journal of Urban Planning and Development* 132(2), 76–79.
- Louf, R., Jensen, P., Barthélemy, M., 2013. Emergence of hierarchy in cost-driven growth of spatial networks. *Proceedings of the National Academy of Sciences* 110(22), 8824–8829.
- Louf, R., Roth, C., Barthélemy, M., 2014. Scaling in Transportation Networks. *PLoS ONE* 9(7), e102007.
- Lund, H., 2003. Testing the claims of New Urbanism. *Journal of the American Planning Association* 69(4), 414–429.
- Lu, Y., Tang, J., 2004. Fractal dimension of a transportation network and its relationship with urban growth: a study of the Dallas - Fort Worth area. *Environment and Planning B: Planning and Design* 31(6), 895–911.
- Lwin, K.K., Murayama, Y., 2011. Modelling of urban green space walkability: Eco-friendly walk score calculator. *Computers, Environment and Urban Systems* 35(5), 408–420.
- Manaugh, K., Kreider, T., 2013. What is mixed use? Presenting an interaction method for measuring land use mix. *The Journal of Transport and Land Use* 6(1), 63–72.
- Mandelbrot, B.B., 1967. How long is the coast of Britain? Statistical Self-Similarity and Fractional Dimension. *Science* 156(3775), 636–638.
- Mandelbrot, B.B., 1977. *The fractal geometry of nature*. W.H. Freeman, San Francisco.
- Mandelbrot, B.B., 2004. *Fractals and chaos: the Mandelbrot set and beyond: selecta volume C*. Springer, New York, N.Y.

- Mandelbrot, B.B., Blumen, A., 1989. Fractal Geometry: What is it, and What Does it do? [and Discussion]. Proceedings of the Royal Society of London. Series A, Mathematical and Physical Sciences 423(1864), pp. 3–16.
- Mandelbrot, B.B., Pfeifer, P., Biham, O., others, 1998. Is nature fractal? Science 279(5352), 783–783.
- Masucci, A.P., Smith, D., Crooks, A., Batty, M., 2009. Random planar graphs and the London street network. The European Physical Journal B 71(2), 259–271.
- Mayne, D., Morgan, G., Wilmore, A., Bauman, A., Jalaludin, B., Bambrick, H., Rose, N., Rodgers, B., Bennett, C., 2012. An objective index of walkability for the Sydney metropolitan region. Journal of Science and Medicine in Sport 15, S32–S33.
- Millward, H., Spinney, J., Scott, D., 2013. Active-transport walking behavior: destinations, durations, distances. Journal of Transport Geography 28, 101–110.
- Milne, B.T., 1988. Measuring the fractal geometry of landscapes. Applied Mathematics and Computation 27(1), 67–79.
- Mitchell, M., 2009. Complexity: a guided tour. Oxford University Press, Oxford [England] ; New York.
- National Research Council (U.S.), Transit Cooperative Research Program, Transit Development Corporation, 2004. Transit-oriented development in the United States: experiences, challenges, and prospects. Transportation Research Board, Washington, D.C.
- NCHRP, National Research Council, 2010. Measuring transportation network performance. Transportation Research Board, Washington, D.C.
- Newman, M.E.J., 2003. The Structure and Function of Complex Networks. SIAM Review 45(2), 167–256.
- Nicolis, G., 2012. Foundations of complex systems: emergence, information and prediction, 2nd ed. ed. World Scientific, Singapore ; Hackensack, N.J. ; London.
- Nussle, J., 2008. Update of statistical area definitions and guidance on their uses. Office of Management and Budget 1–2.

- Ollhoff, J., 2002. Stepping in wholes: : introduction to complex systems: topics in process adaptive systems, 1st ed. ed. Sparrow Media Group, Eden Prairie, MN.
- Owen, N., Cerin, E., Leslie, E., duToit, L., Coffee, N., Frank, L.D., Bauman, A.E., Hugo, G., Saelens, B.E., Sallis, J.F., 2007. Neighborhood Walkability and the Walking Behavior of Australian Adults. *American Journal of Preventive Medicine* 33(5), 387–395.
- Parks, J.R., Schofer, J.L., 2006. Characterizing neighborhood pedestrian environments with secondary data. *Transportation Research Part D: Transport and Environment* 11(4), 250–263.
- Peiravian, F., Derrible, S., Ijaz, F., 2014. Development and application of the Pedestrian Environment Index (PEI). *Journal of Transport Geography* 39, 73–84.
- Phelan, S.E., 2001. What is complexity science, really? *Emergence, A Journal of Complexity Issues in Organizations and Management* 3(1), 120–136.
- Porta, S., Crucitti, P., Latora, V., 2006. The network analysis of urban streets: A dual approach. *Physica A: Statistical Mechanics and its Applications* 369(2), 853–866.
- Preussen Chronik, 2013. Preussen Chronik [WWW Document]. Preussen Chronik. URL <http://www.preussenchronik.de>. (accessed 10.2.14).
- Rodin, V., Rodina, E., 2000. The Fractal Dimension of Tokyo's Streets. *Fractals* 08(04), 413–418.
- Rutt, C., Coleman, K., 2005. Examining the relationships among built environment, physical activity, and body mass index in El Paso, TX. *Preventive Medicine* 40(6), 831–841.
- Saligaros, N., 2010. P2P Urbanism. Creative Commons.
- Samaniego, H., Moses, M.E., 2008a. Cities as Organisms: Allometric Scaling of Urban Road Networks. *Journal of Transport and Land Use* 1(1).
- Samaniego, H., Moses, M.E., 2008b. Cities as organisms: Allometric scaling of urban road networks. *JTLU* 1(1), 21–39.
- Samaniego, H., Moses, M.E., 2008c. Cities as Organisms: Allometric Scaling of Urban Road Networks. *Journal of Transport and Land Use* 1(1).

- Scellato, S., Cardillo, A., Latora, V., Porta, S., 2006. The backbone of a city. *The European Physical Journal B* 50(1-2), 221–225.
- Schlossberg, M., 2006. From TIGER to Audit Instruments: Measuring Neighborhood Walkability with Street Data Based on Geographic Information Systems. *Transportation Research Record* 1982(1), 48–56.
- Schlossberg, M., Brown, N., 2004. Comparing Transit-Oriented Development Sites by Walkability Indicators. *Transportation Research Record* 1887(1), 34–42.
- Schroeder, M.R., 1991. *Fractals, chaos, power laws: minutes from an infinite paradise*. W.H. Freeman, New York.
- Scopus, 2014. Scopus [WWW Document]. Scopus. URL <http://www.scopus.com>
- Sen, A., 1973. *On economic inequality*. Clarendon Press, Oxford.
- Shannon, C., 1948. A mathematical theory of communication. *Bell System Technical Journal* 27, 379–423.
- Shen, G., 2002. Fractal dimension and fractal growth of urbanized areas. *International Journal of Geographical Information Science* 16(5), 419–437.
- Simon, H.A., 1965. The architecture of complexity. *General systems* 10(1965), 63–76.
- Smith, K.R., Brown, B.B., Yamada, I., Kowaleski-Jones, L., Zick, C.D., Fan, J.X., 2008. Walkability and Body Mass Index. *American Journal of Preventive Medicine* 35(3), 237–244.
- Smith, K.R., Zick, C.D., Kowaleski-Jones, L., Brown, B.B., Fan, J.X., Yamada, I., 2011. Effects of neighborhood walkability on healthy weight: Assessing selection and causal influences. *Social Science Research* 40(5), 1445–1455.
- Song, C., Gallos, L.K., Havlin, S., Makse, H.A., 2007. How to calculate the fractal dimension of a complex network: the box covering algorithm. *Journal of Statistical Mechanics: Theory and Experiment* 2007(03), P03006–P03006.
- Strano, E., Nicosia, V., Latora, V., Porta, S., Barthélemy, M., 2012. Elementary processes governing the evolution of road networks. *Scientific Reports* 2.

- Sundquist, K., Eriksson, U., Kawakami, N., Skog, L., Ohlsson, H., Arvidsson, D., 2011. Neighborhood walkability, physical activity, and walking behavior: The Swedish Neighborhood and Physical Activity (SNAP) study. *Social Science & Medicine* 72(8), 1266–1273.
- Sun, Z., Zheng, J., Hu, H., 2012. Fractal Pattern in Spatial Structure of Urban Road Networks. *International Journal of Modern Physics B* 26(30), 1250172.
- Taaffe, E.J., 1973. *Geography of transportation*. Prentice Hall, Englewood Cliffs, New Jersey.
- Tang, J., 2003. Evaluating the relationship between urban road pattern and population using fractal geometry. In: *UCGIS Summer Assembly*. University Consortium for Geographic Information Science, Pacific Grove, CA.
- Tannier, C., Vuidel, G., Houot, H., Frankhauser, P., 2012. Spatial accessibility to amenities in fractal and nonfractal urban patterns. *Environment and Planning B: Planning and Design* 39(5), 801–819.
- Tero, A., Takagi, S., Saigusa, T., Ito, K., Bebber, D.P., Fricker, M.D., Yumiki, K., Kobayashi, R., Nakagaki, T., 2010. Rules for Biologically Inspired Adaptive Network Design. *Science* 327(5964), 439–442.
- Terzi, F., Kaya, H.S., 2011. Dynamic spatial analysis of urban sprawl through fractal geometry: the case of Istanbul. *Environment and Planning B: Planning and Design* 38(1), 175–190.
- Tilahun, N., Levinson, D., 2011. Work and home location: Possible role of social networks. *Transportation Research Part A: Policy and Practice* 45(4), 323–331.
- Tilahun, N.Y., Levinson, D.M., Krizek, K.J., 2007. Trails, lanes, or traffic: Valuing bicycle facilities with an adaptive stated preference survey. *Transportation Research Part A: Policy and Practice* 41(4), 287–301.
- United Nations, 2014. *World Urbanization Prospects (Highlights): The 2014 Revision*. United Nations.
- U.S. Census Bureau, “TIGER/Lines Shapefiles.” TIGER/Lines Shapefiles [WWW Document]. URL [census.gov/geo/maps-data/data/tiger.html](http://census.gov/geo/maps-data/data/tiger.html) (accessed 11.7.12).

- U.S. Census Bureau, “American Community Survey (ACS).” American Community Survey (ACS) [WWW Document]. URL [census.gov/acs/www/](http://census.gov/acs/www/) (accessed 11.16.12).
- U.S. Office of Management and Budget, 2008. Update of Statistical Area Definitions and Guidance on Their Uses.
- Van Dyck, D., Cerin, E., Cardon, G., Deforche, B., Sallis, J.F., Owen, N., de Bourdeaudhuij, I., 2010. Physical activity as a mediator of the associations between neighborhood walkability and adiposity in Belgian adults. *Health & Place* 16(5), 952–960.
- Voss, R.F., 1987. Fractals in Nature: Characterization, Measurement, and Simulation. IBM Thomas J. Watson Research Center.
- Wang, P., Hunter, T., Bayen, A.M., Schechtner, K., Gonzalez, M.C., 2012. Understanding Road Usage Patterns in Urban Areas. *Sci. Rep.* 2.
- Watts, D.J., 2003. Six Degrees, the Science of a Connected Age.
- Watts, D.J., Strogatz, S.H., 1998. Collective Dynamics of “Small-World” Networks. *Nature* 393(6684), 440–2.
- Weinberger, R., Sweet, M.N., 2012. Integrating Walkability into Planning Practice. *Transportation Research Record: Journal of the Transportation Research Board* 2322(-1), 20–30.
- West, G.B., 1999. The Fourth Dimension of Life: Fractal Geometry and Allometric Scaling of Organisms. *Science* 284(5420), 1677–1679.
- Weyman, J.T., Raposo, P.J., Cannata, R., Jaeho, O.H., Motz, M., Gozdyla, P., Booth, G.L., Glazier, R.H., 2008. Urban Environments and Walkability: Definition and Calculation of a Walkability Index for Toronto, Canada. *Canadian Journal of Diabetes* 32(4), 320.
- Wikimedia, 2014. Coast of Britain [WWW Document]. URL [http://commons.wikimedia.org/wiki/File:Great\\_Britain\\_Box.svg](http://commons.wikimedia.org/wiki/File:Great_Britain_Box.svg)
- Wikipedia, 2014a. Coast of Britain [WWW Document]. URL [en.wikipedia.org/wiki/How\\_Long\\_Is\\_the\\_Coast\\_of\\_Britain%3F\\_Statistical\\_Self-Similarity\\_and\\_Fractional\\_Dimension](http://en.wikipedia.org/wiki/How_Long_Is_the_Coast_of_Britain%3F_Statistical_Self-Similarity_and_Fractional_Dimension) (accessed 10.1.13).

- Wikipedia, 2014b. North American settlements by year of foundation [WWW Document]. URL [en.wikipedia.org/wiki/List\\_of\\_North\\_American\\_settlements\\_by\\_year\\_of\\_foundation](http://en.wikipedia.org/wiki/List_of_North_American_settlements_by_year_of_foundation) (accessed 10.1.13).
- Wolfram, S., 2002. A new kind of science. Wolfram Media, Champaign, IL.
- Wong, D.W.S., Fotheringham, A.S., 1990. Urban Systems as Examples of Bounded Chaos. *Geografiska Annaler. Series B, Human Geography* 72(2/3), 89–99.
- Woodcock, J., Banister, D., Edwards, P., Prentice, A.M., Roberts, I., 2007. Energy and transport. *The Lancet* 370(9592), 1078–1088.
- Xie, F., Levinson, D., 2007. Measuring the Structure of Road Networks. *Geographical Analysis* 39(3), 336–356.
- Xie, F., Levinson, D., 2009a. Topological evolution of surface transportation networks. *Computers, Environment and Urban Systems* 33(3), 211–223.
- Xie, F., Levinson, D., 2009b. Modeling the Growth of Transportation Networks: A Comprehensive Review. *Networks and Spatial Economics* 9(3), 291–307.
- Xie, F., Levinson, D.M., 2011. *Evolving Transportation Networks*. Springer New York, New York, NY.
- Yamins, D., Rasmussen, S., Fogel, D., 2003. Growing Urban Roads. *Networks and Spatial Economics* 3, 69–85.
- Yerra, B., 2003. *The Emergence of Hierarchy in Transportation Networks*. University of Minnesota.
- Yerra, B.M., Levinson, D.M., 2005. The emergence of hierarchy in transportation networks. *The Annals of Regional Science* 39(3), 541–553.
- Zhang, H., Li, Z., 2011. Weighted ego network for forming hierarchical structure of road networks. *International Journal of Geographical Information Science* 25(2), 255–272.
- Zhang, L., Levinson, D., 2004. A Model of the Rise and Fall of Roads. Presented at the Engineering Systems Symposium, Massachusetts Institute of Technology.
- Zheng, X., 2010. Box-counting dimension related to the boundary of hexagonal arrays for an efficient digital earth model. *Fractals* 18(2), 223–233.



## **APPENDICES**

## **APPENDIX A: List of 50 U.S. Urban Systems Studied**

Table 4 List of 50 U.S. urban systems studied

<b>Urban Area, State</b>	<b>Founded in<sup>1</sup></b>	<b>Population<sup>2</sup></b>	<b>Area (km<sup>2</sup>)<sup>3</sup></b>	<b>Pop Density</b>	<b>Road Length (km)<sup>3</sup></b>	<b># of Intersections<sup>3</sup></b>
Atlanta, GA	1843	5486738	20306.8	270.2	67215.1	243462
Austin, TX	1835	1784094	9440.8	189.0	30382.0	111234
Baltimore, MD	1729	2895944	5624.9	514.8	35556.3	220784
Boston, MA	1630	4892136	8368.7	584.6	49139.9	261949
Buffalo, NY	1789	1191744	3821.4	311.9	12293.0	41429
Carson, NV	1858	87743	109.0	804.9	900.6	3045
Charlotte, NC	1755	1927130	7177.5	268.5	24978.8	93988
Chicago, IL	1803	9594379	17783.6	539.5	86788.9	396704
Cincinnati, OH	1788	2252951	10398.8	216.7	33834.5	141744
Cleveland, OH	1796	2272776	4827.5	470.8	19472.2	64630
Columbus, OH	1812	1949603	9483.2	205.6	27764.3	106156
Dallas, TX	1841	6501589	21833.1	297.8	83815.2	350762
Denver, CO	1858	2666592	18262.0	146.0	46547.0	182157
Detroit, MI	1701	4369224	9664.6	452.1	46880.4	187960
Grand Rapids, MI	1825	895227	6665.8	134.3	16684.6	42990
Hartford, CT	1637	1400709	3487.6	401.6	14992.7	56695
Honolulu, HI	1809	953207	775.4	1229.3	4678.9	22904

Table 4 List of 50 U.S. urban systems studied

Urban Area, State	Founded in <sup>1</sup>	Population <sup>2</sup>	Area (km <sup>2</sup> ) <sup>3</sup>	Pop Density	Road Length (km) <sup>3</sup>	# of Intersections <sup>3</sup>
Houston, TX	1837	6052475	20585.7	294.0	83365.0	353831
Indianapolis, IN	1821	1856996	9289.1	199.9	32389.9	150469
Jacksonville, FL	1822	1451740	7182.3	202.1	22067.4	76396
Kansas City, KS	1868	2138010	19148.1	111.7	50639.6	184748
Las Vegas, NV	1905	2010951	7330.1	274.3	20926.8	104925
Lewiston, ID	1861	85096	2104.6	40.4	4206.1	6334
Los Angeles, CA	1781	13059105	10913.2	1196.6	70096.7	335638
Louisville, KY	1778	1443801	9227.8	156.5	24453.7	82680
Memphis, TN	1819	1398172	10049.2	139.1	25028.4	74462
Miami, FL	1896	5571523	8410.3	662.5	42827.1	178680
Milwaukee, WI	1833	1602022	3507.8	456.7	17207.1	66802
Minneapolis, MN	1867	3412291	15365.8	222.1	57532.0	259788
Nashville, TN	1779	1740134	13588.3	128.1	32653.8	90700
New Orleans, LA	1718	1247062	3715.5	335.6	18340.7	83361
New York, NY	1624	19217139	15551.5	1235.7	105344.0	499969
Oklahoma, OK	1889	1359027	13051.0	104.1	34167.6	120303
Orlando, FL	1875	2257901	7996.6	282.4	28876.5	123076

Table 4 List of 50 U.S. urban systems studied

Urban Area, State	Founded in <sup>1</sup>	Population <sup>2</sup>	Area (km <sup>2</sup> ) <sup>3</sup>	Pop Density	Road Length (km) <sup>3</sup>	# of Intersections <sup>3</sup>
Philadelphia, PA	1682	6234336	11271.7	553.1	58104.3	256023
Phoenix, AZ	1868	4262838	25763.0	165.5	60738.6	241836
Pittsburgh, PA	1758	2503836	12859.9	194.7	45196.4	167027
Portland, OR	1845	2363554	14669.4	161.1	44544.0	174765
Providence, RI	1636	1695760	3773.5	449.4	18431.5	83871
Raliegh, NC	1792	1258825	4830.5	260.6	18678.0	81802
Rochester, NY	1803	1159166	7037.2	164.7	17863.9	47275
Sacramento, CA	1839	2277843	10167.0	224.0	34020.6	124839
Salt Lake, UT	1847	1246208	10895.1	114.4	22387.0	59736
San Antonio, TX	1718	2239307	16213.5	138.1	44137.5	127773
San Diego, CA	1769	3144425	7668.0	410.1	29499.1	144194
San Francisco, CA	1776	4472992	5352.1	835.7	33483.0	172400
San Jose, CA	1777	1992872	4921.2	405.0	19824.6	93610
St. Louis, MO	1763	2934412	20184.1	145.4	57670.8	205269
Tampa, FL	1823	2858974	5756.8	496.6	31421.2	143714
Washington D.C.	1790	5916033	12735.0	464.5	74190.6	437470

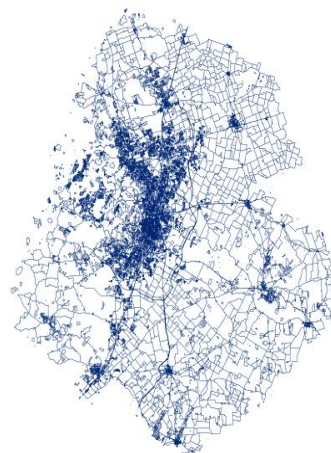
1. Wikipedia, Accessed 2014-06: <http://www.wikipedia.org/>
2. U.S. Census Bureau American FactFinder, 2010: <http://factfinder2.census.gov/>
3. Calculated from U.S. Census Bureau TIGER/Line Shapefiles, 2010: <https://www.census.gov/geo/maps-data/data/tiger-line.html>

## **APPENDIX B: Road Networks for 50 U.S. Urban Systems**



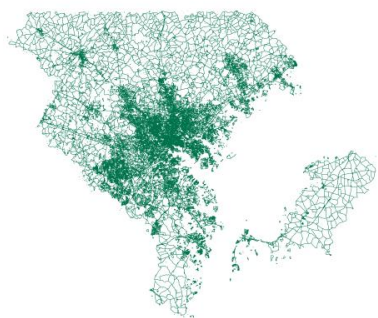
0 12.5 25 50 km

Atlanta, GA



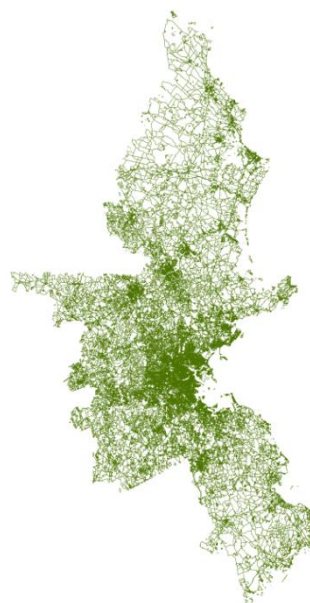
0 12.5 25 50 km

Austin, TX



0 12.5 25 50 km

Baltimore, MD



0 12.5 25 50 km

Boston, MA





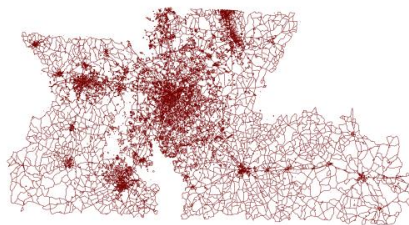
0 12.5 25 50 km

Buffalo, NY



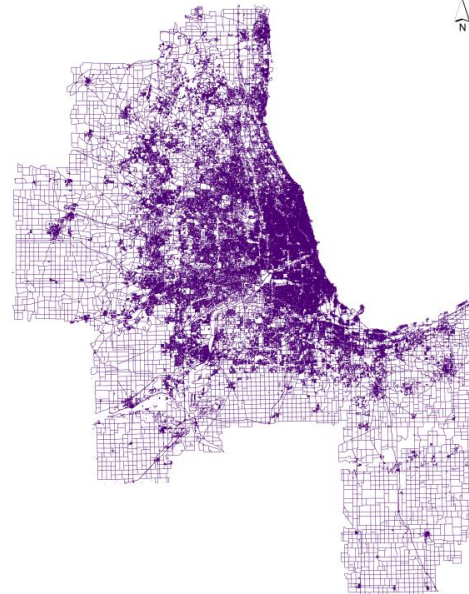
0 12.5 25 50 km

Carson, NV



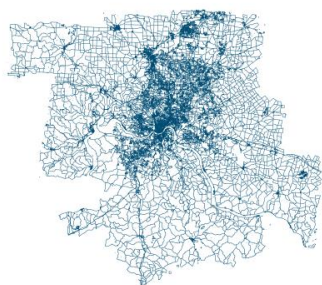
0 12.5 25 50 km

Charlotte, NC



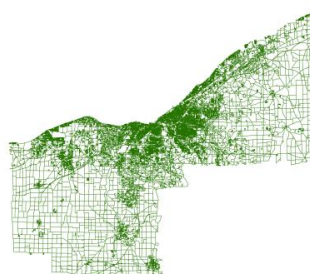
0 12.5 25 50 km

Chicago, IL



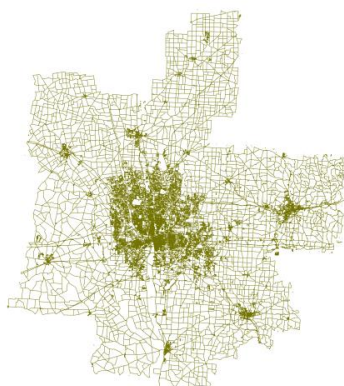
0 12.5 25 50 km

Cincinnati, OH



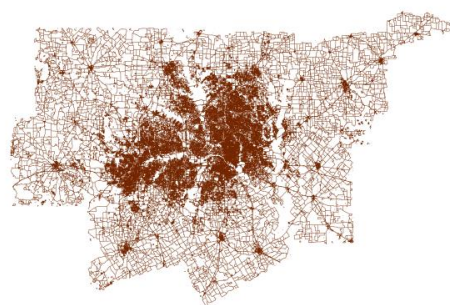
0 12.5 25 50 km

Cleveland, OH



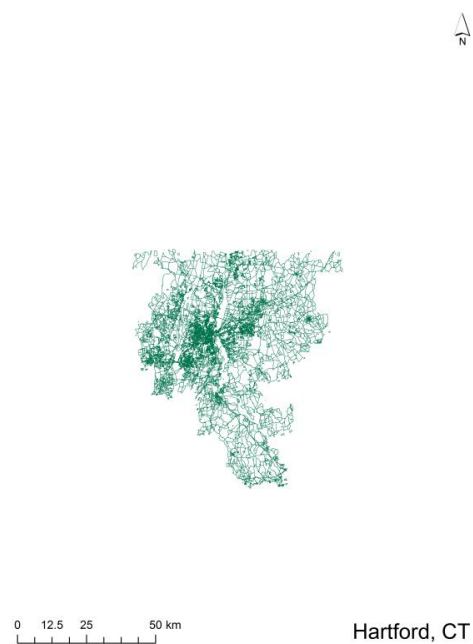
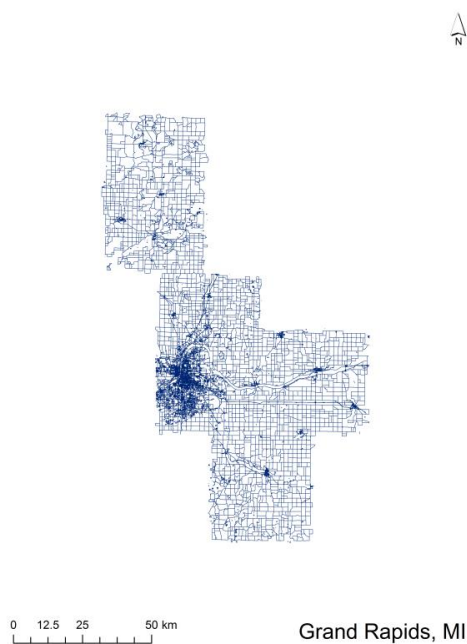
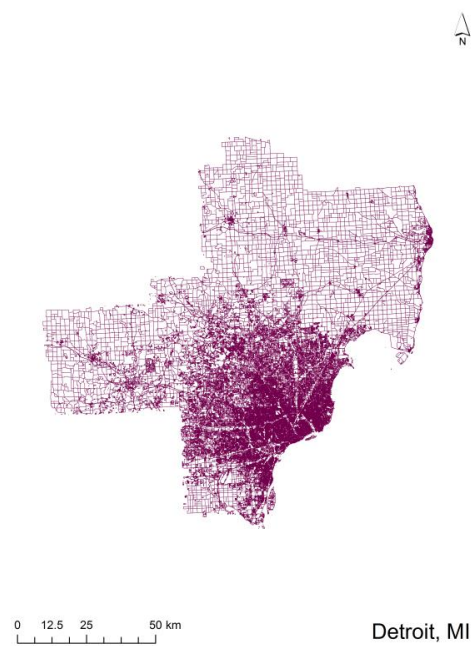
0 12.5 25 50 km

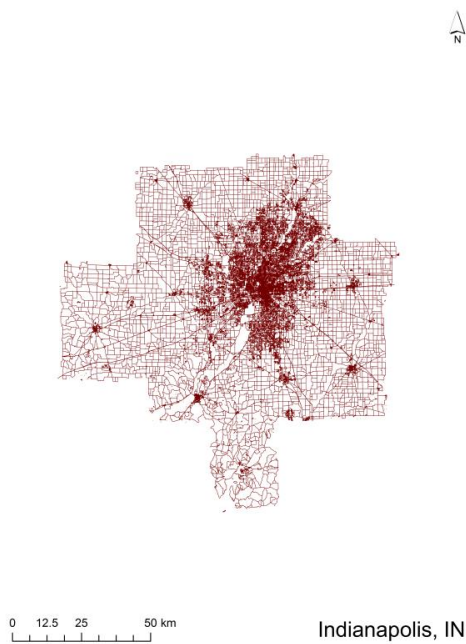
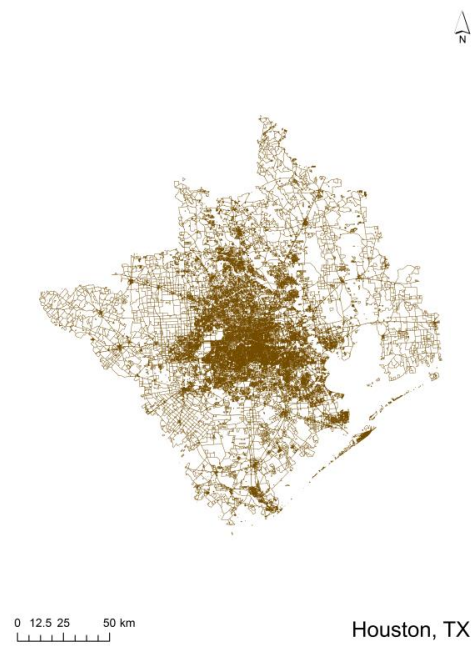
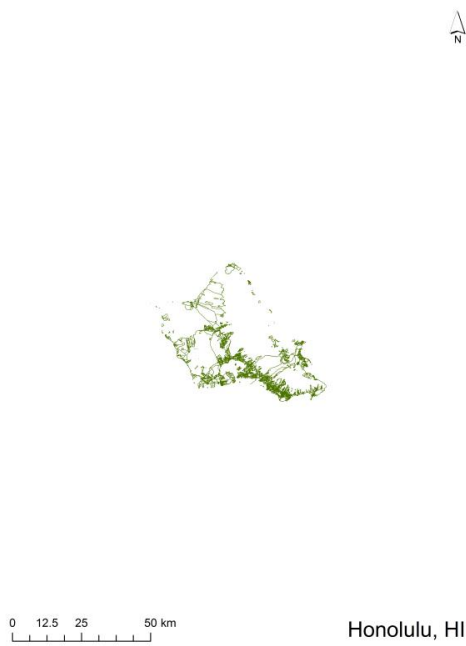
Columbus, OH

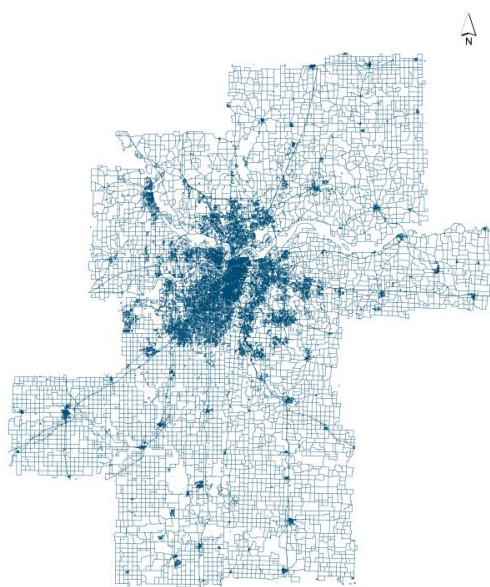


0 12.5 25 50 km

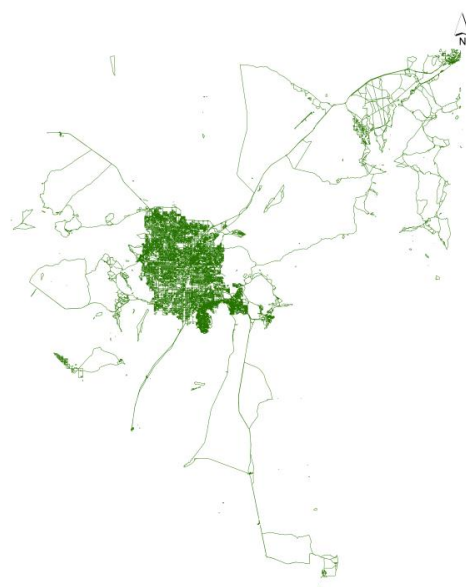
Dallas, TX



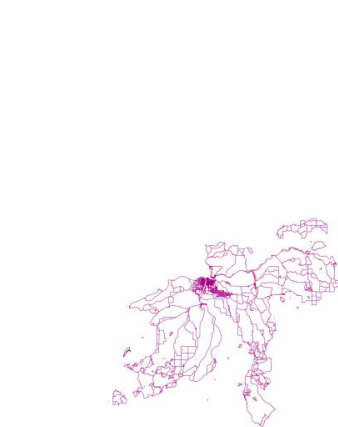




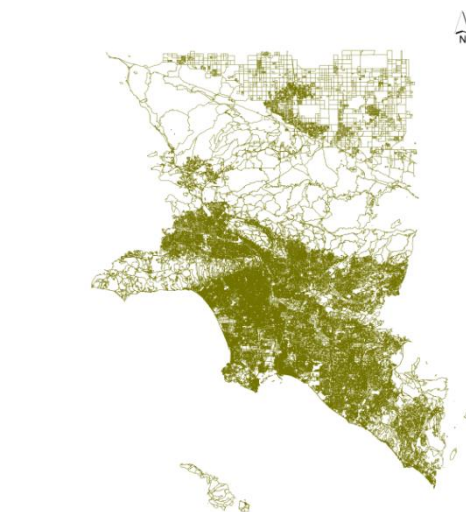
Kansas, KS



Las Vegas, NV

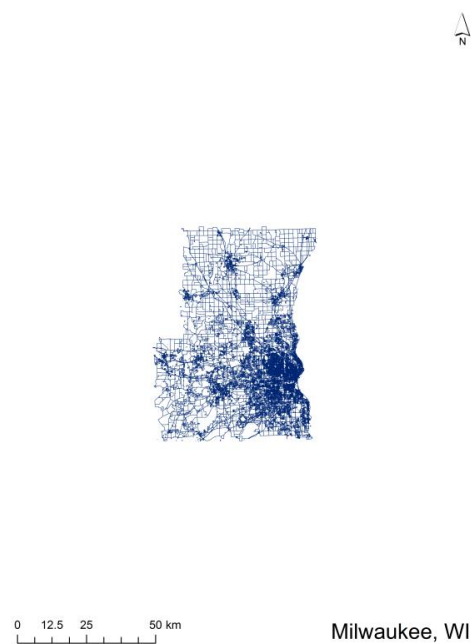
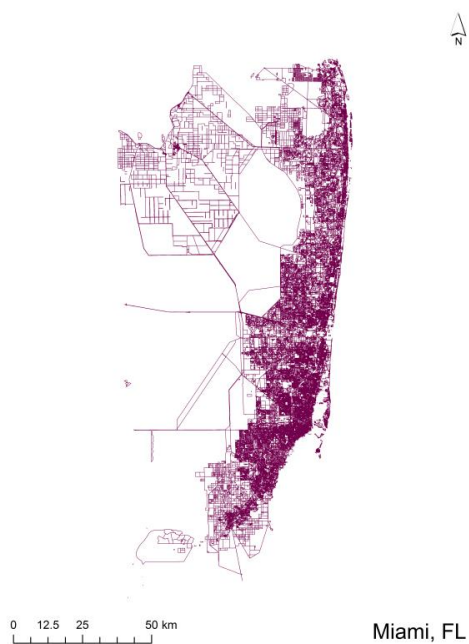
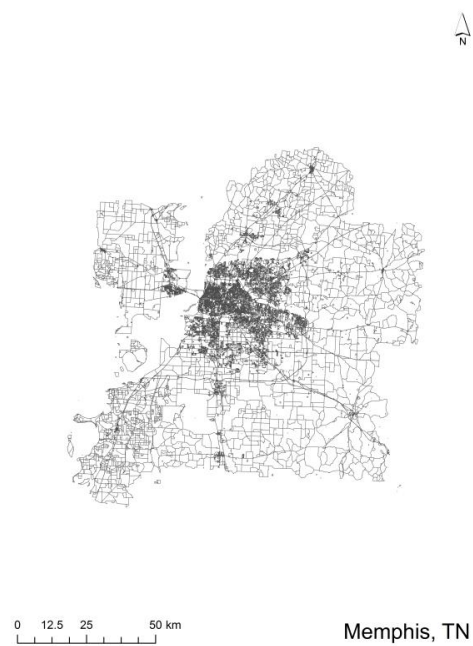
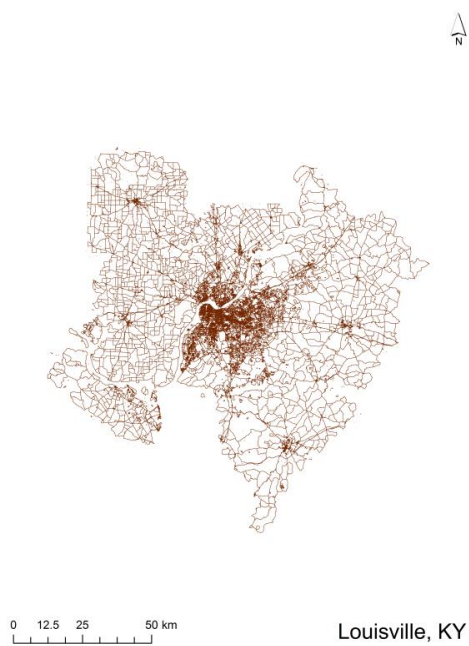


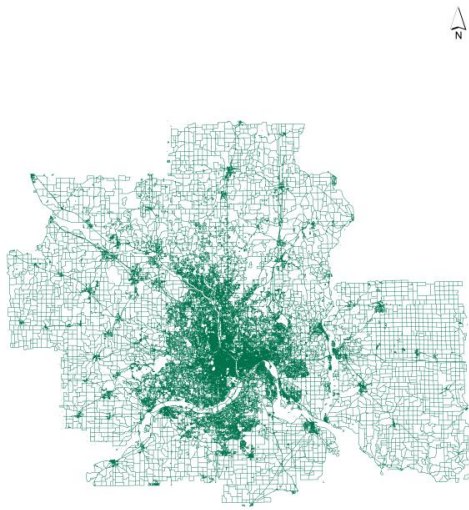
Lewiston, ID



Los Angeles, CA

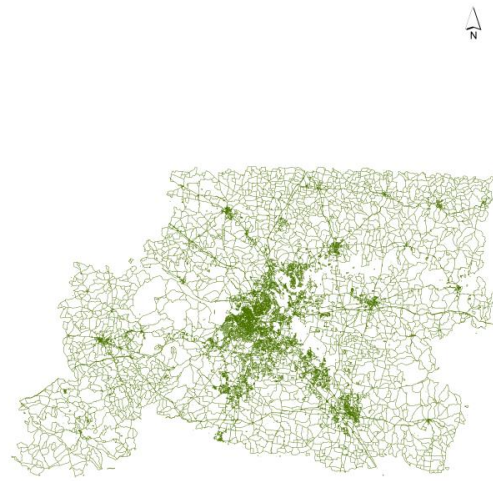






0 12.5 25 50 km

Minneapolis, MN



0 12.5 25 50 km

Nashville, TN



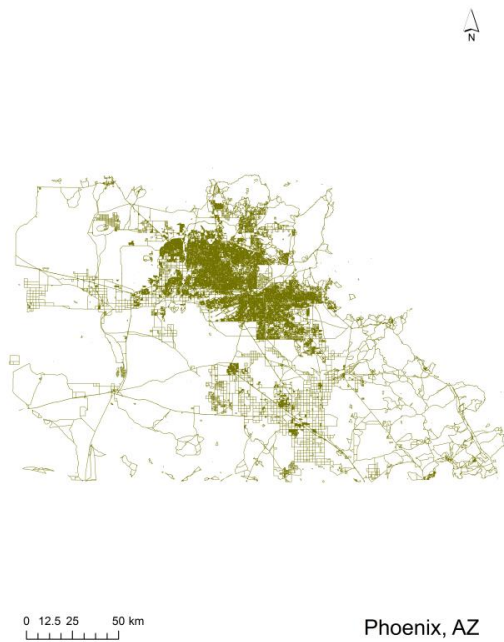
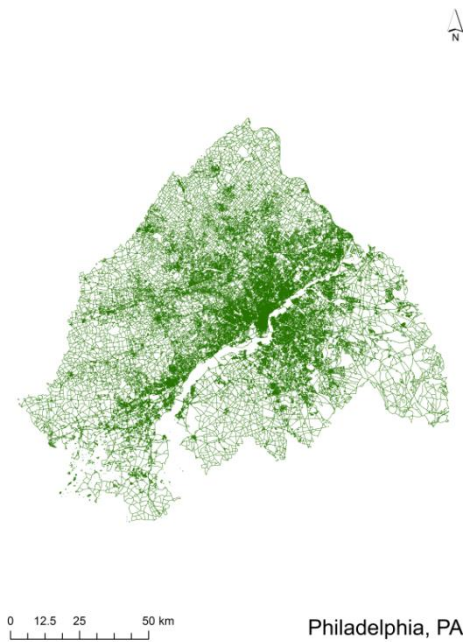
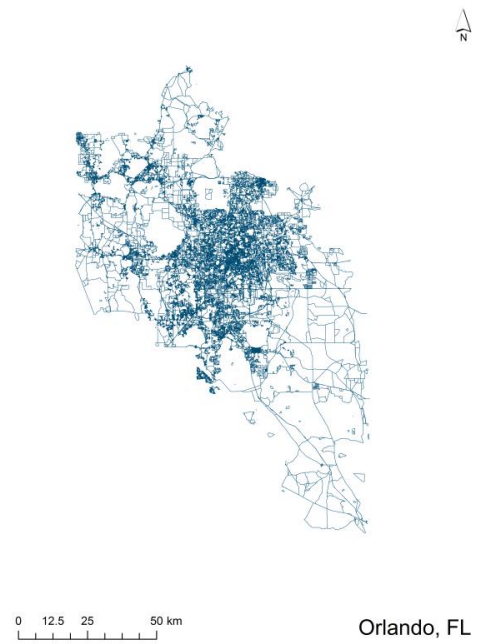
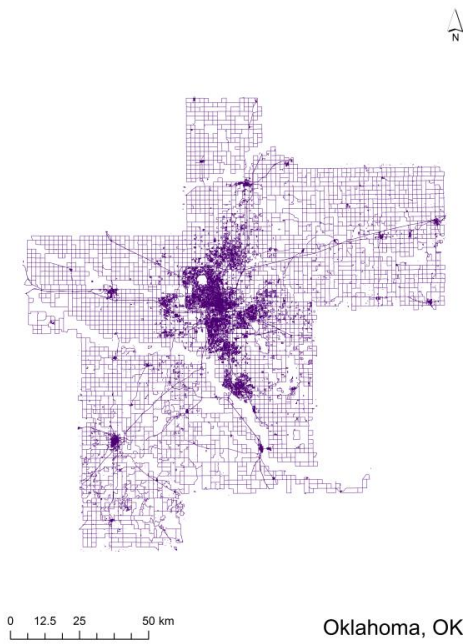
0 12.5 25 50 km

New Orleans, LA

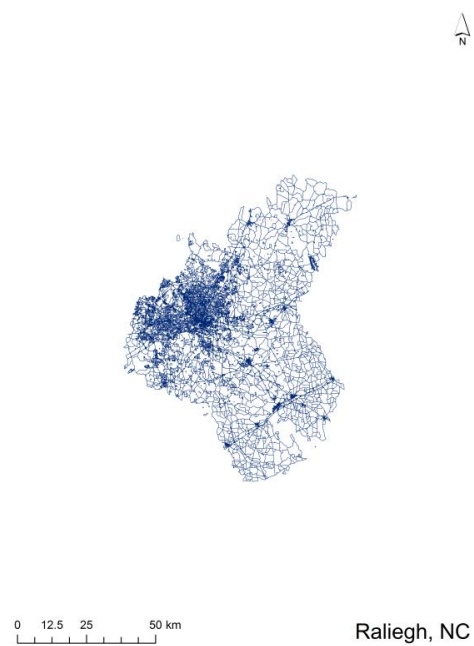
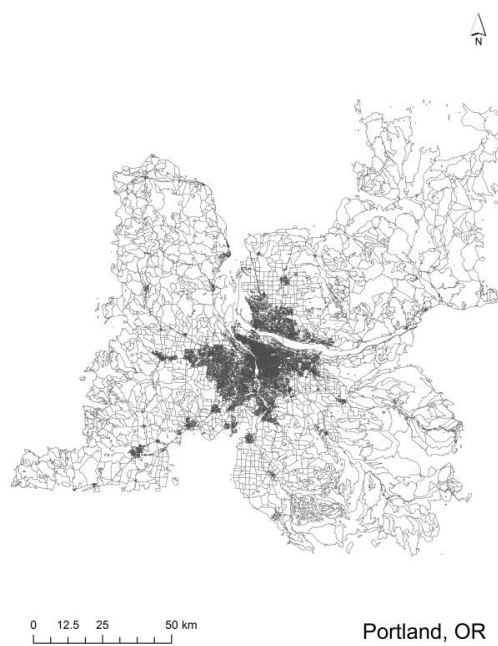
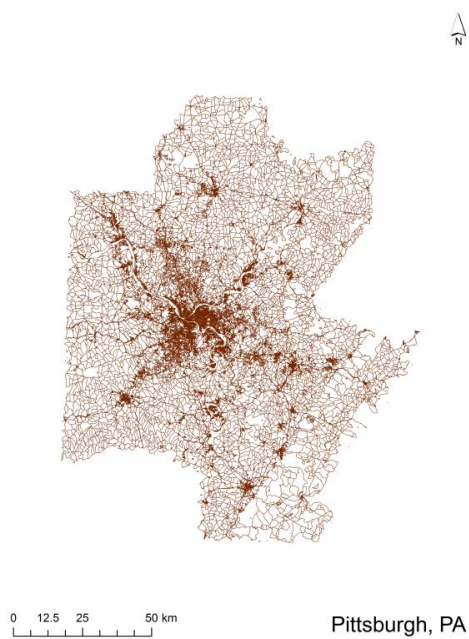


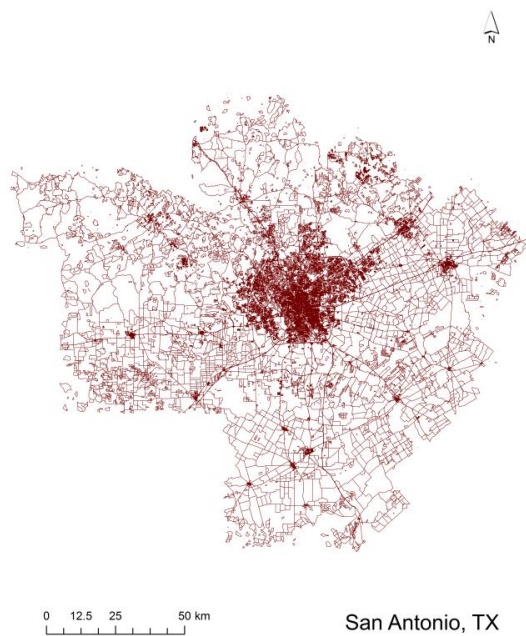
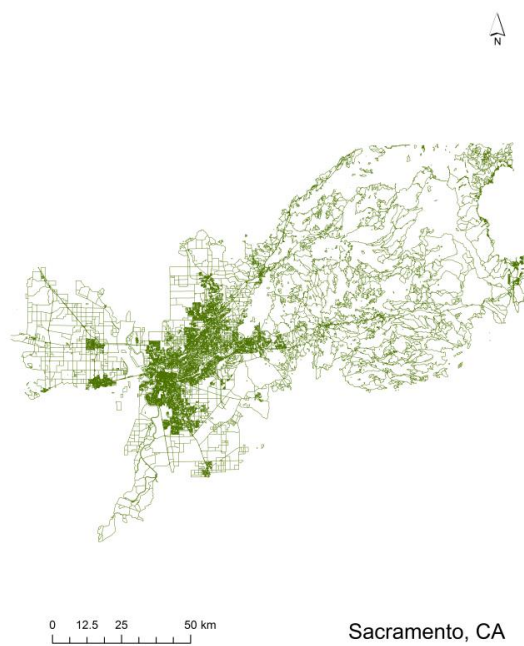
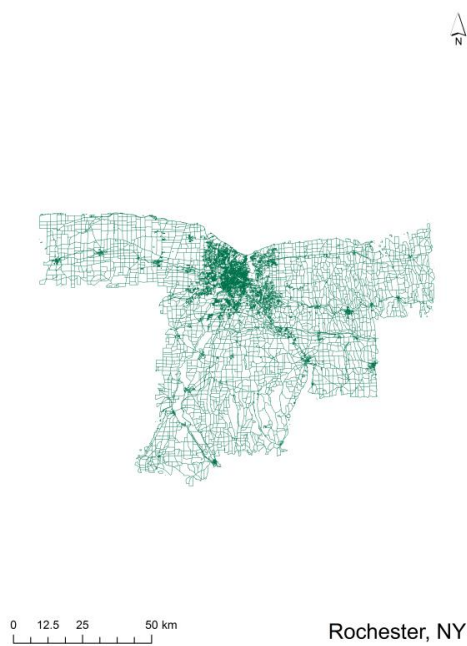
0 12.5 25 50 km

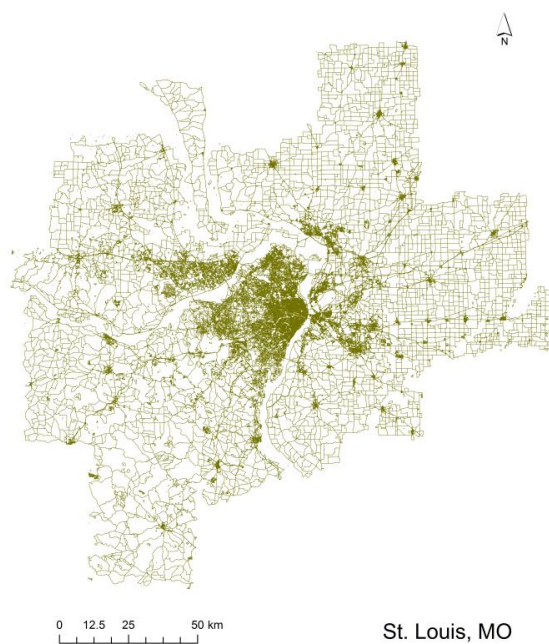
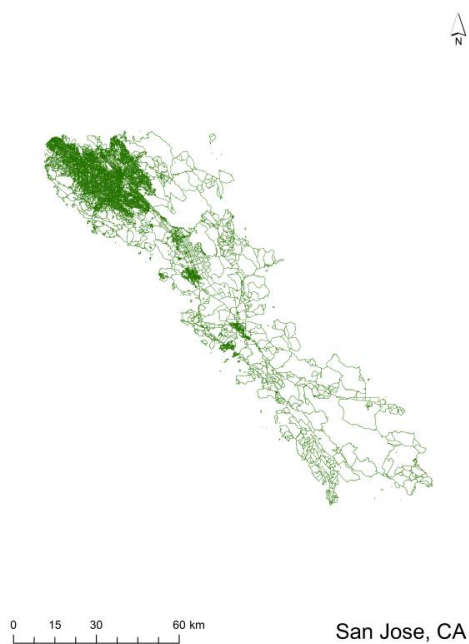
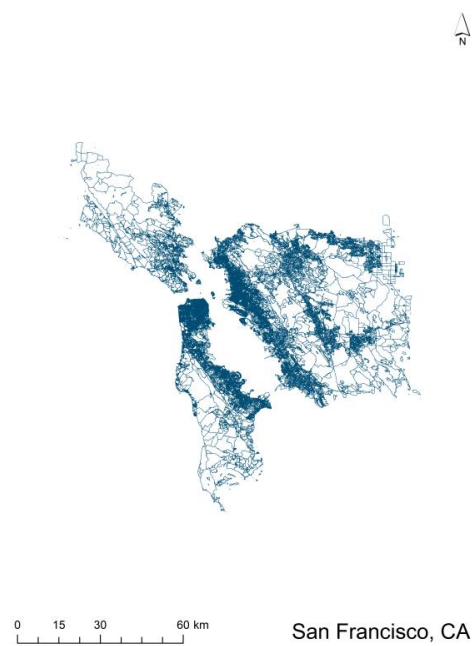
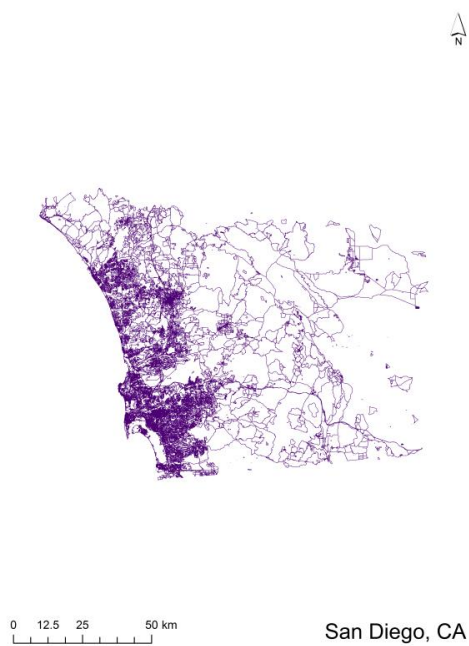
New York, NY











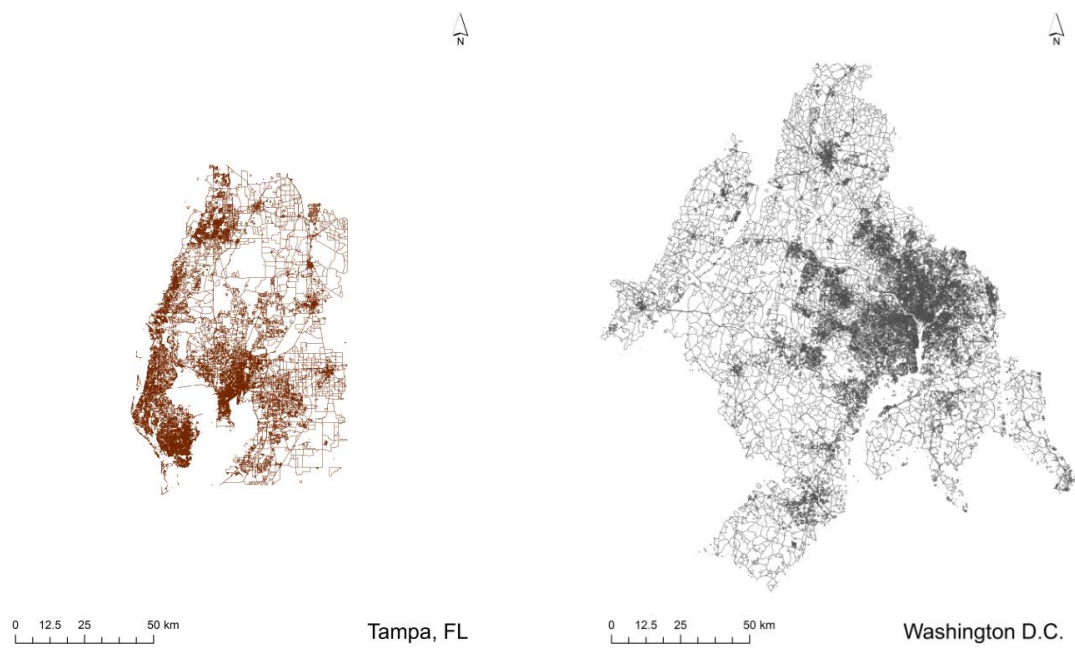
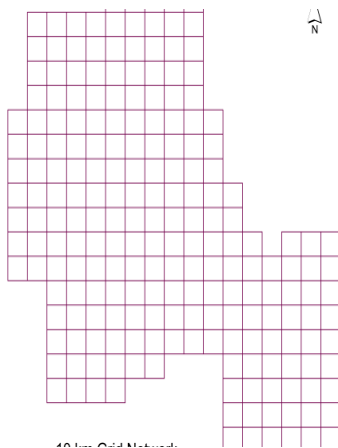


Figure B1. Relative sizes and shapes of the 50 urban road polygons analyzed in this study

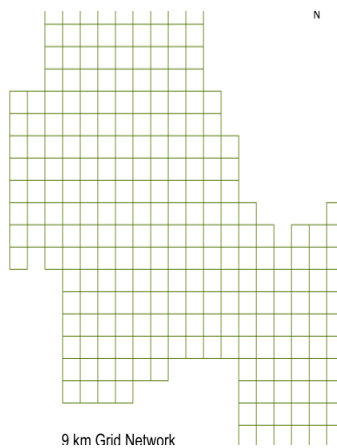
## **APPENDIX C: Details of Grid Creation for Chicago MSA**

### Details of grid creation for Chicago MSA

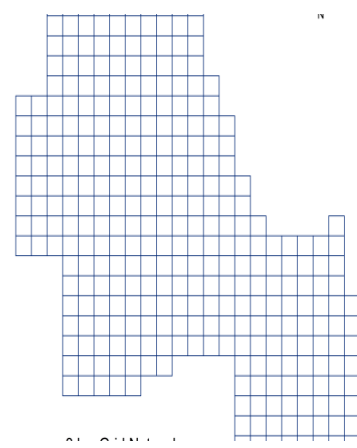
As explained in the methodology, at first the MSA of the given urban area was chosen as its extent. In the next step, successive grids with varying block sizes were created and then overlaid on the road network, from which the cells needed to cover all the road segments within the MSA were extracted. Figures below demonstrate the creation of grids with cells ranging from 10 km to 100 m for Chicago MSA road network. They show how the grid network evolves towards the real road network. During this process, there are thresholds at which the grid network becomes equivalent to the road network from area, line, and point dimensional perspectives. The last figure demonstrates the real road network for visual comparison.



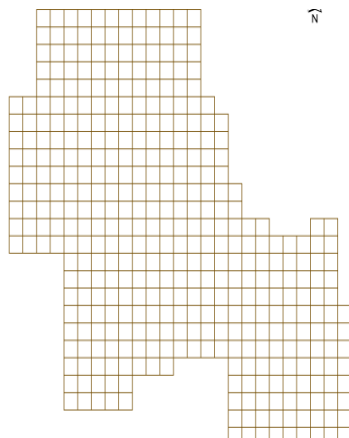
a) 10 km Grid Network



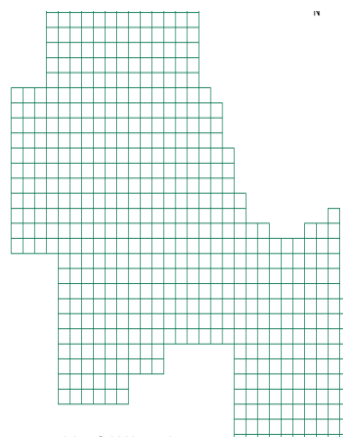
b) 9 km Grid Network



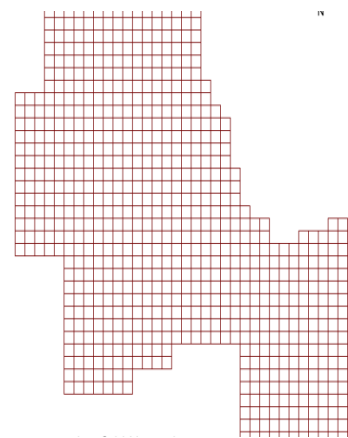
c) 8 km Grid Network



d) 7 km Grid Network

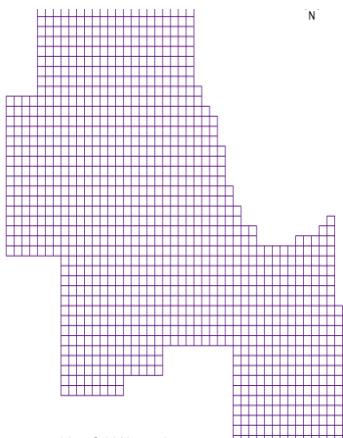


e) 6 km Grid Network

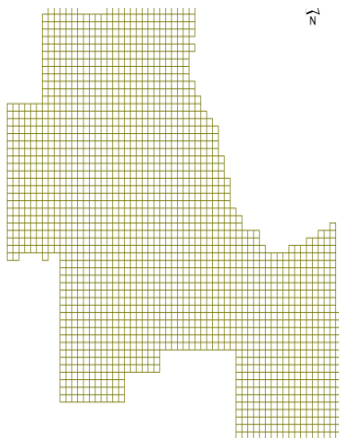


f) 5 km Grid Network

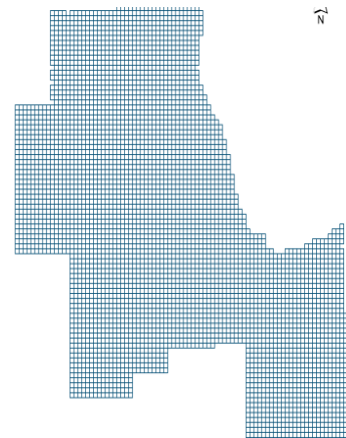




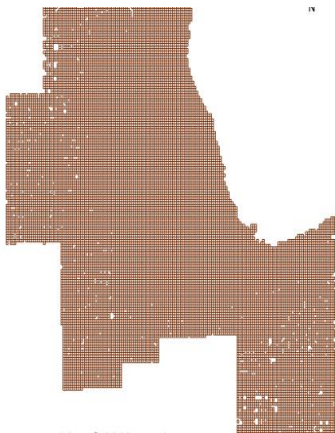
g) 4 km Grid Network



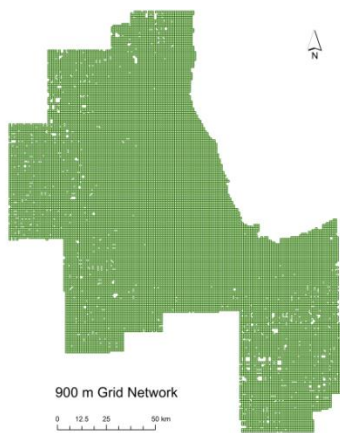
h) 3 km Grid Network



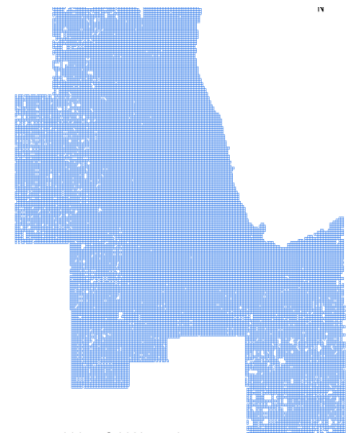
i) 2 km Grid Network



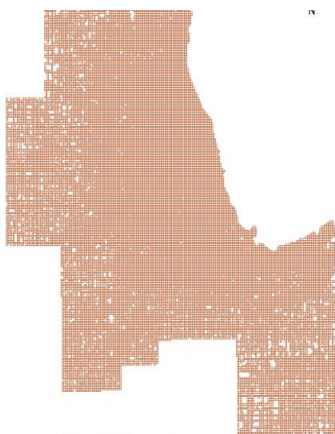
j) 1 km Grid Network



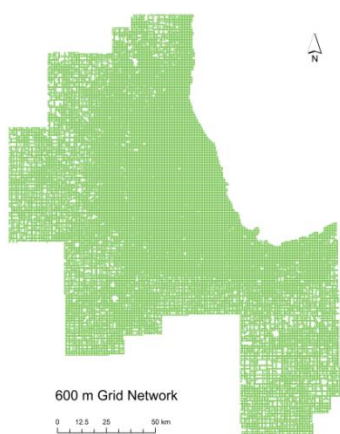
k) 900 m Grid Network



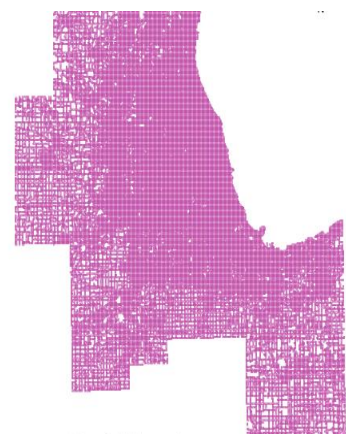
l) 800 m Grid Network



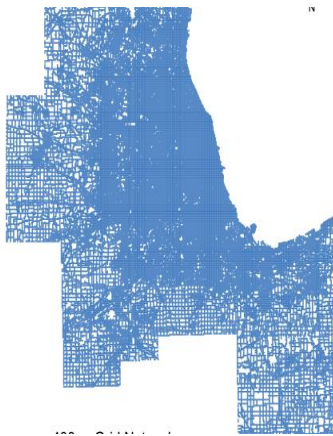
m) 700 m Grid Network



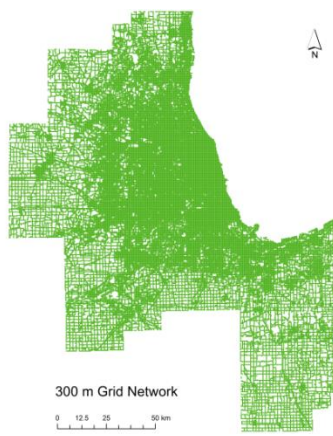
n) 600 m Grid Network



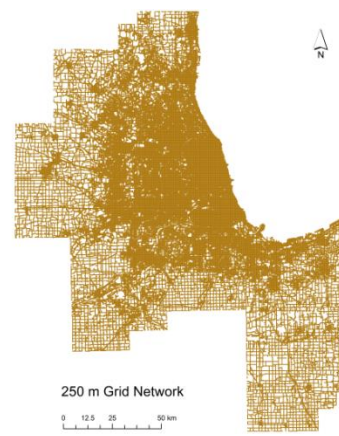
o) 500 m Grid Network



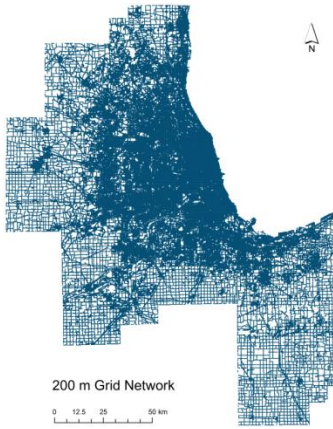
p) 400 m Grid Network



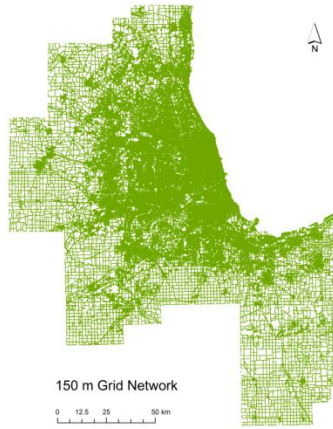
q) 300 m Grid Network



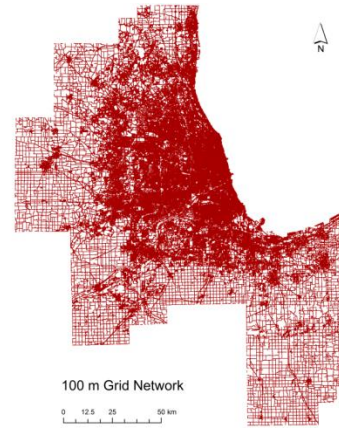
r) 250 m Grid Network



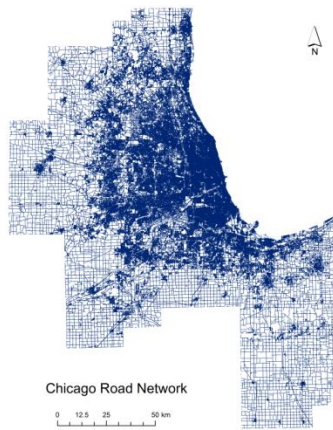
s) 200 m Grid Network



t) 150 m Grid Network



u) 100 m Grid Network



v) Chicago Road Network

Figure C1. Details of grid creation for Chicago MSA



## **APPENDIX D: Area, Point, and Line Thresholds for 50 U.S. Urban Road Networks**

Table 5 Area, point, and line thresholds for 50 U.S. urban road systems

<b>Urban Area, State</b>	<b>Area Threshold (m)</b>	<b>Line Threshold (m)</b>	<b>Point Threshold (m)</b>
Atlanta, GA	872	610	270
Austin, TX	794	666	272
Baltimore, MD	390	352	153
Boston, MA	480	353	174
Buffalo, NY	971	615	270
Carson, NV	156	778	279
Charlotte, NC	672	627	267
Chicago, IL	984	321	179
Cincinnati, OH	745	668	249
Cleveland, OH	821	479	251
Columbus, OH	907	722	267
Dallas, TX	971	472	215
Denver, CO	1671	654	241
Detroit, MI	751	381	204
Grand Rapids, MI	792	926	395
Hartford, CT	545	514	245
Honolulu, HI	454	361	178
Houston, TX	904	450	210
Indianapolis, IN	863	575	213
Jacksonville, FL	923	670	271
Kansas City, KS	1028	793	282
Las Vegas, NV	1330	484	181
Lewiston, ID	663	980	727
Los Angeles, CA	962	230	152
Louisville, KY	767	879	327

Table 5 Area, point, and line thresholds for 50 U.S. urban road systems

<b>Urban Area, State</b>	<b>Area Threshold (m)</b>	<b>Line Threshold (m)</b>	<b>Point Threshold (m)</b>
Memphis, TN	960	891	348
Miami, FL	1660	248	174
Milwaukee, WI	700	386	212
Minneapolis, MN	904	502	207
Nashville, TN	868	919	383
New Orleans, LA	699	372	189
New York, NY	501	282	170
Oklahoma, OK	955	828	296
Orlando, FL	1374	418	200
Philadelphia, PA	648	378	197
Phoenix, AZ	1200	535	221
Pittsburgh, PA	707	596	267
Portland, OR	787	722	270
Providence, RI	531	444	201
Raliegh, NC	637	562	231
Rochester, NY	881	874	380
Sacramento, CA	821	627	260
Salt Lake, UT	1033	957	397
San Antonio, TX	875	806	347
San Diego, CA	1129	413	186
San Francisco, CA	640	272	155
San Jose, CA	773	478	195
St. Louis, MO	880	753	287
Tampa, FL	756	315	180
Washington D.C.	467	361	162

## **APPENDIX E: Density and Decay Indices for 50 U.S. Urban Road Networks**

Table 6 Density and Decay Indices for 50 U.S. Urban Road Networks

Urban Area, State	Density Index (km)	Decay Index (1/km)	Fit Type
Atlanta, GA	20.24	3.9	Logarithmic
Austin, TX	44.855	0.673	Power Law
Baltimore, MD	31.692	6.633	Logarithmic
Boston, MA	29.722	5.79	Logarithmic
Buffalo, NY	19.897	4.344	Logarithmic
Carson, NV	22.281	0.914	Power Law
Charlotte, NC	16.034	3.198	Logarithmic
Chicago, IL	24.43	0.017	Exponential
Cincinnati, OH	49.53	0.675	Power Law
Cleveland, OH	13.39	0.023	Exponential
Columbus, OH	47.732	0.692	Power Law
Dallas, TX	22.61	4.244	Logarithmic
Denver, CO	19.475	0.026	Exponential
Detroit, MI	18.225	0.018	Exponential
Grand Rapids, MI	30.192	0.632	Power Law
Hartford, CT	26.681	0.541	Power Law
Honolulu, HI	22.073	0.586	Power Law
Houston, TX	18.448	0.019	Exponential
Indianapolis, IN	72.927	0.755	Power Law
Jacksonville, FL	32.15	0.625	Power Law
Kansas City, KS	20.921	4.207	Logarithmic
Las Vegas, NV	148.2	1.105	Power Law
Lewiston, ID	15.368	0.721	Power Law
Los Angeles, CA	27.803	4.908	Logarithmic
Louisville, KY	18.781	4.192	Logarithmic

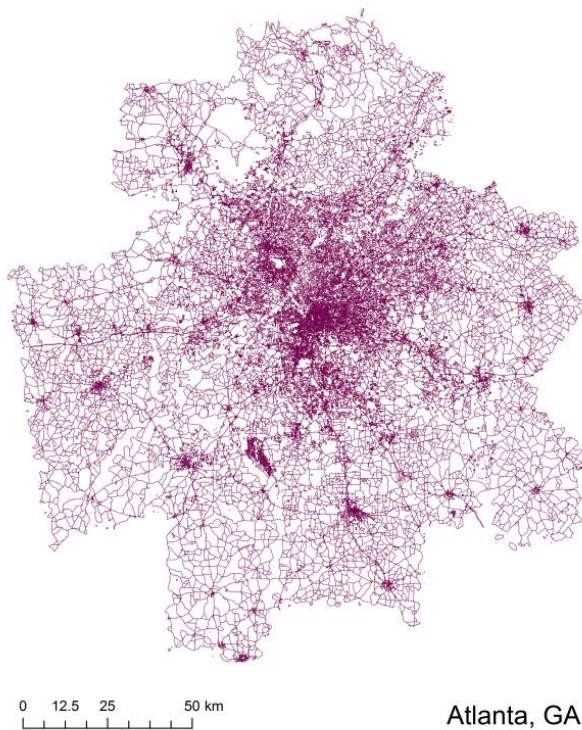
Table 6 Density and Decay Indices for 50 U.S. Urban Road Networks

Urban Area, State	Density Index (km)	Decay Index (1/km)	Fit Type
Memphis, TN	32.929	0.656	Power Law
Miami, FL	17.908	0.021	Exponential
Milwaukee, WI	27.063	5.803	Logarithmic
Minneapolis, MN	92.52	0.742	Power Law
Nashville, TN	26.233	0.576	Power Law
New Orleans, LA	63.23	0.854	Power Law
New York, NY	20.149	0.013	Exponential
Oklahoma, OK	51.494	0.712	Power Law
Orlando, FL	21.955	4.632	Logarithmic
Philadelphia, PA	52.557	0.571	Power Law
Phoenix, AZ	19.883	0.026	Exponential
Pittsburgh, PA	43.931	0.606	Power Law
Portland, OR	29.404	6.371	Logarithmic
Providence, RI	36.808	0.586	Power Law
Raliegh, NC	53.298	0.723	Power Law
Rochester, NY	40.877	0.709	Power Law
Sacramento, CA	42.276	0.643	Power Law
Salt Lake, UT	55.928	0.818	Power Law
San Antonio, TX	59.363	0.725	Power Law
San Diego, CA	44.855	0.666	Power Law
San Francisco, CA	18.316	0.019	Exponential
San Jose, CA	24.289	5.063	Logarithmic
St. Louis, MO	92.722	0.801	Power Law
Tampa, FL	46.73	0.576	Power Law
Washington D.C.	28.348	5.341	Logarithmic

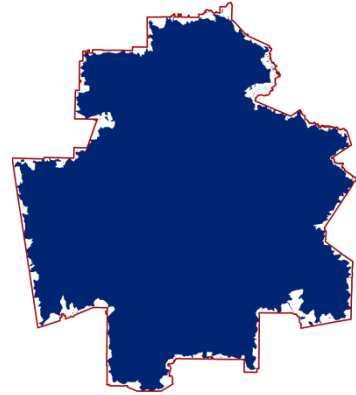
## **APPENDIX F: Characteristic Maps for 50 U.S. Urban Systems**

## Atlanta, GA

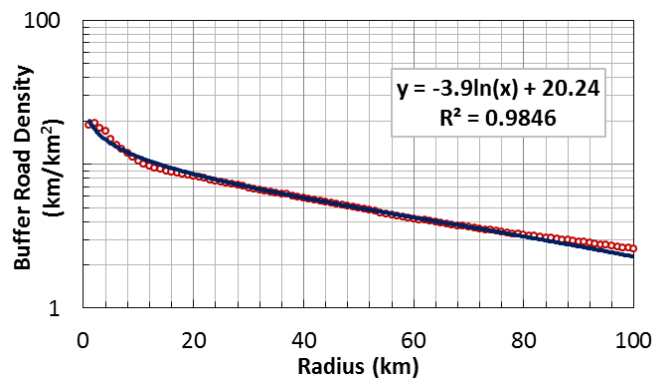
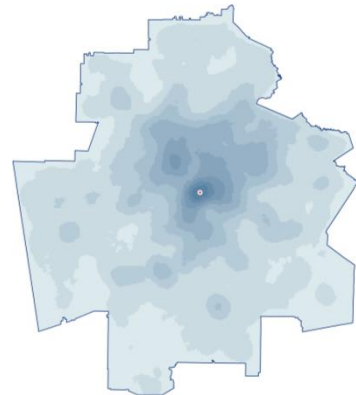
Road Network



Road Polygon Area



Road Density Map



Road Density Fit

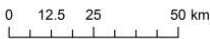
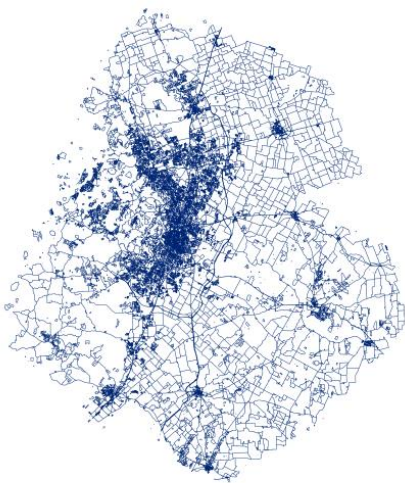
### Characteristics

Founded in	1843
Population	5486738
Pop Density	270.2
Area (km <sup>2</sup> )	20306.8
Road Length (km)	67215.1
# of Intersections	243462
Area Threshold	872
Line Threshold	610
Point Threshold	270
Density Index	20.24
Decay Index	3.9



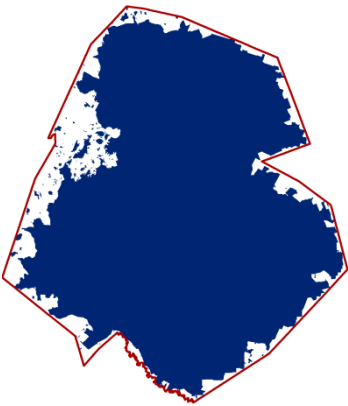
Austin, TX

Road Network

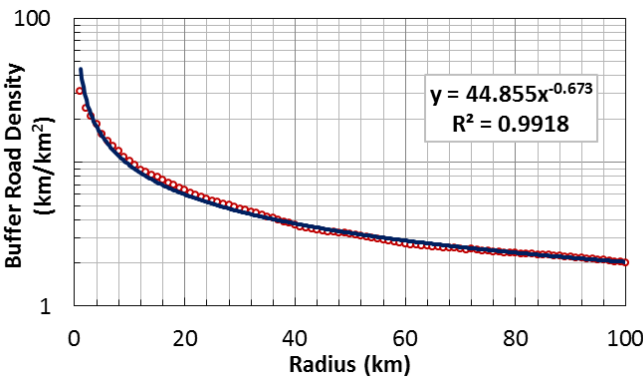
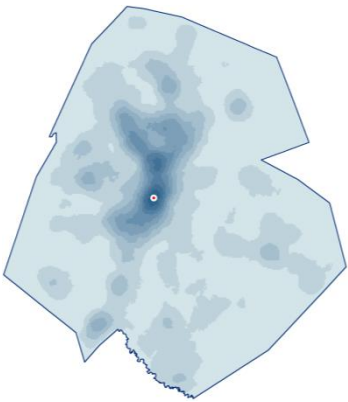


Austin, TX

Road Polygon Area



Road Density Map



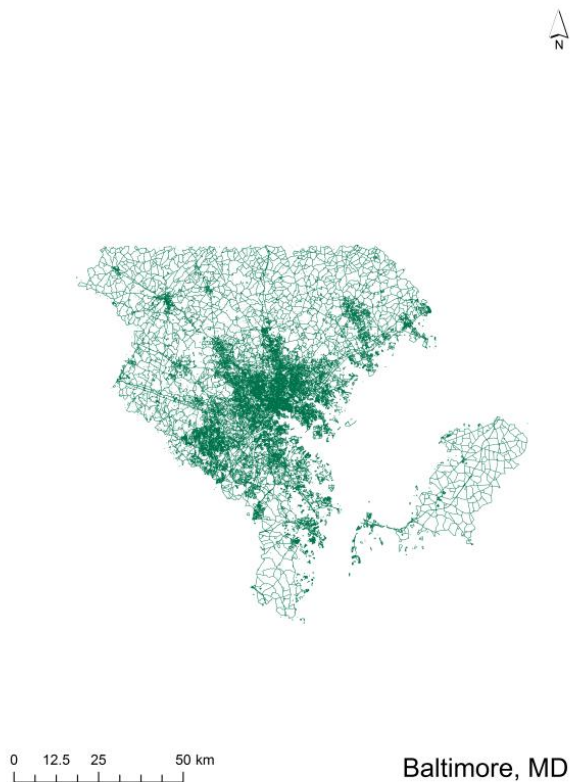
Road Density Fit

Characteristics

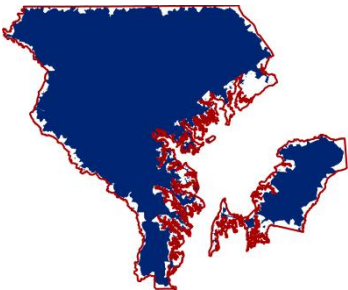
Founded in	1835
Population	1784094
Pop Density	189
Area (km <sup>2</sup> )	9440.8
Road Length (km)	30382
# of Intersections	111234
Area Threshold	794
Line Threshold	666
Point Threshold	272
Density Index	44.855
Decay Index	0.673

**Baltimore, MD**

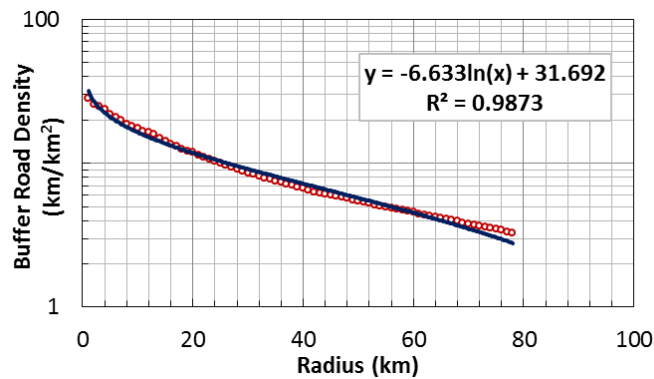
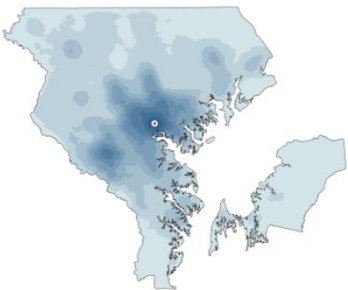
Road Network



Road Polygon Area



Road Density Map



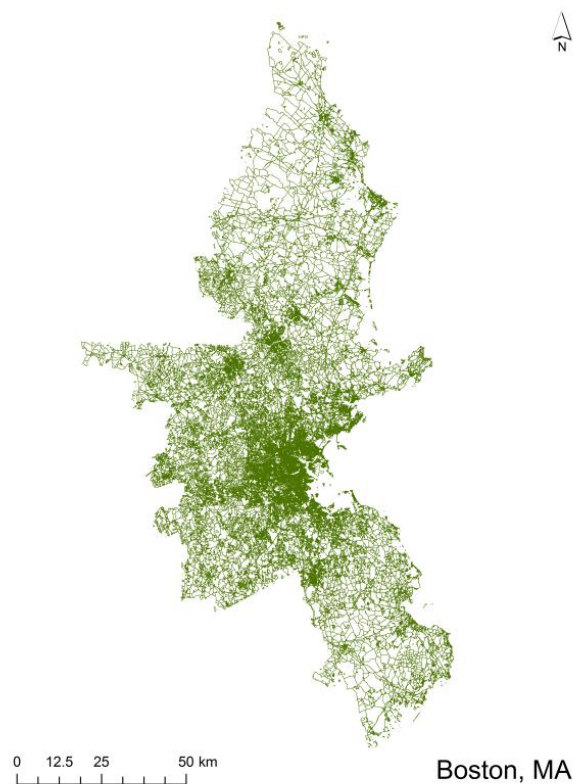
Road Density Fit

**Characteristics**

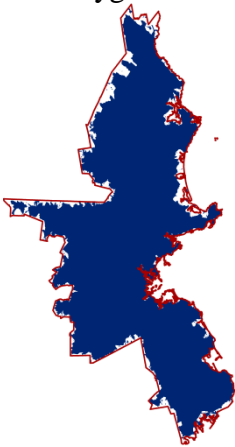
Founded in	1729
Population	2895944
Pop Density (/km <sup>2</sup> )	514.8
Area (km <sup>2</sup> )	5624.9
Road Length (km)	35556.3
# of Intersections	220784
Area Threshold (m)	390
Line Threshold (m)	352
Point Threshold (m)	153
Density Index (km <sup>2</sup> )	31.692
Decay Index (1/km)	6.633

**Boston, MA**

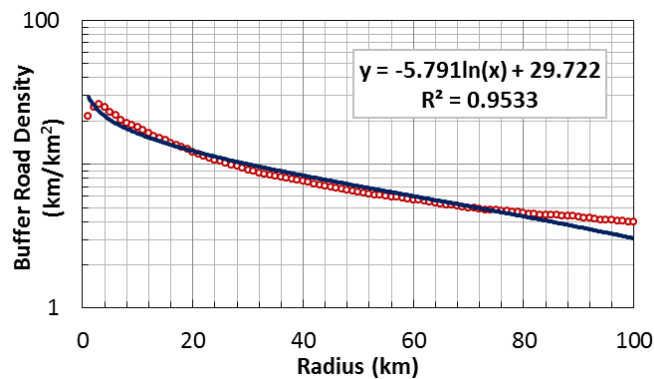
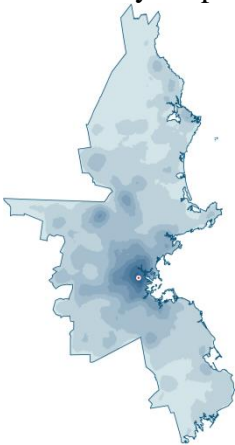
Road Network



Road Polygon Area



Road Density Map



Road Density Fit

**Characteristics**

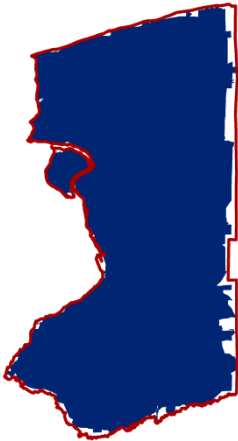
Founded in	1630
Population	4892136
Pop Density (/km <sup>2</sup> )	584.6
Area (km <sup>2</sup> )	8368.7
Road Length (km)	49139.9
# of Intersections	261949
Area Threshold (m)	480
Line Threshold (m)	353
Point Threshold (m)	174
Density Index (km <sup>2</sup> )	29.722
Decay Index (1/km)	5.79

**Buffalo, NY**

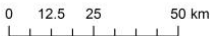
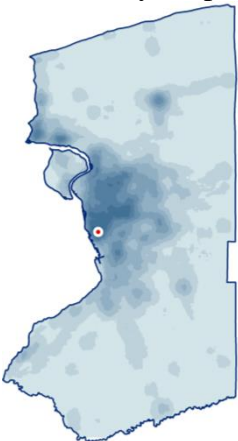
Road Network



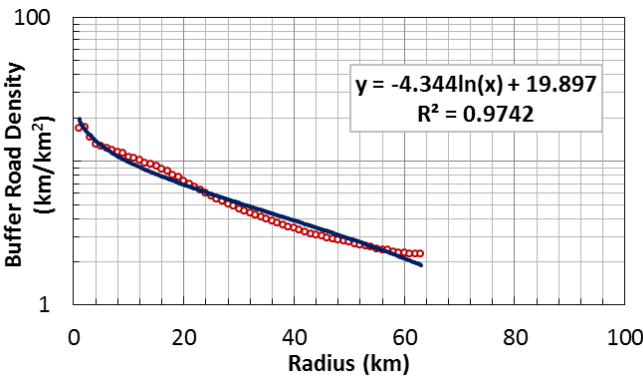
Road Polygon Area



Road Density Map



Buffalo, NY



Road Density Fit

**Characteristics**

Founded in	1789
Population	1191744
Pop Density (/km <sup>2</sup> )	311.9
Area (km <sup>2</sup> )	3821.4
Road Length (km)	12293
# of Intersections	41429
Area Threshold (m)	971
Line Threshold (m)	615
Point Threshold (m)	270
Density Index (km <sup>2</sup> )	19.897
Decay Index (1/km)	4.344

**Carson, NV**

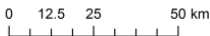
Road Network



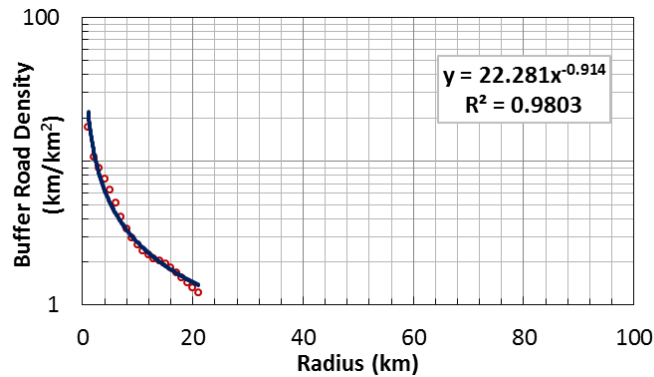
Road Polygon Area



Road Density Map



Carson, NV



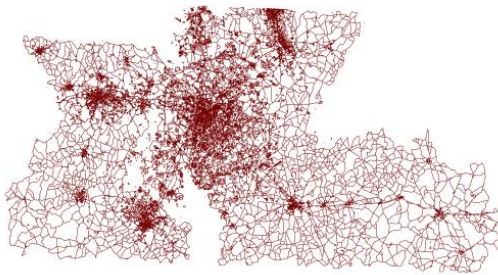
Road Density Fit

**Characteristics**

Founded in	1858
Population	87743
Pop Density (/km²)	804.9
Area (km²)	109
Road Length (km)	900.6
# of Intersections	3045
Area Threshold (m)	156
Line Threshold (m)	778
Point Threshold (m)	279
Density Index (km²)	22.281
Decay Index (1/km)	0.914

## Charlotte, NC

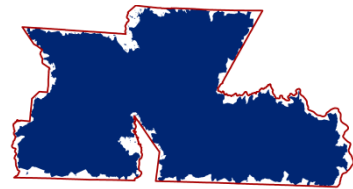
Road Network



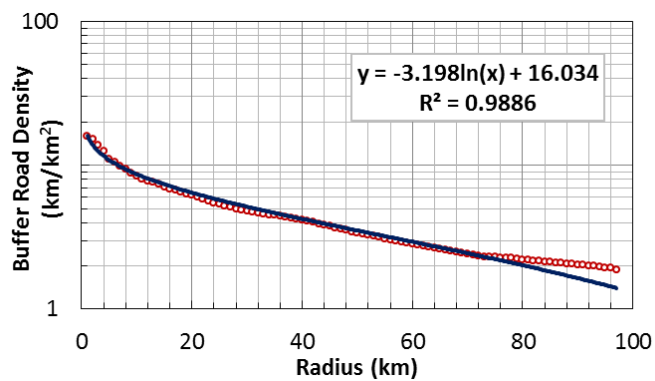
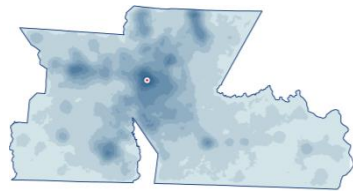
0 12.5 25 50 km

Charlotte, NC

Road Polygon Area



Road Density Map



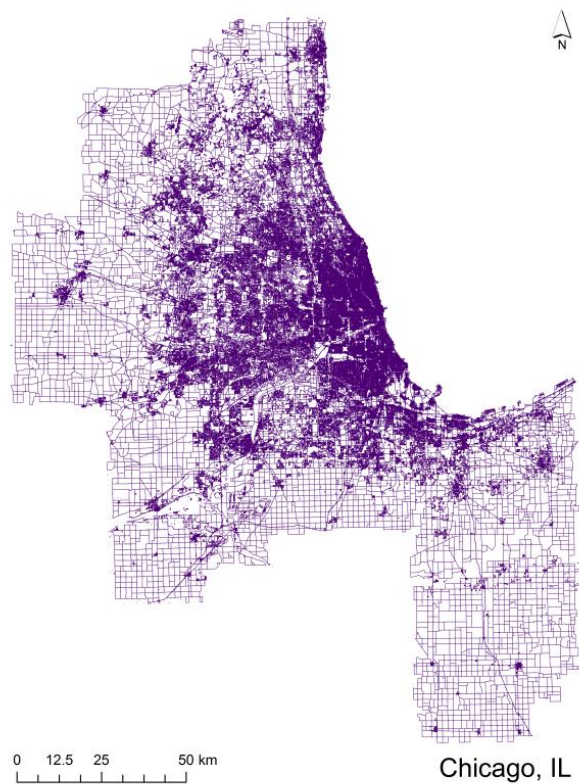
Road Density Fit

### Characteristics

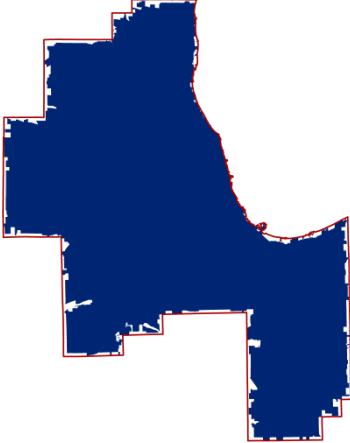
Founded in	1755
Population	1927130
Pop Density (/km <sup>2</sup> )	268.5
Area (km <sup>2</sup> )	7177.5
Road Length (km)	24978.8
# of Intersections	93988
Area Threshold (m)	672
Line Threshold (m)	627
Point Threshold (m)	267
Density Index (km <sup>2</sup> )	16.034
Decay Index (1/km)	3.198

**Chicago, IL**

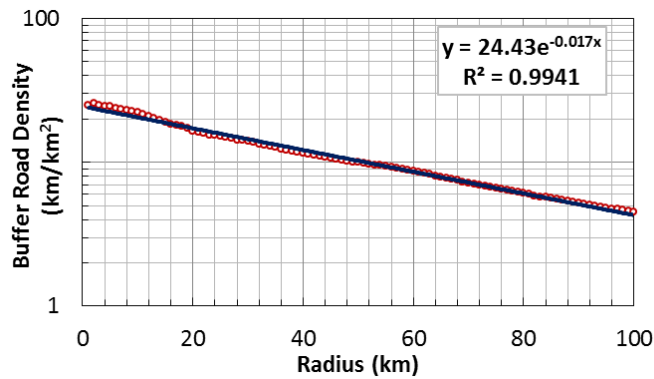
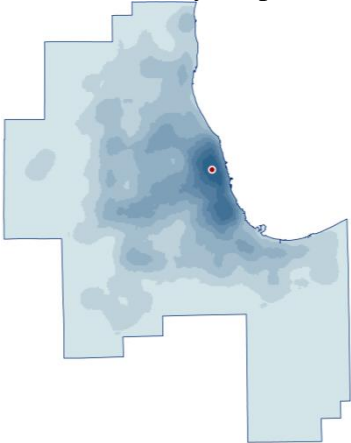
Road Network



Road Polygon Area



Road Density Map



Road Density Fit

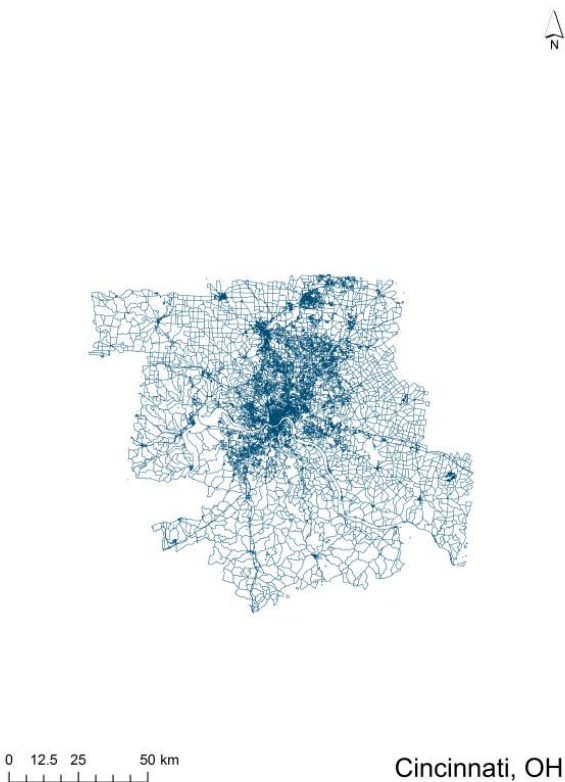
**Characteristics**

Founded in	1803
Population	9594379
Pop Density (/km <sup>2</sup> )	539.5
Area (km <sup>2</sup> )	17783.6
Road Length (km)	86788.9
# of Intersections	396704
Area Threshold (m)	984
Line Threshold (m)	321
Point Threshold (m)	179
Density Index (km <sup>2</sup> )	24.43
Decay Index (1/km)	0.017

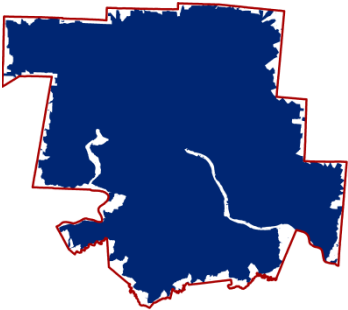


**Cincinnati, OH**

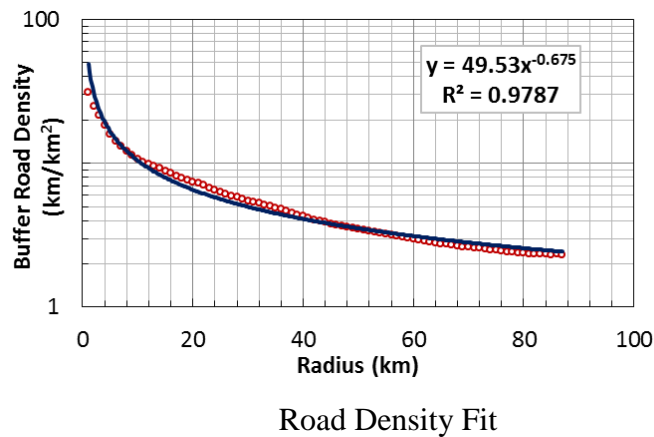
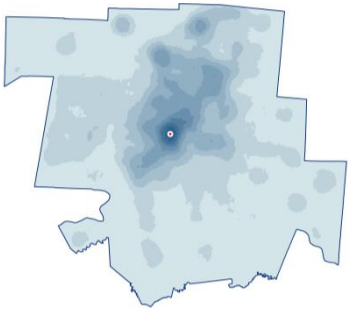
Road Network



Road Polygon Area



Road Density Map



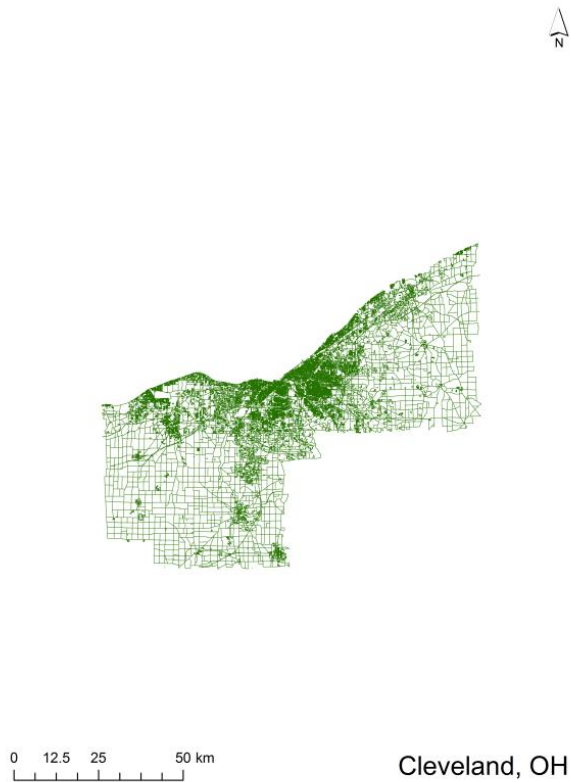
**Characteristics**

Founded in	1788
Population	2252951
Pop Density (/km <sup>2</sup> )	216.7
Area (km <sup>2</sup> )	10398.8
Road Length (km)	33834.5
# of Intersections	141744
Area Threshold (m)	745
Line Threshold (m)	668
Point Threshold (m)	249
Density Index (km <sup>2</sup> )	49.53
Decay Index (1/km)	0.675

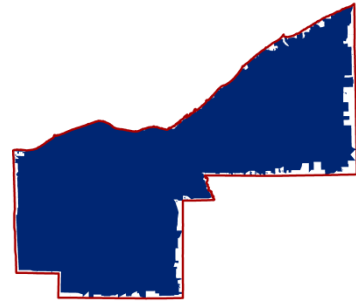


**Cleveland, OH**

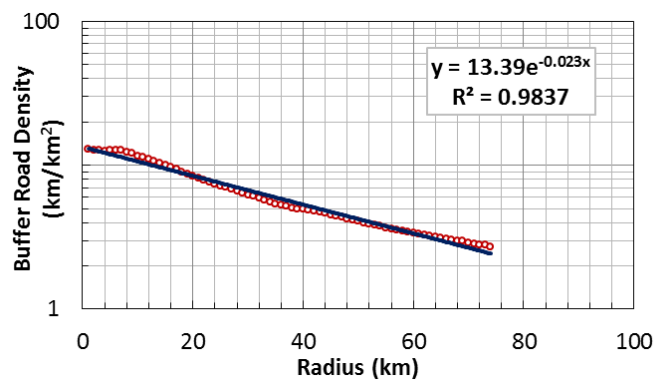
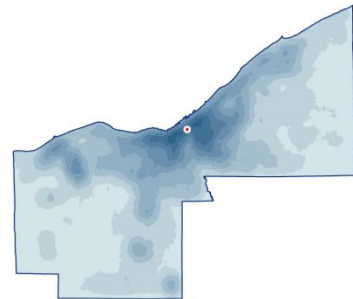
Road Network



Road Polygon Area



Road Density Map



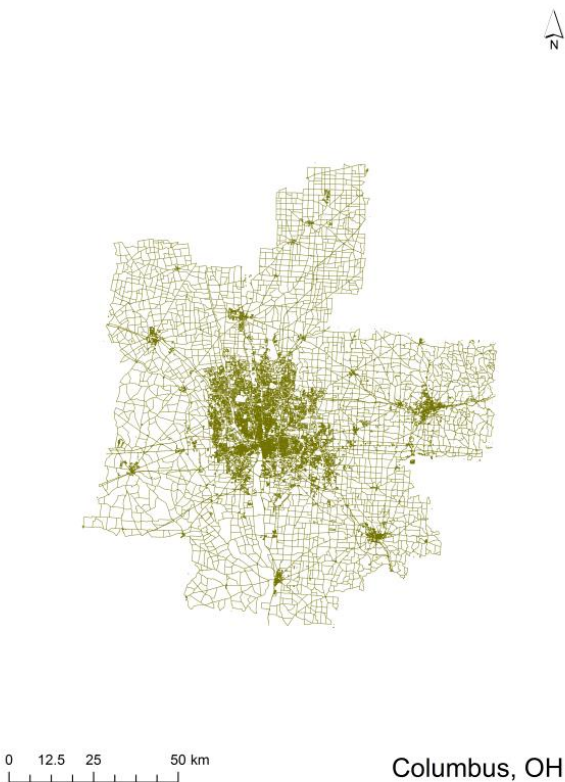
Road Density Fit

**Characteristics**

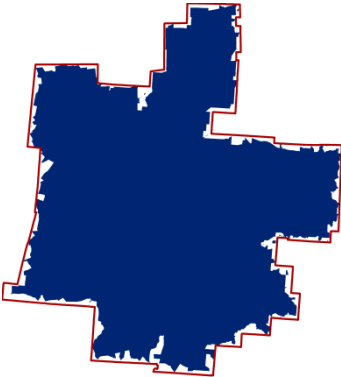
Founded in	1796
Population	2272776
Pop Density (/km <sup>2</sup> )	470.8
Area (km <sup>2</sup> )	4827.5
Road Length (km)	19472.2
# of Intersections	64630
Area Threshold (m)	821
Line Threshold (m)	479
Point Threshold (m)	251
Density Index (km <sup>2</sup> )	13.39
Decay Index (1/km)	0.023

**Columbus, OH**

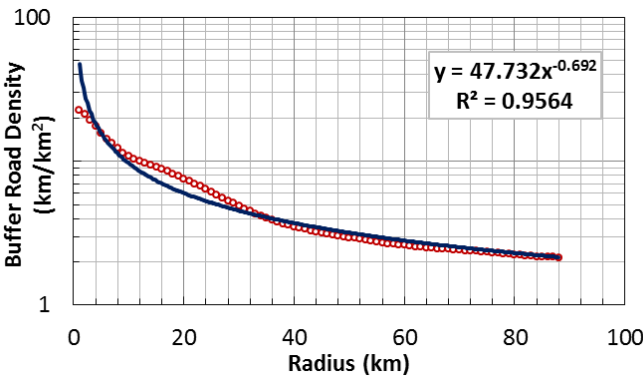
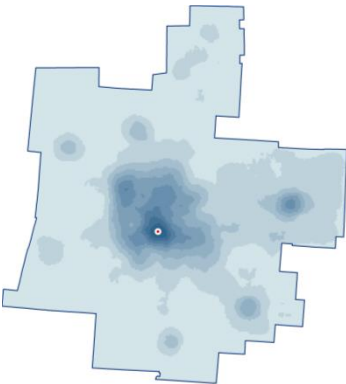
Road Network



Road Polygon Area



Road Density Map



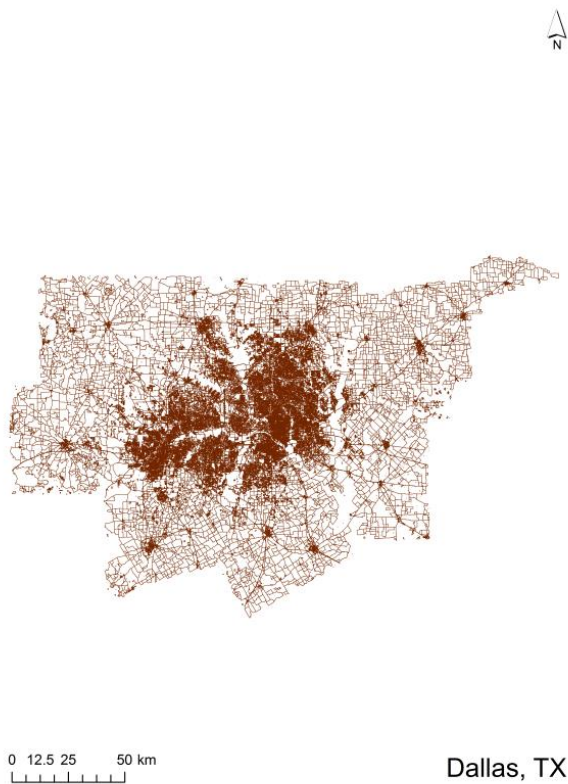
Road Density Fit

**Characteristics**

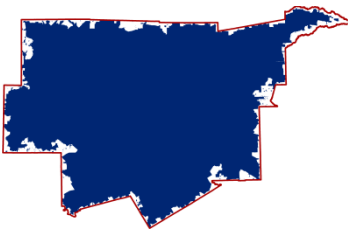
Founded in	1812
Population	1949603
Pop Density (/km <sup>2</sup> )	205.6
Area (km <sup>2</sup> )	9483.2
Road Length (km)	27764.3
# of Intersections	106156
Area Threshold (m)	907
Line Threshold (m)	722
Point Threshold (m)	267
Density Index (km <sup>2</sup> )	47.732
Decay Index (1/km)	0.692

**Dallas, TX**

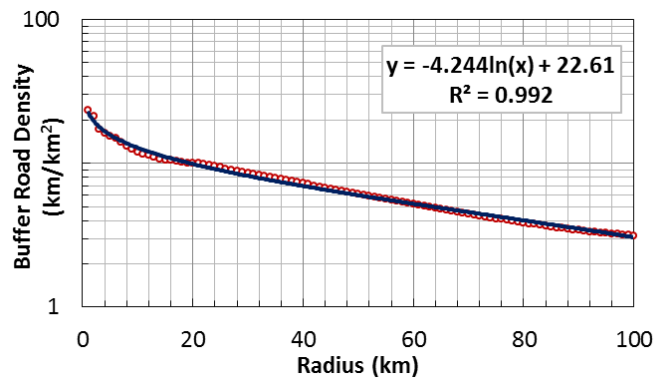
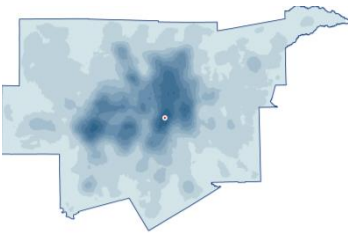
Road Network



Road Polygon Area



Road Density Map



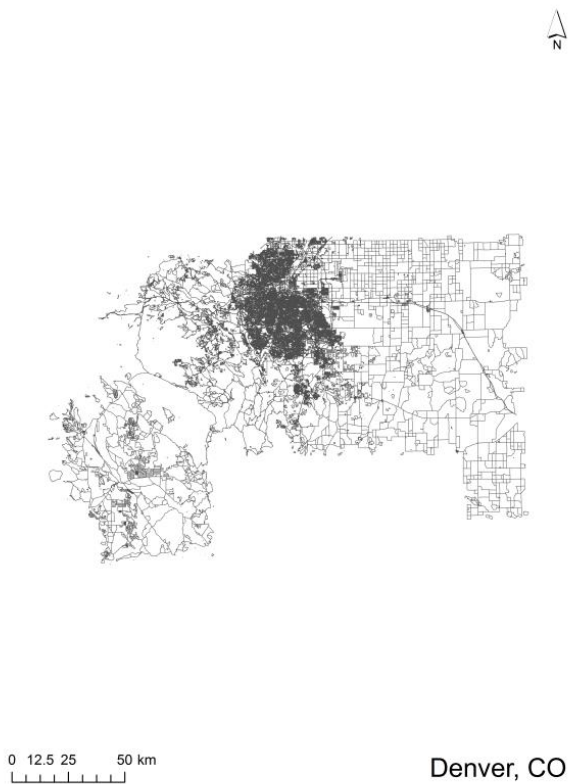
Road Density Fit

**Characteristics**

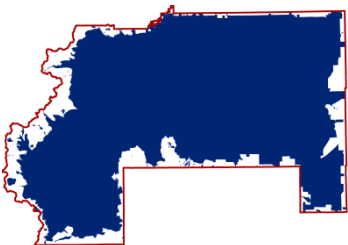
Founded in	1841
Population	6501589
Pop Density (/km <sup>2</sup> )	297.8
Area (km <sup>2</sup> )	21833.1
Road Length (km)	83815.2
# of Intersections	350762
Area Threshold (m)	971
Line Threshold (m)	472
Point Threshold (m)	215
Density Index (km <sup>2</sup> )	22.61
Decay Index (1/km)	4.244

Denver, CO

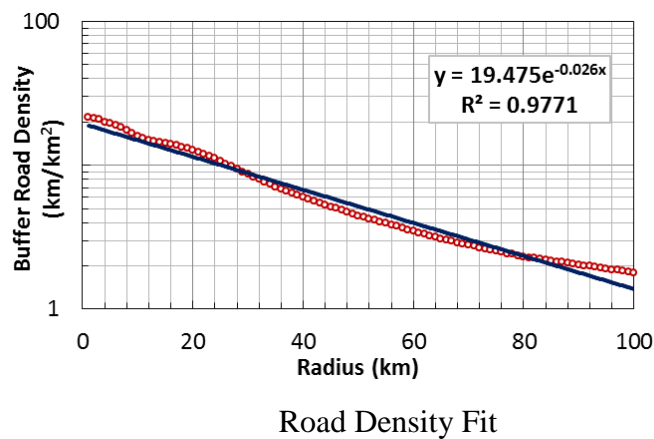
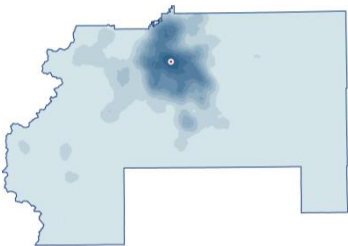
Road Network



Road Polygon Area



Road Density Map

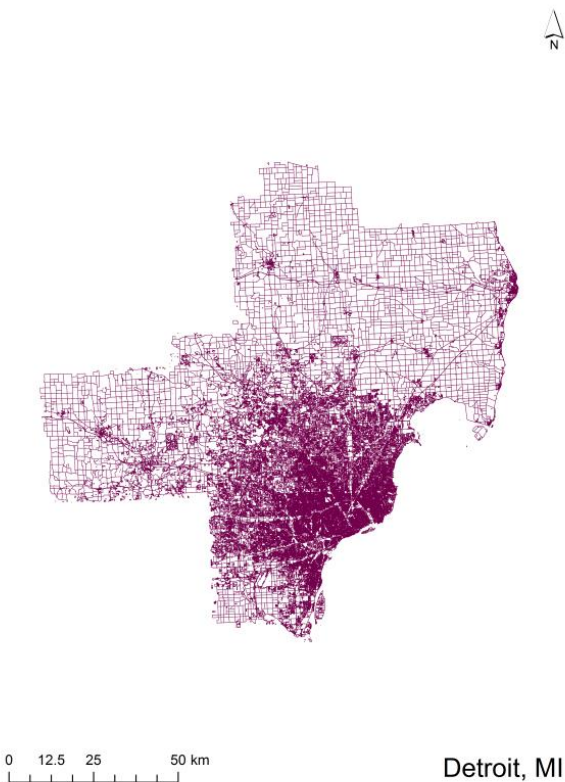


Characteristics

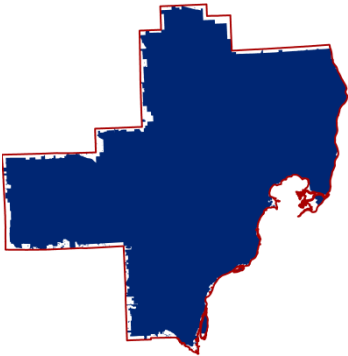
Founded in	1858
Population	2666592
Pop Density (/km <sup>2</sup> )	146
Area (km <sup>2</sup> )	18262
Road Length (km)	46547
# of Intersections	182157
Area Threshold (m)	1671
Line Threshold (m)	654
Point Threshold (m)	241
Density Index (km <sup>2</sup> )	19.475
Decay Index (1/km)	0.026

**Detroit, MI**

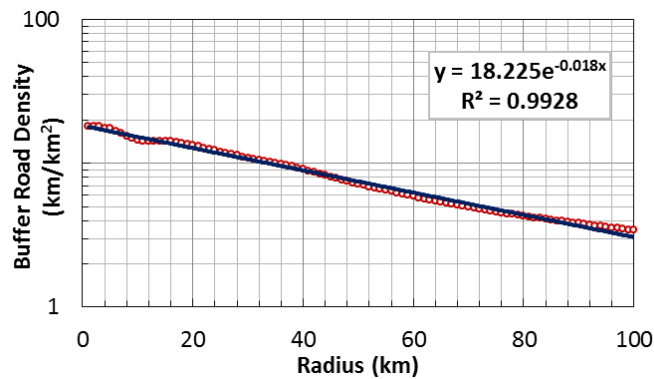
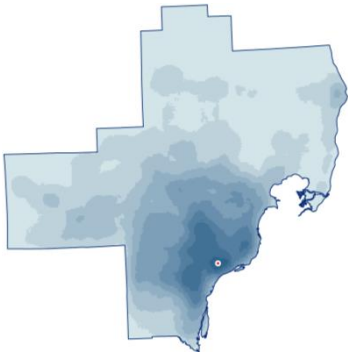
Road Network



Road Polygon Area



Road Density Map



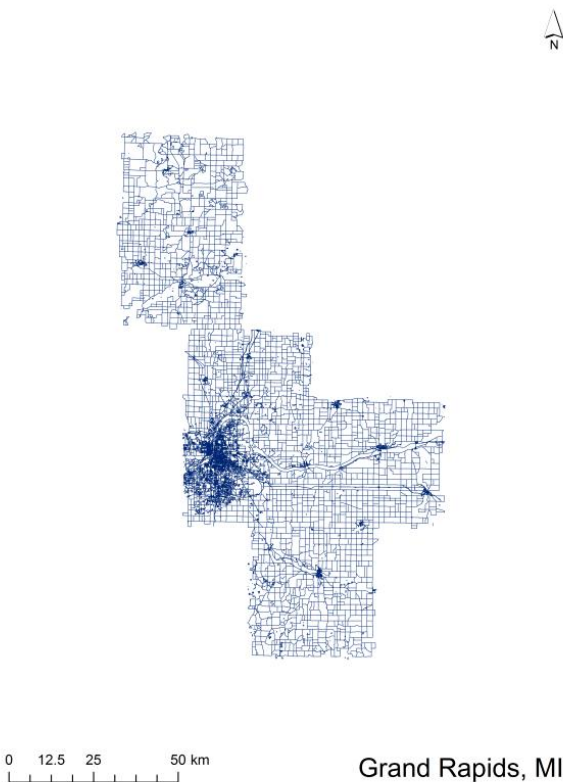
Road Density Fit

**Characteristics**

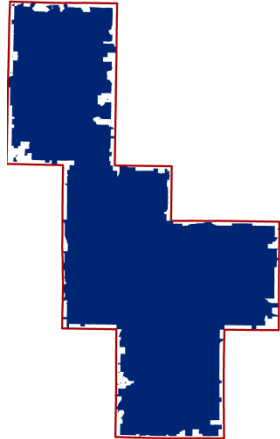
Founded in	1701
Population	4369224
Pop Density (/km <sup>2</sup> )	452.1
Area (km <sup>2</sup> )	9664.6
Road Length (km)	46880.4
# of Intersections	187960
Area Threshold (m)	751
Line Threshold (m)	381
Point Threshold (m)	204
Density Index (km <sup>2</sup> )	18.225
Decay Index (1/km)	0.018

**Grand Rapids, MI**

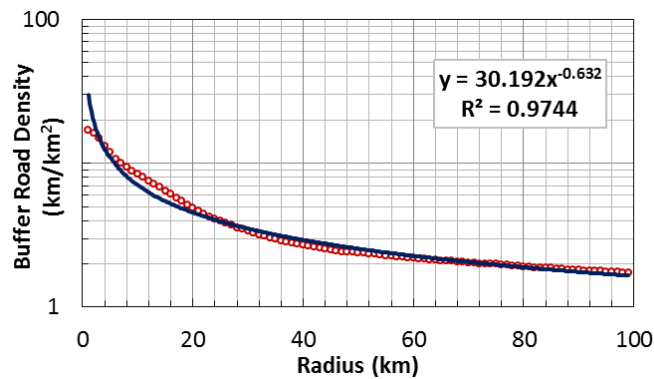
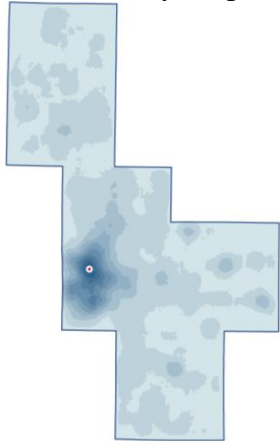
Road Network



Road Polygon Area



Road Density Map



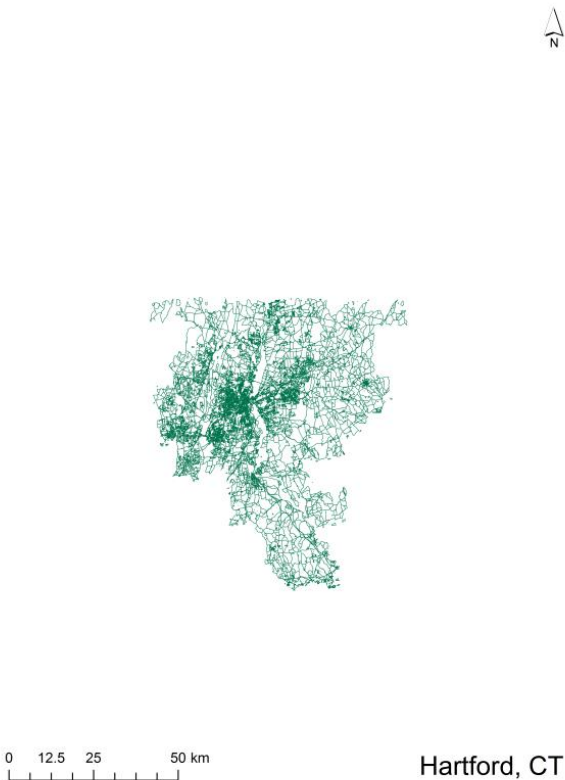
Road Density Fit

**Characteristics**

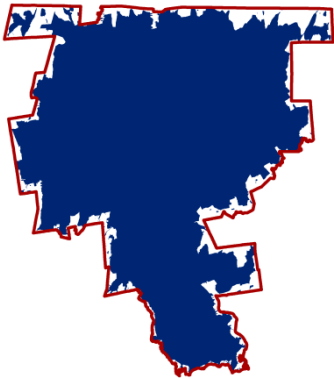
Founded in	1825
Population	895227
Pop Density (/km <sup>2</sup> )	134.3
Area (km <sup>2</sup> )	6665.8
Road Length (km)	16684.6
# of Intersections	42990
Area Threshold (m)	792
Line Threshold (m)	926
Point Threshold (m)	395
Density Index (km <sup>2</sup> )	30.192
Decay Index (1/km)	0.632

**Hartford, CT**

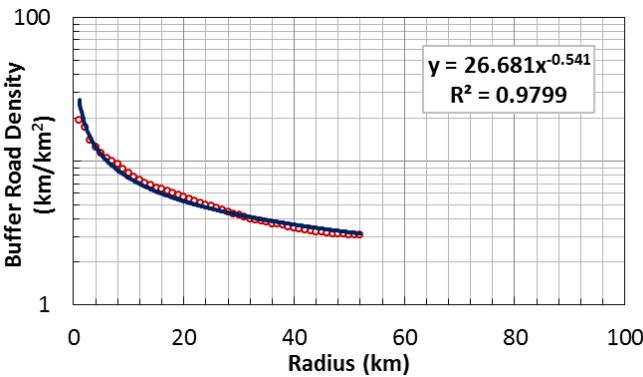
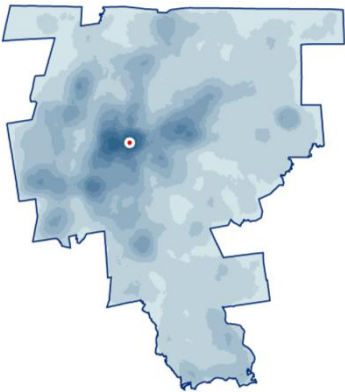
Road Network



Road Polygon Area



Road Density Map



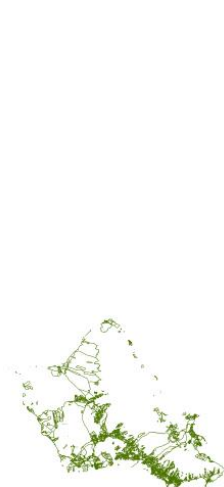
Road Density Fit

**Characteristics**

Founded in	1637
Population	1400709
Pop Density (/km <sup>2</sup> )	401.6
Area (km <sup>2</sup> )	3487.6
Road Length (km)	14992.7
# of Intersections	56695
Area Threshold (m)	545
Line Threshold (m)	514
Point Threshold (m)	245
Density Index (km <sup>2</sup> )	26.681
Decay Index (1/km)	0.541

**Honolulu, HI**

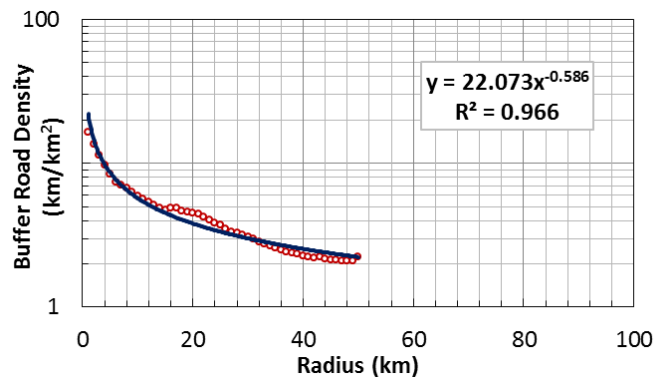
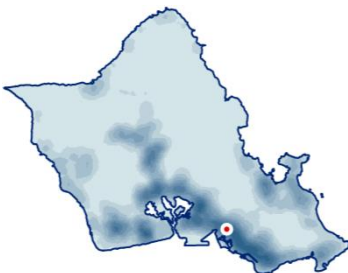
Road Network



Road Polygon Area



Road Density Map



Road Density Fit

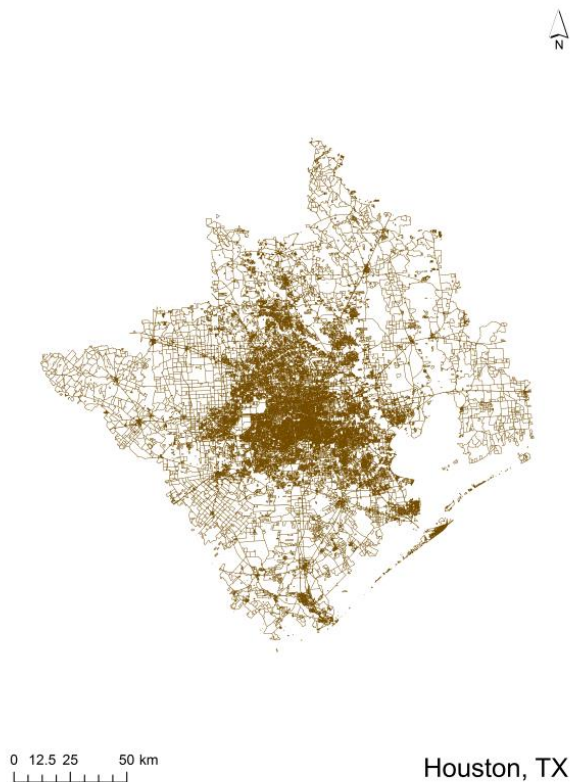
**Characteristics**

Founded in	1809
Population	953207
Pop Density (/km <sup>2</sup> )	1229.3
Area (km <sup>2</sup> )	775.4
Road Length (km)	4678.9
# of Intersections	22904
Area Threshold (m)	454
Line Threshold (m)	361
Point Threshold (m)	178
Density Index (km <sup>2</sup> )	22.073
Decay Index (1/km)	0.586

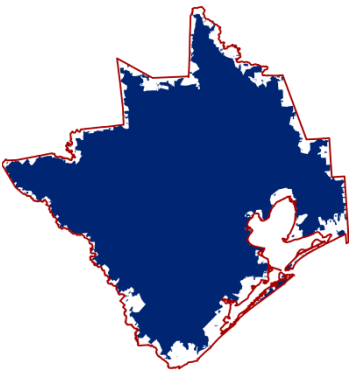


**Houston, TX**

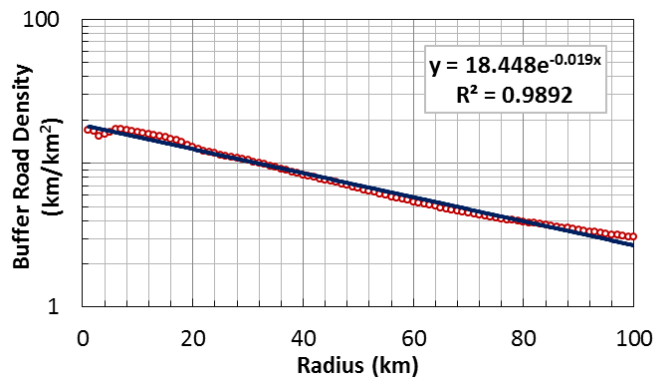
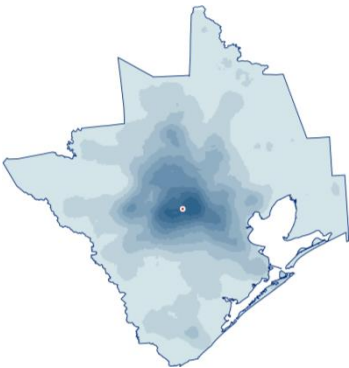
Road Network



Road Polygon Area



Road Density Map



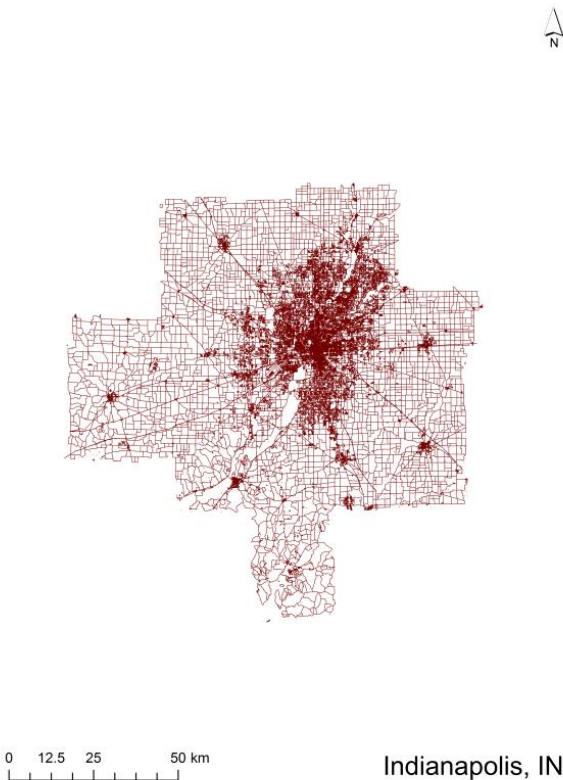
Road Density Fit

**Characteristics**

Founded in	1837
Population	6052475
Pop Density (/km <sup>2</sup> )	294
Area (km <sup>2</sup> )	20585.7
Road Length (km)	83365
# of Intersections	353831
Area Threshold (m)	904
Line Threshold (m)	450
Point Threshold (m)	210
Density Index (km <sup>2</sup> )	18.448
Decay Index (1/km)	0.019

**Indianapolis, IN**

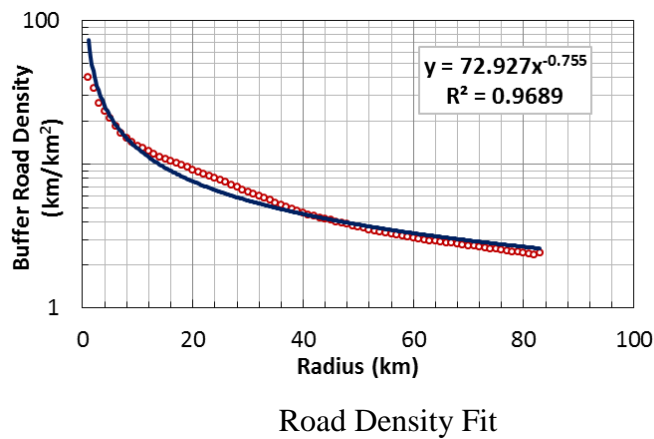
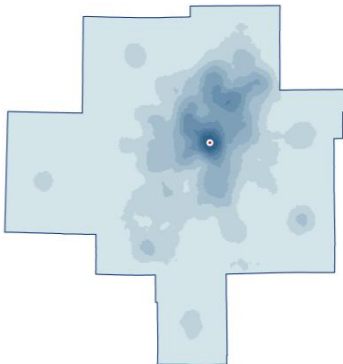
Road Network



Road Polygon Area



Road Density Map



**Characteristics**

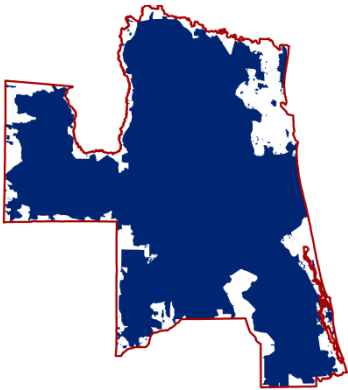
Founded in	1821
Population	1856996
Pop Density (/km <sup>2</sup> )	199.9
Area (km <sup>2</sup> )	9289.1
Road Length (km)	32389.9
# of Intersections	150469
Area Threshold (m)	863
Line Threshold (m)	575
Point Threshold (m)	213
Density Index (km <sup>2</sup> )	72.927
Decay Index (1/km)	0.755

**Jacksonville, FL**

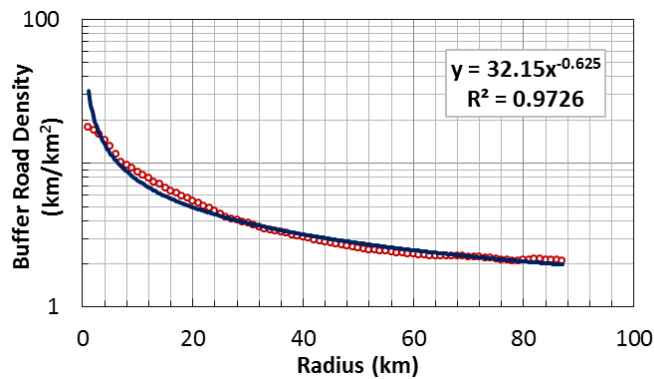
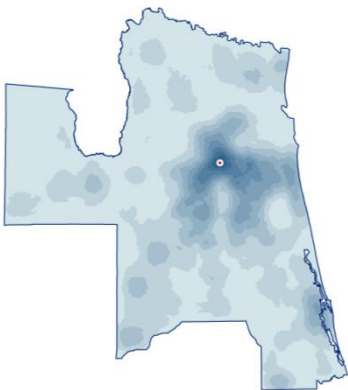
Road Network



Road Polygon Area



Road Density Map



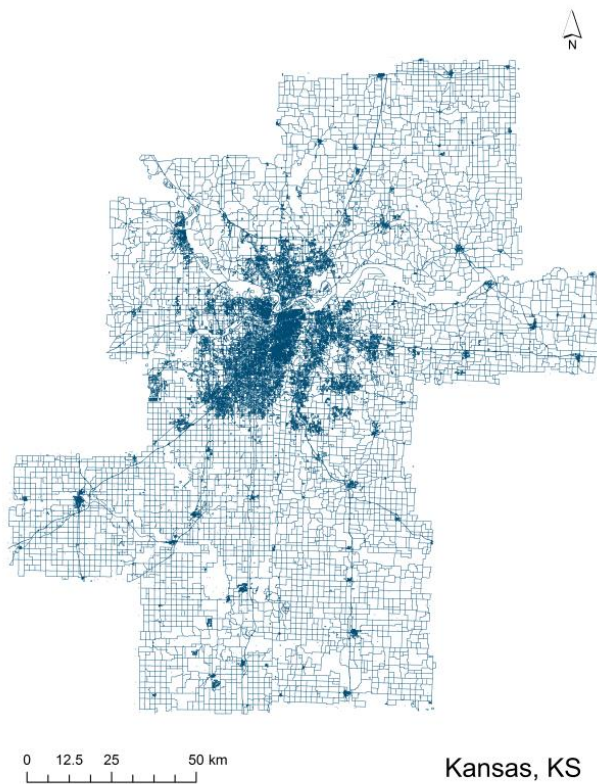
Road Density Fit

**Characteristics**

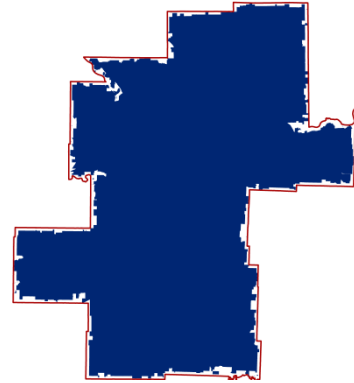
Founded in	1822
Population	1451740
Pop Density (/km <sup>2</sup> )	202.1
Area (km <sup>2</sup> )	7182.3
Road Length (km)	22067.4
# of Intersections	76396
Area Threshold (m)	923
Line Threshold (m)	670
Point Threshold (m)	271
Density Index (km <sup>2</sup> )	32.15
Decay Index (1/km)	0.625

## Kansas, KS

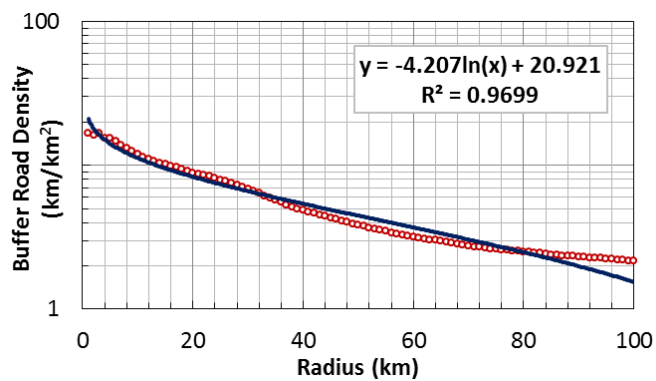
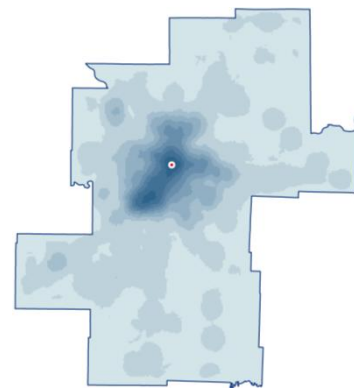
Road Network



Road Polygon Area



Road Density Map



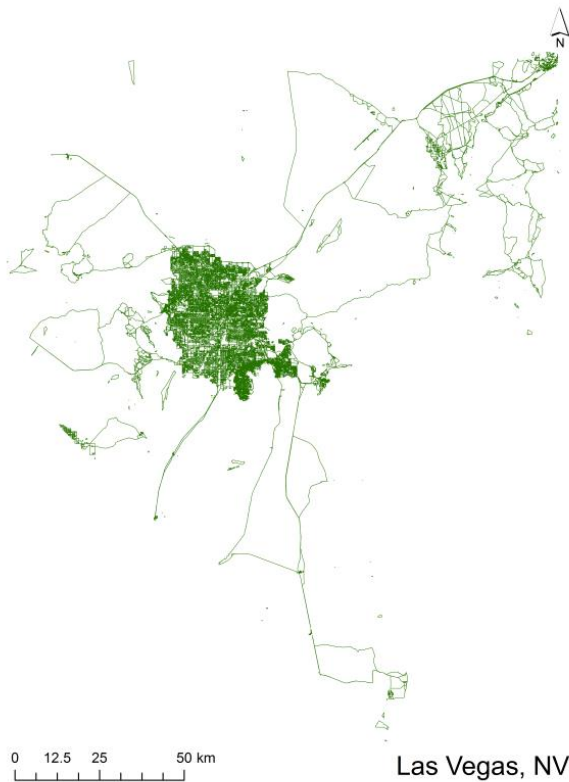
Road Density Fit

### Characteristics

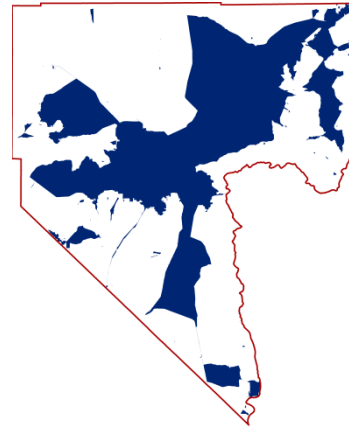
Founded in	1868
Population	2138010
Pop Density (/km <sup>2</sup> )	111.7
Area (km <sup>2</sup> )	19148.1
Road Length (km)	50639.6
# of Intersections	184748
Area Threshold (m)	1028
Line Threshold (m)	793
Point Threshold (m)	282
Density Index (km <sup>2</sup> )	20.921
Decay Index (1/km)	4.207

## Las Vegas, NV

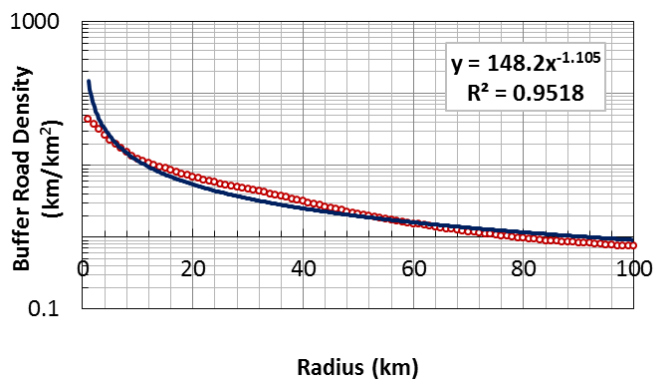
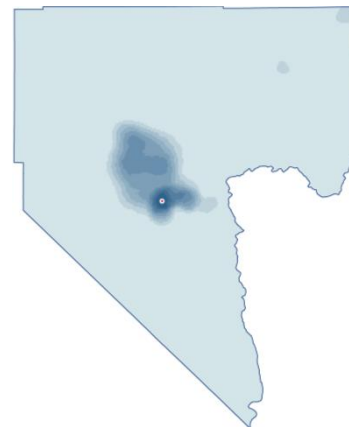
Road Network



Road Polygon Area



Road Density Map



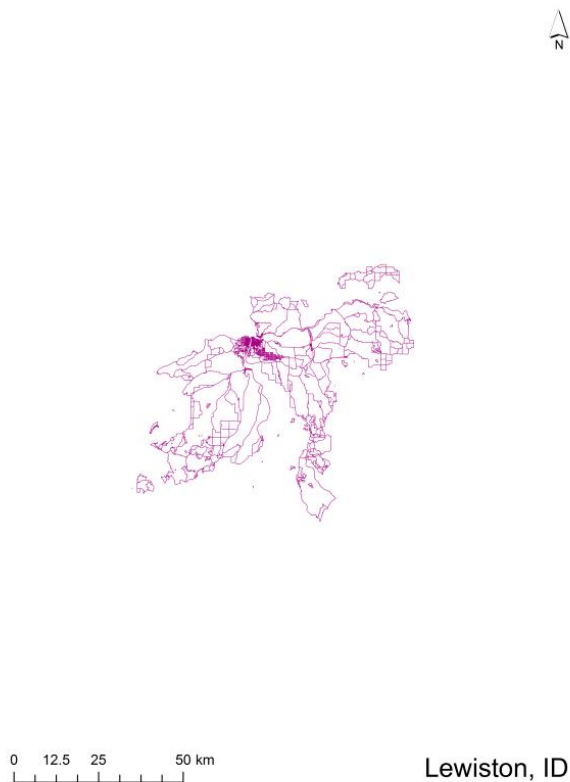
Road Density Fit

### Characteristics

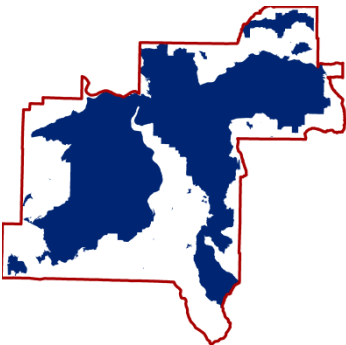
Founded in	1905
Population	2010951
Pop Density (/km <sup>2</sup> )	274.3
Area (km <sup>2</sup> )	7330.1
Road Length (km)	20926.8
# of Intersections	104925
Area Threshold (m)	1330
Line Threshold (m)	484
Point Threshold (m)	181
Density Index (km <sup>2</sup> )	148.2
Decay Index (1/km)	1.105

**Lewiston, ID**

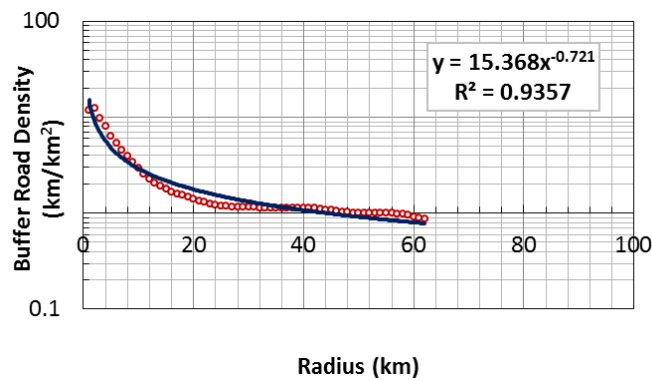
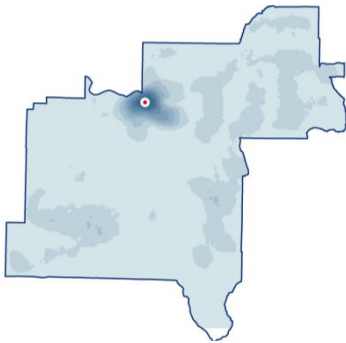
Road Network



Road Polygon Area



Road Density Map



Road Density Fit

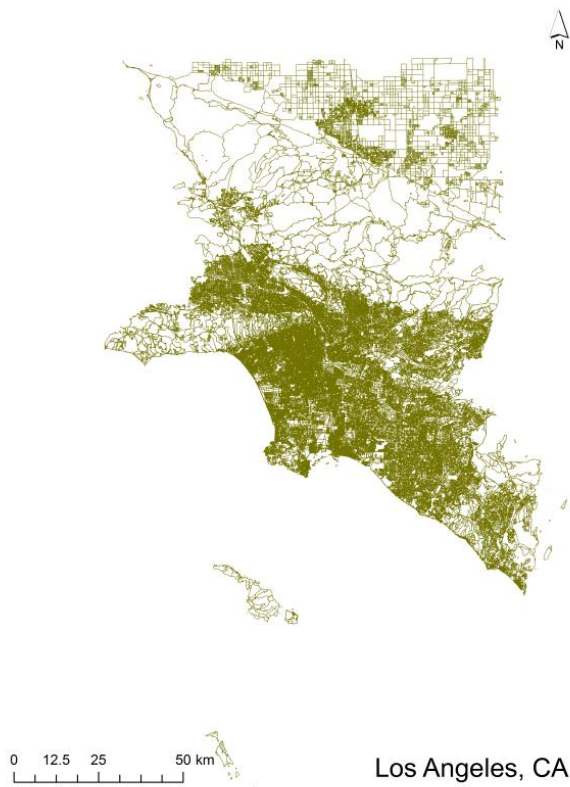
**Characteristics**

Founded in	1861
Population	85096
Pop Density (/km <sup>2</sup> )	40.4
Area (km <sup>2</sup> )	2104.6
Road Length (km)	4206.1
# of Intersections	6334
Area Threshold (m)	663
Line Threshold (m)	980
Point Threshold (m)	727
Density Index (km <sup>2</sup> )	15.368
Decay Index (1/km)	0.721



## Los Angeles, CA

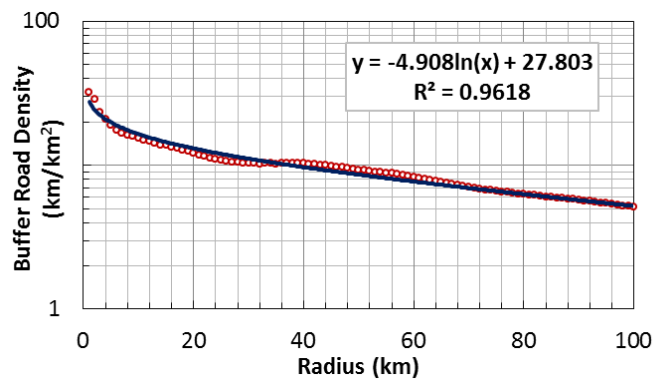
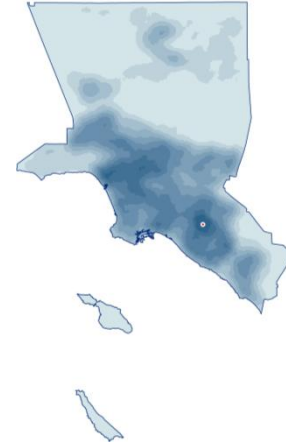
Road Network



Road Polygon Area



Road Density Map



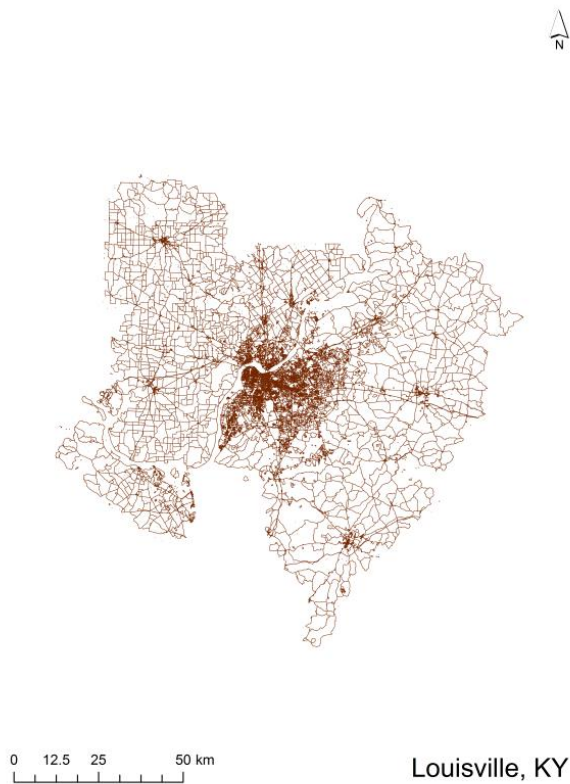
Road Density Fit

### Characteristics

Founded in	1781
Population	13059105
Pop Density (/km <sup>2</sup> )	1196.6
Area (km <sup>2</sup> )	10913.2
Road Length (km)	70096.7
# of Intersections	335638
Area Threshold (m)	962
Line Threshold (m)	230
Point Threshold (m)	152
Density Index (km <sup>2</sup> )	27.803
Decay Index (1/km)	4.908

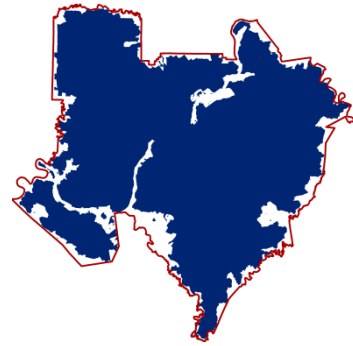
## Louisville, KY

Road Network

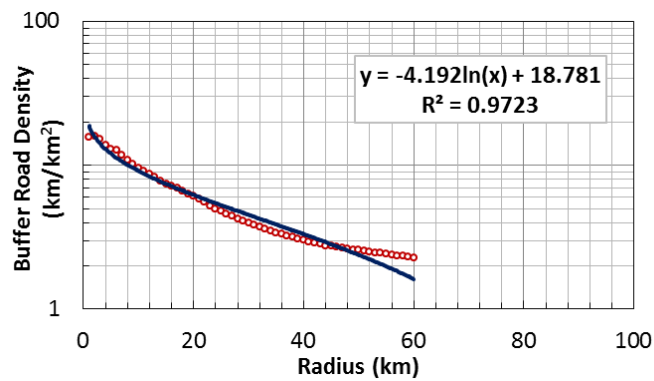
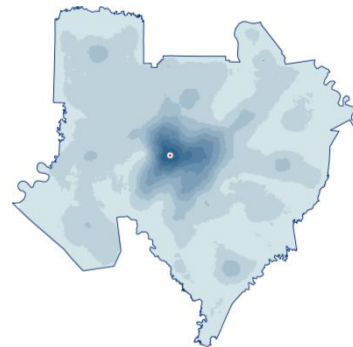


Louisville, KY

Road Polygon Area



Road Density Map



Road Density Fit

### Characteristics

Founded in	1778
Population	1443801
Pop Density (/km <sup>2</sup> )	156.5
Area (km <sup>2</sup> )	9227.8
Road Length (km)	24453.7
# of Intersections	82680
Area Threshold (m)	767
Line Threshold (m)	879
Point Threshold (m)	327
Density Index (km <sup>2</sup> )	18.781
Decay Index (1/km)	4.192

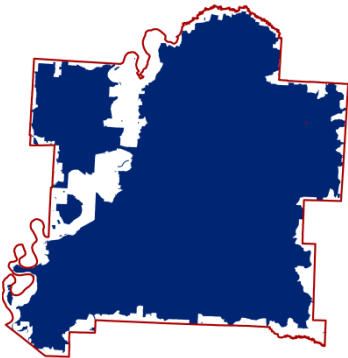


**Memphis, TN**

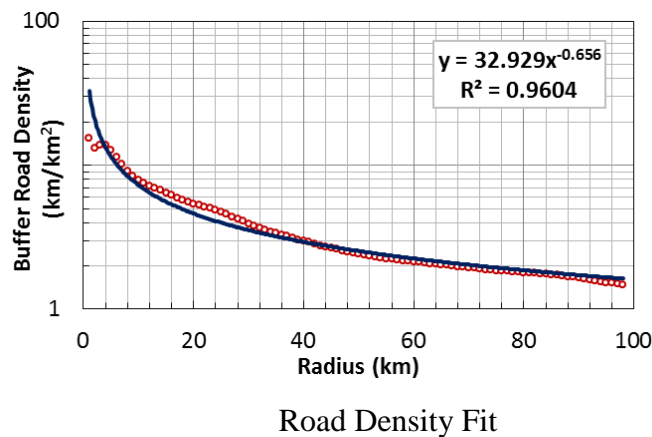
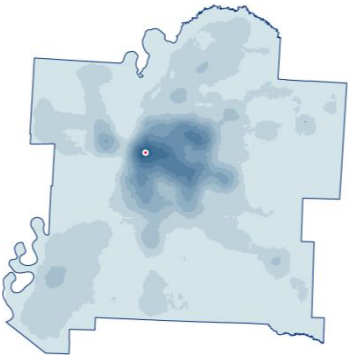
Road Network



Road Polygon Area



Road Density Map

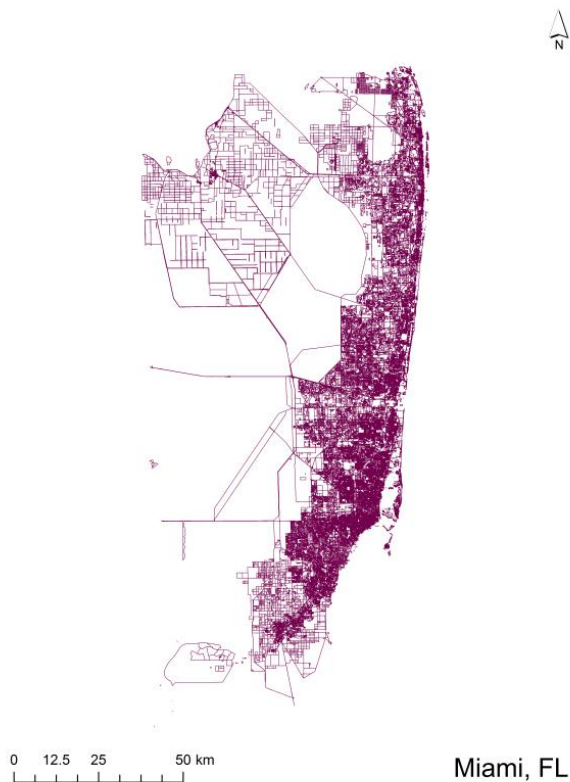


**Characteristics**

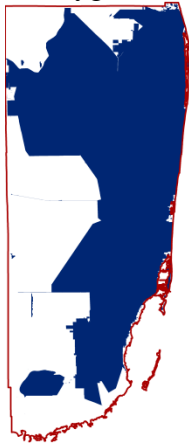
Founded in	1819
Population	1398172
Pop Density (/km <sup>2</sup> )	139.1
Area (km <sup>2</sup> )	10049.2
Road Length (km)	25028.4
# of Intersections	74462
Area Threshold (m)	960
Line Threshold (m)	891
Point Threshold (m)	348
Density Index (km <sup>2</sup> )	32.929
Decay Index (1/km)	0.656

**Miami, FL**

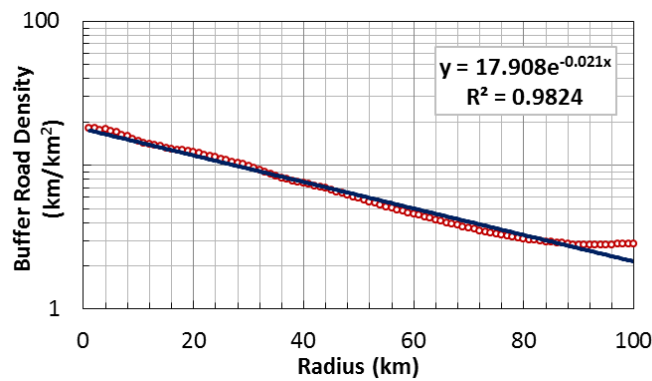
Road Network



Road Polygon Area



Road Density Map



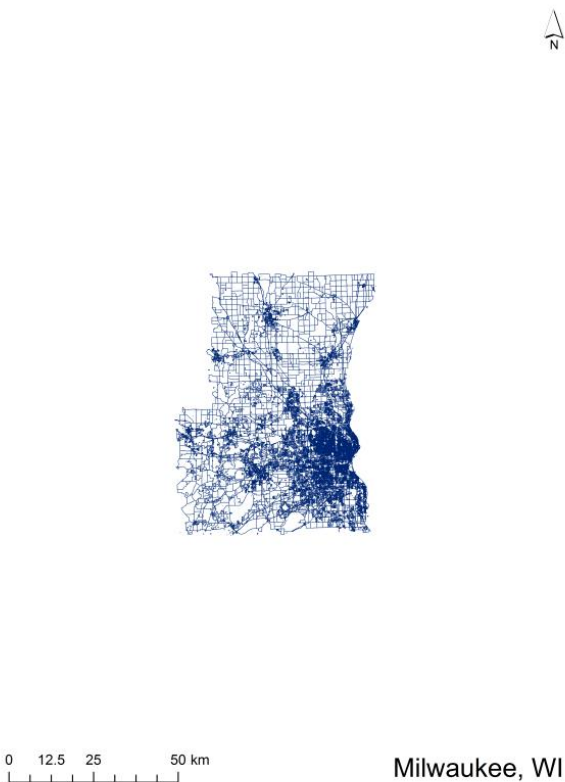
Road Density Fit

**Characteristics**

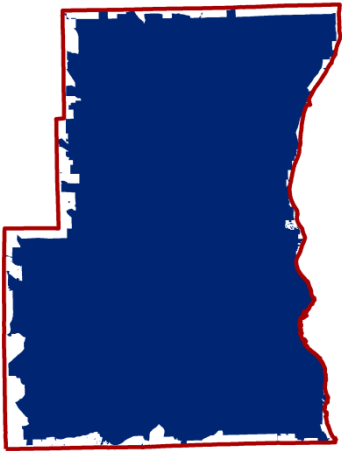
Founded in	1896
Population	5571523
Pop Density (/km <sup>2</sup> )	662.5
Area (km <sup>2</sup> )	8410.3
Road Length (km)	42827.1
# of Intersections	178680
Area Threshold (m)	1660
Line Threshold (m)	248
Point Threshold (m)	174
Density Index (km <sup>2</sup> )	17.908
Decay Index (1/km)	0.021

**Milwaukee, WI**

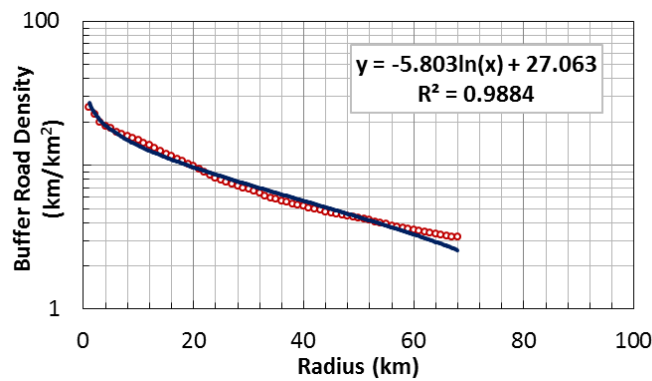
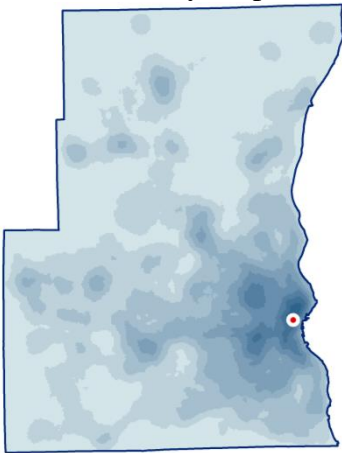
Road Network



Road Polygon Area



Road Density Map



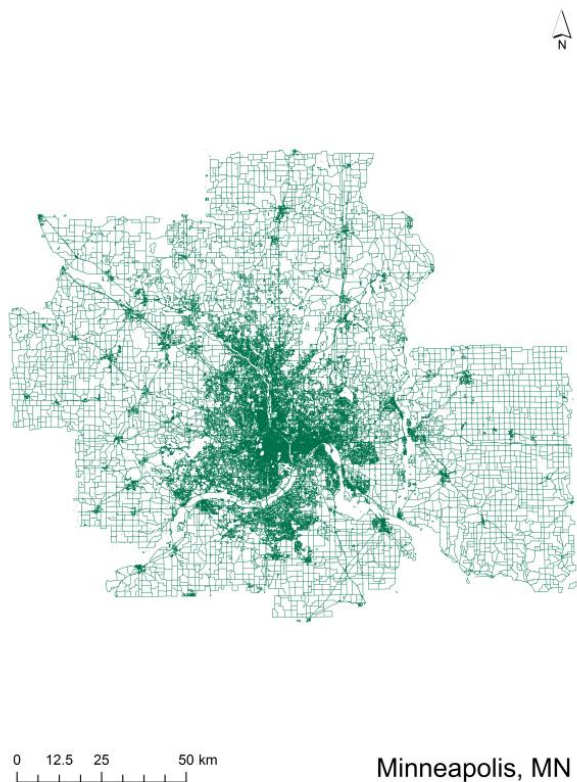
Road Density Fit

**Characteristics**

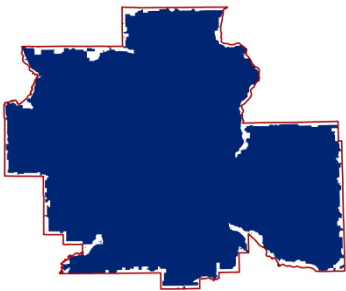
Founded in	1833
Population	1602022
Pop Density (/km <sup>2</sup> )	456.7
Area (km <sup>2</sup> )	3507.8
Road Length (km)	17207.1
# of Intersections	66802
Area Threshold (m)	700
Line Threshold (m)	386
Point Threshold (m)	212
Density Index (km <sup>2</sup> )	27.063
Decay Index (1/km)	5.803

**Minneapolis, MN**

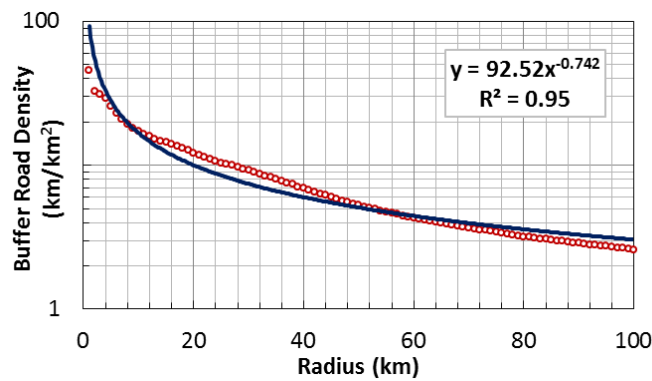
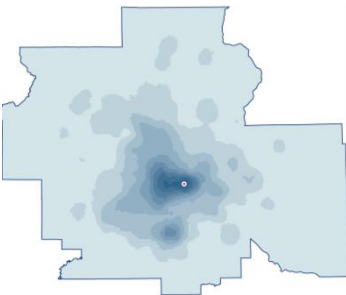
Road Network



Road Polygon Area



Road Density Map



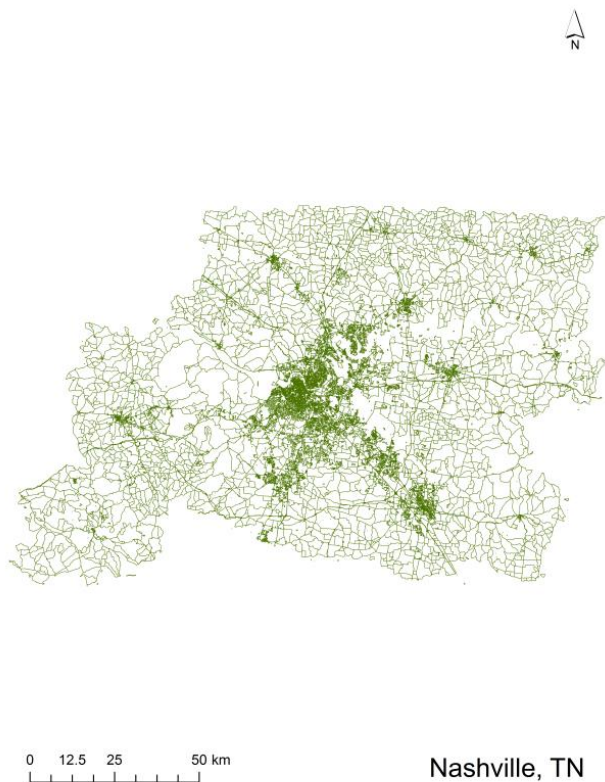
Road Density Fit

**Characteristics**

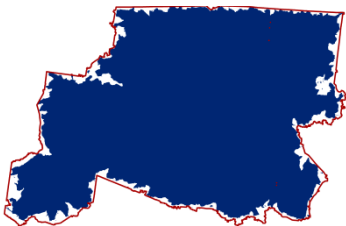
Founded in	1867
Population	3412291
Pop Density (/km <sup>2</sup> )	222.1
Area (km <sup>2</sup> )	15365.8
Road Length (km)	57532
# of Intersections	259788
Area Threshold (m)	904
Line Threshold (m)	502
Point Threshold (m)	207
Density Index (km <sup>2</sup> )	92.52
Decay Index (1/km)	0.742

**Nashville, TN**

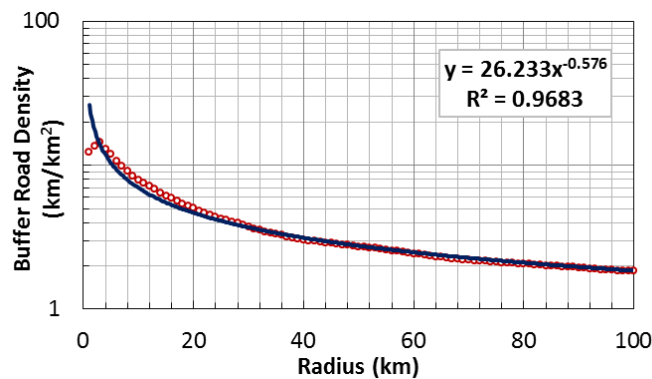
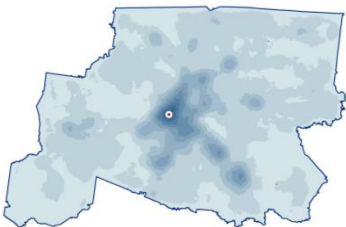
Road Network



Road Polygon Area



Road Density Map



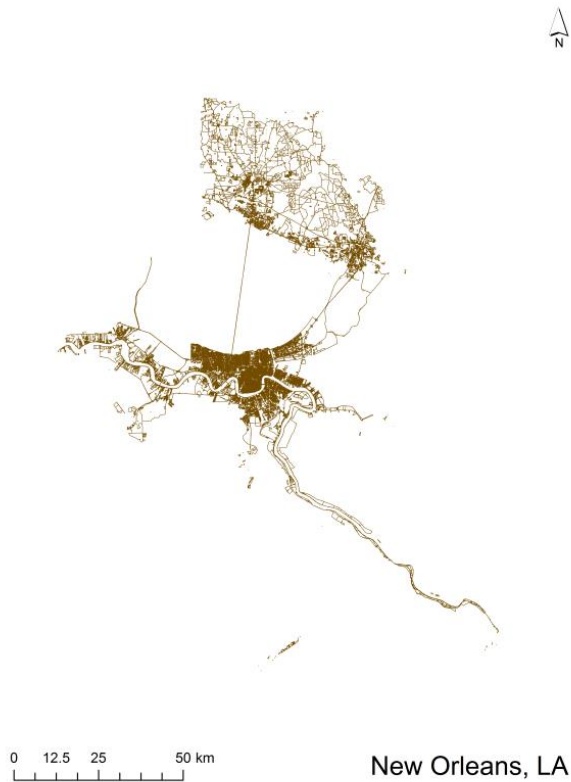
Road Density Fit

**Characteristics**

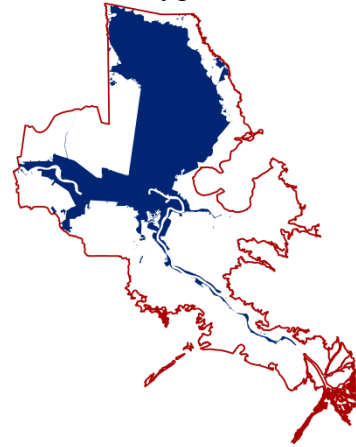
Founded in	1779
Population	1740134
Pop Density (/km <sup>2</sup> )	128.1
Area (km <sup>2</sup> )	13588.3
Road Length (km)	32653.8
# of Intersections	90700
Area Threshold (m)	868
Line Threshold (m)	919
Point Threshold (m)	383
Density Index (km <sup>2</sup> )	26.233
Decay Index (1/km)	0.576

## New Orleans, LA

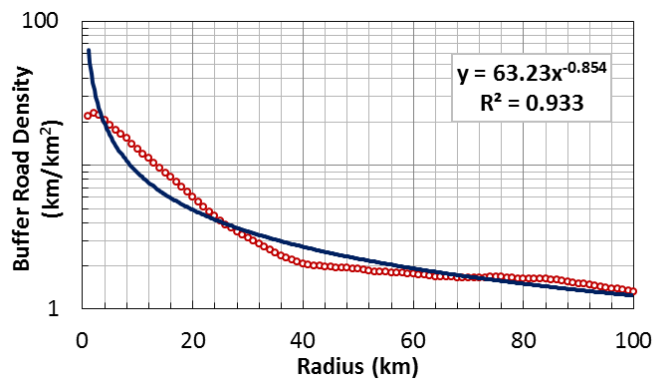
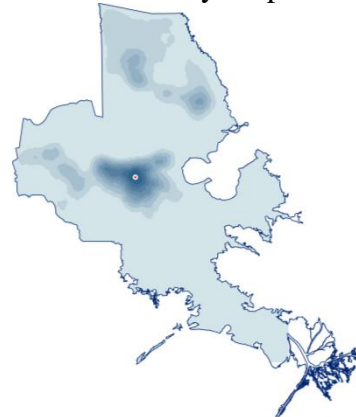
Road Network



Road Polygon Area



Road Density Map



Road Density Fit

### Characteristics

Founded in	1718
Population	1247062
Pop Density (/km <sup>2</sup> )	335.6
Area (km <sup>2</sup> )	3715.5
Road Length (km)	18340.7
# of Intersections	83361
Area Threshold (m)	699
Line Threshold (m)	372
Point Threshold (m)	189
Density Index (km <sup>2</sup> )	63.23
Decay Index (1/km)	0.854

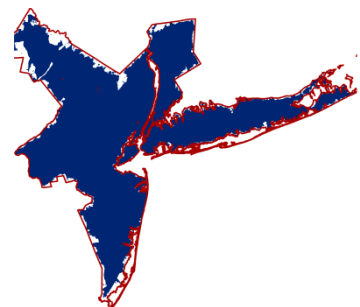


New York, NY

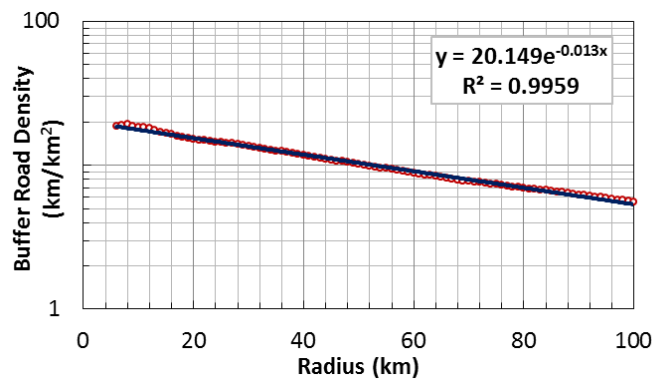
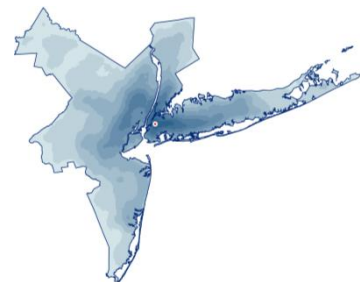
Road Network



Road Polygon Area



Road Density Map



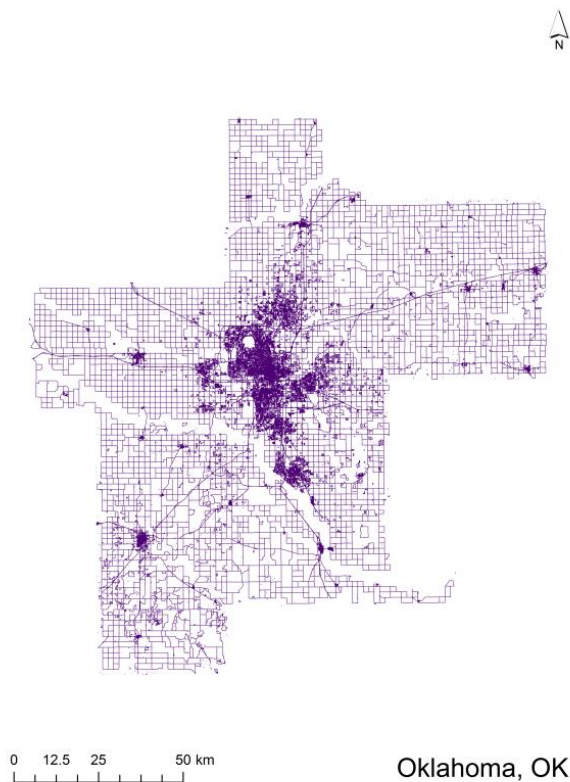
Road Density Fit

Characteristics

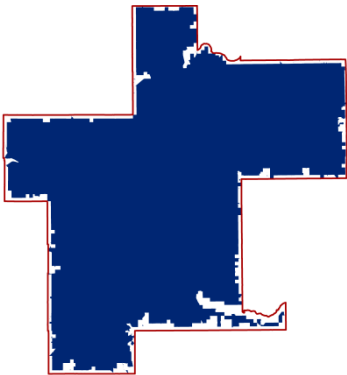
Founded in	1624
Population	19217139
Pop Density (/km <sup>2</sup> )	1235.7
Area (km <sup>2</sup> )	15551.5
Road Length (km)	105344
# of Intersections	499969
Area Threshold (m)	501
Line Threshold (m)	282
Point Threshold (m)	170
Density Index (km <sup>2</sup> )	20.149
Decay Index (1/km)	0.013

**Oklahoma, OK**

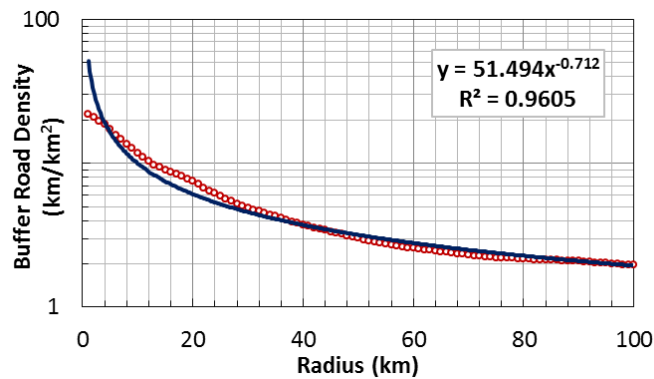
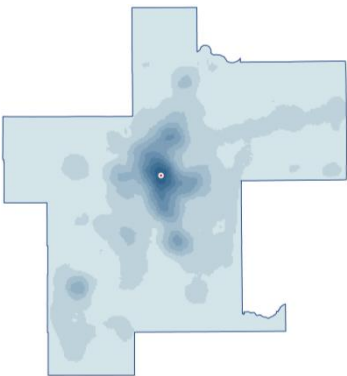
Road Network



Road Polygon Area



Road Density Map



Road Density Fit

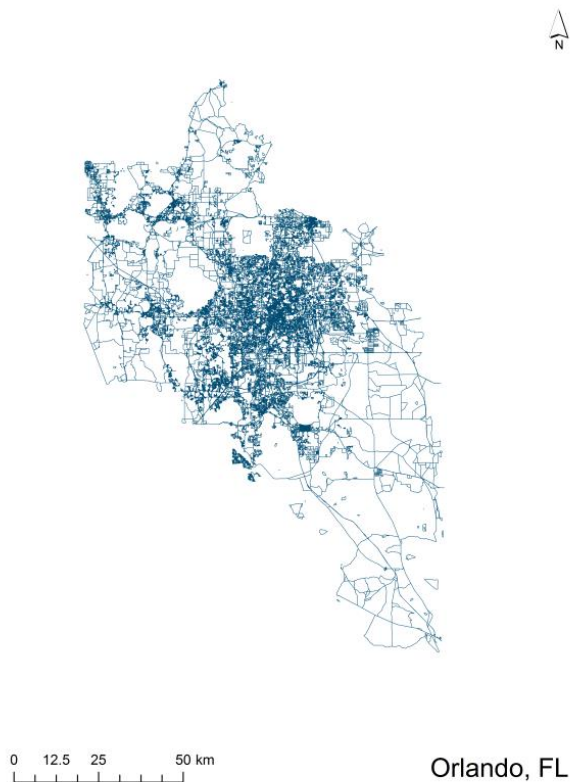
**Characteristics**

Founded in	1889
Population	1359027
Pop Density (/km <sup>2</sup> )	104.1
Area (km <sup>2</sup> )	13051
Road Length (km)	34167.6
# of Intersections	120303
Area Threshold (m)	955
Line Threshold (m)	828
Point Threshold (m)	296
Density Index (km <sup>2</sup> )	51.494
Decay Index (1/km)	0.712

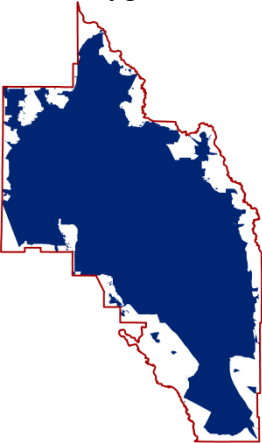


**Orlando, FL**

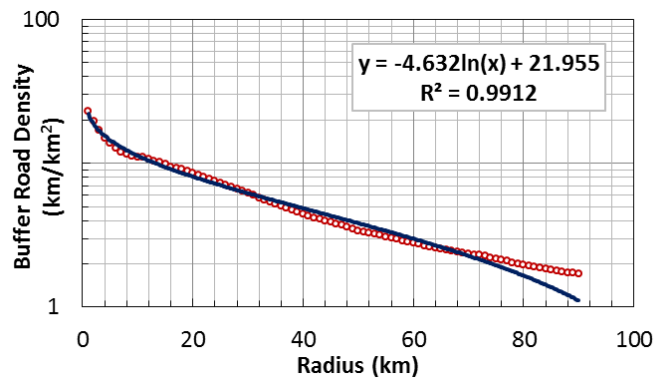
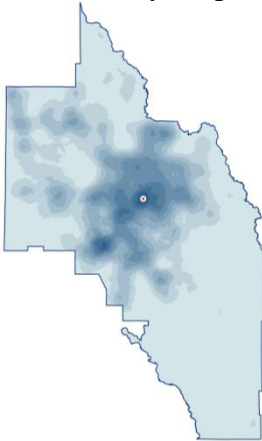
Road Network



Road Polygon Area



Road Density Map



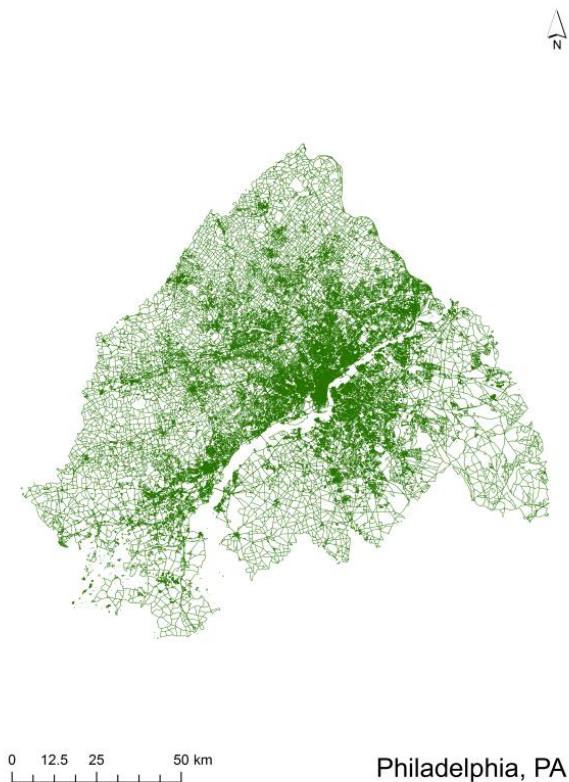
Road Density Fit

**Characteristics**

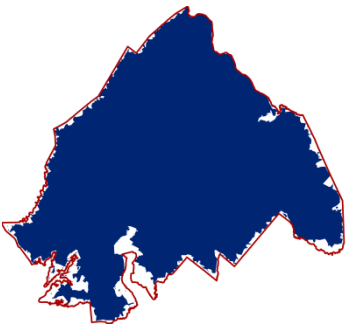
Founded in	1875
Population	2257901
Pop Density (/km <sup>2</sup> )	282.4
Area (km <sup>2</sup> )	7996.6
Road Length (km)	28876.5
# of Intersections	123076
Area Threshold (m)	1374
Line Threshold (m)	418
Point Threshold (m)	200
Density Index (km <sup>2</sup> )	21.955
Decay Index (1/km)	4.632

**Philadelphia, PA**

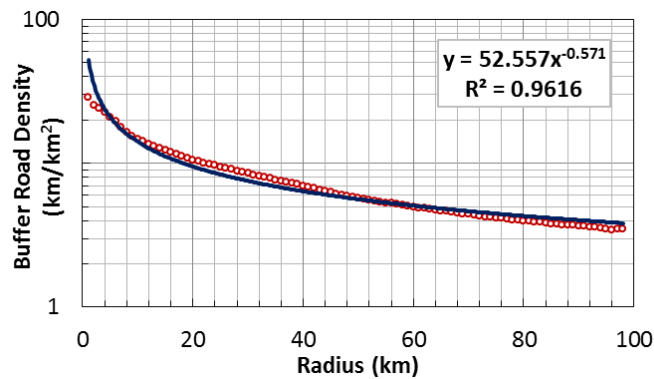
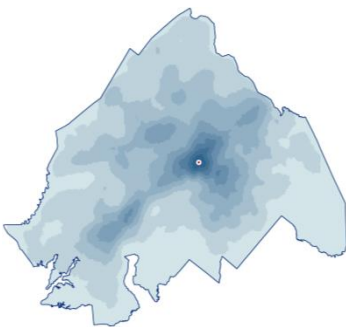
Road Network



Road Polygon Area



Road Density Map



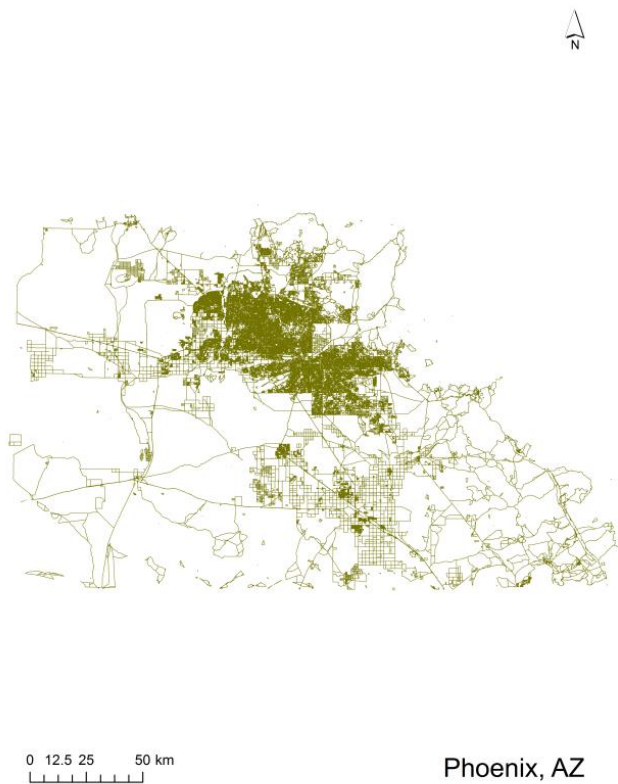
Road Density Fit

**Characteristics**

Founded in	1682
Population	6234336
Pop Density (/km <sup>2</sup> )	553.1
Area (km <sup>2</sup> )	11271.7
Road Length (km)	58104.3
# of Intersections	256023
Area Threshold (m)	648
Line Threshold (m)	378
Point Threshold (m)	197
Density Index (km <sup>2</sup> )	52.557
Decay Index (1/km)	0.571

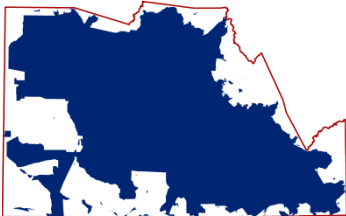
**Phoenix, AZ**

Road Network

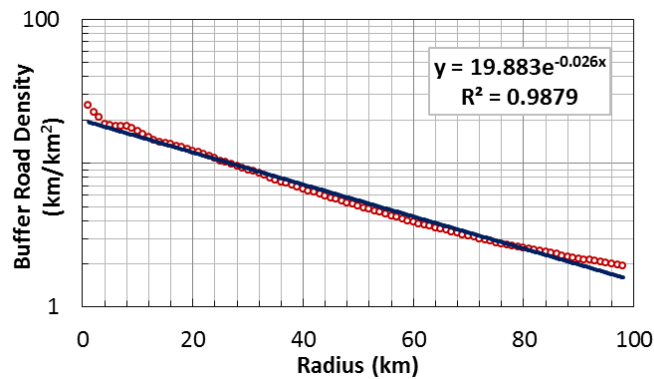
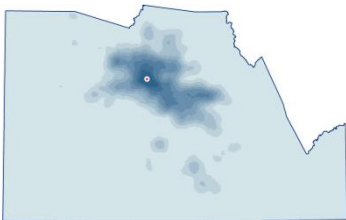


Phoenix, AZ

Road Polygon Area



Road Density Map



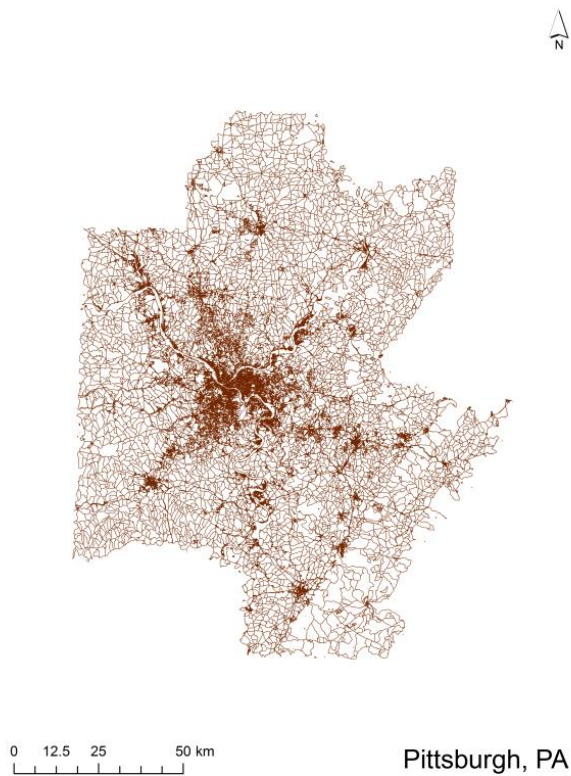
Road Density Fit

**Characteristics**

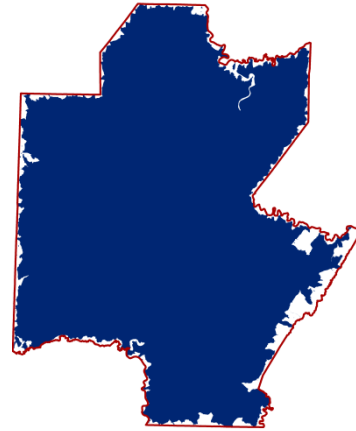
Founded in	1868
Population	4262838
Pop Density (/km <sup>2</sup> )	165.5
Area (km <sup>2</sup> )	25763
Road Length (km)	60738.6
# of Intersections	241836
Area Threshold (m)	1200
Line Threshold (m)	535
Point Threshold (m)	221
Density Index (km <sup>2</sup> )	19.883
Decay Index (1/km)	0.026

## Pittsburgh, PA

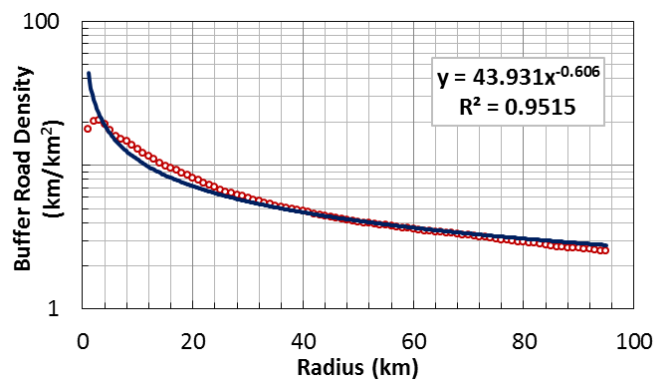
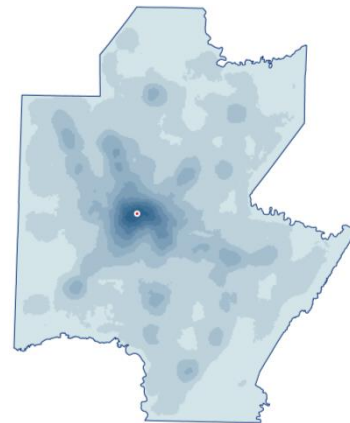
Road Network



Road Polygon Area



Road Density Map



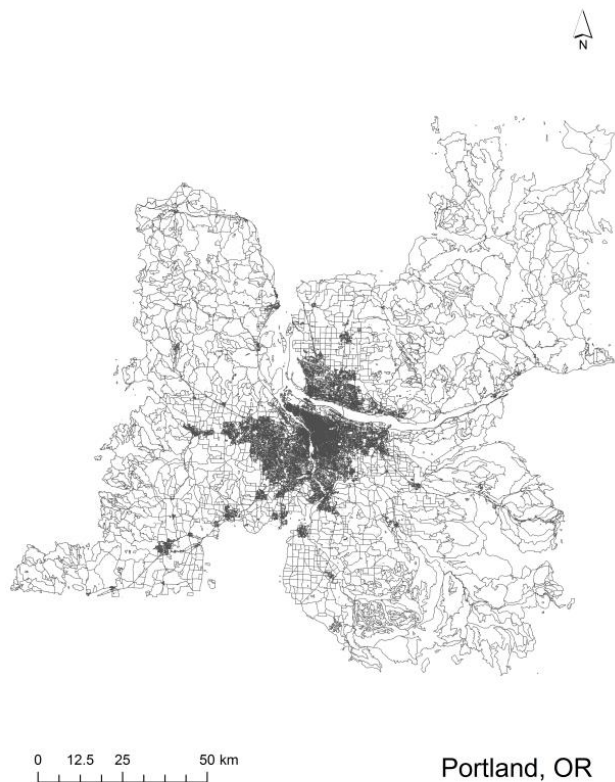
Road Density Fit

### Characteristics

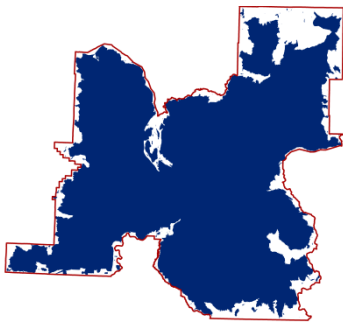
Founded in	1758
Population	2503836
Pop Density (/km <sup>2</sup> )	194.7
Area (km <sup>2</sup> )	12859.9
Road Length (km)	45196.4
# of Intersections	167027
Area Threshold (m)	707
Line Threshold (m)	596
Point Threshold (m)	267
Density Index (km <sup>2</sup> )	43.931
Decay Index (1/km)	0.606

**Portland, OR**

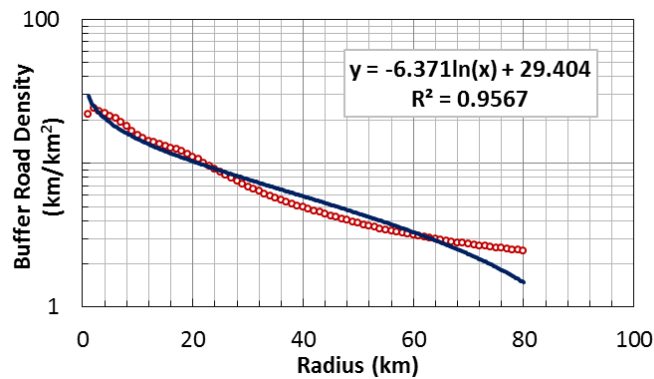
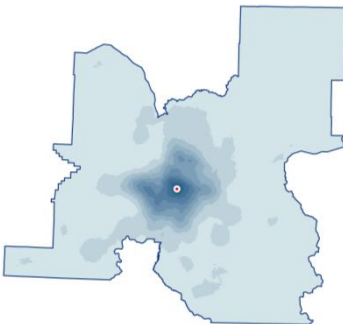
Road Network



Road Polygon Area



Road Density Map



Road Density Fit

**Characteristics**

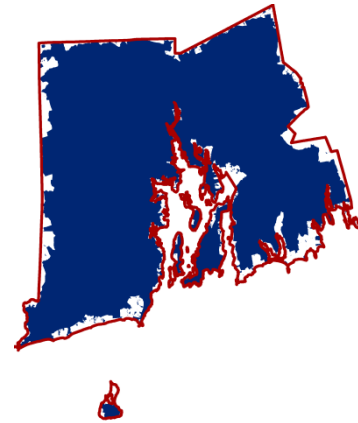
Founded in	1845
Population	2363554
Pop Density (/km <sup>2</sup> )	161.1
Area (km <sup>2</sup> )	14669.4
Road Length (km)	44544
# of Intersections	174765
Area Threshold (m)	787
Line Threshold (m)	722
Point Threshold (m)	270
Density Index (km <sup>2</sup> )	29.404
Decay Index (1/km)	6.371

## Providence, RI

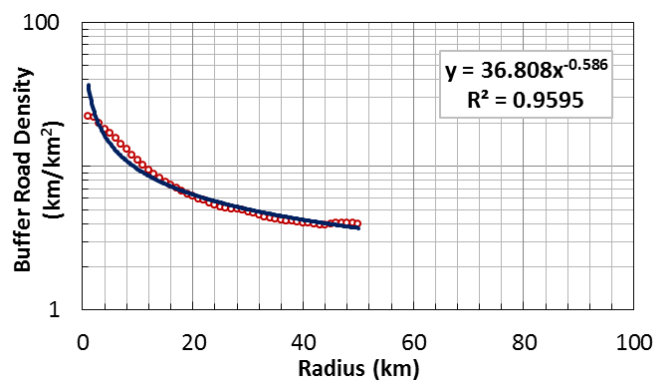
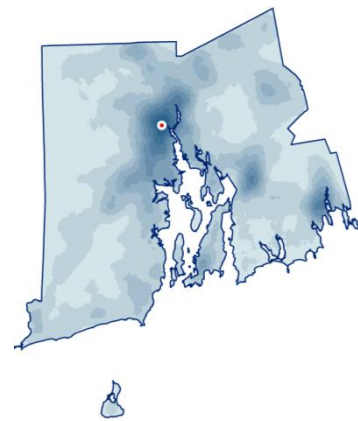
Road Network



Road Polygon Area



Road Density Map



Road Density Fit

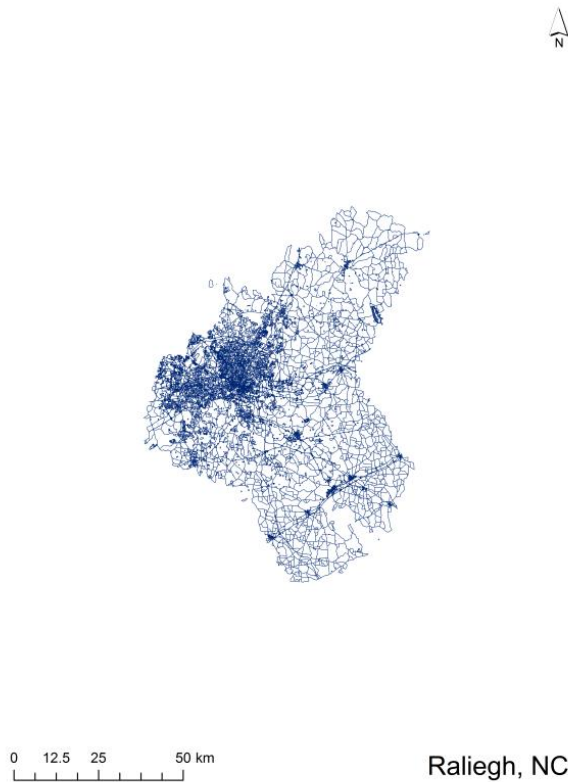
### Characteristics

Founded in	1636
Population	1695760
Pop Density (/km <sup>2</sup> )	449.4
Area (km <sup>2</sup> )	3773.5
Road Length (km)	18431.5
# of Intersections	83871
Area Threshold (m)	531
Line Threshold (m)	444
Point Threshold (m)	201
Density Index (km <sup>2</sup> )	36.808
Decay Index (1/km)	0.586

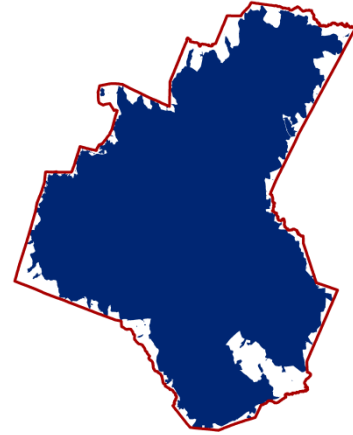


## Raleigh, NC

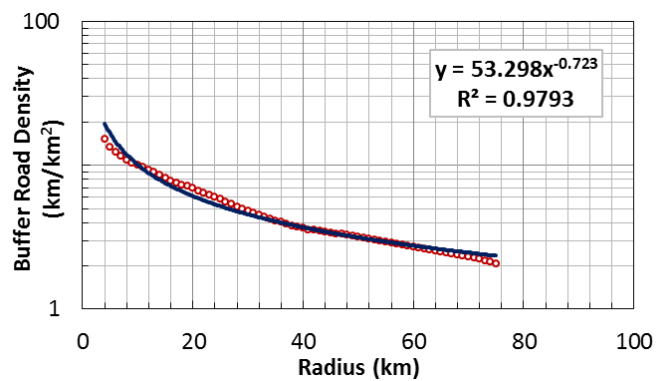
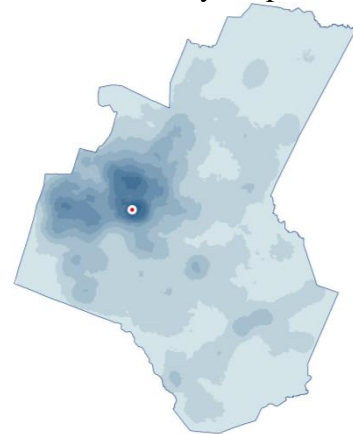
Road Network



Road Polygon Area



Road Density Map



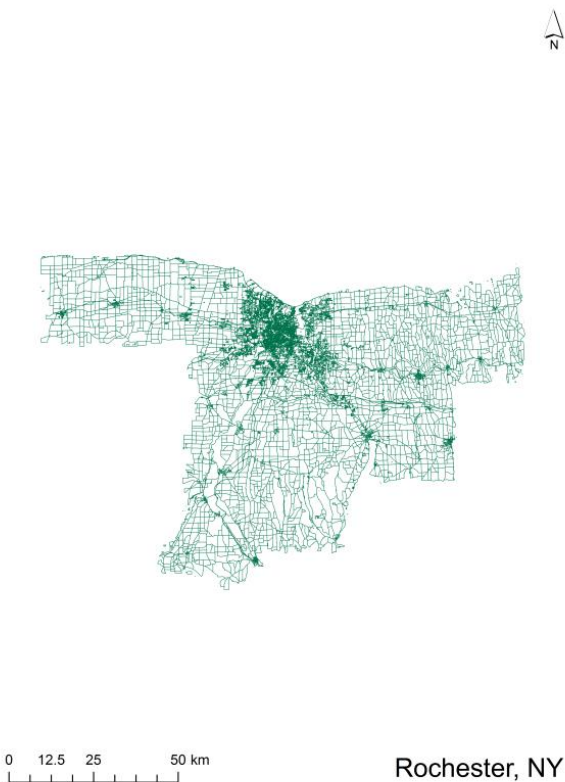
Road Density Fit

### Characteristics

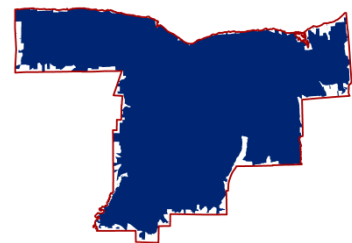
Founded in	1792
Population	1258825
Pop Density (/km <sup>2</sup> )	260.6
Area (km <sup>2</sup> )	4830.5
Road Length (km)	18678
# of Intersections	81802
Area Threshold (m)	637
Line Threshold (m)	562
Point Threshold (m)	231
Density Index (km <sup>2</sup> )	53.298
Decay Index (1/km)	0.723

**Rochester, NY**

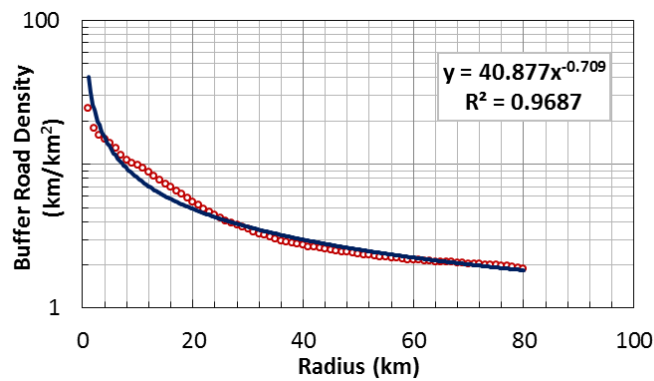
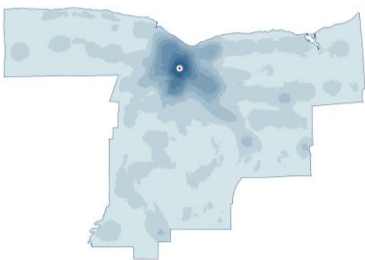
Road Network



Road Polygon Area



Road Density Map



Road Density Fit

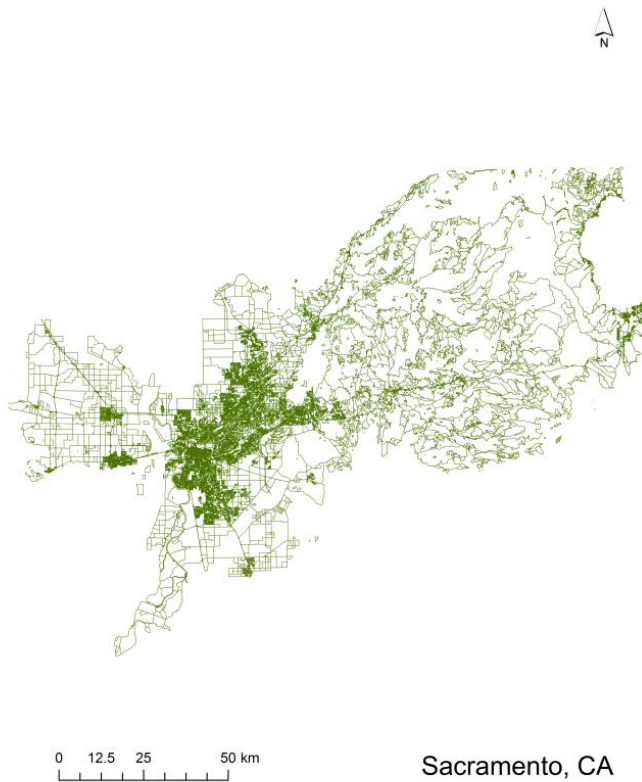
**Characteristics**

Founded in	1803
Population	1159166
Pop Density (/km²)	164.7
Area (km²)	7037.2
Road Length (km)	17863.9
# of Intersections	47275
Area Threshold (m)	881
Line Threshold (m)	874
Point Threshold (m)	380
Density Index (km²)	40.877
Decay Index (1/km)	0.709

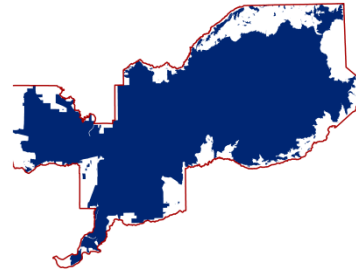


## Sacramento, CA

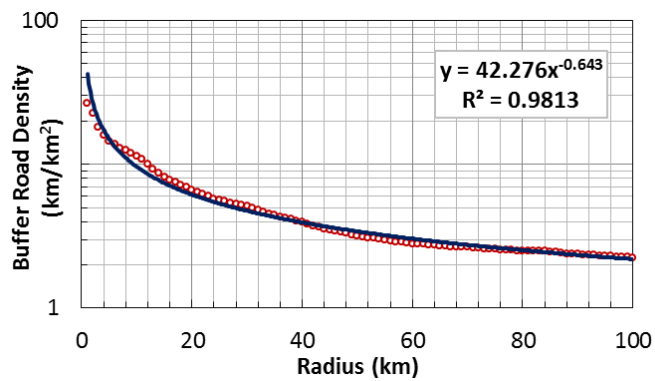
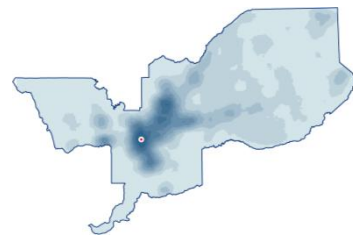
Road Network



Road Polygon Area



Road Density Map



Road Density Fit

### Characteristics

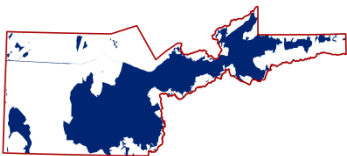
Founded in	1839
Population	2277843
Pop Density (/km <sup>2</sup> )	224
Area (km <sup>2</sup> )	10167
Road Length (km)	34020.6
# of Intersections	124839
Area Threshold (m)	821
Line Threshold (m)	627
Point Threshold (m)	260
Density Index (km <sup>2</sup> )	42.276
Decay Index (1/km)	0.643

**Salt Lake, UT**

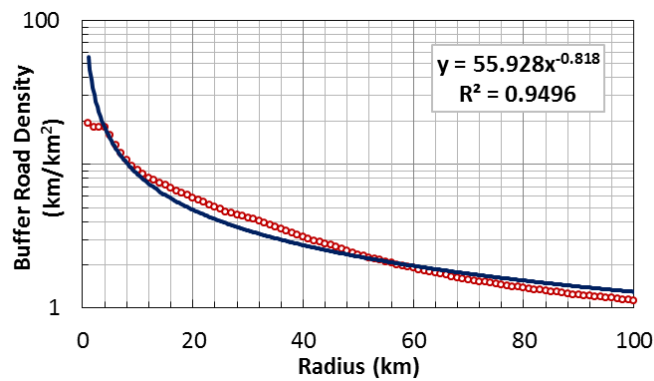
Road Network



Road Polygon Area



Road Density Map



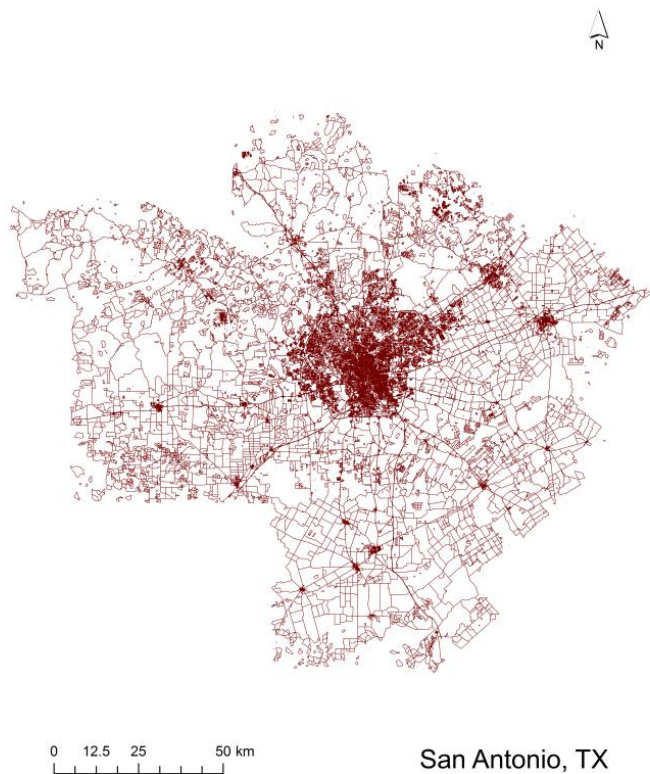
Road Density Fit

**Characteristics**

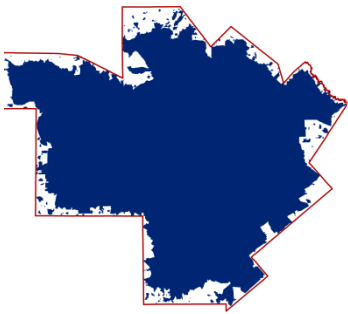
Founded in	1847
Population	1246208
Pop Density (/km <sup>2</sup> )	114.4
Area (km <sup>2</sup> )	10895.1
Road Length (km)	22387
# of Intersections	59736
Area Threshold (m)	1033
Line Threshold (m)	957
Point Threshold (m)	397
Density Index (km <sup>2</sup> )	55.928
Decay Index (1/km)	0.818

**San Antonio, TX**

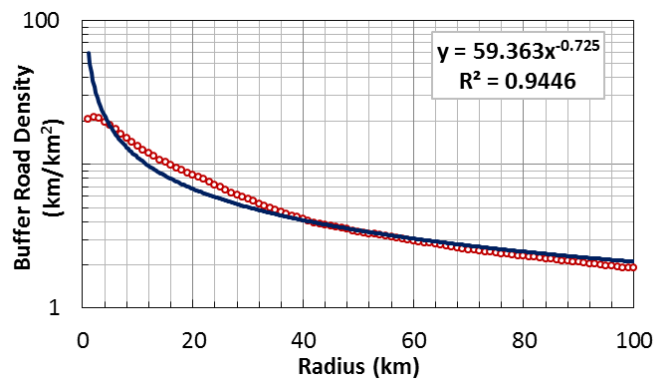
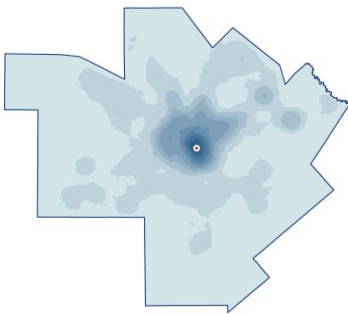
Road Network



Road Polygon Area



Road Density Map



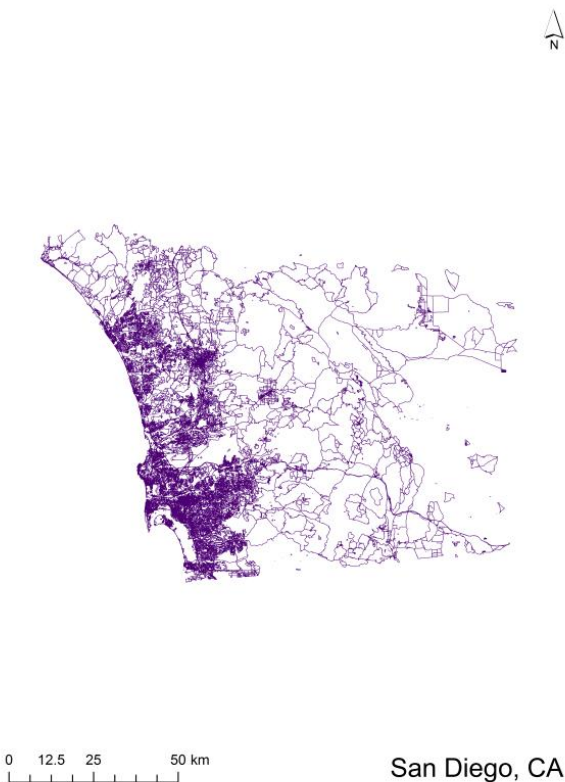
Road Density Fit

**Characteristics**

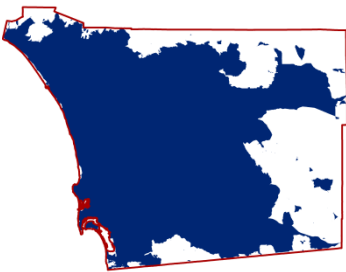
Founded in	1718
Population	2239307
Pop Density (/km <sup>2</sup> )	138.1
Area (km <sup>2</sup> )	16213.5
Road Length (km)	44137.5
# of Intersections	127773
Area Threshold (m)	875
Line Threshold (m)	806
Point Threshold (m)	347
Density Index (km <sup>2</sup> )	59.363
Decay Index (1/km)	0.725

**San Diego, CA**

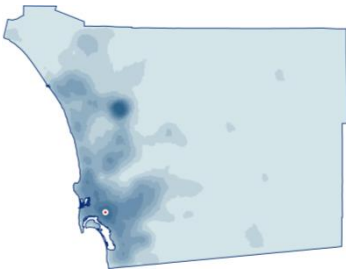
Road Network



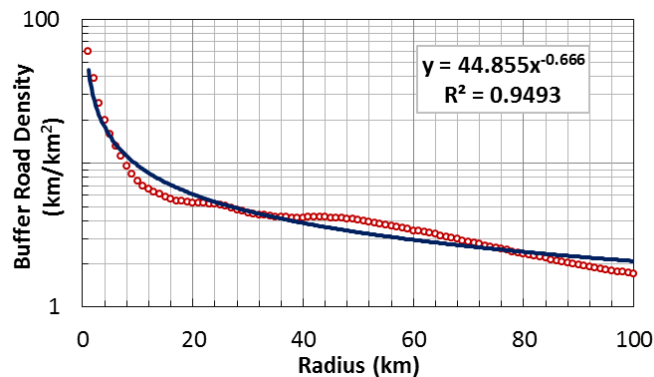
Road Polygon Area



Road Density Map



San Diego, CA



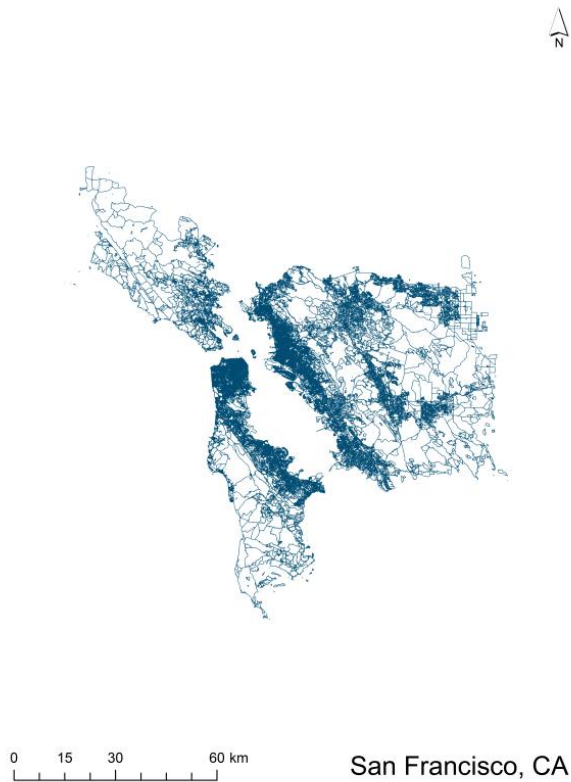
Road Density Fit

**Characteristics**

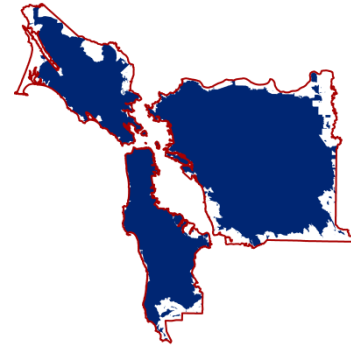
Founded in	1769
Population	3144425
Pop Density (/km <sup>2</sup> )	410.1
Area (km <sup>2</sup> )	7668
Road Length (km)	29499.1
# of Intersections	144194
Area Threshold (m)	1129
Line Threshold (m)	413
Point Threshold (m)	186
Density Index (km <sup>2</sup> )	44.855
Decay Index (1/km)	0.666

## San Francisco, CA

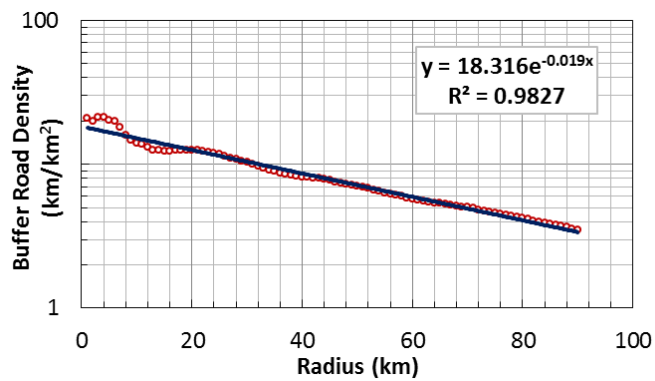
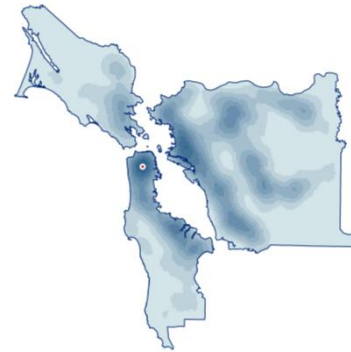
Road Network



Road Polygon Area



Road Density Map



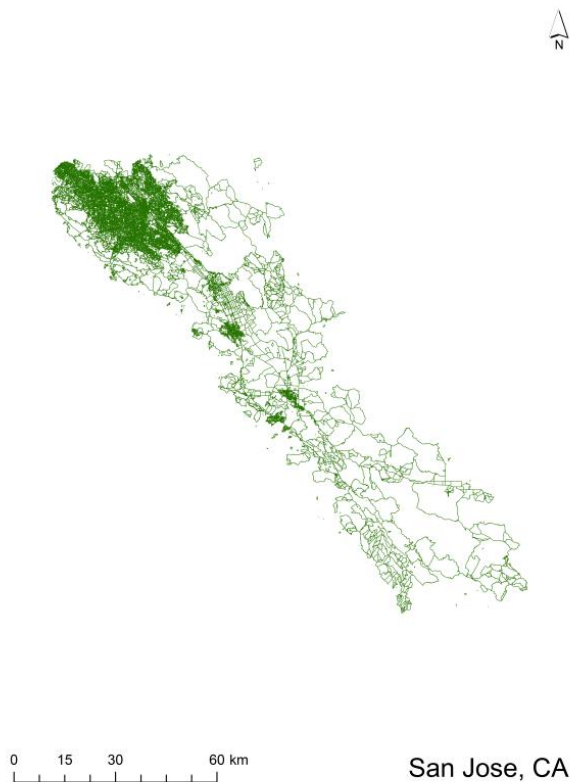
Road Density Fit

### Characteristics

Founded in	1776
Population	4472992
Pop Density (/km <sup>2</sup> )	835.7
Area (km <sup>2</sup> )	5352.1
Road Length (km)	33483
# of Intersections	172400
Area Threshold (m)	640
Line Threshold (m)	272
Point Threshold (m)	155
Density Index (km <sup>2</sup> )	18.316
Decay Index (1/km)	0.019

**San Jose, CA**

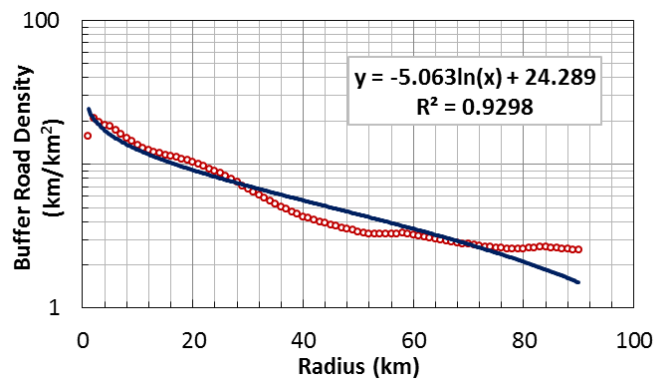
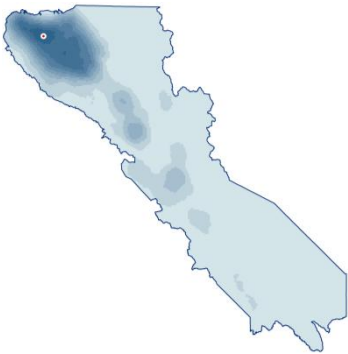
Road Network



Road Polygon Area



Road Density Map



Road Density Fit

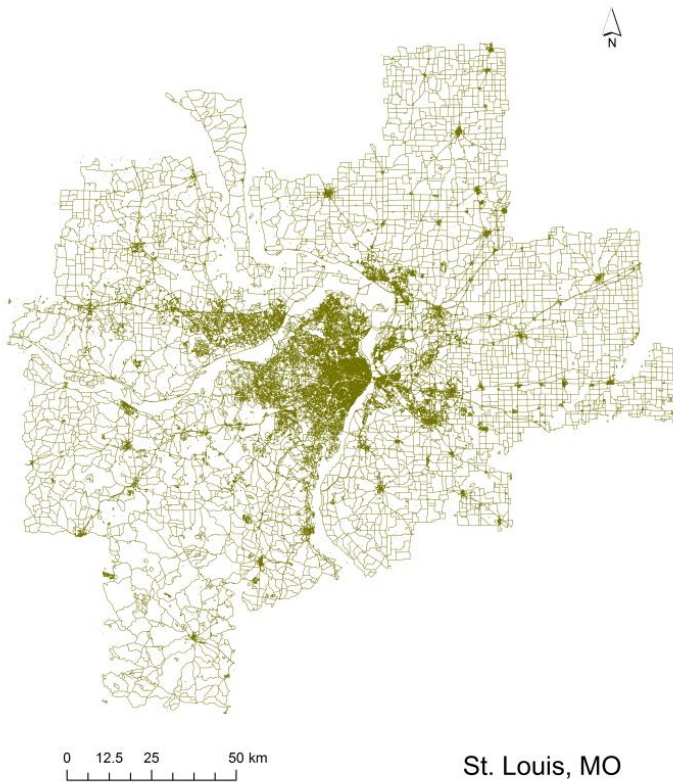
**Characteristics**

Founded in	1777
Population	1992872
Pop Density (/km <sup>2</sup> )	405
Area (km <sup>2</sup> )	4921.2
Road Length (km)	19824.6
# of Intersections	93610
Area Threshold (m)	773
Line Threshold (m)	478
Point Threshold (m)	195
Density Index (km <sup>2</sup> )	24.289
Decay Index (1/km)	5.063

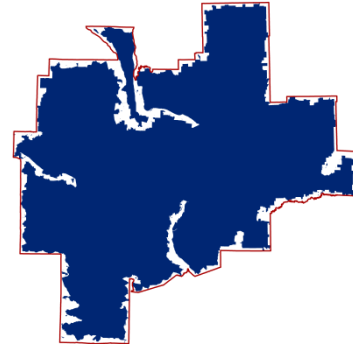


## St. Louis, MO

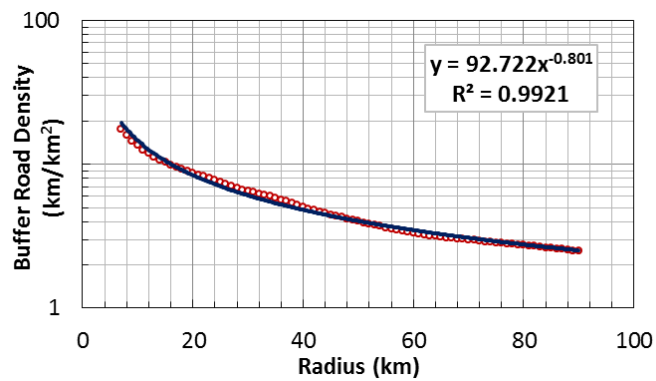
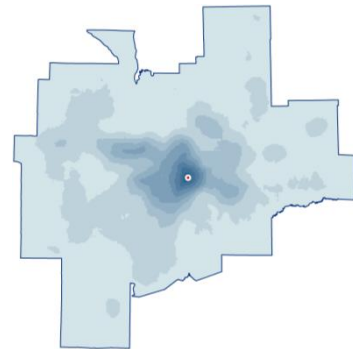
Road Network



Road Polygon Area



Road Density Map



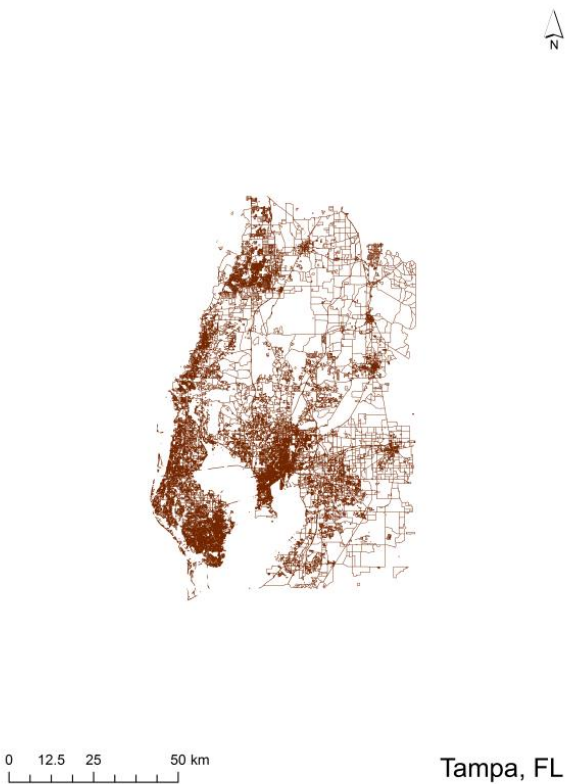
Road Density Fit

### Characteristics

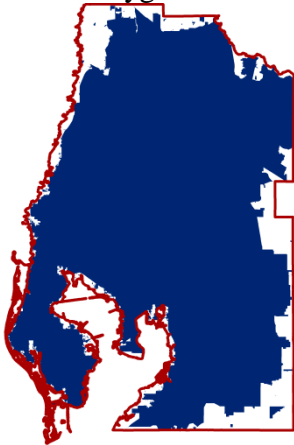
Founded in	1763
Population	2934412
Pop Density (/km <sup>2</sup> )	145.4
Area (km <sup>2</sup> )	20184.1
Road Length (km)	57670.8
# of Intersections	205269
Area Threshold (m)	880
Line Threshold (m)	753
Point Threshold (m)	287
Density Index (km <sup>2</sup> )	92.722
Decay Index (1/km)	0.801

**Tampa, FL**

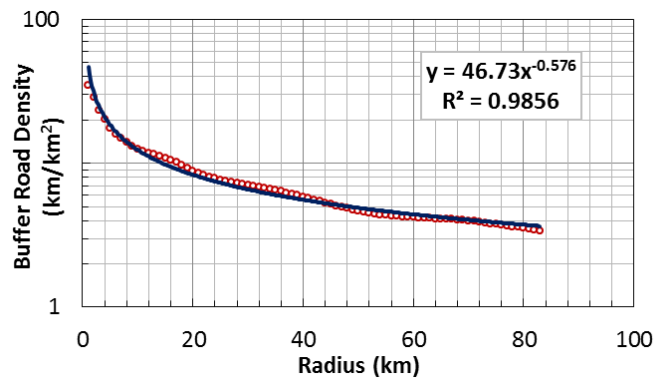
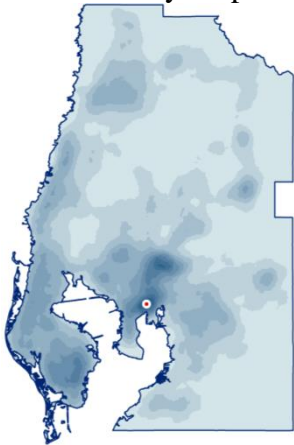
Road Network



Road Polygon Area



Road Density Map



Road Density Fit

**Characteristics**

Founded in	1823
Population	2858974
Pop Density (/km <sup>2</sup> )	496.6
Area (km <sup>2</sup> )	5756.8
Road Length (km)	31421.2
# of Intersections	143714
Area Threshold (m)	756
Line Threshold (m)	315
Point Threshold (m)	180
Density Index (km <sup>2</sup> )	46.73
Decay Index (1/km)	0.576

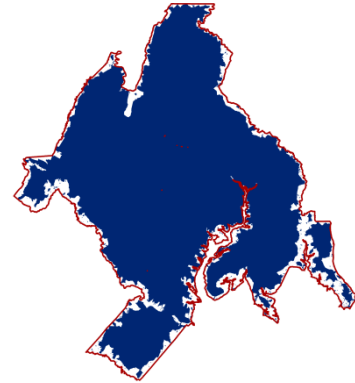


## Washington, DC

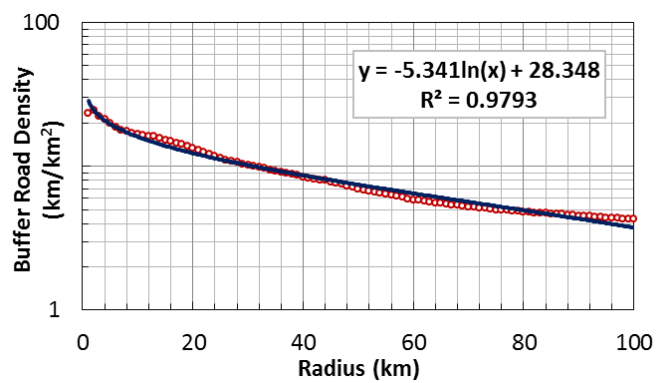
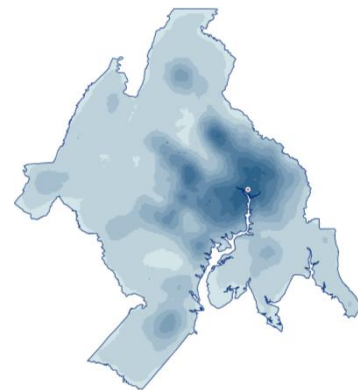
Road Network



Road Polygon Area



Road Density Map



Road Density Fit

### Characteristics

Founded in	1790
Population	5916033
Pop Density (/km <sup>2</sup> )	464.5
Area (km <sup>2</sup> )	12735
Road Length (km)	74190.6
# of Intersections	437470
Area Threshold (m)	467
Line Threshold (m)	361
Point Threshold (m)	162
Density Index (km <sup>2</sup> )	28.348
Decay Index (1/km)	5.341

## **APPENDIX G: Copyright Authorizations**

Farideddin Peiravian  
Civil and Materials Engineering Department  
University of Illinois at Chicago  
842 W Taylor St, MC 246  
Chicago, IL 60607

Sep. 29, 2014

Mr. Robert Wolstenholme  
wolstenholme.images@yahoo.co.uk  
<http://www.robwolstenholme.co.uk/>

**RE: Permission to use a photo taken by you in my PhD thesis**

I am writing to request permission to use the following photo taken by you in my PhD thesis with proper reference to you:



If you kindly agree, please sign and date below and return a scan of this request to me.

Thank you for your kind consideration of my request.

Sincerely,

*F. Peiravian*

Farideddin Peiravian

---

The above request is approved.

Approved by: *RSW* ROB WOLSTENHOLME

Date: *4 Oct 2014*

Authorization for Figure 5





http://www.elsevier.com/journal-authors/author-rights-and-responsibilities

http://www.elsevier.com/journal-authors/author-rights-and-responsibilities#author-use

**ELSEVIER**

Type here to search on Elsevier.com

Advanced search

Follow us:    

Help & Contact

Journals & books

Solutions

Authors, editors & reviewers

About Elsevier

Community

Store

For Authors

[Journal authors' home](#)

**Author Rights**

[Ethics](#)

[Agreements](#)

[Open access](#)

[Author services](#)

[Early career researchers](#)

[Authors' Update](#)

[Book authors' home](#)

[Sharing your article](#)

[Journal and article metrics](#)

[Promote your article](#)

Author Rights

Elsevier supports the need for authors to share, disseminate and maximize the impact of their research. We take our responsibility as stewards of the online record seriously, and work to ensure our policies and procedures help to protect the integrity of scholarly works.

Author's rights to reuse and post their own articles published by Elsevier are defined by Elsevier's copyright policy. For our proprietary titles, the type of copyright agreement used depends on the author's choice of publication:

**For subscription articles:** These rights are determined by a copyright transfer, where authors retain scholarly rights to post and use their articles.

**For open access articles:** These rights are determined by an exclusive license agreement, which applies to all our open access content.
















In both cases, the fundamental rights needed to publish and distribute an article remain the same and Elsevier authors will be able to use their articles for a wide range of scholarly purposes.

Details on how authors can reuse and post their own articles are provided below.

**Help and support**

For reuse and posting not detailed below, please see our [posting policy](#), or for authors who would like to:

- Include material from other sources in your work being published by Elsevier, please visit: [Permission seeking guidelines](#) for Elsevier authors.
- Obtain permission to re-use material from Elsevier books, journals, databases, or other products, please visit: [Obtaining permission to reuse Elsevier material](#)
- Or if you are an Elsevier author and are contacted by a requestor who wishes to re-use all or part of your article or chapter, please also refer them to our [Obtaining Permission to Re-Use Elsevier Material page](#).
- See our [FAQ on posting and copyright queries](#).
- Contact us directly, please email our [Permissions Help Desk](#).

Definitions	Author Posting	Author Use										
<div><b>How authors can use their own journal articles</b></div> <p>Authors can use their articles for a wide range of scholarly, non-commercial purposes as outlined below. These rights apply for all Elsevier authors who publish their article as either a subscription article or an open access article.</p> <p>We require that all Elsevier authors always include a full acknowledgement and, if appropriate, a link to the final published version hosted on Science Direct.</p> <p>For open access articles these rights are separate from how readers can reuse your article as defined by the author's choice of <a href="#">Creative Commons user license options</a>.</p>												
<div><div>Authors can use either their <b>accepted author manuscript</b> or <b>final published article</b> for:</div><table><tr><td></td><td>Use at a conference, meeting or for teaching purposes</td></tr><tr><td></td><td>Internal training by their company</td></tr><tr><td></td><td>Sharing individual articles with colleagues for their research use* (also known as 'scholarly sharing')</td></tr><tr><td></td><td>Use in a subsequent compilation of the author's works</td></tr><tr><td></td><td>Inclusion in a thesis or dissertation</td></tr></table></div>				Use at a conference, meeting or for teaching purposes		Internal training by their company		Sharing individual articles with colleagues for their research use* (also known as 'scholarly sharing')		Use in a subsequent compilation of the author's works		Inclusion in a thesis or dissertation
	Use at a conference, meeting or for teaching purposes											
	Internal training by their company											
	Sharing individual articles with colleagues for their research use* (also known as 'scholarly sharing')											
	Use in a subsequent compilation of the author's works											
	Inclusion in a thesis or dissertation											

## Authorization for Chapter 6.2

Monday, September 29, 2014

260

## VITA

### FARIDEDDIN PEIRAVIAN

#### EDUCATION

---

- 2011-2014    Ph.D. Degree, Civil/Transportation Engineering  
University of Illinois at Chicago, Chicago, Illinois, U.S.A.  
Dissertation: “*Geometric Complexity of Urban Road Networks*”  
GPA: A
- 1992-1994    Master’s Degree, Civil Engineering  
McMaster University, Hamilton, Ontario, Canada  
Thesis: “*Interpretation of In-situ Pavement Properties Using FWD Testing Technique*”  
GPA: A
- 1985         B.Sc. Degree, Civil Engineering  
Shiraz University, Shiraz, Fars, Iran  
GPA: 3.67/4.00, Ranked 1<sup>st</sup> among the graduating class

#### SPECIAL INTERESTS

---

- Mathematical Paradoxes
- The Human Nation
- Sustainability
- Complexity
- Fractals